Distributed control of power networks

Trip, Sebastian

Distributed control of power networks

Passivity, optimality and energy functions

Sebastian Trip

university of groningen / faculty of science and engineering

The research described in this dissertation has been carried out at the Faculty of Science and Engineering, University of Groningen, the Netherlands.

disc dutch institute of systems and control

The research described in this dissertation is part of the research program of the Dutch Institute of Systems and Control (DISC).

The Danish Council for Strategic Research

The research described in this dissertation is supported by the Danish Council for Strategic Research (contract no. 11-116843) within the Programme Sustainable Energy and Environment, under the EDGE (Efficient Distribution of Green Energy) research project.

ISBN: 978-94-034-0062-4 (printed version)
ISBN: 978-94-034-0061-7 (electronic version)

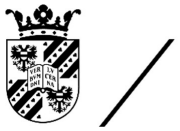

rijksuniversiteit
groningen

Distributed control of power networks

Passivity, optimality and energy functions

Proefschrift

ter verkrijging van de graad van doctor aan de
Rijksuniversiteit Groningen
op gezag van de
rector magnificus prof. dr. E. Sterken
en volgens besluit van het College voor Promoties.

De openbare verdediging zal plaatsvinden op

vrijdag 6 oktober 2017 om 11.00 uur

door

Sebastian Trip

geboren op 31 januari 1985
te Stadskanaal

Promotor
Prof. dr. C. De Persis

Beoordelingscommissie
Prof. dr. M. Cao
Prof. dr. F. Dörfler
Prof. dr. P. Tabuada

"Die Grenzen meiner Sprache bedeuten die Grenzen meiner Welt"

— Ludwig Wittgenstein

Acknowledgments

Working towards this thesis has been a wonderful journey. Many people have helped me, have shaped my research and have joined me on this journey for shorter or longer moments. I wish to thank all of you. The guidance of my promotor has been invaluable. Claudio, thank you for everything you taught me.

Sebastian Trip
Groningen
September 7, 2017

Contents

Chapter 1

Introduction

Various social and technological developments have resulted in an increased share of renewable generation within our energy mix, posing significant challenges to the planning and operation of the existing (energy) networks. Although the shift towards more sustainable energy generation can be seen throughout the whole energy chain, it is the effect on the electricity network that received most attention. Besides the fact that the availability of electricity is essential to our modern society, it is the physical nature of the grid that poses unique and difficult challenges. Traditionally, power networks addressed uncertainty of demand, by controlling the supply. However, due to the increased share of volatile and uncontrollable sources, like wind and solar energy, the uncertainty of the generation side needs to be managed as well. Within such management, the IT-infrastructure plays an important role, and therefore, future 'smarter' grids cannot be longer regarded as a pure physical network, and requires the incorporation of the cyber-infrastructure into the physical model. As the resulting cyber-physical network will consist of many small devices, addressing the stability of such a network becomes more difficult. Modeling each individual device is infeasible, yet their combined response must be accurately described. It is therefore important to derive general properties of systems, without explicitly modelling each component in detail, that are useful to study and improve the stability of the overall network. Furthermore, the collective behaviour of the network must be close to optimal to avoid inefficiencies, and requires coordination among the individual parts. This requires the development of new distributed control schemes that exploit the, widely distributed, sensors and actuators. It is infeasible for a centralized controller to address every controllable load individually, yet actions taken by local controllers must be consistent with global performance objectives. Although contributions from many disciplines are required to make the energy chain more sustainable, the field of system and control theory can provide an important role in creating a reliable network due to its holistic view on the whole system. This work particulary contributes to the establishment of system theoretical properties of the physical power network, the cyber network, and its interconnection. This enables the design op distributed controllers that improve the stability of the network, while increasing the (economic) efficiency of its operation.

1.1 Outline of this thesis

This thesis consists of three main parts, each addressing a particular aspect of the the distributed control of smart grids. Every part consists of a separate introduction and a statement of its contributions. Part I, focusses on the design of distributed controllers, achieving output regulation in a network, by optimally allocating the inputs in distribution networks. Chapter 1 (high voltage networks) and Chapter 2 (microgrids), discuss electrical networks, where the considered output of the system is the frequency deviation. In Chapter 3, a general class of flow networks is studied that includes the model of a high voltage direct current network. The considered model differs particularly from the aforementioned chapters in that the network does not dissipate energy. The stability analysis in this part, as well as in Part II and Part III, relies foremost on an incremental passivity property of the underlying network, the internal model principle and an invariance principle. A continuous consensus algorithm is employed to achieve the desired optimality features. In Part II, we continue studying high voltage networks and incorporate the generation side in a more realistic manner. Commonly, the generation side is modelled by a second order turbine-governor system. Since the turbine-governor system does not enjoy a useful passivity property, the stability analysis is more challenging. We propose two methods. First, in Chapter 4, an overall dissipation inequality is developed for the combined generator and turbine-governor dynamics. Second, in Chapter 5, a sliding mode control strategy is employed to constrain the turbine-governor to a manifold where a passivity property is recovered. Part III relaxes the requirement of continuous communication between the controllers to achieve optimality. Particularly, we study the interconnected continuous physical system and the discrete communication layer, leading to hybrid dynamics of the overall cyber-physical system. In Chapter 6 we study a centralized control scheme, whereas in Chapter 7 we study a distributed setting. Eventually, we provide some conclusions and directions for future research.

1.2 List of publications

Journal publications

- S. Trip, M. Bürger and C. De Persis – *"An internal model approach to (optimal) frequency regulation in power grids with time-varying voltages,"* Automatica, vol. 64, pp. 240–253, 2016. (Chapter 2)

- S. Trip, T.W. Scholten and C. De Persis – *"Optimal regulation of flow networks*

with transient constraints," 2017, under review. (Chapter 4)

- S. Trip and C. De Persis – *"Distributed optimal Load Frequency Control with non-passive dynamics,"* IEEE Transactions on Control of Network Systems, 2017, to appear. (Chapter 5)
- S. Trip, M. Cucuzella, C. De Persis, A.J. van der Schaft and A. Ferrara – *"Passivity based design of sliding modes for optimal Load Frequency Control,"* 2017, under review. (Chapter 6)
- S. Trip, C. De Persis and P. Tesi – *"Coordination of nonlinear cyber-physical systems, from a continuous consensus to a discrete broadcasting protocol (tentative),"* 2017, in preparation. (Chapter 8)
- M. Cucuzella, S.Trip, C. De Persis, A. Ferrara and A.J. van der Schaft – *"A robust consensus algorithm for current sharing and voltage regulation in DC Microgrids,"* 2017, under review.
- M. Cucuzzella, R. Lazzari, S. Trip, S. Rosti, C. Sandroni and A. Ferrara – *"Sliding mode voltage control of boost-based DC microgrids,"* 2017, under review.
- T.W. Scholten, S.Trip and C. De Persis – *"Pressure Regulation in Large Scale Hydraulic Networks with Positivity Constraints (tentative),"* 2017, in preparation.

Conference publications

- M. Bürger, C. De Persis and S. Trip – *"An internal model approach to (optimal) frequency regulation in power grids,"* Proceedings of the 2014 21st International Symposium on Mathematical Theory of Networks and Systems (MTNS), pp. 577–583, Groningen, the Netherlands, 2014. (Chapter 2)
- S. Trip, M. Bürger and C. De Persis – *"An internal model approach to frequency regulation in inverter-based microgrids with time-varying voltages,"* Proceedings of the IEEE 53rd Conference on Decision and Control (CDC)," pp. 223–228, Los Angles, CA, USA, 2014. (Chapter 3)
- S. Trip, T.W. Scholten and C. De Persis – *"Optimal regulation of flow networks with input and flow constraints,"* Proceedings of the 2017 IFAC World Congress, pp. 9854–9859, Toulouse, FR, 2017. (Chapter 4)
- S. Trip and C. De Persis – *"Optimal frequency regulation in nonlinear structure preserving power networks including turbine dynamics: an incremental passivity approach,"* Proceedings of the 2016 American Control Conference (ACC), pp. 4132–4137, Boston, MA, USA, 2016. (Chapter 5)

- S. Trip and C. De Persis – *"Optimal generation in structure-preserving power networks with second order turbine-governor dynamics,"* Proceedings of the 15th European Control Conference (ECC), pp. 916–921, Aalborg, DK, 2016. (Chapter 5)
- M. Cucuzella, S. Trip, C. De Persis and A. Ferrara – *"Distributed second order sliding modes for Optimal Load Frequency Control,"* Proceedings of the 2017 American Control Conference (ACC), pp. 3451–3456, Seattle, WA, USA, 2017. (Chapter 6)
- S. Trip, M. Cucuzella, A. Ferrara and C. De Persis – *"An energy function based design of second order sliding modes for Automatic Generation Control,"* Proceedings of the 2017 IFAC World Congress, pp. 12118–12123, Toulouse, FR, 2017.
- S. Trip and C. De Persis – *"Communication requirements in a master-slave control structure for optimal load frequency control,"* Proceedings of the 2017 IFAC World Congress, pp. 10519–10524, Toulouse, FR, 2017. (Chapter 7)
- T.W. Scholten, S. Trip, and C. De Persis – *"Pressure Regulation in Large Scale Hydraulic Networks with Input Constraints,"* Proceedings of the 2017 IFAC World Congress, pp. 5534–5539, Toulouse, FR, 2017.

Book chapters

- S. Trip and C. De Persis – *"Frequency regulation in power grids by optimal load and generation control"* In A. Beaulieu, J. Wilde, and J.M.A. Scherpen (Ed.), *"Smart grids from a global perspective"*, Springer International Publishing, pp. 129–146, 2016. (Chapter 2)

1.3 Notation

Let $\mathbf{0}$ be the vector or matrix of all zeros of suitable dimension and let $\mathbb{1}_n$ be the vector containing all ones of length n. A diagonal matrix, with diagonal elements given by vector x, is denoted by $\mathrm{diag}(x)$ and occasionally by $[x]$. We define $\mathcal{R}(f(x))$ to be the range of function $f(x)$. A steady state solution to system $\dot{x} = f(x)$, satisfying $\mathbf{0} = f(x)$, is denoted by $\overline{x}$, *i.e.* $\mathbf{0} = f(\overline{x})$, except in Chapter 2, where $\overline{x}$ denotes also a solution to the regulator equations. In case the argument of a function is clear from the context, we occasionally write $f(x)$ as $f(\cdot)$ or f. Let A be a matrix, then $\mathrm{Im}(A)$ is the image of A and $\mathrm{Ker}(A)$ is the kernel of A. In case A is a positive definite (positive semi-definite) matrix, we write $A \in \mathbb{R}^{n\times n}_{>0}$ ($A \in \mathbb{R}^{n\times n}_{\geq 0}$), or $A > \mathbf{0}$ ($A \geq \mathbf{0}$).

Similarly, for negative definite (negative semi-definite) matrices. Lastly, we denote the cardinality of a set $\mathcal{V}$ as $|\mathcal{V}|$.

1.4 Preliminaries

In this section a minimum amount of preliminaries are provided, that are useful to the development of the various results appearing in this thesis. An important topic that is left out here, is a discussion on power networks. The considered power network models in this thesis are standard, and derivations as well as further discussions can be found in e.g (Machowski et al. 2008) and (Kundur et al. 1994).

1.4.1 Nonlinear systems

We suppose the reader is familiar with standard notions for the analysis and control of nonlinear system, and foremost with dissipative systems (Willems 2007). For detailed discussions on nonlinear systems, the textbooks (van der Schaft 1999), (Haddad and Chellaboina 2008) and (Sepulchre et al. 1997), provide excellent starting points. We merely recall a few essential definitions and results, starting with 'incremental passivity'.

Definition 1.4.1 (Incremental passivity, (Pavlov and Marconi 2008))**.** *Consider the system*

$$\begin{aligned} \dot{x} &= f(x,u) \\ y &= h(x), \end{aligned} \tag{1.1}$$

with state $x \in \mathbb{R}^n$ input $u \in \mathbb{R}^m$ and output $y \in \mathbb{R}^m$. We say that (1.1) is incrementally passive if there exists a continuous differentiable, positive definite, radially unbounded, storage function $\mathcal{S}(x_1, x_2) : \mathbb{R}_{\geq 0} \times \mathbb{R}^{2n} \to \mathbb{R}_{\geq 0}$ such that for any two inputs $u_1(t)$ and $u_2(t)$ and any two solutions of system (1.1) $x_1(t), x_2(t)$ corresponding to these inputs, the respective outputs $y_1(t) = h(x_1(t))$ and $y_2(t) = h(x_2(t))$ satisfy the inequality

$$\dot{\mathcal{S}} = \tfrac{\partial \mathcal{S}}{\partial x_1} f(x_1, u_1) + \tfrac{\partial \mathcal{S}}{\partial x_2} f(x_2, u_2) \quad \leq \quad (y_1 - y_2)^T (u_1 - u_2). \tag{1.2}$$

The following extension will be useful as well.

Definition 1.4.2 (Output strictly incremental passivity)**.** *We say that (1.1) is output strictly incrementally passive if in Definition 1.4.1, (1.3) is replaced by*

$$\dot{\mathcal{S}} = \tfrac{\partial \mathcal{S}}{\partial x_1} f(x_1, u_1) + \tfrac{\partial \mathcal{S}}{\partial x_2} f(x_2, u_2) \quad \leq \quad -\rho(y_1 - y_2) + (y_1 - y_2)^T (u_1 - u_2), \tag{1.3}$$

where $\rho(y_1 - y_2) : \mathbb{R}^{2n} \to \mathbb{R}_{\geq 0}$ is a positive definite function.

Note that in Definition 1.4.1, the storage function $\mathcal{S}$ is required to be radially unbounded, which is absent in (Pavlov and Marconi 2008, Definition 1). To accommodate the possibility that $\mathcal{S}$ is not radially unbounded, we introduce the following definition:

Definition 1.4.3 (Incremental cyclo-passivity)**.** *We say that (1.1) is incrementally cyclo-passive if in Definition 1.4.1, (1.3) the incremental storage function $\mathcal{S}$ is not required to be radially unbounded.*

The definition of 'incremental cyclo-passivity' is particularly useful, if we can can only establish that the incremental storage function $\mathcal{S}(x_1, x_2)$ is positive definite at a point $(\overline{x}_1, \overline{x}_2)$. Often it is useful to establish incremental passivity with respect to a particular solution (often the steady state solution), and we introduce the following definition:

Definition 1.4.4 (Incremental passivity with respect to a particular solution)**.** *We say that (1.1) is incrementally passive with respect to a particular solution $x_2(t)$, with input $u_2(t)$ satisfying*

$$\begin{aligned} \dot{x}_2 &= f(x_2, u_2) \\ y_2 &= h(x_2), \end{aligned} \tag{1.4}$$

if in Definition 1.4.1, the dissipation inequality holds with respect to the particular solution $x_2(t)$, instead of any *solution to (1.1).*

In case incremental passivity is established with respect to a steady state solution, (1.4) becomes

$$\begin{aligned} \mathbf{0} &= f(\overline{x}, \overline{u}) \\ \overline{y} &= h(\overline{x}). \end{aligned} \tag{1.5}$$

Remark 1.4.5 (Equilibrium independent passivity)**.** *Note that the definition above shows similarities with the definition of 'equilibrium independent passivity' (Hines et al. 2011). However, the 'integrator system'*

$$\dot{x} = u \tag{1.6}$$

$$y = x, \tag{1.7}$$

is not equilibrium independent passive, as the definition in (Hines et al. 2011) requires that for a given $\overline{u}$, there exists a unique $\overline{x}$, such that (in this case) $\mathbf{0} = \overline{u}$. On the other hand, (1.6) is according to our definition 'incrementally passive with respect to the steady $(\overline{x}, \overline{u})$ satisfying $\mathbf{0} = \overline{u}$', as can be established by considering the incremental storage function $\mathcal{S} = \frac{1}{2}(x - \overline{x})^T(x - \overline{x})$.

Until now we considered dynamical systems with input u. One of the objectives of this work is to design (feedback) controllers, obtaining eventually a closed loop system. We recall three lemmas that will be essential to study the asymptotic behaviour of the closed loop (autonomous) system.

Lemma 1.4.6 (Stability (Sepulchre et al. 1997)). *Let* $\mathbf{0}$ *be an equilibrium of system*

$$\dot{x} = f(x), \tag{1.8}$$

and suppose that f *is locally Lipschitz continuous. Let* $\mathcal{S} : \mathbb{R}^n \to \mathbb{R}_{\geq 0}$ *be a continuous differentiable, positive definite and radially unbounded function* $\mathcal{S}(x)$ *such that*

$$\dot{\mathcal{S}} = \frac{\partial \mathcal{S}(x)}{\partial x} f(x) \leq 0. \quad \forall x \in \mathbb{R}^n \tag{1.9}$$

Then, $x = \mathbf{0}$ *is globally stable and all solutions to (1.8) converge to the set* E *where* $\dot{\mathcal{S}} = 0$.

Lemma 1.4.7 (LaSalle's invariance principle, (Sepulchre et al. 1997)). *Let* Ω *be a positive invariant set of*

$$\dot{x} = f(x). \tag{1.10}$$

Suppose that every solution starting in Ω *converges to a set* $E \subset \Omega$ *and let* M *be the largest invariant set contained in* E*. Then, every bounded solution starting in* Ω *converges to* M *as* $t \to \infty$.

Lemma 1.4.8 (Convergence to a constant vector (Haddad and Chellaboina 2008)). *Consider the system*

$$\dot{x} = f(x), \tag{1.11}$$

and let Ω *be an open neighborhood of* $f^{-1}(\mathbf{0})$*. Suppose the positive orbit of (1.11) is bounded for all* $x \in \Omega$ *and assume that there exists a continuously differentiable function* $\mathcal{S} : \Omega \to \mathbb{R}$ *such that*

$$\dot{\mathcal{S}} = \frac{\partial \mathcal{S}(x)}{\partial x} f(x) \leq 0, \quad \forall x \in \Omega. \tag{1.12}$$

If every point in the largest invariant subset M *of*

$$\{x \in \Omega : \frac{\partial \mathcal{S}(x)}{\partial x} f(x) = 0\} \tag{1.13}$$

is Lyapunov stable, then 1.11 converges to a constant vector.

1.4.2 Optimization

The optimization problems we consider are *convex*, and we exploit a few standard properties of this class of problems. For a more detailed discussion on the topic of convex optimization, possibly in relation to networks, the reader can consult e.g. (Boyd and Vandenberghe 2004) and (Bertsekas 1998). We present a few basic, but essential, results from (Boyd and Vandenberghe 2004) that are tailored to our needs. Consider the optimization problem

$$\begin{aligned} &\min_x C(x) \\ \text{s.t} \quad &Ax - b = \mathbf{0}, \end{aligned} \tag{1.14}$$

with $C(x)$ a strictly convex function.

Assumption 1.4.9 (Feasibility)**.** *There exists a solution $x^\star$ to (1.14), with optimal value of $p^\star = C(x^\star)$.*

Definition 1.4.10 (Lagrangian function)**.** *The Lagrangian function of (1.14) is*

$$L(x, \lambda) = C(x) - \lambda^T (Ax - b), \tag{1.15}$$

where λ is the Lagrange multiplier.

Based on the definition of the Lagrangian function, we can formulate the so-called 'dual problem'.

Definition 1.4.11 (Dual problem)**.** *The dual problem of (1.14) is*

$$\max_\lambda g(\lambda), \tag{1.16}$$

with

$$g(\lambda) = \min_x L(x, \lambda). \tag{1.17}$$

The optimal value is given by $d^\star = g(\lambda^\star)$.

In case $p^\star = d^\star$, we say that strong duality holds. For the considered case we have that strong duality always holds, if the primal problem is feasible.

Lemma 1.4.12 (Slater's condition)**.** *Strong duality holds if (1.14) is feasible.*

Having formulated the primal and the dual problem, one can obtain the following results that are useful to explicitly characterize the solution to (1.14).

Lemma 1.4.13 (Saddle point)**.** *Let Assumption 1.4.9 hold. $x^\star$ is optimal for (1.14) and $\lambda^\star$ is optimal for (dual problem) if and only if $(x^\star, \lambda^\star)$ is a saddle point of (1.15), i.e.*

$$L(x^\star, \lambda) \leq L(x^\star, \lambda^\star) \leq L(x, \lambda^\star). \tag{1.18}$$

Lemma 1.4.14 (First order optimality conditions)**.** *The vector $x^\star$ is optimal for 1.14 if and only if there exists a $\lambda^\star$ such that*

$$\begin{aligned} \nabla C(x^\star) - A^T \lambda^\star &= \mathbf{0} \\ Ax^\star - b &= \mathbf{0}. \end{aligned} \tag{1.19}$$

Note that $\frac{\partial L(x,\lambda)}{\partial x} = \nabla C(x) - A^T\lambda$ and $\frac{\partial L(x,\lambda)}{\partial \lambda} = Ax - b$.

1.4.3 Hybrid systems

The combination of discrete and continuous time dynamics, results in a so-called hybrid system. In this thesis we follow closely the formalism introduced in (Goebel et al. 2012). We recall a few basic notations and concepts that are helpful to understand the exposition in Chapter 7 and Chapter 8. Foremost, we recall some definitions and results that allows us to introduce an invariance principle for hybrid systems. The considered hybrid systems are of the form

$$\begin{aligned} \dot{x} &\in F(x) \quad \text{for } x \in C \\ x^+ &\in G(x) \quad \text{for } x \in D, \end{aligned} \tag{1.20}$$

where

- C is the flow set,
- F is the flow map,
- D is the jump set,
- G is the jump map.

The hybrid system, with state $x \in \mathbb{R}^n$, is denoted as $\mathcal{H} = (C, F, D, G)$, or briefly $\mathcal{H}$. A subset $E \subset \mathbb{R}_{\geq 0} \times \mathbb{Z}_{\geq 0}$ is a *hybrid time domain* if for all $(T, K) \in E$, $E \cap ([0, T] \times \{0, \ldots, K\}) = \bigcup_{k \in \{0,\ldots,K-1\}} ([t_k, t_{k+1}], k)$ for some finite sequence of times $0 = t_0 \leq t_1, \ldots, \leq t_K$. A function $\phi : E \to \mathbb{R}^n$ is a *hybrid arc* if E is a hybrid time domain and if for each $k \in \mathbb{Z}_{\geq 0}$, $t \to \phi(t, k)$ is locally absolutely continuous on $I^k = \{t : (t, k) \in E\}$. The hybrid arc $\phi \to \operatorname{dom} \phi \to \mathbb{R}^n$ is a *solution* to (1.20) if: (i) $\phi(0, 0) \in C \cup D$; (ii) for any $k \in \mathbb{Z}_{\geq 0}, \phi(t, k) \in C$ and $(d/dt)\phi(t, k) \in F(\phi(t, k))$ for almost all $t \in I^k$ (recall that $I^k = \{t : (t, k) \in \operatorname{dom} \phi\}$; (iii) for every $(t, k) \in \operatorname{dom} \phi$ such that $(t, k + 1) \in$

$\mathrm{dom}\,\phi$, $\phi(t,k) \in D$ and $\phi(t,k+1) \in G(\phi(t,k))$. A solution to (1.20) is: *nontrivial* if $\mathrm{dom}\,\phi$ contains at least two points; *maximal* if it cannot be extended; *complete* if $\mathrm{dom}\,\phi$ is unbounded; *precompact* if it is complete and the closure of its range is compact, where the range of ϕ is $\mathrm{rge}\,\phi := \{y \in \mathbb{R}^n : \exists (t,k) \in \mathrm{dom}\,\phi \text{ such that } y = \phi(t,k)\}$.

Lemma 1.4.15 (Nominally well-posedness)**.** *A hybrid system $\mathcal{H} = (C, F, D, G)$ is nominally well-posed if it satisfies the following hybrid basic conditions:*

1. *C and D are closed subsets of $\mathbb{R}^n$,*
2. *$F : \mathbb{R}^n \rightrightarrows \mathbb{R}^n$ is outer semicontinuous and locally bounded relative to C, $C \subset$ dom F, and $F(x)$ is convex for every $x \in C$,*
3. *$G : \mathbb{R}^n \rightrightarrows \mathbb{R}^n$ is outer semicontinuous and locally bounded relative to D, $D \subset$ dom G.*

Definition 1.4.16 (Weakly invariant)**.** *A set $S \subset \mathbb{R}^n$ is* weakly invariant *for system (1.20) if it is:*

1. weakly forward invariant, *i.e., for any $\xi \in \mathcal{S}$ there exists a least one complete solution ϕ with initial condition ξ such that $\mathrm{rge}\,\phi \subset S$;*
2. weakly backward invariant, *i.e., for any $\xi \in \mathcal{S}$ and $\tau > 0$, there exists a least one solution ϕ such that for some $(t^*, k^*) \in \mathrm{dom}\,\phi$, $t^* + k^* \leq \tau$, it is the case that $\phi(t^*, k^*) = \xi$ and $\phi(t,k) \in S$ for all $(t,k) \in \mathrm{dom}\,\phi$ with $t + k \leq t^* + k^*$.*

Lemma 1.4.17 (An invariance principle)**.** *Assume the hybrid system is nominally well posed. Consider a continuous function $V : \mathbb{R}^n \to \mathbb{R}$, continuously differentiable on a neighborhood of C. Suppose that for a given $U \subset \mathbb{R}^n$.*

$$u_C(z) \leq 0, \quad u_D \leq 0 \quad \text{for all } z \in U. \tag{1.21}$$

Let a precompact $\phi^* \in \mathcal{S}_{\mathcal{H}}$ be such that $\overline{\mathrm{rge}\,\phi^*} \subset U$. Then, for some $r \in V(U)$, ϕ^* approaches the nonempty set which is the largest weakly invariant subset of

$$\Upsilon = V^{-1}(r) \cap U \cap \left[\overline{u_C^{-1}(0)} \cup \left(u_D^{-1}(0) \cap G(u_D^{-1}(0))\right)\right]. \tag{1.22}$$

Part I

Optimal coordination of power networks

Introduction

Power networks can be regarded as dynamical networks that interact with the environment. As such, they are often affected by external perturbations, e.g. a change in power demand, that can disrupt their desired output or state. An important objective in AC power networks is to maintain the frequency close to their nominal value. By regarding the frequency as the output of the network, we can therefore study the frequency regulation objective, within the setting of output regulation theory for dynamical systems on networks. Depending on the specific application, another common requirement is to optimally distribute the input to the network among the various nodes. Traditionally, the associated optimization problems are considered static and their study have long history within the field of network optimization (Bertsekas 1998), (Rockafellar 1984). In the case of power networks, the optimal allocation of generated power is commonly called 'economic dispatch'. Due to an increasing volatility of the disturbances, the networks must on the other hand react dynamically on changes in the external conditions. In these cases continuous feedback controllers are required that dynamically adjust inputs at the nodes and the design of such controllers is a subject of Part I.

In Part I we design distributed controllers achieving output regulation and optimality for three different, but related, models. Particularly, we develop our methodology for high voltage networks, modelled by interconnected control areas. Automatic regulation of the frequency in power networks is traditionally achieved by primary proportional control (droop-control) and a secondary PI-control. In this secondary control, commonly known as automatic generation control (AGC), each control area determines its "Area Control Error" (ACE) and changes its production accordingly to compensate for local load changes in order to regulate the frequency back to its nominal value and to maintain the scheduled power flows between different area's. By requiring each control area to compensate for their local load changes

the possibility to achieve economic efficiency is lost. Indeed, the scheduled production in the different control area's is currently determined by economic criteria relatively long in advance. To be economically efficient an accurate prediction of load changes is necessary. Large scale introduction of volatile renewable energy sources and the use of electrical vehicles will however make accurate prediction difficult as the net load (demand minus renewable generation) will change on faster time scales and by larger amounts. A more detailed account on the Optimal Load Frequency control is provided in Part II of this thesis.

Another example of power networks are the 'so-called' microgrids. Microgrids are generally either AC or DC. We study the AC variant, that shows many similarities with the high voltage power network discussed above. The DC microgrid on the other hand has been studied in e.g. (De Persis et al. 2016) and (Zhao and Dörfler 2015). Recently, research focus has shifted from centralized control in microgrids (Guerrero et al. 2011), towards distributed control (Simpson-Porco et al. 2013), (De Persis and Monshizadeh 2017), (Dörfler et al. 2016) (Shafiee et al. 2014), (Trip et al. 2014). Here, optimal allocation of the input to the microgrid, is called 'active power sharing', where the objective is to let each inverter generate the same (or proportionally to their rating) amount of power.

Beside the two particular examples of electricity networks, flow or distribution networks are used to model the distribution of a quantity. The design and regulation of these networks received significant attention due to its many applications, including supply chains (Alessandri et al. 2011), heating, ventilation and air conditioning (HVAC) systems (Gupta et al. 2015), data networks (Moss and Segall 1982), water irrigation (Lee et al. 2017), traffic networks (Iftar 1999), (Coogan and Arcak 2015) and compartmental systems (Blanchini et al. 2016), (Como 2017). Besides these many interesting application, we are particularly interested in its use to model multi-terminal high voltage direct current networks, where the proposed controllers achieve sharing in the current injections to the network, maintaining desired voltage levels.

Contributions

Due to the difficulty of precisely predicting the power demand, the design of algorithms controlling the power generation, maintaining the network at nominal operating conditions, while retaining economic efficiency has attracted considerable attention and a vast amount of literature is available. The aim this part is to provide a different framework in which the problem can be tackled exploiting the incremental passive nature of the dynamical system adopted to model the power network

and internal-model-based controllers ((Pavlov and Marconi 2008), (Bürger and De Persis 2015)) able to achieve an economically efficient power generation control in the presence of unknown, and possibly time-varying, power demand. And although the proposed incrementally passive controllers share similarities with others presented in the literature, the way in which they are derived is new and show a few advantages. First, we allow for time-varying power demand (disturbances) in the power network, and based on the internal-model principle, the proposed controllers can deal with this scenario and it turns out that proportional-integral controllers that are more often found in the literature are a special instance of these controllers. Furthermore, being based on output regulation theory for systems over networks ((Bürger and De Persis 2015), (Bürger and De Persis 2013), (Wieland et al. 2011), (Isidori et al. 2014), (De Persis and Jayawardhana 2014)), our approach has the potential to deal with fairly rich classes of external perturbations (Cox et al. 2012), (Serrani et al. 2001), thus paving the way towards regulators in the presence of a large variety of consumption patterns. Passivity is an important feature shared by more accurate models of the power network, as already recognized for different models in e.g. (Shaik et al. 2013), (Caliskan and Tabuada 2014), (Schiffer et al. 2013), implying that the methods that are employed in this part might be used to deal with more complex (and more realistic) dynamical models. Although we do not pursue the most extensive level of generality in this work, the passivity framework allows us to include voltage dynamics in our model, a feature that is usually neglected in other approaches (Andreasson et al. 2013), (Zhang and Papachristodoulou 2015) (Li et al. 2016). Furthermore, passivity is a very powerful tool in the analysis and design of dynamical control networks (Arcak 2007), (Bai et al. 2011), (van der Schaft and Maschke 2013), such that the obtained results might turn out to be useful besides our focus on power networks. An example is given in Chapter 4, that is dealing with a more general class of flow networks. Also, to show incremental passivity, we introduce storage functions that interestingly can be interpreted as energy functions, thus establishing a connection with classical work in the field of power systems (see e.g. (Bergen and Hill 1981), (Chiang et al. 1995) and references therein), that can guide a further investigation of the problem.

Outline

Chapter 2

In Chapter 2 we provide a framework in which the problem of economically efficient frequency regulation in power networks can be tackled, exploiting the incremental passive nature of the dynamical system and internal-model-based controllers. We

focus on a third-order model with time-varying voltages known as 'flux-decay model' (Section 2.1), which, although simplistic, is tractable and meaningful. We move along the lines of (Bürger and De Persis 2015), (Bürger and De Persis 2013), where a framework to deal with nonlinear output agreement and optimal flow problems for dynamical networks has been proposed. After showing (Section 3.2) that the dynamical model adopted to describe the power network is an incrementally passive system with respect to solutions that are of interest (solutions for which the frequency deviation is zero), we provide a systematic method to design internal-model-based power generation controllers that are able to balance power demand, while minimizing the generation costs at steady state. This design is carried out first by solving the regulator equations (Pavlov and Marconi 2008), (Bürger and De Persis 2015) associated with the frequency regulation problem. Among the feedforward power generation inputs that solve the regulator equations, we single out the one for which the static optimal generation problem is solved (Section 3.3). Distributed controllers are proposed for the case of constant power demand (Section 3.4) and the case of time-varying demand (Section 3.5). For both cases we provide a case study in Section 3.6.

Chapter 3

In Chapter 3 we study frequency regulation and power sharing in AC microgrids. We adopt a third-order inverter model, allowing for time-varying voltages, and therefore addressing a more general setting than typical first order inverter models that assume constant voltages (Section 3.1). Although the problem considered is well known and different control strategies have been suggested, the way we analyze the problem and design the controllers is new. After studying the stability of a microgrid, with constant inputs (Section 3.2), we show that the microgrid is an incrementally passive system, so we can build upon our previous result on optimal frequency regulation in an ordinary power network (Chapter 2). The incremental passivity property of the system at hand enables us, along the lines of Chapter 2, to develop distributers controllers that regulate the frequency and share the active power generation optimally among the inverters (Section 3.3). In Section 3.4 we provide a case study of a small inverter network, and additionally consider voltage controllers that have been left out in the stability analysis.

Chapter 4

In Chapter 4 we consider a general class of flow networks, where edges are used to model the exchange of material (flow) between the nodes (Section 4.1). We propose

a *distributed* controller, dynamically adjusting inputs and flows, to achieve *optimal output regulation* under *capacity constraints* on the input and the flows and in the presence of *unknown* demand (disturbances). The various control objectives and the underlying constraints will be discussed first (Section 4.2), whereafter the proposed controllers at the nodes and the flow controllers are introduced in Section 4.3. The controllers on the edges render the flow network incrementally passive with respect to the desired steady state. This passivity property is then exploited in the design of a distributed controller acting on the nodes. Optimal coordination among the inputs, minimizing a suitable cost function, is achieved by exchanging relevant information over a communication network, whereas the constraints are enforced by using suitably selected saturation functions. Global convergence to the desired steady state is proven relying on Lyapunov arguments and an invariance principle (Section 4.4). We provide two case studies (a district heating system and a multi-terminal high voltage direct current network) to illustrate how physical systems are described as a flow network and to demonstrate the performance of the proposed solution (Section 4.5).

Published in:

S. Trip, M. Bürger and C. De Persis – *"An internal model approach to (optimal) frequency regulation in power grids with time-varying voltages,"* Automatica, vol. 64, pp. 240–253, 2016.

M. Bürger, C. De Persis and S. Trip – *"An internal model approach to (optimal) frequency regulation in power grids,"* Proceedings of the 2014 21st International Symposium on Mathematical Theory of Networks and Systems (MTNS), Groningen, the Netherlands, pp. 577–583, 2014.

S. Trip and C. De Persis – *"Frequency regulation in power grids by optimal load and generation control"* In A. Beaulieu, J. Wilde, and J.M.A. Scherpen (Ed.), *"Smart grids from a global perspective"*, Springer International Publishing, pp. 129–146, 2016.

Chapter 2

Optimal frequency regulation in power networks with time-varying disturbances

Abstract

This chapter studies the problem of frequency regulation in power networks under unknown and possible time-varying load changes, while minimizing the generation costs. We formulate this problem as an output agreement problem for distribution networks and address it using incremental passivity and distributed internal-model-based controllers. Incremental passivity enables a systematic approach to study convergence to the optimal steady state with zero frequency deviation and to design the controller in the presence of time-varying voltages, whereas the internal-model principle is applied to tackle the uncertain nature of the loads.

2.1 Control areas with dynamic voltages

The history of power network modelling is rich and the models we adopt can be found in most textbooks on power systems such as (Machowski et al. 2008) and (Kundur et al. 1994).We focus on an extended swing equation that captures, beside the frequency dynamics, also the essential voltage dynamics (Chiang et al. 1995). In this chapter we show that the considered model possesses some incremental passivity properties that are essential to our approach to the problem. We assume that the power network is partitioned into smaller areas, such as control areas, where the dynamic behavior of an area can be described by an equivalent single generator as a result of coherency and aggregation techniques (Chakrabortty et al. 2011), (Ourari et al. 2006). As a consequence we do not distinguish between individual generator

and load buses. This is in contrast with the structure-preserving models, where the load buses are explicitly modelled (see also Chapter 5), or with Kron-reduced models, where load buses can be eliminated by modeling them as constant admittances or currents (see also Chapter 3).

Consider a power network consisting of n areas. The network is represented by a connected and undirected graph $\mathcal{G} = (\mathcal{V}, \mathcal{E})$, where the nodes, $\mathcal{V} = \{1, \dots, n\}$, represent control areas and the edges, $\mathcal{E} = \{1, \dots, m\}$, represent the transmission lines connecting the areas. The network structure can be represented by its corresponding incidence matrix $\mathcal{B} \in \mathbb{R}^{n \times m}$. The ends of edge k are arbitrarily labeled with a '$+$' and a '$-$'. Then

$$\mathcal{B}_{ik} = \begin{cases} +1 & \text{if } i \text{ is the positive end of } k \\ -1 & \text{if } i \text{ is the negative end of } k \\ 0 & \text{otherwise.} \end{cases}$$

Every node represents an aggregated area of generators and loads and its dynamics are described by the so called 'flux-decay' or 'single-axis' model. It extends the classical second order 'swing equations', that describe the dynamics for the voltage angle δ and the frequency ω, by including a differential equation describing voltage dynamics. A detailed derivation can be found e.g. in (Machowski et al. 2008).

The dynamics of node i are given by:

$$\begin{aligned} \dot{\delta}_i &= \omega_i^b \\ M_i \dot{\omega}_i^b &= u_i - \sum_{j \in \mathcal{N}_i} V_i V_j B_{ij} \sin\big(\delta_i - \delta_j\big) - D_i\big(\omega_i^b - \omega^n\big) - P_{di} \\ \frac{T_{doi}}{(X_{di} - X_{di}^{'})} \dot{V}_i &= \frac{\overline{E}_{fi}}{(X_{di} - X_{di}^{'})} - \frac{1 - B_{ii}(X_{di} - X_{di}^{'})}{(X_{di} - X_{di}^{'})} V_i + \sum_{j \in \mathcal{N}_i} V_j B_{ij} \cos\big(\delta_i - \delta_j\big). \end{aligned} \tag{2.1}$$

where B denotes the susceptance and $\mathcal{N}_i$ is the set of nodes connected to node i by a transmission line. In high voltage transmission networks we consider here, the conductance is close to zero and therefore neglected, i.e. we assume that the network is lossless. An overview of the used symbols is provided in Table 2.1. We focus on (optimal) frequency regulation and in order to keep the analysis concise we assume that $\overline{E}_{fi}$ is constant and do not explicitly include exciter dynamics. To study the interconnected power network we write system (2.1) compactly for all

	State variables
δ_i	Voltage angle
ω_i	Frequency deviation
V_i	Voltage
	Parameters
M_i	Moment of inertia
D_i	Damping constant
T_{doi}	Direct axis transient open-circuit constant
X_{di}	Direct synchronous reactance
$X_{di}^{'}$	Direct synchronous transient reactance
X_{di}	Direct synchronous reactance
X_{di}'	Direct synchronous transient reactance
B_{ij}	Transmission line susceptance
	Inputs
u_i	Controllable power generation
$\overline{E}_{fi}$	Constant exciter voltage
P_{di}	Unknown power demand

Table 2.1: Description of the used symbols.

buses $i \in \mathcal{V}$ as

$$\begin{aligned} \dot{\eta} &= \mathcal{B}^T\omega \\ M\dot{\omega} &= u - \mathcal{B}\Gamma(V)\sin(\eta) - D\omega - P_d \\ T\dot{V} &= -E(\eta)V + \overline{E}_{fd} \\ y &= \omega, \end{aligned} \tag{2.2}$$

where ω is the frequency deviation $\omega^b - \omega^n$, $\mathcal{B}$ is the incidence matrix corresponding to the topology of the network, $\Gamma(V) = \text{diag}\{\gamma_1, \ldots, \gamma_m\}$, with $\gamma_k = V_iV_jB_{ij} = V_jV_iB_{ji}$ and the index k denoting the line $\{i, j\}$, $\overline{E}_{fd} = (\frac{\overline{E}_{f1}}{(X_{d1}-X_{d1}')}, \ldots, \frac{\overline{E}_{fn}}{(X_{dn}-X_{dn}')})^T$, $\eta = \mathcal{B}^T\delta$ and $E(\eta)$ is a matrix such that $E_{ii} = \frac{1-B_{ii}(X_{di}-X_{di}^{'})}{X_{di}-X_{di}^{'}}$ and $E_{ij} = -B_{ij}\cos(\eta_k)$, where again the index k denotes the line $\{i, j\}$. We write explicitly the relation $y = \omega$, to stress that only the frequency (deviation) is measured in the system.

Remark 2.1.1 (Reactance and suscpentance)**.** *In a realistic network the reactance is higher than the transient reactance, i.e.* $X_{di} > X_{di}^{'} > 0$ *and the self-susceptance* B_{ii} *satisfies* $B_{ii} < 0$ *and due to the shunt susceptance* $|B_{ii}| > \sum_{j\in\mathcal{N}_i}|B_{ij}|$ *. It follows that* $E(\eta)$ *is a strictly diagonally dominant and symmetric matrix with positive elements on its diagonal*

and is therefore positive definite.

2.2 Incremental passivity of the multi-machine power network

The purpose of this section is to show that system (2.2) is incrementally passive (see Definition 1.4.1), when we consider u as the input and ω as the output. This property turns out to be fundamental in the subsequent analysis pursued in this chapter. While showing the incremental passivity property, a storage function is derived, based upon which the forthcoming analysis of the response of system (2.2) to the power generation u and the load P_d is carried out. Following (Bürger and De Persis 2015) , to show incremental passivity, system (2.2) is first interpreted as two subsystems interconnected via constraints that reflect the topology of the network. As a matter of fact, observe that system (2.2) can be viewed as the feedback interconnection of the system

$$\begin{aligned} M\dot{\omega} &= u + \mu - D\omega - P_d \\ y &= \omega \end{aligned} \tag{2.3}$$

with the system

$$\begin{aligned} \dot{\eta} &= v \\ T\dot{V} &= -E(\eta)V + \overline{E}_{fd} \\ \lambda &= \Gamma(V)\sin(\eta). \end{aligned} \tag{2.4}$$

These systems are interconnected via the relations

$$\begin{aligned} v &= \mathcal{B}^T y \\ \mu &= -\mathcal{B}\lambda, \end{aligned} \tag{2.5}$$

where the incidence matrix $\mathcal{B}$ reflects the topology of the network. Before studying the incremental passivity of the system it is convenient to recall its equilibria, which we will do in the next subsection.

2.2.1 Equilibria of the power network

As a first step we characterize the constant steady state solution $(\overline{\eta}, \overline{\omega}, \overline{V})$ of (2.2), with a generation $u = \overline{u}$, and in the case in which $\overline{\omega}$ is a constant belonging to the space $\mathrm{Ker}(\mathcal{B}^T)$, i.e. it is a constant vector with all elements being equal. The steady

state solution necessarily satisfies

$$\begin{aligned} \mathbf{0} &= \mathcal{B}^T \overline{\omega} \\ \mathbf{0} &= \overline{u} - \mathcal{B}\Gamma(\overline{V})\sin(\overline{\eta}) - D\overline{\omega} - P_d \\ \mathbf{0} &= -E(\overline{\eta})\overline{V} + \overline{E}_{fd}. \end{aligned} \tag{2.6}$$

Notice that $\overline{\eta}$ is the vector of relative voltage angles that guarantee the power exchange among the buses at steady state. The solution to (2.6) can be characterized as follows:

Lemma 2.2.1 (Steady state frequency deviation)**.** *If there exists* $(\overline{\eta}, \overline{\omega}, \overline{V}) \in \mathrm{Im}(\mathcal{B}^T) \times \mathbb{R}^n \times \mathbb{R}^n_{>0}$ *such that (2.6) holds, then necessarily* $\overline{\omega} = \mathbb{1}_n \omega_*$*, with*

$$\omega_* = \frac{\mathbb{1}_n^T(\overline{u} - P_d)}{\mathbb{1}_n^T D \mathbb{1}_n} = \frac{\sum_{i\in\mathcal{V}}(\overline{u}_i - P_{di})}{\sum_{i\in\mathcal{V}} D_i}, \tag{2.7}$$

and the vector $\overline{u} - P_d$ *must satisfy*

$$\left(I - \frac{D\mathbb{1}_n\mathbb{1}_n^T}{\mathbb{1}_n^T D \mathbb{1}_n}\right)(\overline{u} - P_d) \in \mathcal{D}, \tag{2.8}$$

where

$$\mathcal{D} = \{v \in \mathrm{Im}(\mathcal{B}) : v = \mathcal{B}\Gamma(\overline{V})\sin(\overline{\eta}),\ \overline{\eta} \in \mathrm{Im}(\mathcal{B}^T), \overline{V} \in \mathbb{R}^n_{>0}\}. \tag{2.9}$$

Proof. From the first line of (2.6), the steady state frequency necessarily satisfies $\overline{\omega} = \mathbb{1}_n\omega^*$, with $\omega^* \in \mathbb{R}$. Premultiplying both sides of the second equation with $\mathbb{1}^T$ yields

$$0 = \mathbb{1}_n^T(\overline{u} - P_d) - \mathbb{1}_n^T D \mathbb{1}_n \omega^*, \tag{2.10}$$

from where 2.7 immediately follows. Condition (2.8) is then a result from substituting the obtained expression for $\overline{\omega}$ into the second line of (2.6), ■

Notice that, in view of (2.6), the requirement for $\overline{\omega}$ to be a constant vector requires the vector $u - P_d$ to be constant as well. A characterization of the equilibria for a related system has been similarly discussed in (Simpson-Porco et al. 2013), (Schiffer et al. 2013), (Zhao et al. 2014) and has its antecedents in e.g. (Bergen and Hill 1981). Motivated by the result above, (2.8) is introduced as a feasibility condition that formalizes the physical intuition that the network is capable of transferring the electrical power at its steady state.

Assumption 2.2.2 (Feasibility)**.** *For a given* $\overline{u} - P_d$*, there exist* $\overline{\eta} \in \mathrm{Im}(\mathcal{B}^T)$*,* $\overline{V} \in \mathbb{R}^n_{>0}$ *and* $\overline{E}_{fd} \in \mathbb{R}^n$ *for which (2.8) is satisfied and* $\mathbf{0} = -E(\overline{\eta})\overline{V} + \overline{E}_{fd}$*.*

In some specific cases, the characterization above can be made more explicit. If the graph has no cycles, then (2.8) holds provided that $\overline{u} - P_d$ and $\overline{V}$ are such that (Simpson-Porco et al. 2013)

$$\|\Gamma(\overline{V})^{-1}\mathcal{B}^\dagger \left(I - \frac{D\mathbb{1}_n\mathbb{1}_n^T}{\mathbb{1}_n^T D\mathbb{1}_n}\right)(\overline{u} - P_d)\|_\infty < 1, \tag{2.11}$$

in which case $\overline{\eta}$ is obtained from

$$\sin(\overline{\eta}) = \Gamma(\overline{V})^{-1}\mathcal{B}^\dagger \left(I - \frac{D\mathbb{1}_n\mathbb{1}_n^T}{\mathbb{1}_n^T D\mathbb{1}_n}\right)(\overline{u} - P_d), \tag{2.12}$$

with $\mathcal{B}^\dagger$ the Moore-Penrose pseudo-inverse.

2.2.2 Incremental passivity

Having characterized the steady state solution of system (2.2) and having assumed that such a steady state solution exists, we are ready to state the main result of this section concerning the incremental passivity of the system with respect to the steady state solution. The proof of the incremental passivity of system (2.2) can be split in a number of basic steps. First, one can show that system (2.3) is incrementally passive with respect to the equilibrium solution, namely:

Lemma 2.2.3 (Incremental passivity of (2.3))**.** *System (2.3) with inputs u and μ and output $y = \omega$, is an output strictly incrementally passive system with respect to a constant solution $\overline{\omega}$. Namely, there exists a regular storage function $\mathcal{S}_1(\omega, \overline{\omega})$ which satisfies the incremental dissipation inequality $\dot{\mathcal{S}}_1(\omega, \overline{\omega}) = -\rho(y-\overline{y})+(y-\overline{y})^T(\mu-\overline{\mu})+(y-\overline{y})^T(u-\overline{u})$, where $\dot{\mathcal{S}}_1$ represents the directional derivative of $\mathcal{S}_1$ along the solutions to (2.3) and $\rho : \mathbb{R}^n \to \mathbb{R}_{\geq 0}$ is a positive definite function.*

Proof. Consider the regular storage function $\mathcal{S}_1(\omega, \overline{\omega}) = \frac{1}{2}(\omega - \overline{\omega})^T M(\omega - \overline{\omega})$. We have

$$\begin{aligned}\dot{\mathcal{S}}_1 &= (\omega - \overline{\omega})^T(u + \mu - D\omega - P_d)\\ &= (\omega - \overline{\omega})^T(-D(\omega - \overline{\omega}) + (\mu - \overline{\mu}) + (u - \overline{u}))\\ &= -(y - \overline{y})^T D(y - \overline{y}) + (y - \overline{y})^T(\mu - \overline{\mu}) + (y - \overline{y})^T(u - \overline{u}),\end{aligned} \tag{2.13}$$

which proves the claim. Notice that in the second equality above, we have exploited the identity $\mathbf{0} = \overline{u} + \overline{\mu} - D\overline{\omega} - P_d$. ■

Second, we can prove a similar statement for system (2.4) under the following condition:

Assumption 2.2.4 (Steady state voltage angles and voltages)**.** *Let $\overline{\eta}_k \in (\frac{-\pi}{2}, \frac{\pi}{2})$ for all $k \in \mathcal{E}$ and let $\overline{V} \in \mathbb{R}^n_{>0}$ be such that*

$$\begin{aligned} E(\overline{\eta}) \quad - \quad & \operatorname{diag}(\overline{V})^{-1}|\mathcal{B}|\Gamma(\overline{V})\operatorname{diag}(\sin(\overline{\eta})) \\ & \operatorname{diag}(\cos(\overline{\eta}))^{-1}\operatorname{diag}(\sin(\overline{\eta}))|\mathcal{B}|^T\operatorname{diag}(\overline{V})^{-1} > \mathbf{0}, \end{aligned} \tag{2.14}$$

where $|\mathcal{B}|$ is the incidence matrix with all elements positive.

Confirming inequality (2.14) can be done using only local information as is stated in the following lemma (De Persis and Monshizadeh 2017):

Lemma 2.2.5 (A local condition to satisfy (2.14))**.** *Inequality (2.14) holds if for all $i \in \mathcal{V}$ it holds that*

$$\frac{1}{X_{di} - X'_{di}} - B_{ii} + \sum_{k \sim \{i,j\} \in \mathcal{E}} \frac{B_{ij}(\overline{V}_i + \overline{V}_j \sin^2(\overline{\eta}_k))}{\overline{V}_i \cos(\overline{\eta}_k)} > 0. \tag{2.15}$$

The role of Assumption 2.2.4 is to guarantee the existence of a suitable incremental storage function with respect to the constant solution $(\overline{\eta}, \overline{V})$, as becomes evident in the following lemma.

Lemma 2.2.6 (Hessian matrix)**.** *Let Assumption 2.2.4 hold. Then the storage function*

$$\begin{aligned} \mathcal{S}_2(\eta, \overline{\eta}, V, \overline{V}) \quad = \quad & -\mathbb{1}^T\Gamma(V)\cos(\eta) + \mathbb{1}^T\Gamma(\overline{V})\cos(\overline{\eta}) \\ & - \left(\Gamma(\overline{V})\sin(\overline{\eta})\right)^T(\eta - \overline{\eta}) \\ & - \overline{E}_{fd}(V - \overline{V}) \\ & + \tfrac{1}{2}V^T F V - \tfrac{1}{2}\overline{V}^T F \overline{V}, \end{aligned} \tag{2.16}$$

where $F_{ii} = \frac{1 - B_{ii}(X_{di} - X'_{di})}{X_{di} - X'_{di}}$, has a strict local minimum at $(\overline{\eta}, \overline{V})$.

Proof. First we consider the gradient of $\mathcal{S}_2$, which is given by

$$\nabla \mathcal{S}_2 \quad = \quad \begin{bmatrix} \frac{\partial \mathcal{S}_2}{\partial \eta} & \frac{\partial \mathcal{S}_2}{\partial V} \end{bmatrix}^T = \begin{bmatrix} \Gamma(V)\sin(\eta) - \Gamma(\overline{V})\sin(\overline{\eta}) \\ E(\eta)V - \overline{E}_{fd} \end{bmatrix}. \tag{2.17}$$

It is immediate to see that we have $\nabla \mathcal{S}_2|_{\eta = \overline{\eta}, V = \overline{V}} = \mathbf{0}$. As the gradient of $\mathcal{S}_2$ is zero at $(\overline{\eta}, \overline{V})$, for $\mathcal{S}_2$ to have a strict local minimum it is sufficient that the Hessian is positive definite at $(\overline{\eta}, \overline{V})$. The Hessian is given by

$$\nabla^2 \mathcal{S}_2 = \begin{bmatrix} \Gamma(V)\operatorname{diag}(\cos(\eta)) & \mathcal{H}^T(\eta, V) \\ \mathcal{H}(\eta, V) & E(\eta) \end{bmatrix}, \tag{2.18}$$

where $\mathcal{H}(\eta, V) = \mathrm{diag}(V)^{-1}|\mathcal{B}|\Gamma(V)\mathrm{diag}(\sin(\eta))$. Since $\Gamma(V)\mathrm{diag}(\cos(\eta))$ is positive definite for $\eta \in (\frac{-\pi}{2}, \frac{\pi}{2})^m$ it follows by invoking the Schur complement that $\nabla^2 \mathcal{S}_2|_{\eta=\overline{\eta}, V=\overline{V}} > \mathbf{0}$ if and only if

$$\begin{aligned} E(\overline{\eta}) \quad - \quad & \mathrm{diag}(\overline{V})^{-1}|\mathcal{B}|\Gamma(\overline{V})\mathrm{diag}(\sin(\overline{\eta})) \\ & \mathrm{diag}(\cos(\overline{\eta}))^{-1}\mathrm{diag}(\sin(\overline{\eta}))|\mathcal{B}|^T\mathrm{diag}(\overline{V})^{-1} > \mathbf{0}. \end{aligned} \tag{2.19}$$

■

Remark 2.2.7 (Boundedness of trajectories)**.** *Assuming $\overline{\eta} \in (\frac{-\pi}{2}, \frac{\pi}{2})^m$ is standard in power network stability studies and is also referred to as a security constraint (Dörfler et al. 2016). Assumption 2.2.4 is a technical condition that allows us to infer boundedness of trajectories. An analogous condition (for a related model in a different reference frame) has been proposed in (Schiffer et al. 2013). In the case of constant voltages Assumption 2.2.4 becomes less restrictive and only the assumption $\overline{\eta} \in (\frac{-\pi}{2}, \frac{\pi}{2})^m$ is required (Bürger et al. 2014). We notice indeed that by setting $V = \overline{V}$, the storage function (2.16) reduces to $-\mathbb{1}^T\Gamma(\overline{V})\cos(\eta) + \mathbb{1}^T\Gamma(\overline{V})\cos(\overline{\eta}) - \big(\Gamma(\overline{V})\sin(\overline{\eta})\big)^T(\eta - \overline{\eta})$, which is regularly used in stability studies of the power grid (see e.g. formula (22) in (Bergen and Hill 1981)) and has been adopted to study the stability of constant steady states of incrementally passive systems (Bürger and De Persis 2015) .*

We are now ready to prove that the feedback path (2.4) is incrementally passive with respect to the equilibrium when Assumption 2.2.4 holds.

Lemma 2.2.8 (Incremental passivity of (2.4))**.** *Let Assumptions 2.2.2 and 2.2.4 hold. System (2.4) with input v and output λ is an incrementally passive system, with respect to the constant equilibrium $(\overline{\eta}, \overline{V})$ which fulfills (2.14). Namely, there exists a storage function $\mathcal{S}_2(\eta, \overline{\eta}, V, \overline{V})$ which satisfies the incremental dissipation inequality*

$$\dot{\mathcal{S}}_2(\eta, \overline{\eta}, V, \overline{V}) = -\|\nabla_V \mathcal{S}_2\|^2_{T^{-1}} + (\lambda - \overline{\lambda})^T(v - \overline{v}), \tag{2.20}$$

where $\dot{\mathcal{S}}_2$ represents the directional derivative of $\mathcal{S}_2$ along the solutions to (2.4) and $\|\nabla_V \mathcal{S}_2\|^2_{T^{-1}}$ is the shorthand notation for $(\nabla_V \mathcal{S}_2)^T T^{-1} \nabla_V \mathcal{S}_2$.

Proof. Consider the storage function $\mathcal{S}_2$ given in (2.16). Under Assumption 2.2.4 we have that $\mathcal{S}_2$ is a positive definite function in a neighborhood of $(\overline{\eta}, \overline{V})$. Since $T\dot{V} = -\nabla_V \mathcal{S}_2$, it is straightforward to check that the dissipation inequality writes as

$$\begin{aligned} \dot{\mathcal{S}}_2(\eta, \overline{\eta}, V, \overline{V}) &= -\|\nabla_V \mathcal{S}_2\|^2_{T^{-1}} + (\Gamma(V)\sin(\eta) - \Gamma(\overline{V})\sin(\overline{\eta}))^T\dot{\eta} \\ &= -\|\nabla_V \mathcal{S}_2\|^2_{T^{-1}} + (\lambda - \overline{\lambda})^T(v - \overline{v}), \end{aligned} \tag{2.21}$$

where the last equality trivially holds since $\dot{\overline{\eta}} = \overline{v} = \mathbf{0}$. This proves the claim. ■

The interconnection of incrementally passive systems via (2.5) is known to be still incrementally passive. Bearing in mind Lemma 2.2.3 and Lemma 2.2.8 the next theorem follows immediately, proving that system (2.2) is output strictly incrementally passive with u as an input and $y = \omega$ as an output. We can exploit this feature to further design incrementally passive controllers that generate u while establishing desired properties for the overall closed-loop system.

Theorem 2.2.9 (Incremental passivity of (2.2))**.** *Let Assumptions 2.2.2 and 2.2.4 hold. System (2.2) with input u and output $y = \omega$ is an output strictly incrementally passive system, with respect to the constant equilibrium $(\overline{\eta}, \overline{\omega}, \overline{V})$ which fulfills (2.14). Namely, there exists a storage function $\mathcal{S}(\omega, \overline{\omega}, \eta, \overline{\eta}, V, \overline{V}) = \mathcal{S}_1(\omega, \overline{\omega}) + \mathcal{S}_2(\eta, \overline{\eta}, V, \overline{V})$ which satisfies the following incremental dissipation inequality*

$$\dot{\mathcal{S}}(\omega, \overline{\omega}, \eta, \overline{\eta}, V, \overline{V}) \quad = \quad -\rho(y - \overline{y}) - \|\nabla_V \mathcal{S}_2\|^2_{T^{-1}} + (y - \overline{y})^T (u - \overline{u}), \tag{2.22}$$

where $\dot{\mathcal{S}}$ represents the directional derivative of $\mathcal{S}$ along the solutions to (2.2) and ρ is a positive definite function.

Proof. The results descends immediately from Lemma 2.2.3 and Lemma 2.2.8 bearing in mind the interconnection constraints (2.5). ■

Remark 2.2.10 (Energy functions)**.** *A function similar to $\mathcal{S}$ (but in a different coordinate frame) was considered in e.g. (Chu and Chiang 1999) and are studied as 'energy functions' of the underlying system. Here we provide a different construction that shows that $\mathcal{S}$ is an incremental storage function with respect to which incremental passivity is proven. Highlighting this property is crucial in the approach and analysis we pursue. Furthermore, in the forthcoming analysis, we extend the storage function $\mathcal{S}$ with a term that takes into account the addition of the controller and use it to infer convergence properties of the overall closed-loop system.*

The incremental passivity property of system (2.2) established above has the immediate consequence that the response of the system converges to an equilibrium when the power injection $\overline{u}$ and the load P_d are such that the total imbalance $\overline{u} - P_d$ is a constant. For the sake of completeness, the details are provided in Corollary 2.2.11 below.

Corollary 2.2.11 (Approaching an equilibrium)**.** *Let Assumptions 2.2.2 and 2.2.4 hold. There exists a neighborhood of initial conditions around the equilibrium $(\overline{\eta}, \overline{\omega}, \overline{V})$, where $\overline{\omega} = \mathbb{1}_n \omega_*$ is as characterized in Lemma 2.2.1, such that the solutions to (2.2) starting from this neighborhood approach an equilibrium where $\overline{\omega} = \mathbb{1}_n \omega_*$.*

Proof. Bearing in mind Theorem 2.2.9 and setting $u = \overline{u}$ and $y = \omega$, the overall storage function $\mathcal{S}(\omega, \overline{\omega}, \eta, \overline{\eta}, V, \overline{V}) = \mathcal{S}_1(\omega, \overline{\omega}) + \mathcal{S}_2(\eta, \overline{\eta}, V, \overline{V})$ satisfies

$$\begin{aligned}\dot{\mathcal{S}} &= -(\omega - \overline{\omega})^T D(\omega - \overline{\omega}) - (\omega - \overline{\omega})^T \mathcal{B}(\lambda - \overline{\lambda}) \\ &\quad + (\lambda - \overline{\lambda})^T \mathcal{B}^T(\omega - \overline{\omega}) - \|\nabla_V \mathcal{S}_2\|^2_{T^{-1}} \\ &= -(\omega - \overline{\omega})^T D(\omega - \overline{\omega}) - \|\nabla_V \mathcal{S}_2\|^2_{T^{-1}},\end{aligned} \tag{2.23}$$

where we have exploited the fact that $\mathcal{B}^T\overline{\omega} = \mathbf{0}$, since $\overline{\omega} \in \mathrm{Im}(\mathbb{1})$. As $\dot{\mathcal{S}} \leq \mathbf{0}$ and $(\overline{\eta}, \overline{\omega}, \overline{V})$ is a strict local minimum as a consequence of Assumption 2.2.4, there exists a compact level set Υ around the equilibrium $(\overline{\eta}, \overline{\omega}, \overline{V})$, which is forward invariant. By LaSalle's invariance principle, the solution starting in Υ asymptotically converges to the largest invariant set contained in

$$\Upsilon \cap \{(\eta, \omega, V) : \omega = \overline{\omega}, \|\nabla_V \mathcal{S}_2\| = \mathbf{0}\}. \tag{2.24}$$

Since we have $T\dot{V} = -\nabla_V \mathcal{S}_2$, on such invariant set the system is

$$\begin{aligned}\dot{\eta} &= \mathbf{0} \\ \mathbf{0} &= \overline{u} - D\overline{\omega} - \mathcal{B}\Gamma(V)\sin(\eta) - P_d \\ \mathbf{0} &= -E(\eta)V + \overline{E}_{fd},\end{aligned} \tag{2.25}$$

Since on the invariant set $\dot{\eta} = \dot{\omega} = \dot{V} = \mathbf{0}$, system (2.2) approaches the set of equilibria contained in Υ. Consider a forward invariant set $\Omega \subseteq \Upsilon$ around $(\overline{\eta}, \overline{\omega}, \overline{V})$, where it holds that $\frac{\partial^2 \mathcal{S}}{\partial(\eta,\omega,V)^2} > \mathbf{0}$. As a result any, equilibrium in Ω is Lyapunov stable. It then follows from Lemma 1.4.8 that the solution starting in Ω converges to a point. I.e., we can conclude that the system approaches the set where where $V = \tilde{V}$ and $\eta = \tilde{\eta}$ are constants. Therefore, one can conclude that the system indeed converges to an equilibrium as characterized in Lemma 2.2.1. ■

Remark 2.2.12 (Multiple equilibria)**.** *We cannot claim that $\tilde{\eta} = \overline{\eta}$ and $\tilde{V} = \overline{V}$, since the system could converge to any equilibrium within Υ. This is due to the fact that we have not made any assumptions on the property of the equilibrium $(\overline{\eta}, \overline{\omega}, \overline{V})$ being isolated. In order to establish that the equilibrium is isolated we should ask that the determinant of the Jacobian matrix at the equilibrium is nonsingular, as follows from the inverse function theorem. This is not automatically guaranteed by $(\overline{\eta}, \overline{\omega}, \overline{V})$ being a strict local minimum of the storage function. To better elucidate this claim, first we notice that system (2.2) can be written in*

the form

$$\begin{bmatrix} \dot{\eta} \\ M\dot{\omega} \\ T\dot{V} \end{bmatrix} = \left(\underbrace{\begin{bmatrix} \mathbf{0} & \mathcal{B}^T & \mathbf{0} \\ -\mathcal{B} & \mathbf{0} & \mathbf{0} \\ \mathbf{0} & \mathbf{0} & \mathbf{0} \end{bmatrix} - \begin{bmatrix} \mathbf{0} & \mathbf{0} & \mathbf{0} \\ \mathbf{0} & D & \mathbf{0} \\ \mathbf{0} & \mathbf{0} & I \end{bmatrix}}_{J-R} \right) \underbrace{\begin{bmatrix} I & \mathbf{0} & \mathbf{0} \\ \mathbf{0} & M^{-1} & \mathbf{0} \\ \mathbf{0} & \mathbf{0} & I \end{bmatrix}}_{Q} \nabla\mathcal{S} + \underbrace{\begin{bmatrix} \mathbf{0} \\ I \\ \mathbf{0} \end{bmatrix}}_{g} (u - \overline{u}),$$

where J is a skew-symmetric matrix and R is a diagonal positive semi-definite matrix and

$$\nabla\mathcal{S} = \begin{bmatrix} \Gamma(V)\sin(\eta) - \Gamma(\overline{V})\sin(\overline{\eta}) \\ M(\omega - \overline{\omega}) \\ E(\eta)V - \overline{E}_{fd} \end{bmatrix}. \tag{2.26}$$

Set $u = \overline{u}$. Then LaSalle's invariance principle outlined in the proof above shows that the solution converges to the largest invariant set where $\nabla\mathcal{S}^T(J-R)Q\nabla\mathcal{S} = 0$, that is $\nabla\mathcal{S}^T RQ\nabla\mathcal{S} = 0$. By the structure of R and Q, the latter identity is equal to $\nabla_\omega\mathcal{S} = \mathbf{0}$ (that is, $\omega = \overline{\omega}$) and $\nabla_V\mathcal{S} = \mathbf{0}$. In view of the second equation in (2.6) and of these identities, on this largest invariant set we have $\mathcal{B}(\Gamma(\tilde{V})\sin(\tilde{\eta}) - \Gamma(\overline{V})\sin(\overline{\eta})) = \mathbf{0}$. If $\mathcal{B}$ has full-column rank, that is if the graph is acyclic, then $\Gamma(\tilde{V})\sin(\tilde{\eta}) - \Gamma(\overline{V})\sin(\overline{\eta}) = \mathbf{0}$. This would imply that any point on the invariant set satisfies $\nabla\mathcal{S} = \mathbf{0}$ and it is therefore a critical point for $\mathcal{S}$. Since we have assumed that $(\overline{\eta}, \overline{\omega}, \overline{V})$ is a strict minimum for $\mathcal{S}$ then we could conclude that every trajectory locally converges to $(\overline{\eta}, \overline{\omega}, \overline{V})$. However, in the general case in which the graph is not acyclic, then there could be constant vector $(\tilde{V}, \tilde{\eta}) \neq (\overline{V}, \overline{\eta})$ such that $\mathcal{B}(\Gamma(\tilde{V})\sin(\tilde{\eta}) - \Gamma(\overline{V})\sin(\overline{\eta})) = \mathbf{0}$ (and $E(\tilde{\eta})\tilde{V} - \overline{E}_{fd} = \mathbf{0}$). In this case, convergence can only be guaranteed to an equilibrium $(\tilde{\eta}, \overline{\omega}, \tilde{V})$ characterized in Lemma 2.2.1, as remarked in the result above.

2.3 Minimizing generation costs

Before we address the design of controllers generating u, we discuss a desired optimality property the steady state input $\overline{u}$ should have. This is achieved by realizing that the share of total production each generator has to provide to balance the total electricity demand can be varied. Indeed, from equality (2.7) it can be seen that only the sum of the generators' production is important to characterize the steady state frequency. Generally, different generators have different associated cost functions, such that there is potential to reduce costs when the share of generation among the generators is coordinated in an economically efficient way. In this section we characterize such an optimal generation that minimizes total costs. We consider only the

costs of power generation u, as it is predominant over the excitation and transmission costs. The corresponding network optimization problem we tackle is therefore as follows:

$$\begin{aligned} & \min_u C(u) = \min_u \textstyle\sum_{i\in\mathcal{V}} C_i(u_i) \\ \text{s.t.} \quad & 0 = \mathbb{1}_n^T(u - P_d), \end{aligned} \tag{2.27}$$

where $C_i(u_i)$ is a strictly convex cost function associated to generator i. Comparing the equality constraint to (2.7), it is immediate to see that the solution to (2.27) implies a zero frequency deviation at steady state. The relation of (2.27) with the zero steady state frequency deviation as characterized in (2.6) with $\overline{\omega} = 0$ will be made more explicit at the end of this section. Following standard literature on convex optimization we introduce the Lagrangian function $L(u, \lambda) = C(u) + \lambda \mathbb{1}_n^T (u - P_d)$, where $\lambda \in \mathbb{R}$ is the Lagrange multiplier. Since $C(u)$ is strictly convex we have that $L(u, \lambda)$ is strictly convex in u and concave in λ. Therefore, there exists a saddle point solution to $\max_\lambda \min_u L(u, \lambda)$. Applying first order optimality conditions, the saddle point $(\overline{u}, \overline{\lambda})$ must satisfy

$$\begin{aligned} \nabla C(\overline{u}) + \mathbb{1}_n \overline{\lambda} &= \mathbf{0} \\ \mathbb{1}_n^T(\overline{u} - P_d) &= 0. \end{aligned} \tag{2.28}$$

In the remainder we assume that $C(u)$ is quadratic[1], i.e. $C(u) = \frac{1}{2}u^T Q u = \sum_{i\in\mathcal{N}} \frac{1}{2} q_i u_i^2$, with $q_i > 0$. We make now explicit the solution to the previous set of equations in the case of quadratic cost functions.

Lemma 2.3.1 (Optimal generation)**.** *Let $C(u) = \frac{1}{2}u^T Q u$, with $Q > \mathbf{0}$ and diagonal. There exists a solution $(\overline{u}, \overline{\lambda})$ to (2.28) if and only if the optimal control is*

$$\overline{u} = Q^{-1} \frac{\mathbb{1}_n \mathbb{1}_n^T P_d}{\mathbb{1}_n^T Q^{-1} \mathbb{1}_n}, \tag{2.29}$$

and the optimal Lagrange multiplier is

$$\overline{\lambda} = -\frac{\mathbb{1}_n^T P_d}{\mathbb{1}_n^T Q^{-1} \mathbb{1}_n}. \tag{2.30}$$

Proof. For the considered quadratic cost function, the optimality conditions become

$$\begin{aligned} Q\overline{u} + \mathbb{1}_n \overline{\lambda} &= \mathbf{0} \\ \mathbb{1}_n^T(\overline{u} - P_d) &= 0. \end{aligned} \tag{2.31}$$

Expression (2.29) and (2.30) are obtained by solving 2.31 for $\overline{u}$ and $\overline{\lambda}$. ■

[1] The results hold for linear-quadratic cost functions as well, i.e. $C(u) = \frac{1}{2}u^T Q u + R^T u + \mathbb{1}_n^T s$. In that case $\overline{u} = Q^{-1}(\overline{\theta} - R)$, where $\overline{\theta} = \frac{\mathbb{1}_n \mathbb{1}_n^T (P_d + Q^{-1} R)}{\mathbb{1}_n^T Q^{-1} \mathbb{1}_n} \in \mathrm{Im}(\mathbb{1}_n)$. For the sake of brevity we focus in this chapter on the quadratic case, and explicitly consider the linear and constant components of the cost function in e.g. Chapter 5 and Chapter 6 that also deal with optimal frequency control.

For the optimal control characterized above to guarantee a zero frequency deviation, the equalities (2.6) should now be satisfied with $\overline{u}$ as in (2.29) and $\overline{\omega} = \mathbf{0}$. In this case, the second equality becomes

$$\mathcal{B}\Gamma(\overline{V})\sin(\overline{\eta}) = \Big(Q^{-1}\frac{\mathbb{1}_n\mathbb{1}_n^T}{\mathbb{1}_n^TQ^{-1}\mathbb{1}_n} - I_n\Big)P_d. \tag{2.32}$$

The equality (2.32) shows that an optimal solution may require a nonzero $\mathcal{B}\Gamma(\overline{V})\sin(\overline{\eta})$ at steady state. That implies that at steady state power flows may be exchanged among the control areas in the network and that the local demand P_{di} may not necessarily be all compensated by $\overline{u}_i$. In fact, from (2.29) it is seen that to balance the overall demand $\mathbb{1}^TP_d$ each generator should contribute an amount of power that is inversely proportional to its marginal cost q_i. From (2.29), we also notice that the optimal power generation is independent of the steady state voltage $\overline{V}$. Motivated by Lemma 2.3.1 and the remark that led to (2.32), we introduce the following condition that replaces the previous Assumption 2.2.2:

Assumption 2.3.2. *For a given P_d, there exist $\overline{\eta} \in \mathrm{Im}(\mathcal{B}^T)$, $\overline{V} \in \mathbb{R}^n_{>0}$ and $\overline{E}_{fd} \in \mathbb{R}^n$ for which*

$$\Big(Q^{-1}\frac{\mathbb{1}_n\mathbb{1}_n^T}{\mathbb{1}_n^TQ^{-1}\mathbb{1}_n} - I_n\Big)P_d \in \mathcal{D}, \tag{2.33}$$

with $\mathcal{D}$ defined as in Lemma 2.2.1, is satisfied and $\mathbf{0} = -E(\overline{\eta})\overline{V} + \overline{E}_{fd}$.

We can relate optimization problem (2.27) to another optimization problem in which the zero frequency deviation requirement at steady state is more explicit.

Lemma 2.3.3 (An equivalent optimization problem)**.** *Let Assumption 2.3.2 hold and let $C(u) = \frac{1}{2}u^TQu$, with $Q > 0$ and diagonal. Then the optimal $\overline{u}$ solving (2.27) is equivalent to the optimal $\overline{u}'$ solving*

$$\begin{aligned} & \min_{u,\eta} C(u) = \min_{u,\eta} \textstyle\sum_{i\in\mathcal{V}} C_i(u_i) \\ \text{s.t.} \quad & \mathbf{0} = u - \mathcal{B}\Gamma(\overline{V})\sin(\eta) - P_d \\ & \eta \in \mathrm{Im}(\mathcal{B}^T). \end{aligned} \tag{2.34}$$

Proof. By multiplying both sides of the equality constraint of (2.34) from the left by $\mathbb{1}_n^T$, we obtain the constraint of (2.27). Hence, $\overline{u}'$ satisfies (2.27), and we have $C(\overline{u}) \leq C(\overline{u}')$. By the equality constraint in (2.27), we have $\overline{u} - P_d \in \mathrm{Im}(\mathbb{1}_n)^\perp$. Thus, $\overline{u} - P_d \in \mathrm{Ker}(\mathcal{B}^T)^\perp$ which yields $\overline{u} - P_d \in \mathrm{Im}(\mathcal{B})$. Therefore, $\overline{u} - P_d = \mathcal{B}v$ for some vector v. By the choice $v = \Gamma(\overline{V})\sin(\overline{\eta})$, which exists under Assumption 2.3.2, $\overline{u} - P_d = \mathcal{B}v$ satisfies (2.34) and we have $C(\overline{u}') \leq C(\overline{u})$. Consequently, $C(\overline{u}') = C(\overline{u})$ which results in $\overline{u}' = \overline{u}$ due to the strict convexity of $C(\cdot)$. ■

Lemma 2.3.3 provides insights on how the nonconvex optimization problem (2.34) can be solved for $\overline{u}'$ by (2.27) without the approximation $\sin(\eta) = \eta$ as long as Assumption 2.3.2 holds. This can be seen as an alternative approach to solving for (2.34) by an equivalant 'DC' problem (see e.g. (Dörfler et al. 2016)) where the constraint reads as $\mathbf{0} = u - \mathcal{B}\Gamma(\overline{V})\eta^{DC}$ and requires the graph to be a tree (Dörfler and Bullo 2013). The characterization of $\overline{u}$ in (2.29) will enable the design of controllers regulating the frequency in an optimal manner, which we pursue in the next section. We also remark that even in the case in which P_d is a time-varying signal, the optimal power generation control that guarantees a zero frequency deviation is still given by $\overline{u}$ in (2.29). This property will be used in Section 2.5. Finally, we notice, following (Bürger and De Persis 2015) , that the optimal generation $\overline{u}$ characterized above can be interpreted as the optimal feedfoward control which solves the regulator equations connected with the frequency regulation problem. We will elaborate on this more in the next section.

Remark 2.3.4 (Positivity of the voltages)**.** *It is worth stressing that the explicit request of having $\overline{V} \in \mathbb{R}^n_{>0}$ in Assumptions 2.2.2, 2.2.4 and 2.3.2 is not necessary. As a matter of fact, for any $\overline{V}$ which satisfies $-E(\overline{\eta})\overline{V} + \overline{E}_{fd} = \mathbf{0}$, it trivially holds true that $\overline{V} = E(\overline{\eta})^{-1}\overline{E}_{fd}$. Let $\overline{E}_{fd} \in \mathbb{R}^n_{>0}$. Since $E(\overline{\eta})$ has all the off-diagonal entries non-positive, then it is inverse-positive ((Plemmons 1977), Theorem 1, F_{15}), i.e. each entry of the inverse $E(\overline{\eta})^{-1}$ is non-negative. Furthermore, since $E(\overline{\eta})^{-1}$ is invertible, each row has at least one strictly positive entry. Therefore, the product $\overline{V} = E(\overline{\eta})^{-1}\overline{E}_{fd}$ must necessarily return a vector with all strictly positive entries.*

2.4 Economic efficiency in the presence of constant power demand

Corollary 2.2.11 shows attractivity of the steady state solution under a constant imbalance vector $u - P_d$, which generally results in a nonzero steady state frequency deviation. In this section we consider the problem of designing the generation u in such a way that at steady state the system achieves a zero frequency deviation. We adopt the framework provided in (Bürger and De Persis 2015) This framework provides a constructive and straightforward procedure to the design of the frequency regulator. We start the analysis by reminding that Theorem 2.2.9 states the incre-

mental passivity property of the system

$$\begin{array}{rcl} \dot{\eta} & = & \mathcal{B}^T\omega \\ M\dot{\omega} & = & u - D\omega - \mathcal{B}\Gamma\sin(\eta) - P_d \\ T\dot{V} & = & -E(\eta)V + \overline{E}_{fd} \\ y & = & \omega. \end{array} \tag{2.35}$$

The incremental passivity property holds with respect to two solutions of (2.35). As one of the two solutions, we adopt here a solution to the *regulator equations* (2.36) below. This is the state $(\overline{\eta}, \overline{\omega}, \overline{V})$, the feedforward input $\overline{u}$ and the output $\overline{y} = \overline{\omega} = \mathbf{0}$ such that

$$\begin{array}{rcl} \dot{\overline{\eta}} & = & \mathcal{B}^T\overline{\omega} \;=\; \mathbf{0} \\ \mathbf{0} & = & \overline{u} - \mathcal{B}\Gamma(\overline{V})\sin(\overline{\eta}) - P_d \\ \mathbf{0} & = & -E(\overline{\eta})\overline{V} + \overline{E}_{fd} \\ \overline{y} & = & \overline{\omega} \;=\; \mathbf{0}. \end{array} \tag{2.36}$$

Among the many possible choices, we focus on the steady state solution that arises from the solution of the optimal control problem in the previous section, namely

$$\overline{u} = Q^{-1}\frac{\mathbb{1}_n\mathbb{1}_n^T P_d}{\mathbb{1}_n^T Q^{-1}\mathbb{1}_n}, \tag{2.37}$$

characterized in (2.29) above, and $\overline{\eta}$ such that

$$\mathcal{B}\Gamma(\overline{V})\sin(\overline{\eta}) = \Big(Q^{-1}\frac{\mathbb{1}_n\mathbb{1}_n^T}{\mathbb{1}_n^T Q^{-1}\mathbb{1}_n} - I_n\Big)P_d. \tag{2.38}$$

The framework presented in (Bürger and De Persis 2015) prescribes to design an incrementally passive feedback controller that is able to generate the feedforward input (2.37). The interconnection of the process (2.35) and of the incrementally feedback controller to be introduced below yields a closed-loop system whose solutions asymptotically converge to the desired steady state solution. This idea is made precise in the theorem below, that is the main result of the section and where we propose a dynamic controller that converges asymptotically to the optimal feedforward input that guarantees zero frequency deviation. The result deals with constant power demand, the extension to time-varying power demands being postponed to a later section. As will become clear it is essential that the controllers exchange information, leading to the following assumption.

Assumption 2.4.1 (Communication graph)**.** *The undirected graph reflecting the topology of information exchange among the nodes is connected.*

Theorem 2.4.2 (Optimal regulation in the presence of constant unknown demand)**.** *Consider the system (2.35) with constant power demand P_d and let Assumptions 2.2.4, 2.3.2 and 2.4.1 hold. Then controllers at the nodes*[2]

$$\begin{aligned} \dot{\theta}_i &= \textstyle\sum_{j\in\mathcal{N}_i^{comm}}(\theta_j-\theta_i) - q_i^{-1}\omega_i \\ u_i &= q_i^{-1}\theta_i, \end{aligned} \tag{2.39}$$

for $i \in \mathcal{V}$, where $\mathcal{N}_i^{comm}$ denotes the set of neighbors of node i in a graph describing the exchange of information among the controllers, guarantee the solutions to the closed-loop system that start in a neighborhood of $(\overline{\eta},\overline{\omega},\overline{V},\overline{\theta})$ to converge asymptotically to the largest invariant set where $\omega_i = 0$ for all $i \in \mathcal{V}$, $\|\nabla_V \mathcal{S}_2\| = 0$, and $\theta = \overline{\theta}$, $\overline{\theta}$ being the vector

$$\overline{\theta} = \frac{\mathbb{1}_n \mathbb{1}_n^T P_d}{\mathbb{1}_n^T Q^{-1} \mathbb{1}_n}, \tag{2.40}$$

such that $\overline{u} = Q^{-1}\overline{\theta}$ satisfies

$$\begin{aligned} \dot{\tilde{\eta}} &= \mathbf{0} \\ \mathbf{0} &= \overline{u} - \mathcal{B}\Gamma(\tilde{V})\sin(\tilde{\eta}) - P_d \\ \mathbf{0} &= -E(\tilde{\eta})\tilde{V} + \overline{E}_{fd} \\ y &= \mathbf{0}. \end{aligned} \tag{2.41}$$

Proof. Bearing in mind Theorem 2.2.9, one can notice that the incremental storage function $\mathcal{S}(\omega,\overline{\omega},\eta,\overline{\eta},V,\overline{V}) = \mathcal{S}_1(\omega,\overline{\omega}) + \mathcal{S}_2(\eta,\overline{\eta},V,\overline{V})$ satisfies $\dot{\mathcal{S}} = -(\omega-\overline{\omega})^T D(\omega-\overline{\omega}) - \|\nabla_V \mathcal{S}_2\|^2_{T^{-1}} + (\omega-\overline{\omega})^T(u-\overline{u})$, thus showing that the system is output strictly incrementally passive. This equality holds in particular for $\overline{\omega} = \mathbf{0}$, $\overline{u}$ given in (2.29) and $\overline{\eta}, \overline{V}$ as in Assumption 2.3.2. The internal model principle design pursued in (Bürger and De Persis 2015) and (Bürger and De Persis 2013) prescribes the design of a controller able to generate the feedforward input $\overline{u}$. To this purpose, we introduce the overall controller

$$\begin{aligned} \dot{\theta} &= -\mathcal{L}^{com}\theta + \overline{H}^T v \\ u &= \overline{H}\theta, \end{aligned} \tag{2.42}$$

where $\theta \in \mathbb{R}^n$, $\mathcal{L}^{com}$ the Laplacian associated with a graph that describes the exchange of information among the controllers, and with the term $\overline{H}^T v$ needed to guarantee the incremental passivity property of the controller Here, $v \in \mathbb{R}^n$ is an extra control input to be designed later, while $\overline{H} = \overline{H}^T = Q^{-1}$. If $v = \mathbf{0}$ and $\overline{\theta}(0) = \frac{\mathbb{1}_n \mathbb{1}_n^T P_d}{\mathbb{1}_n^T Q^{-1}\mathbb{1}_n}$, then $\overline{\theta}(t) := \overline{\theta}(0)$ satisfies the differential equation in (2.42) and

[2] For linear-quadratic cost functions the controller output becomes $u_i = q_i^{-1}(\theta_i - r_i)$.

moreover the corresponding output $\overline{H}\,\overline{\theta}(t)$ is identically equal to the feedforward input $\overline{u}(t)$ defined in (2.29), provided that $\overline{H} = Q^{-1}$. More explicitly, we have

$$\begin{aligned} \dot{\overline{\theta}} &= -\mathcal{L}^{com}\overline{\theta} \\ \overline{u} &= \overline{H}\,\overline{\theta}. \end{aligned} \tag{2.43}$$

Notice that this is a manifestation of the internal model principle, that is the ability of the controller to generate, in open-loop and when properly initialized, the prescribed feedforward input. Consider now the incremental storage function $\Theta(\theta, \overline{\theta}) = \frac{1}{2}(\theta - \overline{\theta})^T(\theta - \overline{\theta})$. It satisfies

$$\begin{aligned} \dot{\Theta}(\theta, \overline{\theta}) &= (\theta - \overline{\theta})^T(-\mathcal{L}^{com}\theta + \overline{H}^T v + \mathcal{L}^{com}\overline{\theta}) \\ &= -(\theta - \overline{\theta})^T\mathcal{L}^{com}(\theta - \overline{\theta}) + (\theta - \overline{\theta})^T\overline{H}^T v \\ &= -(\theta - \overline{\theta})^T\mathcal{L}^{com}(\theta - \overline{\theta}) + (u - \overline{u})^T v. \end{aligned} \tag{2.44}$$

We now interconnect the third-order model (2.35) and the controller (2.42), obtaining

$$\begin{aligned} \dot{\eta} &= \mathcal{B}^T\omega \\ M\dot{\omega} &= \overline{H}\theta - \mathcal{B}\Gamma(V)\sin(\eta) - D\omega - P_d \\ T\dot{V} &= -E(\eta)V + \overline{E}_{fd} \\ \dot{\theta} &= -\mathcal{L}^{com}\theta + \overline{H}^T v \\ y &= \omega. \end{aligned} \tag{2.45}$$

Observe that the quadruple $(\overline{\eta}, \overline{\omega}, \overline{V}, \overline{\theta})$ is a solution to the closed-loop system just defined when $v = \mathbf{0}$. Consider the incremental storage function

$$Z(\eta, \overline{\eta}, \omega, \overline{\omega}, V, \overline{V}, \theta, \overline{\theta}) = \mathcal{S}(\eta, \overline{\eta}, \omega, \overline{\omega}, V, \overline{V}) + \Theta(\theta, \overline{\theta}), \tag{2.46}$$

where $(\overline{\eta}, \overline{V})$ fulfills Assumption 2.2.4. Following the arguments of Lemma 2.2.6, it is immediate to see that under condition (2.14) we have that $\nabla Z|_{\eta=\overline{\eta},\omega=\overline{\omega},V=\overline{V},\theta=\overline{\theta}} = \mathbf{0}$ and $\nabla^2 Z|_{\eta=\overline{\eta},\omega=\overline{\omega},V=\overline{V},\theta=\overline{\theta}} > \mathbf{0}$, such that Z has a strict local minimum at $(\overline{\eta}, \overline{\omega}, \overline{V}, \overline{\theta})$. It turns out that

$$\begin{aligned} \dot{Z} = &-(\omega - \overline{\omega})^T D(\omega - \overline{\omega}) - \|\nabla_V \mathcal{S}_2\|^2_{T^{-1}} \\ &+ (\omega - \overline{\omega})^T(u - \overline{u}) - (\theta - \overline{\theta})^T\mathcal{L}^{com}(\theta - \overline{\theta}) \\ &+ (u - \overline{u})^T v. \end{aligned} \tag{2.47}$$

As we are still free to design v, the choice $v = -(\omega - \overline{\omega}) = -\omega$ returns

$$\begin{aligned} \dot{Z} = &-(\omega - \overline{\omega})^T D(\omega - \overline{\omega}) - \|\nabla_V \mathcal{S}_2\|^2_{T^{-1}} \\ &-(\theta - \overline{\theta})^T\mathcal{L}^{com}(\theta - \overline{\theta}) \leq 0. \end{aligned} \tag{2.48}$$

As $\dot{Z} \leq 0$, there exists a compact level set Υ around the equilibrium $(\overline{\eta}, \overline{\omega}, \overline{V}, \overline{\theta})$ which is forward invariant. By LaSalle's invariance principle the solution starting in Υ asymptotically converges to the largest invariant set contained in $\Upsilon \cap \{(\eta, \omega, V, \theta) : \omega = \overline{\omega} = \mathbf{0}, \|\nabla_V \mathcal{S}_2\| = 0, \theta = \overline{\theta} + \mathbb{1}_n \alpha\}$, where $\alpha : \mathbb{R}_{\geq 0} \to \mathbb{R}$ is a function and $\theta = \overline{\theta} + \mathbb{1}_n \alpha$ follows from the communication graph being connected, i.e. $\mathrm{Ker}(\mathcal{L}^{com}) = \mathrm{Im}(\mathbb{1}_n)$. On such invariant set the system is

$$\begin{aligned} \dot{\eta} &= \mathcal{B}^T \overline{\omega} = \mathbf{0} \\ \mathbf{0} &= -\mathcal{B}(\Gamma(V)\sin(\eta) - \Gamma(\overline{V})\sin(\overline{\eta})) - \overline{H}\mathbb{1}_n \alpha \\ \mathbf{0} &= -E(\eta)V + \overline{E}_{fd} \\ \dot{\overline{\theta}} + \mathbb{1}_n \dot{\alpha} &= -\mathcal{L}^{com}(\overline{\theta} + \mathbb{1}_n \alpha). \end{aligned} \tag{2.49}$$

In the second equality above, we have exploited the identity $\mathbf{0} = \overline{H\theta} - \mathcal{B}\Gamma(\overline{V})\sin(\overline{\eta}) - D\overline{\omega} - P_d$. Bearing in mind that $\overline{H} = Q^{-1}$, it follows that necessarily $\alpha = 0$ (it is sufficient to multiply both sides of the second line in (2.49) by $\mathbb{1}_n^T$). Hence on the invariant set $\theta = \overline{\theta}$ and the output of the controller is $\overline{H\theta}$ which equals the optimal feedforward input (2.37). We conclude that the dynamical controller guarantees asymptotic regulation to zero of the frequency deviation and convergence to the optimal feedforward input. Furthermore, we can similarly as in the proof of Corollary 2.2.11, conclude that solutions to the closed-loop system that start in a neighborhood of $(\overline{\eta}, \overline{\omega}, \overline{V}, \overline{\theta})$ converge to a constant vector. ■

The interpretation of the theorem is straightforward: it shows that the dynamic controllers based on an internal model design synchronize to a steady state solution of the exosystem that generates the feedforward input that minimizes generation costs and is able to guarantee a zero frequency deviation. These controllers must be initialized in the vicinity of $\overline{\theta}$ which represents a nominal estimate of the total demand. Starting from this initial guess, the controllers adjust the power production depending on the frequency deviation which in turn depends on *actual* (and *unmeasured*) demand.

2.5 Frequency regulation in the presence of time-varying power demand

Until now we assumed that the power demand term P_d is unknown but constant, as is a standard practice in current research. Future smart grids should however be able to cope with rapid fluctuations of the power demand at the same timescale as the dynamics describing the physical infrastructure, such that approximating the

power demand by a constant can become unrealistic. This asks for controllers able to deal with time-varying power demand. In the previous section we studied within the framework of (Bürger and De Persis 2015) dynamical controllers able to achieve zero frequency deviation with steady state optimal production in the presence of constant power demand. Since the framework lends itself to deal with time-varying disturbances, it is natural to wonder whether the approach can be used to design frequency regulators in the presence of time-varying power demand. This is investigated in this section.

Although the power demand is not known, we will assume that it is the output of a known exosystem, as it is customary in output regulation theory. Let P_d depend linearly on σ, namely, let

$$P_d = \Pi\sigma, \tag{2.50}$$

for some matrix Π, where σ is the state variable of the exosystem

$$\dot{\sigma} = s(\sigma). \tag{2.51}$$

Here the map s is assumed to satisfy the incremental passivity property $(s(\sigma) - s(\sigma'))^T(\sigma - \sigma') \leq 0$ for all σ, σ'. It will be useful to limit ourselves to the case $s(\sigma) = S\sigma$, with S a skew-symmetric matrix. In this case, the exosystem (2.50), (2.51) generates linear combinations of constant and sinusoidal signals. We will however continue to refer to $s(\sigma)$ for the sake of generality, using explicitly $S\sigma$ only when needed. The choice (2.51) is further motivated by spectral decomposition of load patterns (Aguirre et al. 2008), ocean wave energy (Falnes 2007) and wind energy (Van der Hoven 1957), (Milan et al. 2013) that indicate that the net load can indeed be approximated by a superposition of a constant and a few sinusoidal signals. More explicit, we model the power demand P_{di} as a superposition of a constant power demand ($\Pi_{1i}\sigma_1$), a periodic power demand that can be compensated optimally ($\Pi_{2i}\sigma_2(t)$) and a periodic power demand that cannot be compensated optimally ($\Pi_{3i}\sigma_{3i}(t)$), such that $P_{di}(t) = \Pi_{1i}\sigma_1 + \Pi_{2i}\sigma_2(t) + \Pi_{3i}\sigma_{3i}(t)$. The reason why we distinguish between $\Pi_{2i}\sigma_2$ and $\Pi_{3i}\sigma_{3i}$ becomes evident in the next subsection. Similarly, we write the steady state input as a sum of its components, $\overline{u}_i(t) = \overline{u}_{1i} + \overline{u}_{2i}(t) + \overline{u}_{3i}(t)$. The explicit dependency on time will be dropped in the remainder and was added here to stress the differences between constant and time-varying signals.

Example 2.5.1 (Exosystem)**.** *Consider the case of a periodic power demand with frequency μ superimposed to a constant power demand. This demand can be modeled as $P_{di} = \Pi_{1i}\sigma_1 +$*

$\Pi_{2i}\sigma_2$ *where* $\dot{\sigma} = S\sigma$ *with*

$$S = \begin{bmatrix} 0 & \mathbf{0}_{1\times 2} \\ \mathbf{0}_{2\times 1} & S_2 \end{bmatrix} = \begin{bmatrix} 0 & 0 & 0 \\ 0 & 0 & \mu \\ 0 & -\mu & 0 \end{bmatrix}, \tag{2.52}$$

Π_{1i} *is a real number and* $\Pi_{2i} = q_i^{-1}[1\ 0] = q_i^{-1}R_2$. *In this case* $R_2 = [1\ \ 0]$ *and notice that the pair* (R_2, S_2) *is observable.*

2.5.1 Economically efficient frequency regulation in the presence of a class of time-varying power demand

We focus in this subsection on the case in which the power demand at each node has the form $P_{di} = \Pi_{1i}\sigma_1 + \Pi_{2i}\sigma_2$, where σ_1, σ_2 will be specified below. At steady state we have that $\dot{\eta} = \mathbf{0}$, $\dot{V} = \mathbf{0}$ and therefore power flows between different control areas need to be constant. This observation restricts the class of time-varying power demand that can be compensated for by an optimal generation u. We will make this more specific. Recall that the optimal power generation at steady state is given by

$$\overline{u} = Q^{-1}\frac{\mathbb{1}_n\mathbb{1}_n^T P_d}{\mathbb{1}_n^T Q^{-1}\mathbb{1}_n}, \tag{2.53}$$

characterized in (2.29) above. In this case, the second equality in (2.36) writes as in (2.32)

$$\mathcal{B}\Gamma(\overline{V})\sin(\overline{\eta}) = \Big(Q^{-1}\frac{\mathbb{1}_n\mathbb{1}_n^T}{\mathbb{1}_n^T Q^{-1}\mathbb{1}_n} - I_n\Big)P_d. \tag{2.54}$$

This implies that the quantity on the right-hand side must be constant and that there must exist a vector $\overline{\eta} \in \mathrm{Im}(\mathcal{B}^T)$ which satisfies the equality. If we differentiate in the disturbance term $\Pi\sigma$ between a constant component $\Pi_1\sigma_1$ and a time-varying component $\Pi_2\sigma_2$, i.e. $\Pi\sigma = \Pi_1\sigma_1 + \Pi_2\sigma_2$, and there exists a solution to the identity (2.54) when $\Pi\sigma$ is replaced by $\Pi_1\sigma_1$, then such a solution continues to exist provided that the time-varying component of $\Pi\sigma$ belongs to the null space of $(Q^{-1}\frac{\mathbb{1}_n\mathbb{1}_n^T}{\mathbb{1}_n^T Q^{-1}\mathbb{1}_n} - I_n)$. The null space above can be easily characterized.

Lemma 2.5.2 (Nullspace)**.** *The null space of* $(Q^{-1}\frac{\mathbb{1}_n\mathbb{1}_n^T}{\mathbb{1}_n^T Q^{-1}\mathbb{1}_n} - I_n)$ *is given by* $\mathrm{Im}(Q^{-1}\mathbb{1}_n)$.

Proof. First consider the matrix $-\mathbb{1}_n^T Q^{-1}\mathbb{1}_n \cdot (Q^{-1}\frac{\mathbb{1}_n\mathbb{1}_n^T}{\mathbb{1}_n^T Q^{-1}\mathbb{1}_n} - I_n)$, which takes the

expression

$$L^T = \begin{bmatrix} L_{11}^T & -q_1^{-1} & \dots & -q_1^{-1} \\ -q_2^{-1} & L_{22}^T & \dots & -q_2^{-1} \\ \vdots & \vdots & \vdots & \vdots \\ -q_n^{-1} & -q_n^{-1} & \dots & L_{nn}^T \end{bmatrix}, \tag{2.55}$$

where $L_{ii}^T = (\sum_{j \in \mathcal{V} \setminus \{i\}} q_j^{-1})$. Hence, L is the Laplacian matrix of a weighted complete graph. The rank of the Laplacian matrix of a connected graph is $n-1$. Thus the rank of the matrix L^T is also $n-1$. Since the rank of a matrix is not altered by the multiplication by a nonzero constant, one infers that the matrix $(Q^{-1}\frac{\mathbb{1}_n\mathbb{1}_n^T}{\mathbb{1}_n^TQ^{-1}\mathbb{1}_n} - I_n)$ has rank $n-1$ as well. Thus its null space has dimension 1. Now, it is easily checked that the range of $Q^{-1}\mathbb{1}_n$ is included in the null space of $(Q^{-1}\frac{\mathbb{1}_n\mathbb{1}_n^T}{\mathbb{1}_n^TQ^{-1}\mathbb{1}_n} - I_n)$. ■

From Lemma 2.5.2 it follows that the time varying component $\Pi_2\sigma_2$ of the unknown demand must satisfy $\Pi_2\sigma_2 \in \mathrm{Im}(Q^{-1}\mathbb{1}_n)$. This leads to the following model for the power demand

$$\begin{aligned} \dot{\sigma}_1 &= 0 \\ \dot{\sigma}_2 &= s_2(\sigma_2) \\ P_d &= \Pi_1\sigma_1 + Q^{-1}\mathbb{1}_nR_2\sigma_2, \end{aligned} \tag{2.56}$$

where Π_1 is a diagonal matrix, R_2 is some suitable row vector such that the pair (R_2, S_2) is observable and that $Q^{-1}\mathbb{1}_nR_2\sigma_2$ generates the desired time-varying component of the power demand. Notice that the frequencies of the sinusoidal modes in the power demand have to be the same for all nodes. As a result, if we consider the contribution of the time-varying component of the disturbance to the optimal steady-state controller, it must be true that

$$\overline{u}_2 = Q^{-1}\frac{\mathbb{1}_n\mathbb{1}_n^T\Pi_2\sigma_2}{\mathbb{1}_n^TQ^{-1}\mathbb{1}_n} = Q^{-1}\mathbb{1}_nR_2\sigma_2, \tag{2.57}$$

where we have exploited the identity $\Pi_2\sigma_2 = Q^{-1}\mathbb{1}_nR_2\sigma_2$. This identity will also be used later in this section. This characterization points out that, for the existence of a steady state solution with a zero frequency deviation in the presence of time-varying demand, the exchange of power among the different areas must be constant at steady state and this requires that the intensity of the power demand at one aggregate area should be inversely proportional to the power production cost at the same area. We stress that this is not a limitation of the approach pursued, but rather a constraint imposed by the model of the power network and the optimal zero frequency regulation problem. We are now ready to state the main result of this section:

Theorem 2.5.3 (Optimal regulation in the presence of a class of varying demand)**.** *Let Assumptions 2.2.4, 2.3.2 and 2.4.1 hold and suppose that there exists a solution to the regulator equations (2.36) with P_d as in* (2.56)*. Then, given the system (2.35), with exogenous power demand P_d generated by* (2.56)*, with $s_2(\sigma_2) = S_2\sigma_2$, S_2 skew-symmetric and with purely imaginary eigenvalues*[3]*, and (R_2, S_2) an observable pair, the controllers at the nodes*

$$\begin{aligned} \dot{\theta}_{1i} &= \textstyle\sum_{j\in\mathcal{N}_i^{comm}}(\theta_{1j} - \theta_{1i}) - q_i^{-1}\omega_i \\ \dot{\theta}_{2i} &= S_2\theta_{2i} - q_i^{-1}R_2^T\omega_i \\ u_i &= q_i^{-1}\theta_{1i} + q_i^{-1}R_2\theta_{2i}, \end{aligned} \tag{2.58}$$

for all $i = 1, 2, \dots, n$, guarantee the solutions to the closed-loop system that start in a neighborhood of $(\overline{\eta}, \overline{\omega}, \overline{V}, \overline{\theta})$ to converge asymptotically to the largest invariant set where $\omega_i = 0$ for all $i \in \mathcal{V}$, $\|\nabla_V \mathcal{S}_2\| = 0$ and $u = \overline{u}$, with $\overline{u}$ the optimal feedforward input.

Proof. We follow the proof of Theorem 2.4.2 *mutatis mutandis*. For the sake of generality we continue to use $s_2(\sigma_2)$ instead of $S_2\sigma_2$, referring to the latter only for those passages in the proof where the linearity of the map s_2 simplifies the analysis. We consider controllers at the nodes of the form (2.58) where the first term of u_i is inspired by the analogous term in the case of constant power demand (see Theorem 2.4.2) while the second term is suggested by (2.57). In stacked form, with $\omega = \mathbf{0}$, the controllers write as

$$\begin{aligned} \dot{\theta}_1 &= -\mathcal{L}^{com}\theta_1 \\ \dot{\theta}_2 &= \overline{s}_2(\theta_2) \\ u &= Q^{-1}\theta_1 + Q^{-1}(I_n \otimes R_2)\theta_2, \end{aligned}$$

where $\overline{s}_2(\theta) = (s_2(\theta_{21})^T \dots s_2(\theta_{2n})^T)^T$, $s_2(\cdot)$ is the subvector of $s(\cdot)$ that generates the time-varying component of σ and $\theta_2 = (\theta_{21}^T \dots \theta_{2n}^T)^T$.[4] Under appropriate initialization, the system above generates the optimal feedforward input $\overline{u}$. In fact, if $\overline{\theta}_1(0) = \frac{\mathbb{1}_n \mathbb{1}_n^T \Pi_1 \sigma_1(0)}{\mathbb{1}_n^T Q^{-1} \mathbb{1}_n}$, $\overline{\theta}_2(0) = \mathbb{1}_n \otimes \sigma_2(0)$, then $Q^{-1}\overline{\theta}_1 + Q^{-1}(I_n \otimes R_2)\overline{\theta}_2$, where $\overline{\theta}_1, \overline{\theta}_2$ satisfy

$$\begin{aligned} \mathbf{0} &= -\mathcal{L}^{com}\overline{\theta}_1 \\ \dot{\overline{\theta}}_2 &= \overline{s}_2(\overline{\theta}_2), \end{aligned}$$

coincides with $\overline{u}$ defined in (2.53). Following (Bürger and De Persis 2015) , the stabilizing inputs v_1 and v_2 are introduced in the controller above to make it incrementally passive. We obtain

$$\begin{aligned} \dot{\theta}_1 &= -\mathcal{L}^{com}\theta_1 + Q^{-1}v_1 \\ \dot{\theta}_2 &= \overline{s}_2(\theta_2) + (I_n \otimes R_2^T)Q^{-1}v_2 \\ u &= Q^{-1}\theta_1 + Q^{-1}(I_n \otimes R_2)\theta_2. \end{aligned} \tag{2.59}$$

[3] The zero does not belong to the spectrum of S_2.

[4] In the case $s_2(\theta_n) = S_2\theta_n$, we have $\overline{s}_2(\theta) = (I_n \otimes S_2)\theta_2$.

The incremental storage function

$$\Theta(\theta,\overline{\theta}) = \frac{1}{2}(\theta_1-\overline{\theta}_1)^T(\theta_1-\overline{\theta}_1) + \frac{1}{2}(\theta_2-\overline{\theta}_2)^T(\theta_2-\overline{\theta}_2)$$

satisfies

$$\begin{aligned}\dot{\Theta}(\theta,\overline{\theta}) &= -(\theta_1-\overline{\theta}_1)\mathcal{L}^{com}(\theta_1-\overline{\theta}_1)^T \\ &\quad +(\theta_1-\overline{\theta}_1)Q^{-1}v_1 \\ &\quad +(\theta_2-\overline{\theta}_2)^T(\overline{s}_2(\theta_2)-\overline{s}_2(\overline{\theta}_2)) \\ &\quad +(\theta_2-\overline{\theta}_2)^T(I_n\otimes R_2^T)Q^{-1}v_2.\end{aligned}$$

Consider the incremental storage function

$$Z(\eta,\overline{\eta},\omega,\overline{\omega},V,\overline{V},\theta,\overline{\theta}) = \mathcal{S}(\eta,\overline{\eta},\omega,\overline{\omega},V,\overline{V}) + \Theta(\theta,\overline{\theta}), \tag{2.60}$$

where $(\overline{\eta},\overline{V})$ fulfills Assumption 2.2.4. Following the arguments of Lemma 2.2.6, it is immediate to see that under condition (2.14) we have that $\nabla Z|_{\eta=\overline{\eta},\omega=\overline{\omega},V=\overline{V},\theta=\overline{\theta}} = \mathbf{0}$ and $\nabla^2 Z|_{\eta=\overline{\eta},\omega=\overline{\omega},V=\overline{V},\theta=\overline{\theta}} > \mathbf{0}$, such that Z has a strict local minimum at $(\overline{\eta},\overline{\omega},\overline{V},\overline{\theta})$. Under the stabilizing feedback $v_1 = -(\omega-\overline{\omega})$, $v_2 = -(\omega-\overline{\omega})$, the function $Z(\omega,\overline{\omega},\eta,\overline{\eta},V,\overline{V},\theta,\overline{\theta}) = \mathcal{S}(\omega,\overline{\omega},\eta,\overline{\eta},V,\overline{V}) + \Theta(\theta,\overline{\theta})$ along the solutions to

$$\begin{aligned}\dot{\eta} &= D^T\omega \\ \dot{\overline{\eta}} &= \mathbf{0} \\ M\dot{\omega} &= -D\omega - \mathcal{B}(\Gamma(V)\sin(\eta) - \Gamma(\overline{V})\sin(\overline{\eta})) \\ &\quad +Q^{-1}(\theta_1-\overline{\theta}_1) + Q^{-1}(I_n\otimes R_2)(\theta_2-\overline{\theta}_2) \\ \dot{\overline{\omega}} &= \mathbf{0} \\ T\dot{V} &= -E(\eta)V + \overline{E}_{fd} \\ \dot{\overline{V}} &= \mathbf{0} \\ \dot{\theta}_1 &= -\mathcal{L}^{com}\theta_1 - Q^{-1}\omega \\ \dot{\overline{\theta}}_1 &= \mathbf{0} \\ \dot{\theta}_2 &= \overline{s}_2(\theta_2) - (I_n\otimes R_2^T)Q^{-1}\omega \\ \dot{\overline{\theta}}_2 &= \overline{s}_2(\overline{\theta}_2)\end{aligned}$$

satisfies

$$\begin{aligned}\dot{Z} &= -(\omega-\overline{\omega})^T D(\omega-\overline{\omega}) - \|\nabla_V\mathcal{S}_2\|^2_{T^{-1}} \\ &\quad -(\theta_1-\overline{\theta}_1)^T\mathcal{L}^{com}(\theta_1-\overline{\theta}_1),\end{aligned}$$

where we have exploited the identities

$$\begin{aligned}u_1-\overline{u}_1 &= Q^{-1}(\theta_1-\overline{\theta}_1) \\ u_2-\overline{u}_2 &= Q^{-1}(I_n\otimes R_2)(\theta_2-\overline{\theta}_2).\end{aligned}$$

As $\dot{Z}\leq 0$, one infers convergence to the largest invariant set of points where $\omega=\mathbf{0}$, $\|\nabla_V\mathcal{S}_2\|=\mathbf{0}$, $\theta_1=\overline{\theta}_1+\mathbb{1}_n\alpha$, where $\alpha:\mathbb{R}_{\geq 0}\to\mathbb{R}$ is a function. On the invariant set the dynamics take the form

$$\begin{aligned}
\dot{\eta} &= \mathbf{0} \\
\mathbf{0} &= -\mathcal{B}(\Gamma(V)\sin(\eta) - \Gamma(\overline{V})\sin(\overline{\eta})) \\
&\quad +Q^{-1}\mathbb{1}_n\alpha + Q^{-1}(I_n \otimes R_2)(\theta_2 - \overline{\theta}_2) \\
\mathbf{0} &= -E(\eta)V + \overline{E}_{fd} \\
\dot{\overline{\theta}}_1 + \mathbb{1}_n\dot{\alpha} &= -\mathcal{L}^{com}(\overline{\theta}_1 + \mathbb{1}_n\alpha) \\
\dot{\theta}_2 - \dot{\overline{\theta}}_2 &= \overline{s}_2(\theta_2 - \overline{\theta}_2),
\end{aligned} \tag{2.61}$$

From the fourth line in (2.61) we infer that α is a constant. The second line with $\eta = \tilde{\eta}$ then implies that $q_i^{-1}R_2(\theta_{2i} - \overline{\theta}_{2i}) = c_i$ is a constant as well. Since the term $R_2(\theta_{2i} - \overline{\theta}_{2i})$ contains only sinusoidal modes, necessarily $c_i = 0$ and from the pair (R_2, S_2) being observable it follows that $\theta_{2i} = \overline{\theta}_{2i}$. Equal to the proof of Theorem 2.4.2, pre-multiplying the second line in (2.61) by $\mathbb{1}_n^T$ shows that $\alpha = 0$ and therefore that $\theta_1 = \overline{\theta}_1$. We can now conclude that $u_1 = \overline{u}_1$ and $u_2 = \overline{u}_2$, that is the input u converges to the optimal (time-varying) feedforward input, as claimed. ■

2.5.2 Frequency regulation in the presence of a wider class of time-varying power demand

We continue the previous subsection by considering frequency regulation in the case the power demand is generated by the exosystem

$$\begin{aligned}
\dot{\sigma}_1 &= 0 \\
\dot{\sigma}_2 &= s_2(\sigma_2) \\
\dot{\sigma}_3 &= \overline{s}_3(\sigma_3) \\
P_d &= \Pi_1\sigma_1 + Q^{-1}\mathbb{1}_n R_2\sigma_2 + \overline{R}_3\sigma_3,
\end{aligned} \tag{2.62}$$

where additionally to (2.56) we have $\overline{s}_3(\theta) = (s_{31}(\theta_{31})^T \dots s_{3n}(\theta_{3n})^T)^T$ and $\overline{R}_3 = \text{block.diag}(R_{31}, \dots, R_{3n})$. Notice that $s_{3i}(\theta_{3i})$ and R_{3i} can now vary from node to node. As shown in the previous subsection $\overline{u}$ cannot satisfy (2.53) any longer due to the presence of σ_3. However, compensating for σ_3 is still a meaningful control task, for otherwise the frequency deviation would not converge to zero any longer. Furthermore, for those cases for which the component $\Pi_1\sigma_1 + Q^{-1}\mathbb{1}_n R_2\sigma_2$ is much greater in magnitude than $\overline{R}_3\sigma_3$, $\overline{u}$ will satisfy (2.53) approximately. In order to regulate the frequency deviation to zero when the power demand is generated by (2.62) we propose controllers inspired by the previous subsection and we adjust the proof of Theorem 2.5.3 accordingly.

Corollary 2.5.4 (Regulation in the presence of varying demand)**.** *Let Assumptions 2.2.4, 2.3.2 and 2.4.1 hold and suppose that there exists a solution to the regulator equations (2.36) with P_d as in* (2.62)*. Then, given the system (2.35), with exogenous power demand P_d*

generated by (2.62), $s_k(\sigma_k) = S_k\sigma_k$, S_k *skew-symmetric and with purely imaginary eigenvalues for* $k = 2, 3$, *and* $((R_2\ R_{3i}), \textit{block.diag}(S_2, S_{3i}))$ *an observable pair, the controllers at the nodes*

$$\begin{aligned} \dot{\theta}_{1i} &= \textstyle\sum_{j\in\mathcal{N}_i^{comm}}(\theta_{1j} - \theta_{1i}) - q_i^{-1}\omega_i \\ \dot{\theta}_{2i} &= S_2\theta_{2i} - q_i^{-1}R_2^T\omega_i \\ \dot{\theta}_{3i} &= S_{3i}\theta_{3i} - R_{3i}^T\omega_i \\ u_i &= q_i^{-1}\theta_{1i} + q_i^{-1}R_2\theta_{2i} + R_{3i}\theta_{3i}, \end{aligned} \tag{2.63}$$

for all $i = 1, 2, \ldots, n$, *guarantee the solutions to the closed-loop system that start in a neighborhood of* $(\overline{\eta}, \overline{\omega}, \overline{V}, \overline{\eta})$ *to converge asymptotically to the largest invariant set where* $\omega_i = 0$ *for all* $i \in \mathcal{V}$, $\|\nabla_V \mathcal{S}_2\| = 0$ *and* $u = \overline{u} = \overline{u}_1 + \overline{u}_2 + \overline{u}_3$.

Proof. By adding $\frac{1}{2}(\theta_3 - \overline{\theta}_3)^T(\theta_3 - \overline{\theta}_3)$ to the overall storage function (2.60) and following the same lines of reasoning as the proof of Theorem 2.5.3 we can conclude that the system converges to the largest invariant set of points where $\omega = \mathbf{0}$, $\|\nabla_V \mathcal{S}_2\| = \mathbf{0}$, $\theta_1 = \overline{\theta}_1 + \mathbb{1}_n\alpha$, where $\alpha : \mathbb{R}_{\geq 0} \to \mathbb{R}$ is a function. On the invariant set the dynamics take the form

$$\begin{aligned} \dot{\eta} &= \mathbf{0} \\ \mathbf{0} &= -\mathcal{B}(\Gamma(V)\sin(\eta) - \Gamma(\overline{V})\sin(\overline{\eta})) \\ &\quad +Q^{-1}\mathbb{1}_n\alpha + Q^{-1}(I_n \otimes R_2)(\theta_2 - \overline{\theta}_2) \\ &\quad +\overline{R}_3(\theta_3 - \overline{\theta}_3) \\ \mathbf{0} &= -E(\eta)V + \overline{E}_{fd} \\ \dot{\overline{\theta}}_1 + \mathbb{1}_n\dot{\alpha} &= -\mathcal{L}^{com}(\overline{\theta}_1 + \mathbb{1}_n\alpha) \\ \dot{\theta}_2 - \dot{\overline{\theta}}_2 &= \overline{s}_2(\theta_2 - \overline{\theta}_2) \\ \dot{\theta}_3 - \dot{\overline{\theta}}_3 &= \overline{s}_3(\theta_3 - \overline{\theta}_3) \end{aligned}$$

from where we can conclude in a similar way as in the proof of Theorem 2.5.3 that $(\theta_1, \theta_2, \theta_3)$ converges to $(\overline{\theta}_1, \overline{\theta}_2, \overline{\theta}_3)$ and therefore that u converges to $\overline{u}$. ■

Remark 2.5.5 (Additional gains)**.** *The focus of this work is on the asymptotic behavior of the system. To obtain a desirable transient response, we can adjust the controller of Corollary 2.5.4, by including additional controller gains* $\alpha, \beta_1, \beta_2 \in \mathbb{R}_{>0}$, *and* $\beta_3 \in \mathbb{R}_{>0}^n$ *resulting in a controller of the form*

$$\begin{aligned} \dot{\theta}_1 &= -\alpha\mathcal{L}^{com}\theta_1 - \beta_1 Q^{-1}\omega \\ \dot{\theta}_2 &= \overline{s}_2(\theta_2) - \beta_2(I_n \otimes R_2^T)Q^{-1}\omega \\ \dot{\theta}_3 &= \overline{s}_3(\theta_3) - \overline{R}_3^T\,\mathrm{diag}(\beta_3)\omega \\ u &= \beta_1 Q^{-1}\theta_1 + \beta_2 Q^{-1}(I_n \otimes R_2)\theta_2 + \mathrm{diag}(\beta_3)\overline{R}_3\theta_3. \end{aligned}$$

The tuning of the various parameters depends on the system at hand and is outside of the scope of this work. We notice however that the optimality features of the controller are preserved under the addition of the various gains.

Remark 2.5.6 (Non-harmonic disturbances)**.** *Controller (2.58) (as well as the other controllers introduced in the previous sections) are designed to counteract disturbances generated by exosystems (2.62). These controllers are also robust to other perturbations. Consider system (2.35) with a disturbance $-Q^l$ in addition to $-P_d$. Assume that $-Q^l$ has a finite $\mathcal{L}_2$-norm, namely $\int_0^\infty \|Q^l(s)\|^2 ds < \infty$. In the presence of Q^l, the incremental model is modified in such a way that the function $Z(\omega, \overline{\omega}, \eta, \overline{\eta}, V, \overline{V}, \theta, \overline{\theta})$ satisfies*

$$\begin{aligned} \dot{Z} &= -(\omega - \overline{\omega})^T D(\omega - \overline{\omega}) - \|\nabla_V \mathcal{S}_2\|^2_{T^{-1}} \\ &\quad -(\theta_1 - \overline{\theta}_1)^T \mathcal{L}^{com}(\theta_1 - \overline{\theta}_1) - (\omega - \overline{\omega})^T Q^l. \end{aligned}$$

Further manipulations show that

$$\begin{aligned} \dot{Z} &\leq -(\omega - \overline{\omega})^T \tilde{D}(\omega - \overline{\omega}) - \|\nabla_V \mathcal{S}_2\|^2_{T^{-1}} \\ &\quad -(\theta_1 - \overline{\theta}_1)^T \mathcal{L}^{com}(\theta_1 - \overline{\theta}_1) + \gamma (Q^l)^T Q^l, \end{aligned}$$

where $\gamma = \frac{1}{2\varepsilon}$, $\tilde{A} = A - \frac{\varepsilon}{2} I$, and ε is a number satisfying $0 < \varepsilon < 2 \min_i\{A_i\}$. Integrating both sides yields

$$Z(t) - Z(0) \leq \gamma \int_0^t \|Q^l(s)\|^2 ds \leq \gamma \int_0^\infty \|Q^l(s)\|^2 ds.$$

This shows that, for initial conditions of the system which are sufficiently close to a strict local minimum of Z and for disturbances Q^l with a sufficiently small $\mathcal{L}_2$-norm, the solutions of the system remain in a compact level set of Z and as such are bounded and exist for all time. Furthermore,

$$(\omega(t) - \overline{\omega})^T \tilde{D}(\omega(t) - \overline{\omega}) \leq Z(0) + \gamma \textstyle\int_0^\infty \|Q^l(s)\|^2 ds.$$

Since the left-hand side is bounded for all time, we have

$$\min_i\{\tilde{D}_i\} \sup_{t \geq 0} \|\omega(t) - \overline{\omega}\|^2 \leq Z(0) + \gamma \textstyle\int_0^\infty \|Q^l(s)\|^2 ds,$$

which shows the existence of a finite $\mathcal{L}_2$-to-$\mathcal{L}_\infty$ gain from the disturbance Q^l to the frequency deviation $\omega - \overline{\omega}$. Similarly, one can show the existence of a finite $\mathcal{L}_2$-to-$\mathcal{L}_2$ gain (Kundur et al. 2004).

This section contributed to the development of distributed and dynamic controllers based on an internal model design able to generate a time-varying feedforward input such that a zero frequency deviation is obtained in the presence of time-varying power demand. Furthermore we characterized the time-varying power demand that can be compensated optimally under the requirement of zero frequency regulation.

2.6 Case study

We illustrate the performance of the controllers on a connected four area network (see (Nabavi and Chakrabortty 2013) how a four area network equivalent can be obtained for the IEEE New England 39-bus system or the South Eastern Australian 59-bus system). This simulation is carried out on the network provided in (Li et al. 2014) and its network topology is shown in Figure 2.1. The values of cost coef-

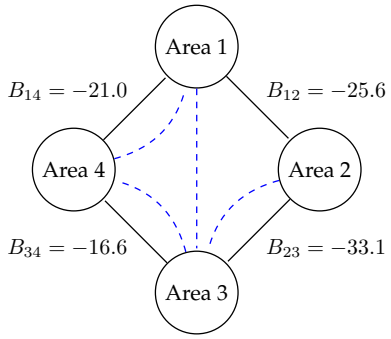

Figure 2.1: A four area equivalent network of the power grid, where B_{ij} denotes the susceptance of the transmission line connecting two areas. The dashed lines represent the communication links.

ficients, generator and transmission line parameters are a slight modification of the ones provided in (Li et al. 2014), (Ourari et al. 2006) and (Bergen and Vittal 2000). An overview of the numerical values of the relevant parameters is provided in Table 2.2. The communication among the controllers is depicted in Figure 2.1 as well and differs from the topology of the power grid. As a first scenario the power demand P_d (per unit) is assumed to be constant and therefore the controller of Section 2.4 is applicable. The system is initially at steady state with a constant load $P_d(t) = (2.00, 1.00, 1.50, 1.00)^T$, $t \in [0, 10)$ and according to their cost functions generators take a different share in the power generation such that the total costs are minimized. At timestep 10 the load[5] is increased to $P_d(t) = (2.20, 1.05, 1.55, 1.10)^T$, $t \geq 10$. The frequency response to the control input is given in Figure 2.2, where the base frequency is 120π rad/s. From Figure 2.2 we can see how the frequency drops due to the increased load. Furthermore we note that the controller regulates the power generation such that a new steady state condition is obtained where the frequency deviation is again zero and costs are minimized. To elaborate on this we note that the generation costs at $t = 100$ are 3.36×10^4 \$/h (assuming a base

[5] We can interpret an increase of load also as a sudden drop of uncontrollable (renewable) generation.

	Area 1	Area 2	Area 3	Area 4
M_i	5.22	3.98	4.49	4.22
D_i	1.60	1.22	1.38	1.42
T_{doi}	5.54	7.41	6.11	6.22
X_{di}	1.84	1.62	1.80	1.94
$X_{di}^{'}$	0.25	0.17	0.36	0.44
E_{fdi}	4.41	4.20	4.37	4.45
B_{ii}	-49.61	-61.66	-52.17	-40.18
q_i	1.00	0.75	1.50	0.50

Table 2.2: An overview of the numerical values used in the simulations. System parameters are provided in 'per unit', except T_{doi} (seconds). The generation cost coefficient q_i is given in $\frac{\$10^4}{h}$.

power of 1000 MVA), which is substantially lower than the generation costs when every control area would produce only for its own demand (4.79×10^4 \$/h). Since we did not include excitor dynamics in this simulation, the voltages are not regulated. Nevertheless the voltages do not deviate much from their nominal value of 1 per unit. At timestep 70 the communication link between area 1 and area 3 is lost, without effecting the frequencies. This is expected since the controller states are already in consensus and it provides numerical evidence that our approach is robust to changes in the communication network as long as the graph stays connected.

As a second scenario we consider a time-varying load as in (2.62), where the constant demand of scenario 1 is modulated by sinusoidal terms with periods of 30 seconds. We note that the controller design does not require that all loads vary with the same frequency and is only assumed here for notational convenience. The resulting load profile is given by

$$P_d(t) = (2.00, 1.00, 1.50, 1.00)^T + 0.040 \times \sin(\frac{2\pi t}{30})(1.10, 1.20, 0.98, 1.00)^T \quad (2.64)$$

for $t \in [0, 10)$ and

$$P_d(t) = (2.20, 1.05, 1.55, 1.10)^T + 0.044 \times \sin(\frac{2\pi t}{30})(1.04, 1.30, 0.99, 1.00)^T, \quad (2.65)$$

for $t \geq 10$. Notice that the sinusoidal term does not belong to $\mathrm{Im}(Q^{-1}\mathbb{1}_n)$. Accordingly we rely on the controller proposed in Section 2.5.2 with $\beta_3 = 0.5\mathbb{1}_n$ (see

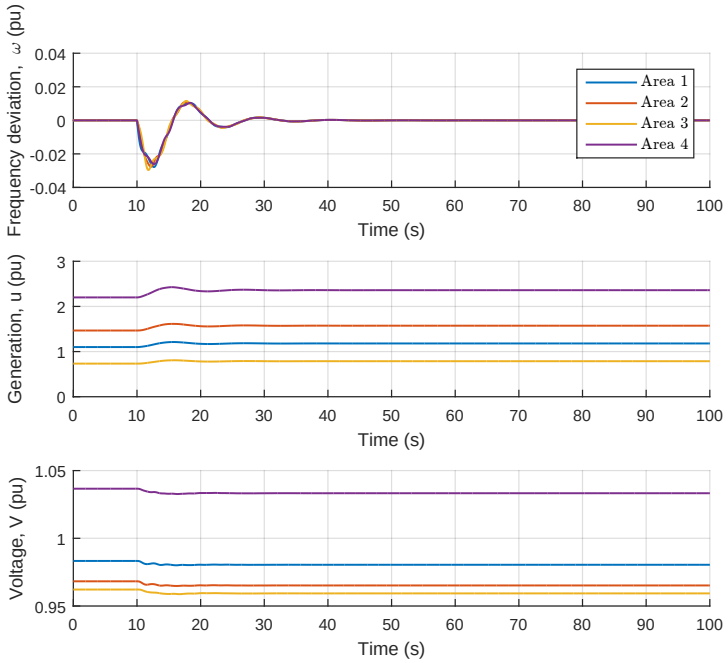

Figure 2.2: Frequency response and control input using the controller of Section 2.4. The constant load is increased at timestep 10, whereafter the frequency deviation is regulated back to zero and generation costs are minimized.

Remark 2.5.5) with matrices

$$S_{3i} = \begin{bmatrix} 0 & \frac{2\pi}{30} \\ \frac{-2\pi}{30} & 0 \end{bmatrix}, \quad R_{3i} = \begin{bmatrix} 1 & 0 \end{bmatrix}. \tag{2.66}$$

From Figure 2.3 we can see how the controller provides a time-varying input such that the frequency deviation is driven to zero even in the presence of a time-varying load. Since the time-varying load does not belong to $\mathrm{Im}(Q^{-1}\mathbb{1}_n)$, the time-varying power generation is not economically optimal anymore. One can check however that the constant term of the generation still converges to the optimum and is equal to the optimal generation in scenario 1. An example of optimal generation in the presence of a time-varying load, where the time-varying load belongs to $\mathrm{Im}(Q^{-1}\mathbb{1}_n)$, is provided in (Bürger et al. 2014) under the assumption of constant voltages.

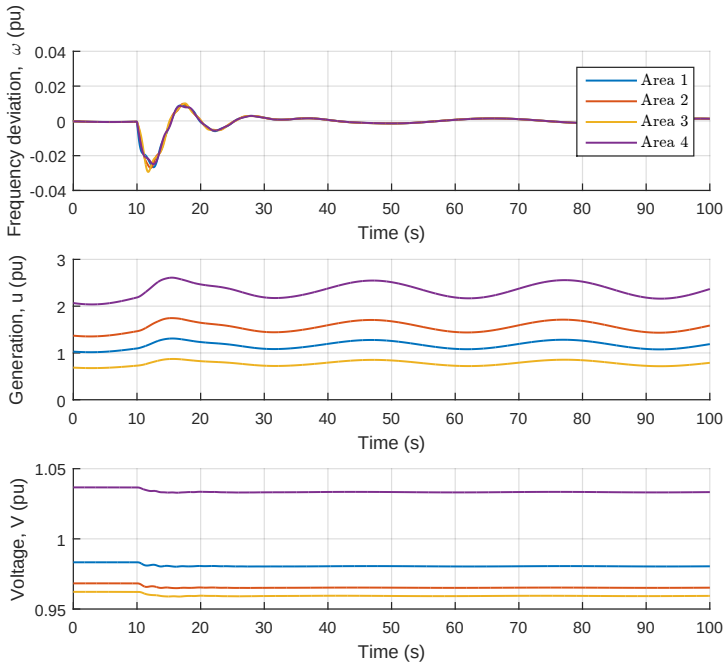

Figure 2.3: Frequency response and control input using the controller of Section 2.5.2. The time-varying load is increased at timestep 10, whereafter the frequency is regulated back to zero. The costs associated to the constant term of the generation are minimized.

Published in:

S. Trip, M. Bürger and C. De Persis – *"An internal model approach to frequency regulation in inverter-based microgrids with time-varying voltages,"* Proceedings of the IEEE 53rd Conference on Decision and Control (CDC)," Los Angles, CA, USA, pp. 223–228, 2014.

Chapter 3

Active power sharing in microgrids

Abstract

This chapter studies the problem of frequency regulation and active power sharing in inverter-based microgrids with time-varying voltages. Building upon the result in the previous chapter, we propose the design of internal-model-based controllers and analyze it within an (incrementally) passivity framework. A small case study indicates the effectiveness of the proposed solution.

3.1 A microgrid model

Consider a microgrid consisting of n generation and m load buses. Every generation bus represents an inverter, connected to a DG unit and a battery. The loads are modelled as constant impedances and corresponding load buses are eliminated, resulting in a Kron-reduced network. Consequently, the network is represented by a connected and undirected graph $\mathcal{G} = (\mathcal{V}, \mathcal{E})$, where $\mathcal{V} = \{1, \dots, n\}$ is the set of nodes (generation buses) and $\mathcal{E} = \{1, \dots, m\}$ is the set of distribution lines connecting the nodes. The network structure can be represented by its corresponding incidence matrix $\mathcal{B} \in \mathbb{R}^{n \times m}$. The ends of edge k are arbitrary labeled with a '$+$' and a '$-$'. Then

$$\mathcal{B}_{ik} = \begin{cases} +1 & \text{if } i \text{ is the positive end of } k \\ -1 & \text{if } i \text{ is the negative end of } k \\ 0 & \text{otherwise.} \end{cases}$$

3.1.1 A network of inverters

The inverter at the node i is assumed to be able to regulate its frequency instantaneous and its voltage in a delayed manner. The inverter is therefore represented

by

$$\begin{aligned} \dot{\delta}_i &= u_i^{\delta}, \\ \tau_{V_i}\dot{V}_i &= -V_i + u_i^{V}, \end{aligned} \tag{3.1}$$

where δ_i and V_i are the voltage angle and voltage respectively, and $\tau_{V_i} \in \mathbb{R}_{>0}$ is the time constant of the filter. The considered controllers are given by

$$\begin{aligned} u_i^{\delta} &= \omega^d - k_{P_i}(P_i^m - P_i^d - p_i), \\ u_i^{V} &= V_i^d - k_{Q_i}(Q_i^m - Q_i^d - q_i), \end{aligned} \tag{3.2}$$

where $\omega^d, V^d, P^d, Q^d \in \mathbb{R}^n$ are respectively the desired frequency, desired voltage, active power setpoint and reactive power setpoint, and are determined according to economic and technical criteria. The constants $k_{P_i} \in \mathbb{R}_{>0}$ and $k_{Q_i} \in \mathbb{R}_{>0}$ are the frequency and voltage droop gains respectively. p_i and q_i are additional control inputs which we will design later to achieve frequency and voltage regulation.

Remark 3.1.1 (Inverter model and controller)**.** *The inverter model (3.1) and controller (3.2) are identical to the ones in (Schiffer et al. 2013), when we set $p_i = 0$ and $q_i = 0$. We refer the reader to (Schiffer et al. 2013) and (Schiffer et al. 2015) for a more in depth treatment of physical interpretation and underlying assumptions.*

The measured active and reactive powers (P_i^m and Q_i^m) are obtained through filters with time constants τ_{P_i} and τ_{Q_i}:

$$\begin{aligned} \tau_{P_i}\dot{P}_i^m &= -P_i^m + P_i \\ \tau_{Q_i}\dot{Q}_i^m &= -Q_i^m + Q_i, \end{aligned} \tag{3.3}$$

where the power flows are given by

$$\begin{aligned} P_i &= G_{ii}V_i^2 - \sum_{j\in\mathcal{N}_i} \big(B_{ij}V_iV_j\sin(\delta_i-\delta_j) + G_{ij}V_iV_j\cos(\delta_i-\delta_j)\big) \\ Q_i &= -B_{ii}V_i^2 - \sum_{j\in\mathcal{N}_i} \big(G_{ij}V_iV_j\sin(\delta_i-\delta_j) - B_{ij}V_iV_j\cos(\delta_i-\delta_j)\big), \end{aligned} \tag{3.4}$$

where B_{ij} and G_{ij} denote the susceptance and the conductance of the distribution line respectively. Additionally, we have $B_{ii} = \hat{B}_{ii} + \sum_{j\in\mathcal{N}_i} B_{ij}$ and $G_{ii} = \hat{G}_{ii} + \sum_{j\in\mathcal{N}_i} G_{ij}$, where $\hat{B}_{ii}$ and $\hat{G}_{ii}$ denote the shunt susceptance and shunt conductance. In the subsequent analysis we approximate the terms involving G by an *unknown* constant, i.e.

$$\begin{aligned} P_i &= \sum_{j\in\mathcal{N}_i} |B_{ij}|V_iV_j\sin(\delta_i-\delta_j) + P_{0i}, \\ Q_i &= |B_{ii}|V_i^2 - \sum_{j\in\mathcal{N}_i} |B_{ij}|V_iV_j\cos(\delta_i-\delta_j) + Q_{0i}. \end{aligned} \tag{3.5}$$

The approximation above (including a lossless network as a particular case by setting $P_{0i} = Q_{0i} = 0$) is common in power grid studies and is made in order to derive a suitable Lyapunov function for the stability analysis. Assuming $\tau_{V_i} \ll \tau_{P_i} \simeq \tau_{Q_i}$ we can simplify the used model by setting $\tau_{V_i} = 0$, resulting in

$$\begin{aligned} \dot{\delta}_i &= \omega_i \\ \tau_{P_i}\dot{\omega}_i &= -\omega_i + \omega^d - k_{P_i}(P_i - P_{0i}^d) + u_i^P \\ \tau_{Q_i}\dot{V}_i &= -V_i + V_i^d - k_{Q_i}(Q_i - Q_{0i}^d) + u_i^Q, \end{aligned} \tag{3.6}$$

with

$$\begin{aligned} u_i^P &= -k_{P_i}(p_i + \tau_{P_i}\dot{p}_i) \\ u_i^Q &= -k_{Q_i}(q_i + \tau_{Q_i}\dot{q}_i). \end{aligned} \tag{3.7}$$

For all nodes the system writes as:

$$\begin{aligned} \dot{\delta} &= \omega \\ T_P\dot{\omega} &= -\omega + \mathbb{1}_n\omega^d - K_P(P - P_0^d) + u^P \\ T_Q\dot{V} &= -V + V^d - K_Q(Q - Q_0^d) + u^Q, \end{aligned} \tag{3.8}$$

where the used symbols follow straightforwardly from the node dynamics, and are vectors or matrices with appropriate dimensions. Since the dynamics are driven by the differences in the voltage angles we introduce $\eta = \mathcal{B}^T\delta$ and write (3.8) as:

$$\begin{aligned} \dot{\eta} &= \mathcal{B}^T\omega, \\ T_P\dot{\omega} &= -\omega + \mathbb{1}_n\omega^d - K_P(\mathcal{B}\mathrm{diag}(\mathcal{B}_+^T V)\mathrm{diag}(\mathcal{B}_-^T V)B^e\sin(\eta) - P_0^d) + u^P, \\ T_Q\dot{V} &= -V + V^d - K_Q(\mathrm{diag}(V)B^nV \\ &\quad - |\mathcal{B}|\mathrm{diag}(\mathcal{B}_+^T V)\mathrm{diag}(\mathcal{B}_-^T V)B^e\cos(\eta) - Q_0^d) + u^Q, \end{aligned} \tag{3.9}$$

where $\mathcal{B}$ is the corresponding incidence matrix. Its positive entries are given by $\mathcal{B}_+$ and its negative entries by $\mathcal{B}_-$, such that we have $\mathcal{B} = \mathcal{B}_+ + \mathcal{B}_-$. Furthermore $|\mathcal{B}| = \mathcal{B}_+ - \mathcal{B}_-$ denotes the incidence matrix with all elements positive. The susceptance of the transmission lines is denoted by $B^e = \mathrm{diag}(B_k)$, where $B_k = |B_{ij}| = |B_{ji}|$ is the susceptance of transmission line k connecting nodes i and j. The shunt susceptance of the nodes is given by $B^n = \mathrm{diag}(|B_{ii}|)$. To simplify the notation further we

introduce

$$\begin{aligned} P_0^d &= P_0^d - P_0 \\ Q_0^d &= Q^d - Q_0 \\ M_P &= K_P^{-1} T_P \\ M_Q &= K_Q^{-1} T_Q \\ \Theta(V) &= \mathrm{diag}(V) B^n V \\ \Gamma(V) &= \mathrm{diag}(\mathcal{B}_+^T V) \mathrm{diag}(\mathcal{B}_-^T V) B^e. \end{aligned} \tag{3.10}$$

Remark 3.1.2 (A new voltage dependent variable)**.** *Notice that $\Gamma(V)$ is a diagonal matrix with $\Gamma(V)_{kk} = |B_{ij}|V_iV_j = |B_{ji}|V_jV_i$ when edge k is incident to nodes i and j. $\Theta(V)$ is a vector with $\Theta(V)_i = |B_{ii}|V_i^2$.*

Using the new variables (3.10), system (3.9) can be written as

$$\begin{aligned} \dot{\eta} &= \mathcal{B}^T \omega \\ M_P \dot{\omega} &= -K_P^{-1}(\omega - \mathbb{1}_n \omega^d) + P_0^d - \mathcal{B}\Gamma(V)\sin(\eta) + u^P \\ M_Q \dot{V} &= -K_Q^{-1}(V - V^d) + Q_0^d - \Theta(V) + |\mathcal{B}|\Gamma(V)\cos(\eta) + u^Q, \end{aligned} \tag{3.11}$$

which we will use throughout this chapter.

3.2 Stability with constant control inputs

First we investigate the stability of the equilibria of system (3.11) under the assumption $u^P = \overline{u}^P$ and $u^Q = \overline{u}^Q$ are constant. This study has been already pursued in e.g. (Schiffer et al. 2013) or in (Simpson-Porco et al. 2013) for a first order model. The approach in this work descends however from the results provided in Chapter 2 and can provide new insight into this problem. Furthermore it paves the way for allowing dynamic controlled u^P and u^Q in later sections, relying on (incremental) passivity and the internal model approach. Our analysis is based on characterizing the equilibria and providing conditions when those equilibria are locally attractive.

3.2.1 Equilibria

Before characterizing the equilibria, we need the following assumption, which guarantees the existence of an equilibrium:

Assumption 3.2.1 (Feasibility). *For a given $\overline{u}^P + P_0^d$ and $\overline{u}^Q + Q_0^d$, there exist $\overline{\eta} \in \mathrm{Im}(\mathcal{B}^T) \cap (\frac{-\pi}{2}, \frac{\pi}{2})^m$, $\overline{\omega} \in \mathrm{Ker}(\mathcal{B}^T)$ and $\overline{V} \in \mathbb{R}^n_{>0}$ such that*

$$\begin{aligned} \mathbf{0} &= -K_P^{-1}(\overline{\omega} - \mathbb{1}_n \omega^d) - \mathcal{B}\Gamma(\overline{V})\sin(\overline{\eta}) + P_0^d + \overline{u}^P \\ \mathbf{0} &= -K_Q^{-1}(\overline{V} - V^d) - \Theta(\overline{V}) + |\mathcal{B}|\Gamma(\overline{V})\cos(\overline{\eta}) + Q_0^d + \overline{u}^Q. \end{aligned} \tag{3.12}$$

Under this assumption the equilibria can be characterized as follows:

Lemma 3.2.2 (Equilibria). *The equilibria of (3.11) are given by*

$$\overline{\omega} = \mathbb{1}_n \omega_*, \tag{3.13}$$

where

$$\omega_* = \omega^d + \frac{\mathbb{1}_n^T(P_0^d + \overline{u}^P)}{\mathbb{1}_n^T K_P^{-1} \mathbb{1}_n}, \tag{3.14}$$

$$\mathcal{B}\Gamma(\overline{V})\sin(\overline{\eta}) = \big(I_n - \frac{-K_P^{-1}\mathbb{1}_n\mathbb{1}_n^T}{\mathbb{1}_n^T K_P^{-1}\mathbb{1}_n}\big)(P_0^d + \overline{u}^P), \tag{3.15}$$

and $\overline{V}$ any vector fulfilling Assumption 3.2.1.

3.2.2 Local attractivity

Having characterized the equilibria of system (3.11), we are now ready to investigate the stability properties of the steady state solution. Recall the underlying assumption that $\overline{V} \in \mathbb{R}^n_{>0}$, and that therefore there exists a compact set around $\overline{V}$ which only contains positive values of V. To analyze the stability consider the incremental storage function:

$$\begin{aligned} &\mathcal{S}(\omega, \overline{\omega}, \eta, \overline{\eta}, V, \overline{V}) \\ &= \frac{1}{2}(\omega - \overline{\omega})^T M_P (\omega - \overline{\omega}) \\ &- \mathbb{1}_m^T \Gamma(V)\cos(\eta) + \mathbb{1}_m^T \Gamma(\overline{V})\cos(\overline{\eta}) - (\Gamma(\overline{V})\sin(\overline{\eta}))^T(\eta - \overline{\eta}) \\ &+ \mathbb{1}_n^T K_Q^{-1}(V - \overline{V}) - (K_Q^{-1}V^d + Q_0^d + \overline{u}^Q)^T(\mathbf{ln}(V) - \mathbf{ln}(\overline{V})) \\ &+ \frac{1}{2}\mathbb{1}_n^T(\Theta(V) - \Theta(\overline{V})). \end{aligned} \tag{3.16}$$

The former terms involving η and ω descend from Chapter 2, whereas latter terms were used previously to analyze voltage stability (Schiffer et al. 2014). Notice that the storage function is not bounded, since unboundedness of η implies that the term $(\Gamma(\overline{V})\sin(\overline{\eta}))^T\eta$ is unbounded as well. In order to invoke LaSalle's invariance principle we therefore require condition 3.17, in the lemma below, to be satisfied.

Lemma 3.2.3 (Local minimum of (3.16))**.** *The storage function (3.16) has, under Assumption 3.2.1, a local minimum at an equilibrium point $(\overline{\eta}, \overline{\omega}, \overline{V})$, if the following condition is met*

$$\Big(\frac{\partial^2 \mathcal{S}}{\partial^2 V} - \frac{\partial^2 \mathcal{S}}{\partial V \partial \eta}\frac{\partial^2 \mathcal{S}}{\partial^2 \eta}\frac{\partial^2 \mathcal{S}}{\partial \eta \partial V}\Big)\Big|_{\eta=\overline{\eta},\omega=\overline{\omega},V=\overline{V}} > \mathbf{0}, \tag{3.17}$$

where

$$\begin{aligned}
\frac{\partial^2 \mathcal{S}}{\partial \eta \partial V} &= (|\mathcal{B}|\Gamma(V)\mathrm{diag}(\sin(\eta)))^T \mathrm{diag}(V)^{-1}, \\
\frac{\partial^2 \mathcal{S}}{\partial V \partial \eta} &= \mathrm{diag}(V)^{-1}(|\mathcal{B}|\Gamma(V)\mathrm{diag}(\sin(\eta))), \\
\frac{\partial^2 \mathcal{S}}{\partial^2 \eta} &= \mathrm{diag}(\Gamma(V)\cos(\eta)), \\
\Big(\frac{\partial^2 \mathcal{S}}{\partial^2 V}\Big)_{ii} &= \Big(|B_{ii}| + \frac{K_Q V^d + Q_0^d + \overline{u}^Q}{V_i^2}\Big),
\end{aligned} \tag{3.18}$$

and $(\frac{\partial^2 \mathcal{S}}{\partial^2 V})_{ij} = (-|B_{ij}|\cos\eta_k)$ for $i \neq j$, where edge k is incident to nodes i and j. When node i is not connected to node j we take $|B_{ij}| = 0$.

Proof. First we consider the gradient of the storage function.

$$\nabla \mathcal{S} = \begin{bmatrix} \frac{\partial \mathcal{S}}{\partial \eta}^T & \frac{\partial \mathcal{S}}{\partial \omega}^T & \frac{\partial \mathcal{S}}{\partial V}^T \end{bmatrix}^T = \begin{bmatrix} \Gamma(V)\sin(\eta) - \Gamma(\overline{V})\sin(\overline{\eta}) \\ M_P(\omega - \overline{\omega}) \\ (-\dot{V}^T M_Q \mathrm{diag}(V)^{-1})^T \end{bmatrix} \tag{3.19}$$

Since $\dot{V}|_{\eta=\overline{\eta},\omega=\overline{\omega},V=\overline{V}} = 0$ it is immediate to see that we have $\nabla\mathcal{S}|_{\eta=\overline{\eta},\omega=\overline{\omega},V=\overline{V}} = \mathbf{0}$. As the gradient of $\mathcal{S}$ is zero at an equilibrium point it is sufficient for $\mathcal{S}$ to have a local minimum when the Hessian is positive definite at an equilibrium. The Hessian is given by

$$\nabla^2 \mathcal{S} = \begin{bmatrix} \mathrm{diag}(\Gamma(V)\cos(\eta)) & \mathbf{0} & \frac{\partial^2 \mathcal{S}}{\partial \eta \partial V} \\ \mathbf{0} & M_P & \mathbf{0} \\ \frac{\partial^2 \mathcal{S}}{\partial V \partial \eta} & \mathbf{0} & \frac{\partial^2 \mathcal{S}}{\partial^2 V} \end{bmatrix}, \tag{3.20}$$

where $(\frac{\partial^2 \mathcal{S}}{\partial V \partial \eta})^T = \frac{\partial^2 \mathcal{S}}{\partial \eta \partial V} = (|\mathcal{B}|\Gamma(V)\mathrm{diag}(\sin(\eta)))^T \mathrm{diag}(V)^{-1}$, $(\frac{\partial^2 \mathcal{S}}{\partial^2 V})_{ii} = |B_{ii}| + \frac{K_Q V^d + Q_0^d + \overline{u}^Q}{V_i^2}$ and $(\frac{\partial^2 \mathcal{S}}{\partial^2 V})_{ij} = -|B_{ij}|\cos\eta_k$ for $i \neq j$, where edge k is incident to nodes i and j. Since M_p and $\mathrm{diag}(\Gamma(V)\cos(\eta))$ are positive definite matrices, it follows by invoking the Schur complement that $\nabla^2\mathcal{S}|_{\overline{\eta},\overline{\omega},\overline{V}} > \mathbf{0}$ if and only if

$$\Big(\frac{\partial^2 \mathcal{S}}{\partial^2 V} - \frac{\partial^2 \mathcal{S}}{\partial V \partial \eta}\frac{\partial^2 \mathcal{S}}{\partial^2 \eta}\frac{\partial^2 \mathcal{S}}{\partial \eta \partial V}\Big)\Big|_{\eta=\overline{\eta},\omega=\overline{\omega},V=\overline{V}} > \mathbf{0}. \tag{3.21}$$

■

We are now ready to state the main result of this section, that is, any solution starting sufficiently close to an equilibrium where the storage function $\mathcal{S}$ has a local minimum, asymptotically converges to an equilibrium fulfilling Assumption 3.2.1.

Theorem 3.2.4 (Convergence to an equilibrium)**.** *Given system (3.11), if the equilibrium fulfills condition (3.17), then the system locally asymptotically converges to an equilibrium fulfilling Assumption 3.2.1.*

Proof. Since the storage function has a local minimum at the equilibria we can invoke LaSalle's invariance principle. For this we show that $\dot{\mathcal{S}} \leq 0$, with the equality holding only at the equilibria. In fact,

$$\dot{\mathcal{S}} = \frac{\partial \mathcal{S}}{\partial \eta}\dot{\eta} + \frac{\partial \mathcal{S}}{\partial \omega}\dot{\omega} + \frac{\partial \mathcal{S}}{\partial V}\dot{V}, \tag{3.22}$$

where

$$\begin{aligned}
\frac{\partial \mathcal{S}}{\partial \eta}\dot{\eta} &= -(\omega - \overline{\omega})^T \mathcal{B}(\Gamma(\overline{V})\sin(\overline{\eta}) - \Gamma(V)\sin(\eta)),\\
\frac{\partial \mathcal{S}}{\partial \omega}\dot{\omega} &= (\omega - \overline{\omega})^T(-K_P^{-1}\omega + K_P^{-1}\overline{\omega})\\
&\quad + (\omega - \overline{\omega})^T \mathcal{B}(\Gamma(\overline{V})\sin(\overline{\eta}) - \Gamma(V)\sin(\eta)),\\
\frac{\partial \mathcal{S}}{\partial V}\dot{V} &= -\dot{V}^T M_Q \mathrm{diag}(V)^{-1}\dot{V},
\end{aligned} \tag{3.23}$$

yielding

$$\dot{\mathcal{S}} = -(\omega - \overline{\omega})^T K_P^{-1}(\omega - \overline{\omega}) - \dot{V}^T M_Q \mathrm{diag}(V)^{-1}\dot{V}. \tag{3.24}$$

Recalling that $V \in \mathbb{R}^n_{>0}$, we have that $\dot{\mathcal{S}} \leq 0$ and therefore there exists a compact level set Υ around the equilibrium $(\overline{\eta}, \overline{\omega}, \overline{V})$, which is forward invariant. By LaSalle's invariance principle the solution starting in Υ converges asymptotically to the largest invariant set contained in $\Upsilon \cap \{(\eta, \omega, V) : \omega = \overline{\omega}, \dot{V} = 0\}$. On such invariant set the system is

$$\begin{aligned}
\dot{\eta} &= \mathcal{B}^T\overline{\omega},\\
\mathbf{0} &= -K_P^{-1}(\overline{\omega} - \mathbb{1}_n\omega^d) - \mathcal{B}\Gamma(V)\sin(\eta) + P_0^d + \overline{u}^P,\\
\mathbf{0} &= -K_Q^{-1}(V - V^d) - \Theta(V) + |\mathcal{B}|\Gamma(V)\cos(\eta) + Q_0^d + \overline{u}^Q.
\end{aligned} \tag{3.25}$$

Recall that $\overline{\omega} = \mathbb{1}_n\omega^*$, such that $\dot{\eta} = \mathcal{B}^T\mathbb{1}_n\omega^* = \mathbf{0}$. Since on the invariant set $\dot{\eta} = \dot{\omega} = \dot{V} = \mathbf{0}$, system (3.11) approaches the set of equilibria contained in Υ. Consider a forward invariant set $\Omega \subseteq \Upsilon$ around $(\overline{\eta}, \overline{\omega}, \overline{V})$, where it holds that $\frac{\partial^2 \mathcal{S}}{\partial(\eta,\omega,V)^2} > \mathbf{0}$. Since every equilibrium in Ω is Lyapunov stable, it then follows from Lemma 1.4.8 that the solution starting in Ω converges to a point. I.e., we can conclude that the system approaches the set where where $V = \tilde{V}$ and $\eta = \tilde{\eta}$ are constants. ■

3.3 Frequency regulation by dynamic control inputs

In the previous section we investigated the stability of system (3.11) with constant $u^P = \overline{u}^P$. As shown in Lemma 3.2.2 this generally results in a steady state frequency $\overline{\omega}$ deviating from the desired frequency ω^d. In this section we adopt the approach pursued in Chapter 2, and based on incremental passivity and the internal model approach, we design a dynamic and distributed controller providing a control input $u^P(t)$ such that $\overline{\omega} = \mathbb{1}_n \omega^d$ is locally asymptotically stable, i.e. the frequency is stabilized at its desired value. Before proposing a stabilizing controller we first discuss possible values of the steady state control input.

3.3.1 Power sharing

From Lemma 3.2.2 it is immediate to see that any input $\overline{u}^P$, satisfying $\mathbb{1}_n^T(P_0^d + \overline{u}^P) = 0$, implies that a stable equilibrium satisfies $\overline{\omega} = \omega^d$. Among the possible choices of $\overline{u}^P$, we focus on the steady state input solving the following optimization problem:The control input $\overline{u}^P$ is a solution to the following optimization problem:

$$\begin{aligned} \min_{u^P, v} \frac{1}{2}(u^P)^T R u^P &= \min_{u^P, v} \sum_{i \in \mathcal{V}} \frac{1}{2} r_i (u_i^P)^2 \\ \text{s.t. } \mathbf{0} &= -\mathcal{B}\Gamma(\overline{V})v + P_0^d + u^P, \end{aligned} \tag{3.26}$$

where we have set $\sin(\eta) = v$. The equality constraint in the optimization problem coincides with the frequency dynamics in (3.11) at steady state where $\omega = \mathbb{1}_n \omega^d$. Following standard literature on convex optimization (see e.g. (Boyd and Vandenberghe 2004)) we introduce the Lagrangian function

$$L(u^P, v, \lambda) = (u^P)^T R u^P + \lambda^T \left(-\mathcal{B}\Gamma(\overline{V})v + P_0^d + u^P\right). \tag{3.27}$$

Assume that R is a positive diagonal matrix and therefore R is strictly convex. It follows that $L(u^P, v, \lambda)$ is convex in (u^P, v) and concave in λ. Therefore there exists a saddle point solution to

$$\max_{\lambda} \min_{u^P, v} L(u^P, v, \lambda).$$

Applying first order optimality conditions, the saddle point $(\overline{u}^P, \overline{v}, \overline{\lambda})$ must satisfy

$$\begin{aligned} R\overline{u}^P + \overline{\lambda} &= \mathbf{0}, \\ \Gamma(\overline{V})\mathcal{B}^T\overline{\lambda} &= \mathbf{0}, \\ -\mathcal{B}\Gamma(\overline{V})\overline{v} + P_0^d + \overline{u}^P &= \mathbf{0}. \end{aligned} \tag{3.28}$$

Solving this set of equations for $\overline{u}^P$ it is straightforward to show that

$$\overline{u}^P = -R^{-1}\frac{\mathbb{1}_n \mathbb{1}_n^T P_0^d}{\mathbb{1}_n^T K_p^{-1} \mathbb{1}_n}. \tag{3.29}$$

Remark 3.3.1 (Active power sharing)**.** *Active power sharing is an important aspect in microgrids. Some results on obtaining a desirable power sharing are provided e.g. in (Simpson-Porco et al. 2013) and (Schiffer et al. 2013). Note that in the present setting, the matrix R can be chosen to obtain an appropriate active power sharing. For instance the choice $R = I_n$ results in $\overline{u}_i^P = \overline{u}_j^P = \overline{u}_*^P$ for all i, j, whereas $R = K_P^{-1}$ results in $\overline{u}_i^P$ proportional to its droop gain.*

3.3.2 Stability

Relying on results of the previous section and our previous work (Bürger et al. 2014), we can design a controller which makes the system (3.11) locally asymptotically converging to an equilibrium where $\overline{\omega} = \mathbb{1}_1 \omega^d$, and thus provides frequency control, which is comparable to secondary control in the classic power grid. The stability result of the previous section assumed $u^P = \overline{u}^P$ and $u^Q = \overline{u}^Q$ are constants. If we let u^P be any control input, it is immediate to see from Lemma 3.2.4 that system (3.11) is incrementally passive from the input $u = u^P$ to the output $y = \omega$.

Corollary 3.3.2 (Incremental passivity)**.** *Let condition (3.17) hold. Then for system (3.11) there exists a regular storage function $\mathcal{S}'(\eta, \overline{\eta}, \omega, \overline{\omega})$ which satisfies the following incremental dissipation inequality*

$$\dot{\mathcal{S}}' \leq -(y - \overline{y})^T K_P^{-1}(y - \overline{y}) + (y - \overline{y})^T (u - \overline{u}), \tag{3.30}$$

where $u = u^P$ and $y = \omega$.

As the main result of this section we propose a dynamic controller that converges asymptotically to the feedforward input (3.29) and guarantees an asymptotical convergence of the frequency ω to its desired value $\mathbb{1}_n \omega^d$.

Theorem 3.3.3 (Frequency regulation and active power sharing)**.** *Given system (3.11), and assuming that condition (3.17) holds, the controllers at the nodes*

$$\begin{aligned} \dot{\theta}_i &= \sum_{j \in \mathcal{N}_i^{comm}} (\theta_j - \theta_i) - r_i^{-1}(\omega_i - \omega^d), \\ u_i^P &= r_i^{-1}\theta_i, \quad i \in \mathcal{V} \end{aligned} \tag{3.31}$$

where $\mathcal{N}_i^{comm}$ denotes the set of neighbors of node i in a graph describing the exchange of information among the controllers, guarantee locally the solutions to the closed-loop system

to converge asymptotically to the largest invariant set where $\omega_i = \omega^d$ for all $i \in \mathcal{V}$, and $\theta = \overline{\theta}$, $\overline{\theta}$ being the vector

$$\overline{\theta} = \frac{\mathbb{1}_n \mathbb{1}_n^T P_0^d}{\mathbb{1}_n^T R^{-1} \mathbb{1}_n}, \tag{3.32}$$

such that $\overline{u}^P = -R^{-1}\overline{\theta}$, is as in (3.29).

Proof. Bearing in mind Corollary 3.3.2 we have that system (3.11), with dynamic u^P and constant $\overline{u}^Q$ is incrementally passive from the input u^P to the output ω. The internal model principle design pursued in (De Persis 2013), (Bürger and De Persis 2013) and (Bürger and De Persis 2015) prescribes the design of a controller able to generate the feedforward input $\overline{u}^P$. To this purpose, we introduce the overall controller

$$\begin{aligned} \dot{\theta} &= -\mathcal{L}^{com}\theta + \overline{H}^T v, \\ u^P &= \overline{H}\theta, \end{aligned} \tag{3.33}$$

where $\theta \in \mathbb{R}^n$, $\mathcal{L}^{com}$ the Laplacian associated with a graph that describes the exchange of information among the controllers, and with the term $\overline{H}^T v$ needed to guarantee the incremental passivity property of the controller (see (Bürger and De Persis 2013), (Bürger and De Persis 2015) for details). Here $v \in \mathbb{R}^n$ is an extra control input to be designed later, while $\overline{H} = \overline{H}^T = -R^{-1}$.
If $v = \mathbf{0}$ and $\overline{\theta}(0) = \frac{\mathbb{1}_n \mathbb{1}_n^T P_0^d}{\mathbb{1}_n^T R^{-1} \mathbb{1}_n}$, then $\overline{\theta}(t) := \overline{\theta}(0)$ satisfies the differential equation in (3.33) and moreover the corresponding output $\overline{H}\,\overline{\theta}(t)$ is identically equal to the feedforward input $\overline{u}^P(t)$ defined in (3.29), provided that $\overline{H} = -R^{-1}$. More explicitly, we have

$$\begin{aligned} \dot{\overline{\theta}} &= -\mathcal{L}^{com}\overline{\theta}, \\ \overline{u}^P &= -R^{-1}\,\overline{\theta}. \end{aligned} \tag{3.34}$$

Consider now the incremental storage function

$$\Phi(\theta, \overline{\theta}) = \frac{1}{2}(\theta - \overline{\theta})^T(\theta - \overline{\theta})$$

It satisfies along the solutions to (3.33)

$$\begin{aligned} \dot{\Phi}(\theta, \overline{\theta}) &= (\theta - \overline{\theta})^T(-\mathcal{L}^{com}\theta - R^{-1}v + \mathcal{L}^{com}\overline{\theta}) \\ &\leq -(\theta - \overline{\theta})^T R^{-1} v = (u^P - \overline{u}^P)^T v. \end{aligned} \tag{3.35}$$

We now interconnect system (3.11) and the controller (3.33), obtaining

$$\begin{aligned}\dot{\eta} &= \mathcal{B}^T\omega,\\ M_P\dot{\omega} &= -K_P^{-1}(\omega - \mathbb{1}_n\omega^d) - \mathcal{B}\Gamma(V)\sin(\eta) + P_0^d - R^{-1}\theta,\\ M_Q\dot{V} &= -K_Q^{-1}(V - V^d) - \Theta(V) + |\mathcal{B}|\Gamma(V)\cos(\eta) + Q_0^d + \overline{u}^Q,\\ \dot{\theta} &= -\mathcal{L}^{com}\theta - R^{-1}v.\end{aligned} \tag{3.36}$$

Consider the incremental storage function

$$Z(\omega, \mathbb{1}_n\omega^d, \eta, \overline{\eta}, V, \overline{V}, \theta, \overline{\theta}) = \mathcal{S}(\omega, \mathbb{1}_n\omega^d, \eta, \overline{\eta}, V, \overline{V}) + \Phi(\theta, \overline{\theta}), \tag{3.37}$$

where $(\overline{\eta}^T, \mathbb{1}_n^T\omega^d, \overline{V}^T)^T$ fulfills Assumption 3.2.1. Following the argumentation of Lemma 3.2.3, it is immediate to see that under condition (3.17) we have that $\nabla Z|_{\eta=\overline{\eta},\omega=\overline{\omega},V=\overline{V},\theta=\overline{\theta}} = \mathbf{0}$ and $\nabla^2 Z|_{\eta=\overline{\eta},\omega=\overline{\omega},V=\overline{V},\theta=\overline{\theta}} > 0$, such that Z has a local minimum at its equilibrium. It turns out that

$$\begin{aligned}\dot{Z} = &-(\omega - \mathbb{1}_n\omega^d)^T K_P^{-1}(\omega - \mathbb{1}_n\omega^d)\\ &- \dot{V}^T M_Q \mathrm{diag}(V)^{-1}\dot{V}\\ &+ (\omega - \mathbb{1}_n\omega^d)^T(u - \overline{u})\\ &- (\theta - \overline{\theta})^T\mathcal{L}^{com}(\theta - \overline{\theta}) + (u - \overline{u})^T v.\end{aligned} \tag{3.38}$$

As we are still free in designing v, the choice $v = -(\omega - \mathbb{1}_n\omega^d)$ returns

$$\begin{aligned}\dot{Z} = &-(\omega - \mathbb{1}_n\omega^d)^T K_P^{-1}(\omega - \mathbb{1}_n\omega^d)\\ &- \dot{V}^T M_Q \mathrm{diag}(V)^{-1}\dot{V}\\ &- (\theta - \overline{\theta})^T\mathcal{L}^{com}(\theta - \overline{\theta}) \leq 0\end{aligned} \tag{3.39}$$

As $\dot{Z} \leq 0$, there exists a compact level set Υ around the equilibrium $(\eta, \mathbb{1}_n\omega^d, \overline{V}, \overline{\theta})$, which is forward invariant. By LaSalle's invariance principle the solution starting in Υ asymptotically converges to the largest invariant set contained in $\Upsilon \cap \{(\eta, \omega, V, \theta) : \overline{\omega} = \mathbb{1}_n\omega^d, \dot{V} = \mathbf{0}, \theta = \overline{\theta} + \mathbb{1}_n\alpha(t)\}$. On such invariant set the system is

$$\begin{aligned}\dot{\eta} &= \mathcal{B}^T\mathbb{1}_n\omega^d,\\ \mathbf{0} &= -\mathcal{B}(\Gamma(V)\sin(\eta) - \Gamma(\overline{V})\sin(\overline{\eta})) - R^{-1}\mathbb{1}_n\alpha(t),\\ \mathbf{0} &= -K_Q^{-1}(V - V^d) + Q_0^d - \Theta(V) + |\mathcal{B}|\Gamma(V)\cos(\eta) + \overline{u}^Q,\\ \dot{\overline{\theta}} &= -\mathcal{L}^{com}(\overline{\theta} + \mathbb{1}_n\alpha(t)).\end{aligned} \tag{3.40}$$

Premultiplying the second line in (3.40) by $\mathbb{1}_n^T$ yields $\mathbb{1}_n^T R^{-1}\mathbb{1}_n\alpha(t) = 0$. As R^{-1} is a positive definite diagonal matrix it follows that necessary $\alpha(t) = 0$ and therefore the control input u^P converges to the optimal control input $\overline{u}^P$ given by (3.29).

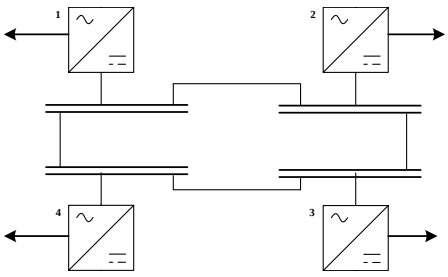

Figure 3.1: A microgrid consisting of 4 interconnected inverters.

Recall that $\overline{\omega} = \mathbb{1}_n \omega^d$, such that $\dot{\eta} = \mathcal{B}^T \mathbb{1}_n \omega^d = \mathbf{0}$. Since on the invariant set $\dot{\eta} = \dot{\omega} = \dot{V} = \dot{\theta} = \mathbf{0}$, the solutions to system (3.11) controlled by (3.31) approach the set of equilibria contained in Υ. Consider a forward invariant set $\Omega \subseteq \Upsilon$ around $(\overline{\eta}, \overline{\omega}, \overline{V}, \overline{\theta})$, where it holds that $\frac{\partial^2 \mathcal{Z}}{\partial(\eta,\omega,V,\theta)^2} > \mathbf{0}$. Since every equilibrium in Ω is Lyapunov stable, it then follows from Lemma 1.4.8 that the solution starting in Ω converges to a point. ■

Bearing in mind that p_i is applied to the physical system, which is related to u_i^P via (3.7), the following corollary provides the overall controller:

Corollary 3.3.4 (Applied control input)**.** *The control input p, applied to the controllers (3.2) is generated by the following system:*

$$\begin{aligned} \dot{\theta} &= -\mathcal{L}^{com}\theta - R^{-1}(\omega - \mathbb{1}\omega^d), \\ u^P &= -R^{-1}\theta, \\ T_P \dot{x}^P &= -x^P - K_P^{-1} u^P, \\ p &= x^P. \end{aligned} \tag{3.41}$$

3.4 Case study

We will illustrate the performance of the controller proposed in Theorem 3.3.3 on an academic example of a microgrid. Consider a network of four interconnected inverters, as shown in Figure 3.1. Noticing that $\overline{\omega}$ is independent of the voltages, we propose additionally the following decentralized controller aiming at voltage

regulation:

$$\begin{aligned} \dot{\mu}_i &= -(V_i - V_i^d) \\ u_i^Q &= \mu_i. \end{aligned} \tag{3.42}$$

The control objective chosen in this simulation is to let the system converge to the desired values $\omega^d = 50$ and $V^d = (1, 1, 1, 1)^T$. The system is initially at steady state with $P_0^d = (0.02, 0.15, 0.1, 0.1)^T$ for $t \in [0, 25)$ and $Q^d = (0.202, 0.014, 0.0131, 0.089)^T$ for $t \in [0, 45)$. At timestep $t > 25$, P_0^d is changed to $P_0^d = (0.04, 0.4, 0.2, 0.2)^T$ and at timestep $t > 45$, Q_0^d is changed to $Q_0^d = (3.78, 1.8, 0, 4)^T$. The frequency and voltage response to the control inputs is provided in Figure 3.2. From Figure 3.2 we can see how the controller proposed in Theorem 3.3.3 regulates the frequency after a disturbance back to its desired value. Furthermore we notice that controller (3.42) is able regulate the voltage to its desired value. Although the proven results hold only locally, the simulations provide evidence that the proposed controllers perform well in a wide range around the desired values.

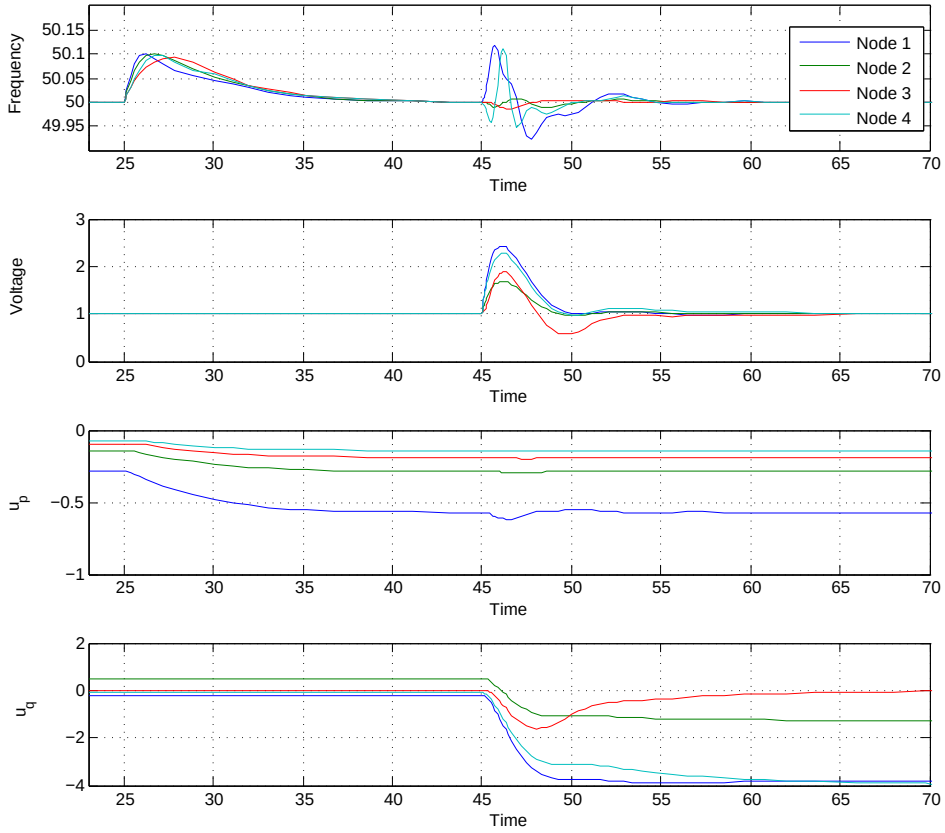

Figure 3.2: Frequency and voltage response to changing values of P_0^d and Q_0^d and its corresponding control inputs u^P and u^Q. The value of P_0^d is changed at timestep 25 and Q_0^d at timestep 45.

Published in:

S. Trip, T.W. Scholten and C. De Persis – *"Optimal regulation of flow networks with transient constraints,"* 2017, under review.

S. Trip, T.W. Scholten and C. De Persis – *"Optimal regulation of flow networks with input and flow constraints,"* Proceedings of the 2017 IFAC World Congress, 2017, pp. 9854–9859, Toulouse, FR, 2017.

Chapter 4

Output regulation of flow networks with input and flow constraints

Abstract

In this chapter we show how techniques that were proven useful in the previous chapters can be adapted, to study the (optimal) coordination of general flow networks with storage capabilities at the nodes. Particularly, we show how a class of high voltage direct current (HVDC) networks fit within the considered model of a flow network. The control objective is to regulate the measured output (e.g storage levels or voltages) towards the desired value. In contrast to Chapter 2 and Chapter 3, the subsystems at the nodes are not 'output strictly incrementally passive' (i.e. the nodes are undamped), posing new challenges to the controller design. We present a distributed controller that dynamically adjusts the node injections and flows, to achieve output regulation in the presence of an unknown disturbance, while satisfying given input and flow constraints. Optimal coordination among the inputs, minimizing a suitable cost function, is achieved by exchanging information over a communication network. Exploiting an incremental passivity property, the desired steady state is proven to be globally asymptotically stable under the closed loop dynamics. In addition to the study of a multi-terminal HVDC network, a study on a district heating system shows the the effectiveness of the proposed solution.

4.1 Flow networks

Consider a network of physically interconnected *undamped* dynamical systems. The topology of the system is described by a graph $\mathcal{G} = (\mathcal{V}, \mathcal{E})$, where $\mathcal{V} = \{1, ..., n\}$ is the set of nodes and $\mathcal{E} = \{1, ..., m\}$ is the set of edges connecting the nodes. We represent the topology by its corresponding incidence matrix $\mathcal{B} \in \mathbb{R}^{n \times m}$, where $\mathcal{B}$ is defined by arbitrarily labelling the ends of the edges in $\mathcal{E}$ with a '$+$' and a '$-$', and

letting

$$\mathcal{B}_{ik} = \begin{cases} +1 & \text{if node } i \text{ is the positive end of edge } k \\ -1 & \text{if node } i \text{ is the negative end of edge } k \\ 0 & \text{otherwise.} \end{cases}$$

The evolution of state x_i at node i is given by[1]

$$\begin{aligned} \tau_{x_i}\dot{x}_i(t) &= -\sum_{k\in\mathcal{N}_i} \mathcal{B}_{ik}u_{fk}(t) + u_{pi}(t) - d_i \\ y_i(t) &= h_i(x_i(t)), \end{aligned} \tag{4.1}$$

where $u_{pi}(t)$ is the input, τ_{x_i} a constant, $\mathcal{N}_i$ is the set of edges connected to node i, $u_{fk}(t)$ is the flow on edge k, $y_i = h_i(x_i)$ is the measured output at node i with $h_i(\cdot)$ a continuously differentiable and strictly increasing function and d_i is a constant *unknown* disturbance. We can represent the complete network compactly as

$$\begin{aligned} \tau_x\dot{x} &= -\mathcal{B}u_f + u_p - d \\ y &= h(x). \end{aligned} \tag{4.2}$$

System (4.2) has been studied in various settings where the state x is often identified with the storage or inventory at the nodes. We provide two case studies where system (4.2) is applicable in Section 6 of this chapter.

4.2 Optimal regulation with input and flow constraints

In this section we discuss the control objective and the various input and flow constraints under which the objective should be reached. We start with discussing the two control objectives. The first objective is concerned with the output $y = h(x)$ in (4.2), at steady state.

Objective 4.2.1 (Output regulation)**.** *Let $\overline{y} \in \mathcal{R}(h(x))$ be a desired constant setpoint, then the output $y = h(x)$ of (4.2) asymptotically converges to $\overline{y}$, i.e.*

$$\lim_{t\to\infty} \|h(x(t)) - \overline{y}\| = \mathbf{0}. \tag{4.3}$$

Any constant steady state $\overline{x}$ that satisfies $h(\overline{x}) = \overline{y}$ necessarily implies that system (4.2) satisfies

$$\mathbf{0} = -\mathcal{B}u_f + u_p - d. \tag{4.4}$$

[1]We assume that on every node i there is an input u_{pi}. An extension towards the partial absence of inputs can be achieved by following a similar argumentation as is presented in this chapter (Trip, Scholten and De Persis 2017b).

Premultiplying both sides of (4.4) with $\mathbb{1}^T$ results in

$$0 = \mathbb{1}^T u_p - \mathbb{1}^T d, \tag{4.5}$$

such that at a steady state the total input to the network needs to be equal to the total disturbance. Since any u_p solving (4.5) is not unique when $n \geq 2$, it is natural to wonder if the total input can be coordinated optimally among the nodes. To this end, we assign a strictly convex linear-quadratic cost function $C_i(u_{pi})$ to each node of the form

$$C_i(u_{pi}) = \frac{1}{2} q_i u_{pi}^2 + r_i u_{pi} + s_i, \tag{4.6}$$

with $q_i \in \mathbb{R}_{>0}$ and $s_i, r_i \in \mathbb{R}$. The total cost can be expressed as

$$\begin{aligned} C(u_p) &= \sum_{i \in \mathcal{V}} C_i(u_{pi}) \\ &= \frac{1}{2} u_p^T Q u_p + r^T u_p + s, \end{aligned} \tag{4.7}$$

where $Q = \text{diag}(q_1, \ldots, q_n)$, $r = (r_1, \ldots, r_n)^T$ and $s = \Sigma_{i=1}^n s_i$. Minimizing (4.7) while satisfying the equilibrium condition

$$\mathbf{0} = -\mathcal{B} u_f + u_p - d, \tag{4.8}$$

gives rise to the following optimization problem:

$$\begin{aligned} \underset{u_p, u_f}{\text{minimize}} \quad & C(u_p) \\ \text{subject to} \quad & \mathbf{0} = -\mathcal{B} u_f + u_p - d. \end{aligned} \tag{4.9}$$

It is possible to explicitly characterize the solution to (4.9), similarly as we have done in Lemma 2.3.1:

Lemma 4.2.2 (Solution to optimization problem (4.9))**.** *The solution to (4.9) is given by*

$$\overline{u}_p = Q^{-1}(\mu - r), \tag{4.10}$$

where

$$\mu = \frac{\mathbb{1}\mathbb{1}^T}{\mathbb{1}^T Q^{-1} \mathbb{1}} (d + Q^{-1} r). \tag{4.11}$$

Remark 4.2.3 (Identical marginal costs)**.** *Note that we can rewrite (4.10) as*

$$\mu = Q \overline{u}_p + r, \tag{4.12}$$

and that $\mu \in \text{Im}(\mathbb{1})$. It follows that at the solution to (4.9) we have that for all $i \in \mathcal{V}$ the so-called marginal costs $q_i u_{pi} + r_i$ are identical.

We are now ready to state the second control objective.

Objective 4.2.4 (Optimal feedforward input)**.** *The input at the nodes asymptotically converge to the solution to (4.9), i.e.*

$$\lim_{t\to\infty} \|u_p(t) - \overline{u}_p\| = 0, \tag{4.13}$$

with $\overline{u}_p$ as in (4.10).

We now turn our attention to possible constraints on the input and the flows under which the objectives should be reached. First, in physical systems the input u_p is generally constrained by a minimum value (often zero, preventing a negative input) and maximum value, representing e.g. a production capacity.

Constraint 4.2.5 (Input limitations)**.** *The inputs at the nodes satisfy*

$$u_p^- < u_p(t) < u_p^+ \quad \text{for all } t \geq 0, \tag{4.14}$$

where $u_p^-, u_p^+ \in \mathbb{R}^n$ are constant vectors and the inequalities hold componentwise.

Second, the flows on the edges are often constrained to be unidirectional and to be within the capacity of the edges.

Constraint 4.2.6 (Flow capacity)**.** *The flows on the edges satisfy*

$$u_f^- < u_f(t) < u_f^+ \quad \text{for all } t \geq 0, \tag{4.15}$$

where $u_f^-, u_f^+ \in \mathbb{R}^m$ are constant vectors and the inequalities hold componentwise.

Note that physical limitations and safety requirements demand that the constraints should be satisfied *for all time* and not only at a steady state.

Remark 4.2.7 (Unconstrained case)**.** *The unconstrained case can be regarded as a particular example of the considered setting. This is obtained by taking as a lower and upper bound for u_{pi}, u_{fi} respectively $-\infty$ and ∞.*

Before we design a distributed control scheme in the next section, we assume that the considered problem is feasible.

Assumption 4.2.8 (Feasibility)**.** *For a given d, its corresponding $\overline{u}_p$ given by (4.10) satisfies $u_p^- < \overline{u}_p < u_p^+$, and there exists a, possibly non-unique, $u_f^- < \overline{u}_f < u_f^+$ that satisfies*

$$\mathbf{0} = -\mathcal{B}\overline{u}_f + \overline{u}_p - d. \tag{4.16}$$

4.3 Controller design

In this section we propose *distributed* input and flow controllers that satisfy the various objectives and constraints discussed in the previous section, whereas the stability of the closed loop system is discussed in the next section. For convenience we summarize the objectives and constraints yielding the following controller design problem.

Problem 4.3.1 (Controller design problem)**.** *Design distributed controllers that regulate inputs u_p at the nodes and the flows u_f on the edges, such that*

$$\begin{aligned} \lim_{t\to\infty} \|h(x(t)) - \overline{y}\| &= 0 \\ \lim_{t\to\infty} \|u_p(t) - \overline{u}_p\| &= 0, \end{aligned} \tag{4.17}$$

where $\overline{u}_p$ is as in (4.10). Furthermore,

$$\begin{aligned} u_p^- < & u_p(t) < u_p^+ \\ u_f^- < & u_f(t) < u_f^+, \end{aligned} \tag{4.18}$$

should hold componentwise for all $t \geq 0$.

First, we focus on the input controller. Inspired by the result in (Trip and De Persis 2016a) (see also Section 8.5), where a similar control problem is considered in the setting of power networks, we propose the controller

$$\begin{aligned} \tau_\theta \dot{\theta} &= -g(\theta) + \phi - (h(x) - \overline{y}) \\ \tau_\phi \dot{\phi} &= -\phi + g(\theta) - \beta Q \mathcal{L}^{com}(Q\phi + r) \\ u_p &= g(\theta), \end{aligned} \tag{4.19}$$

where $\mathcal{L}^{com}$ is the Laplacian matrix reflecting the communication topology, $\beta \in \mathbb{R}_{>0}$ and $g(\theta) : \mathbb{R}^n \to \mathbb{R}^n$ is a mapping with suitable properties that will be discussed in Assumption 3 below. Note that only information on $q_i\phi_i + r_i$ needs to be exchanged among neighbours. As we will discuss in the stability analysis in the next section, controller (4.19) ensures that $g(\theta)$ converges to ϕ, whereas the communication term ensures that additionally at steady state a consensus is obtained in the marginal costs, i.e. $Qg(\overline{\theta})+r \in \mathrm{Im}(\mathbb{1})$. In order to guarantee that all marginal costs converge to the same value we make the following assumption on the communication network.

Assumption 4.3.2 (Communication network)**.** *The graph reflecting the communication topology is undirected and connected.*

Now let us focus on the flow controller. We consider a controller of the following form

$$\begin{aligned} \tau_\lambda \dot{\lambda} &= \mathcal{B}^T(h(x) - \overline{y}) \\ u_f &= f(\lambda), \end{aligned} \tag{4.20}$$

where $\mathcal{B}$ is again the incidence matrix reflecting the topology of the physical network and $f(\lambda) : \mathbb{R}^n \to \mathbb{R}^n$ is a mapping with suitable properties discussed in Assumption 3 below. Note that the flow controller on edge k only requires information of its adjacent nodes. Together with the information exchange among neighbours in (4.19) we have that the proposed control scheme is indeed fully distributed.

The proposed controller guarantees that constraints (4.14) and (4.15) are satisfied by properly selecting $f(\lambda)$ and $g(\theta)$. Since we have that $u_p = g(\theta)$ and $u_f = f(\lambda)$, the following assumption is sufficient to ensure that the inputs and flows do not exceed their limitations.

Assumption 4.3.3 (Bounded controller outputs)**.** *Mappings $g(\theta)$ and $f(\lambda)$, in respectively (4.19) and (4.20) are continuously differentiable and strictly increasing, satisfying*

$$\begin{aligned} u_f^- < f(\lambda) < u_f^+ \\ u_p^- < g(\theta) < u_p^+, \end{aligned} \tag{4.21}$$

where the inequalities hold componentwise. Moreover, $g(\theta)$ and $f(\lambda)$ are such that $\overline{u}_f \in \mathcal{R}(f(\lambda))$ and $\overline{u}_p \in \mathcal{R}(g(\theta))$, with $\overline{u}_f$ and $\overline{u}_p$ as in Assumption 4.2.8.

Note that Assumption 4.3.3 is not restrictive as it includes e.g. $\xi(z) = z$ in absence of any constraints and also the constraint enforcing functions $\xi(z) = \tanh(z)$, $\xi(z) = \arctan(z)$ (see also the case studies in Section 4.5).

Before we analyse the stability of the system we investigate the properties of the steady state. To do so, we write system (4.2) in closed loop with controllers (4.19) and (4.20), obtaining

$$\begin{aligned} \tau_x \dot{x} &= -\mathcal{B} f(\lambda) + g(\theta) - d \\ \tau_\lambda \dot{\lambda} &= \mathcal{B}^T(h(x) - \overline{y}) \end{aligned} \tag{4.22a}$$

$$\begin{aligned} \tau_\theta \dot{\theta} &= -g(\theta) + \phi - (h(x) - \overline{y}) \\ \tau_\phi \dot{\phi} &= -\phi + g(\theta) - \beta Q \mathcal{L}^{com}(Q\phi + r). \end{aligned} \tag{4.22b}$$

We will now show that under Assumptions 4.2.8–4.3.3 there exists at least one steady state of system (4.22). Moreover, all steady states of system (4.22) satisfy the control objectives.

Lemma 4.3.4 (Satisfying objectives 1 and 2)**.** *Let Assumptions 4.2.8, 4.3.2 and 4.3.3 hold, then there exists a steady state of system (4.22). Moreover, all steady states satisfy $h(\overline{x}) = \overline{y}$ and $g(\overline{\theta}) = \overline{u}_p$, where $\overline{u}_p$ is the optimal control input given by (4.10).*

Proof. Due to Assumption 4.2.8 and 4.3.3 we have that there exists a $\overline{\lambda}$ and $\overline{\theta}$ such that

$$\mathbf{0} = -\mathcal{B}f(\overline{\lambda}) + g(\overline{\theta}) - d, \tag{4.23}$$

where $g(\overline{\theta}) = \overline{u}_p$ and $\overline{u}_p$ as in (4.10). Moreover, from $\overline{y} \in \mathcal{R}(h(x))$, there exists a $\overline{x}$ such that

$$\mathbf{0} = h(\overline{x}) - \overline{y}. \tag{4.24}$$

When we additionally take $\overline{\phi} = \overline{u}_p$ it is immediate to veriy that

$$\begin{aligned}
\mathbf{0} =& -\mathcal{B}f(\overline{\lambda}) + g(\overline{\theta}) - d \\
\mathbf{0} =& \ \mathcal{B}^T(h(\overline{x}) - \overline{y}) \\
\mathbf{0} =& -g(\overline{\theta}) + \overline{\phi} - (h(\overline{x}) - \overline{y}) \\
\mathbf{0} =& -\overline{\phi} + g(\overline{\theta}) - \beta Q\mathcal{L}^{com}(Q\overline{\phi} + r),
\end{aligned} \tag{4.25}$$

is satisfied and proves existence of a steady state. We will now show that (4.25) necessarily implies that $h(\overline{x}) = \overline{y}$ and $g(\overline{\theta}) = \overline{u}_p$. From $\mathbf{0} = \mathcal{B}^T(h(\overline{x}) - \overline{y})$, it follows that $h(\overline{x}) - \overline{y} = c_1(t)\mathbb{1}$, where $c_1(t) \in \mathbb{R}$ is a function. It follows that

$$g(\overline{\theta}) - \overline{\phi} = c_1(t)\mathbb{1}. \tag{4.26}$$

Substituting this in the last equation of (4.25) yields

$$\begin{aligned}
\mathbf{0} &= c_1(t)\mathbb{1} - \beta Q\mathcal{L}^{com}(Q\overline{\phi} + r) \\
&= c_1(t)Q^{-1}\mathbb{1} - \beta\mathcal{L}^{com}(Q\overline{\phi} + r).
\end{aligned} \tag{4.27}$$

Premultiplying both sides of the previous equation by $\mathbb{1}^T$ yields

$$0 = c_1(t)\mathbb{1}^T Q^{-1}\mathbb{1}. \tag{4.28}$$

Since Q is a diagonal matrix with only positive elements, it follows that $c_1(t) = 0$ and that $h(\overline{x}) = \overline{y}$. As a consequence we have that $\overline{\phi} = g(\overline{\theta})$ such that

$$\mathbf{0} = -\beta Q\mathcal{L}^{com}(Qg(\overline{\theta}) + r). \tag{4.29}$$

Since also

$$\mathbf{0} = -\beta Q\mathcal{L}^{com}(Q\overline{u}_p + r), \tag{4.30}$$

we have that $g(\overline{\theta}) = \overline{u}_p + c_2(t)Q^{-1}\mathbb{1}$, where $c_2(t) \in \mathbb{R}$ is a scalar. Premultiplying the first equation of (4.25) by $\mathbb{1}^T$ and exploiting that $\mathbb{1}^T(\overline{u}_p - d) = 0$ yields

$$\begin{aligned} 0 &= \mathbb{1}^T(\overline{u}_p + c_2(t)Q^{-1}\mathbb{1} - d) \\ &= c_2(t)\mathbb{1}^T Q^{-1}\mathbb{1}, \end{aligned} \tag{4.31}$$

such that $c_2(t) = 0$ and consequently $g(\overline{\theta}) = \overline{u}_p$. ■

4.4 Stability analysis

In this section we analyze the stability of the closed-loop system (4.22). The analysis is foremost based on LaSalle's invariance principle and exploits useful properties of interconnected incrementally passive systems (Definition 1.4.1). Throughout the coming discussion we will regularly use a storage function containing the term

$$U(z) = \int_{\overline{z}}^{z} \xi(y) - \xi(\overline{z})dy, \tag{4.32}$$

where $z \in \mathbb{R}$. We can show that $U(z)$ is radially unbounded, i.e. $\lim_{\|z\|\to\infty} U(z) = \infty$, under suitable restrictions on ξ. In fact, a sufficient condition on ξ is that it is strictly increasing as we will show below.

Lemma 4.4.1 (Radial unboundedness)**.** *Let $\xi(z)$ be a strictly increasing continuous function, then $U(z)$ as in (4.32) is radially unbounded.*

Proof. First, consider the case where $z \to \infty$. Since $\xi(z)$ is strictly increasing and continuous we have that there exists a $z_+ > \overline{z}$, such that $\xi(z) - \xi(\overline{z}) > \epsilon$, for $\epsilon > 0$ and $z > z_+$. We have that

$$\begin{aligned} \lim_{z\to\infty} U(z) &= \lim_{z\to\infty} \int_{\overline{z}}^{z} \xi(y) - \xi(\overline{z})dy, \\ &= \int_{\overline{z}}^{z_+} \xi(y) - \xi(\overline{z})dy + \lim_{z\to\infty} \int_{z_+}^{z} \xi(y) - \xi(\overline{z})dy \\ &\geq \int_{\overline{z}}^{z_+} \xi(y) - \xi(\overline{z})dy + \lim_{z\to\infty} \int_{z_+}^{z} \epsilon dy \\ &= \infty. \end{aligned} \tag{4.33}$$

A similar argument holds for the case where $z \to -\infty$. ■

We now proceed with establishing the incremental passivity property of (4.22a).

Lemma 4.4.2 (Incremental passivity of (4.22a))**.** *Let Assumptions 4.2.8, 4.3.2 and 4.3.3 hold. System (4.22a) with input $g(\theta)$ and output $h(x)$ is an incrementally passive system, with respect to $(\overline{x}, \overline{\theta}, \overline{\lambda})$ satisfying*

$$\begin{aligned} \mathbf{0} &= -\mathcal{B} f(\overline{\lambda}) + g(\overline{\theta}) - d \\ \mathbf{0} &= \mathcal{B}^T (h(\overline{x}) - \overline{y}). \end{aligned} \tag{4.34}$$

Namely, there exists a radially unbounded storage function $\mathcal{S}_1(x, \overline{x}, \lambda, \overline{\lambda})$ which satisfies the following incremental dissipation equality

$$\dot{\mathcal{S}}_1 = (h(x) - h(\overline{x}))^T (g(\theta) - g(\overline{\theta})), \tag{4.35}$$

along the solutions to (4.22a).

Proof. Consider the storage function

$$\begin{aligned} \mathcal{S}_1 = &\sum_{i \in \mathcal{V}} \tau_{x_i} \int_{\overline{x}_i}^{x_i} h_i(y) - h_i(\overline{x}_i) dy \\ &+ \sum_{i \in \mathcal{E}} \tau_{\lambda_k} \int_{\overline{\lambda}_k}^{\lambda_k} f_k(y) - f_k(\overline{\lambda}_k) dy. \end{aligned} \tag{4.36}$$

Since $h_i(x_i)$ and $f_k(\lambda_k)$ are strictly increasing functions we have, exploiting Lemma 3, that $\mathcal{S}_1$ is radially unbounded. Furthermore, we have that along the solutions to (4.22a) $\mathcal{S}_1$ satisfies

$$\begin{aligned} \dot{\mathcal{S}}_1 &= (h(x) - h(\overline{x}))^T \tau_x \dot{x} + (f(\lambda) - f(\overline{\lambda}))^T \tau_\lambda \dot{\lambda} \\ &= (h(x) - h(\overline{x}))^T (-\mathcal{B} f(\lambda) + g(\theta) - d) \\ &\quad + (f(\lambda) - f(\overline{\lambda}))^T \mathcal{B}^T (h(x) - \overline{y}) \\ &= (h(x) - h(\overline{x}))^T (-(\mathcal{B} f(\lambda) - f(\overline{\lambda})) + (g(\theta) - g(\overline{\theta})) \\ &\quad + (f(\lambda) - f(\overline{\lambda}))^T \mathcal{B}^T (h(x) - \overline{y}) \\ &= (h(x) - h(\overline{x}))^T (g(\theta) - g(\overline{\theta})), \end{aligned} \tag{4.37}$$

where we have exploited (4.34) in the last equality and that $h(\overline{x}) = \overline{y}$. ■

We now prove a similar result for (4.22b).

Lemma 4.4.3 (Incremental passivity of (4.22b))**.** *Let Assumptions 4.2.8, 4.3.2 and 4.3.3 hold. System (4.22a) with input $-h(x)$ and output $g(\theta)$ is an incrementally passive system, with respect to $(\overline{x}, \overline{\theta}, \overline{\phi})$ satisfying*

$$\begin{aligned} \mathbf{0} &= -g(\overline{\theta}) + \overline{\phi} - (h(\overline{x}) - \overline{y}) \\ \mathbf{0} &= -\overline{\phi} + g(\overline{\theta}) - \beta Q \mathcal{L}^{com} (Q\overline{\phi} + r). \end{aligned} \tag{4.38}$$

Namely, there exists a radially unbounded storage function $\mathcal{S}_2(\theta, \overline{\theta}, \phi, \overline{\phi})$ which satisfies the following incremental dissipation equality

$$\begin{aligned}\dot{\mathcal{S}}_2 = &- (g(\theta) - \phi)^T (g(\theta) - \phi) - \beta (Q\phi + r)^T \mathcal{L}^{com} (Q\phi + r) \\ &- (g(\theta) - g(\overline{\theta}))^T (h(x) - h(\overline{x}))\end{aligned} \tag{4.39}$$

along the solutions to (4.22b).

Proof. Consider the storage function

$$\mathcal{S}_2 = \sum_{i \in \mathcal{V}} \tau_{\theta_i} \int_{\overline{\theta}_i}^{\theta_i} g_i(y) - g_i(\overline{\theta}_i) dy + \frac{1}{2} (\phi - \overline{\phi})^T \tau_\phi (\phi - \overline{\phi}). \tag{4.40}$$

Since $g_i(\theta_i)$ is a strictly increasing function we have, exploiting Lemma 3, that $\mathcal{S}_2$ is radially unbounded. Furthermore, we have that along the solutions to (4.22b) $\mathcal{S}_2$ satisfies

$$\begin{aligned}\dot{\mathcal{S}}_2 &= (g(\theta) - g(\overline{\theta}))^T \tau_\theta \dot{\theta} + (\phi - \overline{\phi})^T \tau_\phi \dot{\phi} \\ &= (g(\theta) - g(\overline{\theta}))^T (-g(\theta) + \phi - (h(x) - \overline{y})) \\ &\quad + (\phi - \overline{\phi})^T (-\phi + g(\theta) - \beta Q \mathcal{L}^{com} (Q\phi + r)) \\ &= - (g(\theta) - \phi)^T (g(\theta) - \phi) - \beta (Q\phi + r)^T \mathcal{L}^{com} (Q\phi + r) \\ &\quad - (g(\theta) - g(\overline{\theta}))^T (h(x) - h(\overline{x})),\end{aligned} \tag{4.41}$$

where we have exploited (4.38), $h(\overline{x}) = \overline{y}$, $(Q\overline{\phi} + r)^T \mathcal{L}^{com} = \mathbf{0}$ and that $\overline{\phi} = g(\overline{\theta})$. ■

Exploiting the previous lemmas, we are now ready to prove the main result of this chapter.

Theorem 4.4.4 (Main result)**.** *Let Assumptions 4.2.8, 4.3.2 and 4.3.3 hold. System (4.22) globally approaches the set where $h(x) = \overline{y}$ and where $u_p = \overline{u}_p$ as given in (4.10). Moreover, u_p and u_f satisfy constraints (4.14) and (4.15) for all $t \geq 0$.*

Proof. Satisfying constraints (4.14) and (4.15) for all $t \geq 0$ follows from the design of $g(\theta)$ and $f(\lambda)$ and Assumption 3. From Lemma 4.4.2 and Lemma 4.4.3 we have that $\mathcal{S} = \mathcal{S}_1 + \mathcal{S}_2$ satisfies along the solutions to (4.22)

$$\dot{\mathcal{S}} = - (g(\theta) - \phi)^T (g(\theta) - \phi) - \beta (Q\phi + r)^T \mathcal{L}^{com} (Q\phi + r). \tag{4.42}$$

Since $\mathcal{S}$ is radially unbounded we can conclude that all solutions to (4.22) remain bounded. We can therefore invoke LaSalle's invariance principle and infer that the system approaches the largest invariant set contained in the set where $\dot{\mathcal{S}} = 0$. This set where $\dot{\mathcal{S}} = 0$ is characterized by

$$\Upsilon = \{x, \lambda, \theta, \phi | \phi = g(\theta), Q\phi + r \in \mathrm{Im}(\mathbb{1})\}, \tag{4.43}$$

where $Q\phi + r \in \mathrm{Im}(\mathbb{1})$ follows from the communication graph being connected. Bearing additionally in mind that

$$Qg(\overline{\theta}) + r \in \mathrm{Im}(\mathbb{1}), \tag{4.44}$$

we have that on the invariant set that

$$g(\theta) = g(\overline{\theta}) + Q^{-1}\mathbb{1}c(t), \tag{4.45}$$

where $c(t) : \mathbb{R} \to \mathbb{R}$ is a function. On this set, the solutions to (4.22) satisfy

$$\begin{aligned} \tau_x \dot{x} &= -\mathcal{B}f(\lambda) + g(\overline{\theta}) + Q^{-1}\mathbb{1}c(t) - d \\ \tau_\lambda \dot{\lambda} &= \mathcal{B}^T(h(x) - \overline{y}) \\ \tau_\theta \dot{\theta} &= -(h(x) - \overline{y}) \\ \tau_\phi \dot{\phi} &= \mathbf{0}. \end{aligned} \tag{4.46}$$

We now argue that on the invariant set we need to have

$$(x - \overline{x}) = \mathbf{0}. \tag{4.47}$$

Bearing in mind that $\phi = g(\theta)$ and since the solutions to (4.46) are differentiable, we have that on the invariant set $\dot{\phi} = \frac{\partial g(\theta)}{\partial \theta}\dot{\theta}$. Since $g(\theta)$ is a strictly increasing mapping, it follows that $\frac{\partial g(\theta)}{\partial \theta} \neq \mathbf{0}$ and that $\dot{\theta} = \mathbf{0}$. Therefore, $h(x) = \overline{y}$ on the invariant set and consequently $x = \overline{x}$.

Next we prove that on the invariant set $g(\theta) = g(\overline{\theta})$. Note that it is sufficient to prove that $c(t) = 0$. Since $\overline{x}$ is constant and $x = \overline{x}$ we obtain that $\dot{x} = \mathbf{0}$. From this, together with (4.46) we can conclude that we approach the set where

$$\mathbf{0} = -\mathcal{B}f(\lambda) + g(\overline{\theta}) + Q^{-1}\mathbb{1}c(t) - d. \tag{4.48}$$

Pre-multiplying both sides with $\mathbb{1}^T$ yields

$$\begin{aligned} 0 &= \mathbb{1}^T(g(\overline{\theta}) - d) + \mathbb{1}^T Q^{-1}\mathbb{1}c(t) \\ &= \mathbb{1}^T Q^{-1}\mathbb{1}c(t). \end{aligned} \tag{4.49}$$

Since Q^{-1} is a diagonal matrix with only positive elements, we have that $c(t) = 0$. We can therefore conclude that we indeed approach the set where $h(x) = h(\overline{x})$ and where $u_p = g(\theta) = g(\overline{\theta}) = \overline{u}_p$ and that the constraints (4.14) and (4.15) are satisfied for all $t \geq 0$. ■

Remark 4.4.5 (Avoiding oscillations)**.** *It is natural to compare (4.19) with a controller of the form*

$$\begin{aligned} \tau_\theta \dot{\theta} =& -\beta Q \mathcal{L}^{com}(Qg(\theta) + r) - (h(x) - \overline{y}) \\ u_p =& \, g(\theta), \end{aligned} \tag{4.50}$$

as both admit a steady state where $h(\overline{x}) = \overline{y}$ and $g(\overline{\theta}) = \overline{u}_p$. However, in contrast to (4.22) for which we will prove global convergence to the desired state, system

$$\begin{aligned} \tau_x \dot{x} =& -\mathcal{B} f(\lambda) + g(\theta) - d \\ \tau_\lambda \dot{\lambda} =& \, \mathcal{B}^T (h(x) - \overline{y}) \\ \tau_\theta \dot{\theta} =& -\beta Q \mathcal{L}^{com}(Qg(\theta) + r) - (h(x) - \overline{y}), \end{aligned} \tag{4.51}$$

can converge (depending on Q) to a limit cycle exhibiting oscillatory behavior (Scholten et al. 2016).

Remark 4.4.6 (Local results)**.** *Note that the global convergence result is a consequence of the strictly increasing behavior of the nonlinear functions $f_k(\lambda_k)$, $g_i(\theta_i)$ and $h_i(x_i)$. In case that the functions are increasing on a finite interval, a local result of Theorem 1 can be derived. An important class of functions for which this holds are odd functions that are not necessarily increasing on the whole domain, such as the sinusoidal function.*

4.5 Case study

To illustrate how various physical systems can be regarded as a flow network and to show the performance of the proposed controllers we consider two case studies. The first case study considers a district heating system, whereas the second case study considers a multi-terminal HVDC network.

4.5.1 District heating systems

Building upon the results presented in (Scholten et al. 2015), we consider a district heating system with a topology as depicted in Figure 4.1. Each node represents a producer, a consumer and a stratified storage tank (see Figure 4.2). The storage tank consists of a hot and a cold layer of water, both with variable volumes. We denote the volume of the hot layer of water at node i as x_i (m^3), which is also the output of the system, i.e. $h_i(x_i) = x_i$. The various nodes are interconnected via a pipe network $\mathcal{G}$. Following (Scholten et al. 2015), the dynamics for the hot layer can be derived by applying mass conservation laws resulting in the following representation of the

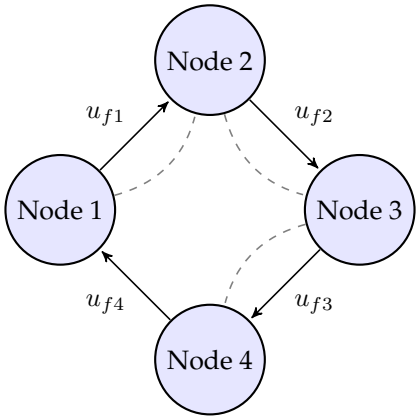

Figure 4.1: Topology of the considered heat network. The arrows indicate the required flow directions in the heat network, while the dashed lines represent the communication network used by the controllers.

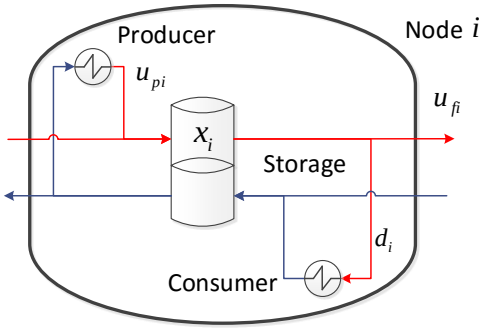

Figure 4.2: A node in the district heating network.

district heating system:

$$\dot{x} = -\mathcal{B}u_f + u_p - d, \tag{4.52}$$

where u_f (m^3/h) denotes the flow through the pipes. Moreover, u_p (m^3/h) and d (m^3/h) are respectively the flows trough the heat exchangers of the producers and the consumers. It is immediate to see that (4.52) has identical dynamics as (4.2) if we set $\tau_x = I$. The controllers (4.19) and (4.20) are therefore applicable and we study the obtained closed-loop system. We perform a simulation over a 40 hour time interval in which we evaluate the response to a change in demand at $t = 12$ and change in

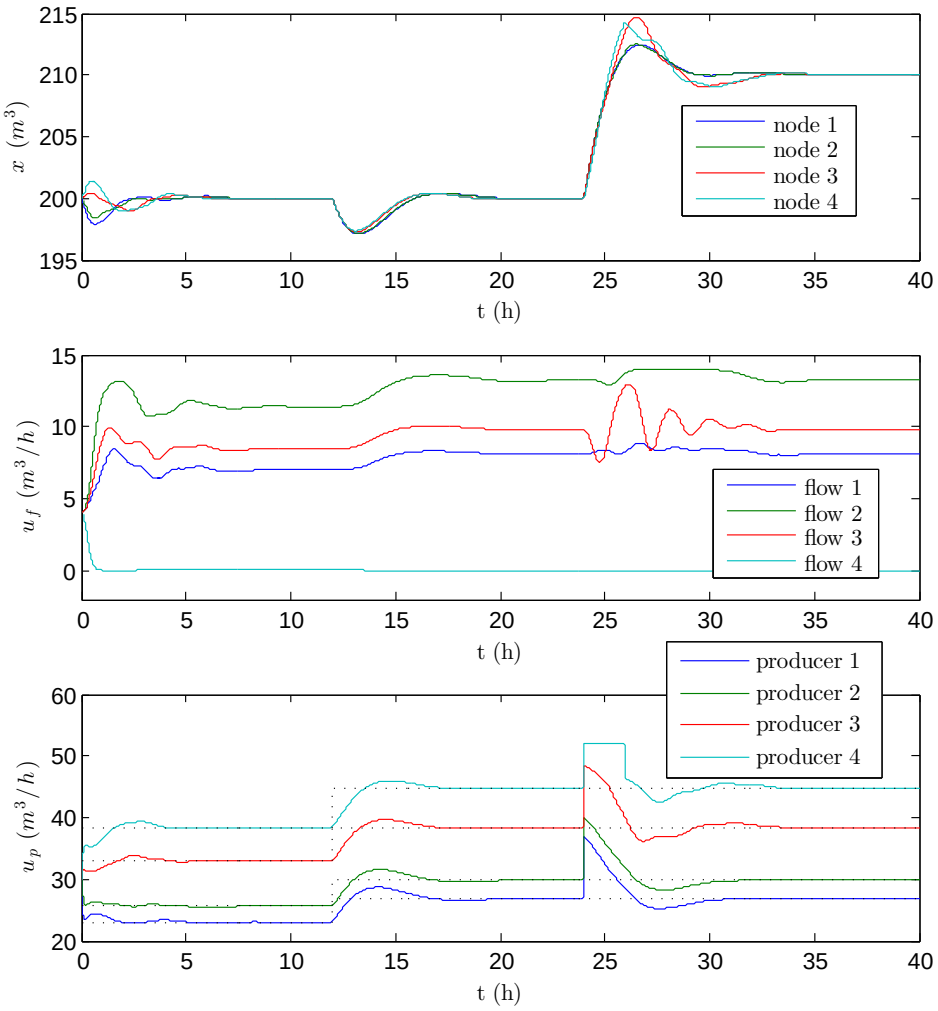

Figure 4.3: Volumes, flows and productions of the district heating system during a 40 hour period. The optimal production $\overline{u}_p$ as in (4.10) is indicated by dotted lines in the lower plot.

setpoint at $t = 24$. The cost functions of the four producers are purely quadratic, i.e. $s = r = \mathbf{0}$ and

$$Q = \operatorname{diag}\begin{pmatrix} 10 & 9 & 7 & 6 \end{pmatrix}.$$

Initially the volume is identical to the first setpoint $x(0) = \overline{x} = \begin{bmatrix}200 & 200 & 200 & 200\end{bmatrix}^T$ for all $t < 24$. The initial demand is given by $d = \begin{bmatrix}30 & 30 & 30 & 30\end{bmatrix}^T$ for all $t < 12$, which is increased at $t = 12$ to $d = \begin{bmatrix}35 & 35 & 35 & 35\end{bmatrix}^T$ The setpoint for the volume $\overline{x}$ is increased at $t = 24$ to $\overline{x} = \begin{bmatrix}210 & 210 & 210 & 210\end{bmatrix}^T$. To guarantee uni-directional flows and positive production we require $u_f > 0$, $u_p > 0$ and due to capacity constraints we additional require them to be upper bounded by $14\ m^3/h$ and $52\ m^3/h$, respectively. To enforce these constraints the input is designed as

$$\begin{aligned} u_{fi}(\lambda_i) &= 7(\tanh(\lambda_i) + 1) \\ u_{pi}(\theta_i) &= 26(\tanh(\theta_i) + 1), \end{aligned}$$

where $\tanh(\cdot)$ is the hyperbolic tangent function. Finally we let $\tau_\lambda = I$, $\tau_\theta = I$, $\tau_\phi = 0.005 \cdot I$ and $\beta = 10$.
The resulting response of the system can be found in Figure 4.3, where we can clearly see the effects of the increased demand at $t = 12$ and change in setpoint at $t = 24$. More specifically, in the upper plot we can see that the controllers indeed let the volumes in the four storage tanks to converge towards the desired setpoints of $200m^3$ ($t < 24$) and $210m^3$ ($t \geq 24$). In the middle plot we see that the flows in the pipes remain within the constraint $0 < u_f < 14$ throughout the entire simulation. Finally, in the bottom plot we see the production at the four nodes and the optimal productions denoted by the dotted lines. We observe that the production converges towards the optimal value $\overline{u}_p$ and satisfies $0 < u_p < 52$ for the entire period.

4.5.2 Multi-terminal HVDC networks

As a second case study we consider multi-terminal high voltage direct current (HVDC) networks that have been recently studied in e.g. (Andreasson et al. 2016). We assume that the lines connecting the terminals are lossless such that the overall network dynamics are given by

$$\begin{aligned} \mathcal{C}\dot{V} &= -\mathcal{B}\lambda + u_p - d \\ L\dot{\lambda} &= \mathcal{B}^T V, \end{aligned} \tag{4.53}$$

where V are the voltages at the terminals, λ are the currents through the lines, d are uncontrollable current injections and u_p are controllable current injections. The corresponding circuit is provided in Figure 4.4, where $\mathcal{C}_i$ is the capacitance at the terminals and L_k is the inductance of line k. The first objective is to stabilize the voltages around the desired setpoint $\overline{V}$ which is identical for each terminal such that $\mathcal{B}^T V = \mathcal{B}^T(V - \overline{V})$. The second objective is to share the controllable current

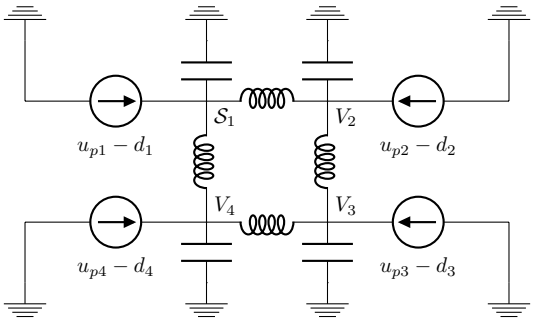

Figure 4.4: Topology of a four bus multi-terminal HVDC network. We take $\mathcal{C}_i = 57\mu F$ and $\mathcal{L}_k = 0.0135H$. for $i, k \in \{1, \ldots, 4\}$.

injections equally among the terminals. Although the currents over the lines follow from physical principles and can not be independently controlled, they have the same dynamics as (4.20) if we set $\tau_\lambda = L$. The controllers (4.19) are applied to the network with $\beta = 100, Q = I, s = \mathbf{0}, r = \mathbf{0}$, $\tau_\theta = 100$, $\tau_\phi = 0.02$. The topology of the communication network is identical to the topology of the physical network. The desired voltage is $\overline{V} = 165kV$ throughout the simulation. Initially all d_i have a value of $100A$. At $t = 0.02s$, the value of d_2 increased to $140A$, whereas d_3 is decreased to $80A$. To prevent low and high current injections during the transient we require for all nodes that $90A \leq u_{pi}(t) \leq 120A$ is satisfied. To achieve this we let

$$g_i(\theta_i) = 90 + 15\left(\tanh(\theta_i) + 1\right), \tag{4.54}$$

while $f_i(\lambda_i) = \lambda_i$, for all $i \in \{1, \ldots, 4\}$. The response to the change in demand is given in Figure 4.5, from where we conclude that the voltages converge towards their set point of $165kV$, while u_p satisfies its constraints at all time.

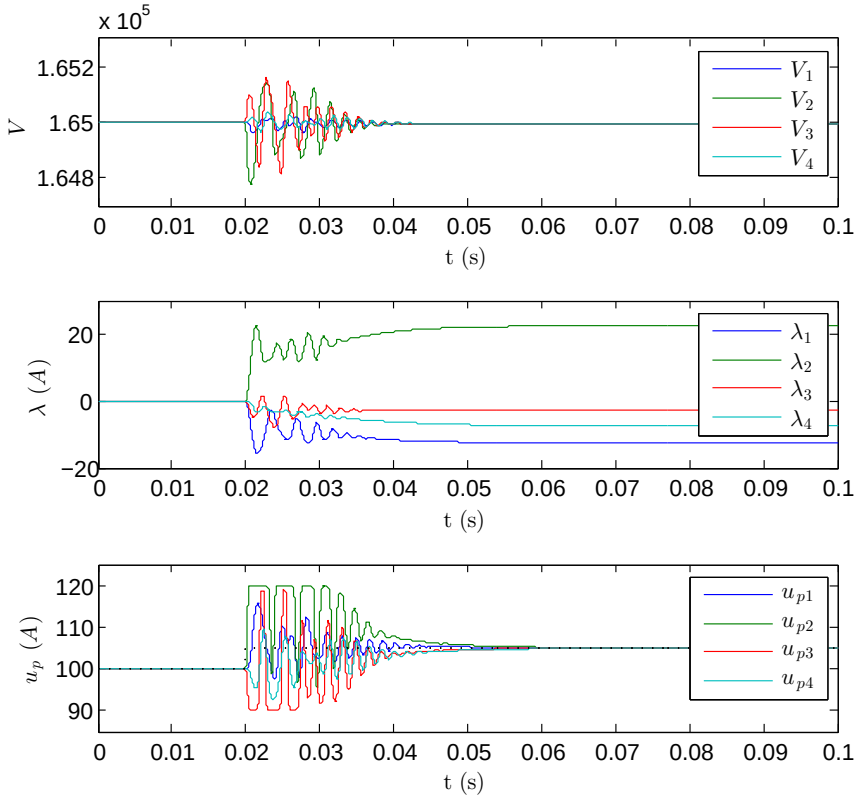

Figure 4.5: Voltages, current flows and current injections for a high voltage direct current network. The optimal production $\overline{u}_p$ as in (4.10) is indicated by dotted lines in the lower plot.

Part II

Optimal load frequency control with non-passive dynamics

Introduction

Whenever there is an imbalance between generation and load, the frequency in the power network deviates from its nominal value. This makes frequency regulation, or 'Load Frequency Control' (LFC), a critical task to maintain the stability of the network. Whereas primary droop control is utilized to act fast on smaller fluctuations to prevent destabilization, the frequency in the power network is conventionally regulated by 'Automatic Generation Control' (AGC) that acts on the reference setting of the governors. To do so, each control area determines its 'Area Control Error' (ACE) and changes the setpoints accordingly to compensate for local load changes and to maintain the scheduled tie-line power flows between the different areas (Machowski et al. 2008), (Wood and Wollenberg 1996). However, due to an ever increasing penetration of renewable energy it is uncertain if the current AGC implementations are still adequate (Apostolopoulou et al. 2016). The use of smart grids, computer-based control and communication networks offer on the other hand possibilities to improve the current practices (Pandey et al. 2013), (Ibraheem et al. 2005). Various solutions have been proposed to improve the performance of the AGC (Pan and Liaw 1989), (Liu and Ilić 2012), (Zhang et al. 2013), (Mi et al. 2013), (Yousef et al. 2014). Specifically, the effect of a large share of volatile renewable energy sources has been investigated (Variani and Tomsovic 2013), (Xu et al. 2016). Economic efficiency over slower timescales is achieved by a tertiary optimization layer, commonly called the economic dispatch, that is outside of the conventional LFC loop.

Since the AGC was designed to be completely decentralized where each control area only reacts to its own ACE, there is loss of economic efficiency on the fast timescales of LFC. Instead of enforcing a predefined power flow over tie-lines, it is cost effective to coordinate the various regulation units within the whole system. This

becomes especially relevant with a larger share of renewable energy sources where generation cannot be as accurately predicted as in the past. It is therefore desirable to further merge the secondary LFC and the tertiary optimization layer, which we call '*optimal* Load Frequency Control' (OLFC). Proposed solutions to obtain OLFC can be roughly divided into two approaches. The first approach formulates the Lagrangian dual of the economic dispatch problem and solves the optimization problem based on a distributed primal-dual gradient algorithm that runs in parallel with the network dynamics (Zhang and Papachristodoulou 2015), (Li et al. 2016), (Stegink et al. 2017), (You and Chen 2014), (Kasis et al. 2016), (Jokic et al. 2009), (Mudumbai et al. 2012), (Miao and Fan 2016), (Cai et al. 2015), (Apostolopoulou et al. 2015),(Yi et al. 2015), (Cherukuri and Cortés 2016), (Yi et al. 2016). The advantage of this approach is that capacity constraints and convex cost functions can be straightforwardly incorporated. A drawback is however that information on the amount of uncontrollable generation and load needs to be available, which is generally unknown in LFC where only the frequency is used as a proxy for the imbalance. This issue is alleviated by the second approach, realizing that in the unconstrained case the marginal costs of the various generation units are identical at a cost effective coordination. In this approach optimality is achieved by employing a distributed consensus algorithm that converges to a state of identical marginal costs (Bürger et al. 2014), (Trip et al. 2016), (Schiffer and Dörfler 2016), (Zhao et al. 2015), (Monshizadeh et al. 2016), (Andreasson et al. 2013), (Kar and Hug 2012), (Binetti et al. 2014), (Rahbari-Asr et al. 2014), (Yang et al. 2013), (Yang et al. 2016). Although OLFC has been proposed as viable alternative to the conventional AGC, it poses the fundamental question if incorporating the economic dispatch into the LFC deteriorates the stability of the power network (Alvarado et al. 2001).

Contributions

Part II of this thesis continues and extends the study of the closed loop stability of OLFC and the power network. Particularity, we build upon the results presented in Chapter 2, where we exploit an incremental passivity property of the power network to design distributed controllers achieving OLFC. However, on the generation side there are still remaining challenges to include realistic models required in the study of frequency regulation. This is mainly due to the fact the the most commonly used second order model of the turbine-governor dynamics does not allow for a passive interconnection with the power network. Despite the recent advances in the analysis of OLFC in closed loop with the power network that allows to study the stability in presence of detailed generator models (Trip et al. 2016), (Stegink et al. 2016)

and improved network representations (Schiffer and Dörfler 2016), including the important turbine-governor dynamics is indeed less understood. We notice that the referred studies on AGC include a second order model for the turbine-governor dynamics, whereas none of analytical studies on the stability of OLFC include such dynamics and are generally restricted to at most a first order model. Part II makes the noteworthy extension towards closing this gap and incorporates the second order turbine-governor dynamics in the stability analysis of the OLFC. We propose two approaches to incorporate the second order turbine-governor dynamics. In the first approach, which we present in Chapter 5, we develop an overall dissipation inequality for the combined power network and turbine-governor system. In the second approach, presented in Chapter 6, we apply a distributed sliding mode controller to recover a suitable passivity property of the turbine-governor system once the system reaches the sliding manifold. A detailed outline is provided below.

Outline

Chapter 5

In Chapter 5 we study the so-called 'Bergen-Hill' network model that represents various relevant power network configurations (Section 5.1). After discussing its equilibria and the optimal generation (Section 5.2), we establish an incremental passivity of the network (Section 5.3). This passivity property of the power network is then exploited to study the stability of the network, including the second order model for the turbine-governor with a constant setpoint. To prove asymptotic stability of the power network we study the eigenvalues of a Hamiltonian matrix depending on (local) system parameters. Doing so, we connect frequency control in power networks to the study of Hamiltonian matrices (Section 5.4). As a result of the constant setpoint, the frequency deviation will generally converge to a nonzero value. Therefore, we relax the requirement of a constant setpoint to the governor and provide a dynamic controller, continuously adjusting the setpoint, to obtain OLFC. Here, we incorporate the first order and second order turbine-governor models in a unifying way. Including the second order turbine-governor dynamics is especially challenging as they are non-passive and we cannot rely on the standard methodology for interconnecting passive systems. Instead, we develop a suitable dissipation inequality for the interconnected generator and turbine-governor. Due to the advantage of reduced generation and demand information requirements, we focus in Chapter 5 on a distributed consensus based controller, where information on marginal costs is exchanged among neighbouring buses. Nevertheless, we provide some guidelines how the higher order turbine-governor dynamics can be included in primal-dual

based approaches as well. Along the stability analysis for the second order turbine-governor model we establish a locally verifiable range of acceptable droop constants that allows us to infer frequency regulation. As a result of the distributed and modular design of the controllers, the proposed solution permits to straightforwardly include load control along the generation control and we provide a brief discussion on this topic. A case study confirms that disregarding the range of acceptable droop constants in the controller design can lead to instability (Section 5.6). We therefore argue that the design of an OLFC algorithm needs to carefully incorporate the effect of the turbine-governor dynamics.

Chapter 6

In Chapter 6 we provide an alternative approach to Chapter 5, to incorporate second order turbine-governor dynamics into an OLFC scheme. Specifically, we propose a distributed sliding mode (SM) controller (Utkin 1992, Edwards and Spurgen 1998) to obtain OLFC. Sliding mode control has been used to improve the conventional AGC schemes (Mi et al. 2013), possibly together with fuzzy logic (Ha 1998) and disturbances observers (Mi et al. 2016). However, the proposed use of SM to obtain a distributed OLFC scheme is new and can offer a few advantages over the previous results on OLFC. In comparison with the Chapter 5, we do not impose constraints on the droop gains. We adopt the nonlinear model of a power network, including voltage dynamics that we have studied before in Chapter 2. We briefly recall its dynamics and an useful passivity property (Section 6.1). The generation side is, compared with Chapter 3, extended with a second order turbine-governor model. The proposed control scheme continuously adjusts the governor set point, to obtain the objectives of OLFC which we briefly recall in Section 6.2. We propose a *distributed* SM controller that is shown to achieve frequency control, while minimizing generation costs (Section 6.3). This result is obtained by avoiding the measurement of the power demand and the use of observers (Rinaldi et al. 2017), which is an element concurring to the ease of practical implementation of the proposed control strategy. Conventional SM controllers can suffer from the notorious drawback known as chattering effect, due to the discontinuous control input. To alleviate this issue, we incorporate the Suboptimal Second Order Sliding Mode (SSOSM) control algorithm (Bartolini et al. 1998a), leading to a continuous control input. A desired passivity property of the controlled turbine-governor system prescribes the design of a suitable manifold. Particularly, the non-passive turbine-governor system, constrained to this manifold, is shown to be incrementally passive. This permits a passive feedback interconnection with the power network, once the closed-loop system evolves on the sliding manifold, and we use this fact to show asymptotic conver-

gence to the desired state (Section 6.4). We believe that the chosen approach, where the design of the sliding manifold is inspired by desired passivity properties, offers new perspectives on the control of networks that have similar control objectives as the one presented, e.g. achieving power sharing in microgrids. A case study confirms the obtained theoretical results, where we study the performance of the controllers on an academic example of the power network (Section 6.5)

Published in:

S. Trip and C. De Persis – *"Distributed optimal Load Frequency Control with non-passive dynamics,"* IEEE Transactions on Control of Network Systems, 2017, to appear.

S. Trip and C. De Persis – *"Optimal frequency regulation in nonlinear structure preserving power networks including turbine dynamics: an incremental passivity approach,"* Proceedings of the 2016 American Control Conference (ACC), 2016, pp. 4132-4137, Boston, MA, USA.

S. Trip and C. De Persis – *"Optimal generation in structure-preserving power networks with second order turbine-governor dynamics,"* Proceedings of the 15th European Control Conference (ECC), 2016, pp. 916-921, Aalborg, DK.

Chapter 5

Dissipation inequalities for non-passive dynamics

Abstract

Motivated by an increase of renewable energy sources we propose a distributed optimal Load Frequency Control scheme achieving frequency regulation and economic dispatch. Based on an energy function of the power network we derive an incremental passivity property for a well known nonlinear structure preserving network model, differentiating between generator and load buses. Exploiting this property we design distributed controllers that adjust the power generation. Notably, we explicitly include the turbine-governor dynamics where first order and the widely used second order dynamics are analyzed in a unifying way. Due to the non-passive nature of the second order turbine-governor dynamics, incorporating them is challenging and we develop a suitable dissipation inequality for the interconnected generator and turbine-governor. This allows us to include the generator side more realistically in the stability analysis of optimal Load Frequency Control than was previously possible.

5.1 The Bergen-Hill model

In this chapter we consider the nonlinear structure-preserving model of the power network proposed in (Bergen and Hill 1981) that we will extend in the following sections to include turbine-governor and load dynamics. The network consists of n_g generator buses and n_l load buses. Each bus is assumed to be either a generator or a load bus, such that the total number of buses in the network is $n_g + n_l = n$. The network is represented by a connected and undirected graph $\mathcal{G} = (\mathcal{V}_g \cup \mathcal{V}_l, \mathcal{E})$,

where $\mathcal{V}_g = \{1, \ldots, n_g\}$ is the set of generator buses, $\mathcal{V}_l = \{n_g + 1, \ldots, n\}$ is the set of load buses and $\mathcal{E} = \{1, \ldots, m\}$ is the set of transmission lines connecting the buses. The network structure can be represented by its corresponding incidence matrix $\mathcal{B} \in \mathbb{R}^{n \times m}$. The ends of transmission line k are arbitrarily labeled with a '$+$' and a '$-$'. The incidence matrix is then given by

$$\mathcal{B}_{ik} = \begin{cases} +1 & \text{if } i \text{ is the positive end of } k \\ -1 & \text{if } i \text{ is the negative end of } k \\ 0 & \text{otherwise.} \end{cases}$$

Following (Bergen and Hill 1981), generator bus $i \in \mathcal{V}_g$ is modelled as

$$\begin{aligned} \dot{\delta}_i &= \omega_{gi} \\ M_i \dot{\omega}_{gi} &= -D_{gi}\omega_{gi} - \sum_{j \in \mathcal{N}_i} V_i V_j B_{ij} \sin(\delta_i - \delta_j) + P_{ti}, \end{aligned} \tag{5.1}$$

where $\mathcal{N}_i$ is the set of buses connected to bus i. In high voltage tranmission networks considered here, the conductance is close to zero and therefore neglected, i.e. we assume the network to be lossless. The uncontrollable loads[1] are assumed (Bergen and Hill 1981), (Kundur et al. 1994) to consist of a constant and a frequency dependent component. We model a load bus for $i \in \mathcal{V}_l$ therefore as

$$\begin{aligned} \dot{\delta}_i &= \omega_{li} \\ 0 &= -D_{li}\omega_{li} - \sum_{j \in \mathcal{N}_i} V_i V_j B_{ij} \sin(\delta_i - \delta_j) - P_{di}. \end{aligned} \tag{5.2}$$

An overview of the used symbols is provided in Table 5.1. Since the power flows are determined by the differences in voltage angles, it is convenient to introduce $\eta_k = \delta_i - \delta_j$, where η_k is the difference of voltage angles across line k joining buses i and j. For all buses the dynamics of the power network are written as

$$\begin{aligned} \dot{\eta} &= \mathcal{B}^T \omega \\ M\dot{\omega}_g &= -D_g\omega_g - \mathcal{B}_g \Gamma \sin(\eta) + P_t \\ \mathbf{0} &= -D_l\omega_l - \mathcal{B}_l \Gamma \sin(\eta) - P_d, \end{aligned} \tag{5.3}$$

where $\omega = (\omega_g^T, \omega_l^T)^T$, $\eta = \mathcal{B}^T\delta$ and $\Gamma = \mathrm{diag}\{\Gamma_1, \ldots, \Gamma_m\}$, with $\Gamma_k = V_iV_jB_{ij} = V_jV_iB_{ji}$ and the index k denoting the line $\{i, j\}$. The matrices $\mathcal{B}_g \in \mathbb{R}^{n_g \times m}$ and $\mathcal{B}_l \in \mathbb{R}^{n_l \times m}$ are obtained by collecting from $\mathcal{B}$ the rows indexed by $\mathcal{V}_g$ and $\mathcal{V}_l$ respectively. The remaining symbols follow straightforwardly from the node dynamics and are

[1] Controllable loads can be incorporated as well. The discussion on this topic is postponed to Remark 5.5.12 to facilitate a concise treatment.

	State variables
δ_i	Voltage angle
ω_{gi}	Frequency deviation at the generator bus
ω_{li}	Frequency deviation at the load bus
	Parameters
M_i	Moment of inertia
D_{gi}	Damping constant of the generator
D_{li}	Damping constant of the load
B_{ij}	Susceptance of the transmission line
V_i	Voltage
	Controllable input
P_{ti}	Turbine output power
	Uncontrollable input
P_{di}	Unknown constant power demand

Table 5.1: Description the variables and parameters appearing in the power network model.

diagonal matrices or vectors of suitable dimensions. It is possible to eliminate ω_l in (5.3) by exploiting the identity $\omega_l = D_l^{-1}(-\mathcal{B}_l\Gamma\sin(\eta) - P_d)$ and realizing that $\mathcal{B}^T\omega = \mathcal{B}_g^T\omega_g + \mathcal{B}_l^T\omega_l$ (Monshizadeh and De Persis 2015). As a result we can write (5.3) equivalently as

$$\begin{aligned} \dot{\eta} &= \mathcal{B}_g^T\omega_g + \mathcal{B}_l^T D_l^{-1}(-\mathcal{B}_l\Gamma\sin(\eta) - P_d) \\ M\dot{\omega}_g &= -D_g\omega_g - \mathcal{B}_g\Gamma\sin(\eta) + P_t. \end{aligned} \tag{5.4}$$

We will however keep ω_l when it enhances the readability.

Remark 5.1.1 (Control areas)**.** *In the absence of load buses, the considered model appears in the study of automatic generation control of control areas, where a control area is described by an equivalent generator. A control area is then typically modelled as*

$$\begin{aligned} \dot{\delta}_i &= \omega_{gi} \\ M_i\dot{\omega}_{gi} &= -D_{gi}\omega_{gi} - \sum_{j\in\mathcal{N}_i} V_iV_jB_{ij}\sin(\delta_i - \delta_j) + P_{ti} - P_{di}, \end{aligned} \tag{5.5}$$

where the loads are collocated at the equivalent generator. All results in this chapter also hold for this particular case.

Remark 5.1.2 (Microgrids)**.** *Besides modelling high voltage power networks, system (5.3) has also been used to model (Kron reduced) microgrids (Schiffer 2015), (Trip et al. 2014),*

(Dörfler et al. 2016), (Shafiee et al. 2014), (De Persis and Monshizadeh 2017), (Schiffer et al. 2014). Smaller synchronous machines and inverters are then represented by (5.1) and (5.2) respectively.

5.2 Steady state and optimality

Before addressing the turbine-governor dynamics that adjust P_t, we discuss the steady state frequency deviation under constant generation $\overline{P}_t$. In particular we study the optimal value of $\overline{P}_t$ that allows for a zero frequency deviation at steady state, i.e. $\overline{\omega} = \mathbf{0}$. The steady state $(\overline{\eta}, \overline{\omega}, \overline{P}_t)$ of (5.3) necessarily satisfies

$$\begin{aligned} \mathbf{0} &= \mathcal{B}^T \overline{\omega} \\ \mathbf{0} &= -D_g \overline{\omega}_g - \mathcal{B}_g \Gamma \sin(\overline{\eta}) + \overline{P}_t \\ \mathbf{0} &= -D_l \overline{\omega}_l - \mathcal{B}_l \Gamma \sin(\overline{\eta}) - P_d. \end{aligned} \tag{5.6}$$

We make the natural assumption that a, possibly non-unique, solution to (5.21) exists, which corresponds to the ability of the network to transfer the required power at steady state.

Assumption 5.2.1 (Solvability)**.** *For a given $P_d \in \mathbb{R}^{n_l}$ and $\overline{P}_t \in \mathbb{R}^{n_g}$, there exist $\overline{\eta} \in \mathrm{Im}(\mathcal{B}^T)$, $\overline{\omega} \in \mathrm{Ker}(\mathcal{B}^T)$ and such that (5.21) is satisfied.*

From algebraic manipulations of (5.21) we can derive the following lemma that makes the frequency deviation at steady state $\overline{\omega}$ explicit.

Lemma 5.2.2 (Steady state frequency deviation)**.** *Let Assumption 5.2.1 hold, then necessarily $\overline{\omega} = \mathbb{1}_n \omega_*$, with*

$$\omega_* = \frac{\mathbb{1}_{n_g}^T \overline{P}_t - \mathbb{1}_{n_l}^T P_d}{\mathbb{1}_{n_g}^T D_g \mathbb{1}_{n_g} + \mathbb{1}_{n_l}^T D_l \mathbb{1}_{n_l}}, \tag{5.7}$$

where $\mathbb{1}_n \in \mathbb{R}^n$ is the vector consisting of all ones.

We recover therefore the well known fact that the total generation needs to be equal to the total load in order to have a zero frequency deviation in a lossless network. As we only require the total generation to be equal to the total load, it is natural to wonder if we can distribute the generation in an optimal manner. To this end, we assign to every generator a strictly convex linear-quadratic cost function that relates the generated power P_{ti} to the generation costs $C_i(P_{ti})$, typically expressed in \$/MWh, i.e.

$$C_i(P_{ti}) = \frac{1}{2} q_i P_{ti}^2 + r_i P_{ti} + s_i. \tag{5.8}$$

To formalize the notion of optimality, we pose the following optimization problem:

$$\begin{aligned} &\min_{P_t} C(P_t) \\ \text{s.t.} \quad &0 = \mathbb{1}_{n_g}^T \overline{P}_t - \mathbb{1}_{n_l}^T P_d, \end{aligned} \tag{5.9}$$

where $C(P_t) = \sum_{i \in \mathcal{V}_g} C_i(P_{ti})$. Defining furthermore $Q = \text{diag}(q_1, \dots, q_{n_g})$, $R = (r_1, \dots, r_{n_g})^T$ and $s = (s_1, \dots, s_{n_g})^T$ we can compactly write

$$C(P_t) = \frac{1}{2} P_t^T Q P_t + R^T P_t + \mathbb{1}_{n_g}^T s. \tag{5.10}$$

From the discussion of Lemma 5.2.2, we note that satisfying the equality constraint in (5.9) implies $\overline{\omega} = \mathbf{0}$. The solution to (5.9), indicated by the superscript opt, therefore satisfies

$$\begin{aligned} \mathbf{0} &= \mathcal{B}^T \mathbf{0} \\ \mathbf{0} &= -D_g \mathbf{0} - \mathcal{B}_g \Gamma \sin(\overline{\eta}) + \overline{P}_t^{opt} \\ \mathbf{0} &= -D_l \mathbf{0} - \mathcal{B}_l \Gamma \sin(\overline{\eta}) - P_d. \end{aligned} \tag{5.11}$$

It is possible to explicitly characterize the solution to (5.9).

Lemma 5.2.3 (Optimal generation)**.** *The solution $\overline{P}_t^{opt}$ to (5.9) satisfies*

$$\overline{P}_t^{opt} = Q^{-1}(\overline{\lambda}^{opt} - R), \tag{5.12}$$

where

$$\overline{\lambda}^{opt} = \frac{\mathbb{1}_{n_g}(\mathbb{1}_{n_l}^T P_d + \mathbb{1}_{n_g}^T Q^{-1} R)}{\mathbb{1}_{n_g}^T Q^{-1} \mathbb{1}_{n_g}}. \tag{5.13}$$

The first derivative of the cost function is commonly called the 'marginal cost function'. From (5.12) and (5.13) it is then immediate to see that

$$Q\overline{P}_t^{opt} + R = \overline{\lambda}^{opt} \in \text{Im}(\mathbb{1}_{n_g}), \tag{5.14}$$

which implies that at the solution to (5.9) all marginal costs are identical.

Remark 5.2.4 (Information requirements)**.** *Solving (5.9) explicitly requires the knowledge of the total load $\mathbb{1}_{n_l}^T P_d$. A popular approach to solve (5.9) in a distributed fashion is based on primal-dual gradient dynamic. These approaches do generally require knowledge of the loads. A remarkable feature of the proposed distributed controllers, that will be discussed in the remaining of this chapter, is that they solve (5.9) without such measurements at the cost of the restriction to linear-quadratic cost functions and the absence of generation and power flow constraints.*

The focus of this section was the characterization of the (optimal) steady state of the power network under constant power generation. In the next section we establish a passivity property of the power network that will be useful to design controllers that dynamically adjust P_t such that P_t converges to the optimal steady state $\overline{P}_t^{opt}$.

5.3 An incremental passivity property of the Bergen-Hill model

We now establish a passivity property for the considered power network model, that is essential to the stability analysis in the following section.

Lemma 5.3.1 (Incremental cyclo-passivity of (5.4))**.** *Let Assumption 5.2.1 hold. System (5.4) with input P_t and output ω_g is an output strictly incrementally cyclo-passive system, with respect to $(\overline{\eta}, \overline{\omega}_g)$ satisfying*

$$\begin{aligned} \mathbf{0} &= \mathcal{B}_g^T \overline{\omega}_g + \mathcal{B}_l^T D_l^{-1}(-\mathcal{B}_l \Gamma \sin(\overline{\eta}) - P_d) \\ \mathbf{0} &= -D_g \overline{\omega}_g - \mathcal{B}_g \Gamma \sin(\overline{\eta}) + \overline{P}_t. \end{aligned} \tag{5.15}$$

Namely, there exists a storage function $U(\omega_g, \overline{\omega}_g, \eta, \overline{\eta})$ which satisfies the following incremental dissipation inequality

$$\dot{U} = -\|\omega_g - \overline{\omega}_g\|_{D_g}^2 - \|\omega_l - \overline{\omega}_l\|_{D_l}^2 + (\omega_g - \overline{\omega}_g)^T (P_t - \overline{P}_t), \tag{5.16}$$

where $\dot{U}$ represents the derivative of $U(\omega_g, \overline{\omega}_g, \eta, \overline{\eta})$ along the solutions to (5.4).

Proof. Consider the incremental storage function

$$\begin{aligned} U(\omega_g, \overline{\omega}_g, \eta, \overline{\eta}) = &\frac{1}{2}(\omega_g - \overline{\omega}_g)^T M (\omega_g - \overline{\omega}_g) \\ &- \mathbb{1}^T \Gamma \cos(\eta) + \mathbb{1}^T \Gamma \cos(\overline{\eta}) - (\Gamma \sin(\overline{\eta}))^T (\eta - \overline{\eta}). \end{aligned} \tag{5.17}$$

We have that $U(\omega_g, \overline{\omega}_g, \eta, \overline{\eta})$ satisfies along the solutions to (5.4)

$$\begin{aligned}
\dot{U} &= (\omega_g - \overline{\omega}_g)^T(-D_g\omega_g - \mathcal{B}_g\Gamma\sin(\eta) + P_t) \\
&\quad + (\Gamma\sin(\eta) - \Gamma\sin(\overline{\eta}))^T(\mathcal{B}_g^T\omega_g + \mathcal{B}_l^T D_l^{-1}(-\mathcal{B}_l\Gamma\sin(\eta) - P_d)) \\
&= - \|\omega_g - \overline{\omega}_g\|_{D_g}^2 + (\omega_g - \overline{\omega}_g)^T(P_t - \overline{P}_t) \\
&\quad + (\Gamma\sin(\eta) - \Gamma\sin(\overline{\eta}))^T\mathcal{B}_l^T(\omega_l - \overline{\omega}_l) \\
&= - \|\omega_g - \overline{\omega}_g\|_{D_g}^2 + (\omega_g - \overline{\omega}_g)^T(P_t - \overline{P}_t) \\
&\quad + (\Gamma\sin(\eta)\mathcal{B}_l + P_d)^T D_l^{-1} D_l(\omega_l - \overline{\omega}_l) \\
&\quad - (\Gamma\sin(\overline{\eta})\mathcal{B}_l + P_d)^T D_l^{-1} D_l(\omega_l - \overline{\omega}_l) \\
&= - \|\omega_g - \overline{\omega}_g\|_{D_g}^2 - \|\omega_l - \overline{\omega}_l\|_{D_l}^2 + (\omega_g - \overline{\omega}_g)^T(P_t - \overline{P}_t),
\end{aligned} \tag{5.18}$$

where we exploit identity (5.15) in the second equation. ■

Note that the result of Lemma 5.3.1 holds in particular if we take $\overline{\omega} = \mathbf{0}$ and $\overline{P}_t = \overline{P}_t^{opt}$. We now consider what conditions ensure that storage function (5.17) has a local minimum at a steady state satisfying (5.15).

Assumption 5.3.2 (Steady state angle differences)**.** *The differences in voltage angles $\overline{\eta}$ in (5.21) satisfy $\overline{\eta}_k \in (\frac{-\pi}{2}, \frac{\pi}{2}) \quad \forall k \in \mathcal{E}$.*

Note that Assumption 5.3.2 is generally satisfied under normal operating conditions of the power network, where a small difference in voltage angle is also referred to as phase-cohesiveness (Dörfler et al. 2013) and is preferred to avoid instability after perturbations (North American Electric Reliability Corporation (NERC) 2016).

Lemma 5.3.3 (Local minimum of (5.17))**.** *Let Assumption 5.3.2 hold. Then the storage function (5.17) has a local minimum at $(\overline{\eta}, \overline{\omega}_g)$.*

Proof. We first recall the definition of a Bregman distance (Bregman 1967). Let $F : \mathcal{X} \to \mathbb{R}$ be a continuously differentiable and strictly convex function defined on a closed convex set $\mathcal{X}$. The Bregman distance associated with F for the points $x, \overline{x}$ is defined as

$$D_F(x, \overline{x}) = F(x) - F(\overline{x}) - \nabla F(\overline{x})^T(x - \overline{x}). \tag{5.19}$$

A useful property of D_F is that it is positive definite in its first argument, due to the strict convexity of F. Lemma 5.3.3 then follows from (5.17) being the Bregman distance associated with the function $F(\omega_g, \eta) = \frac{1}{2}\omega_g^T M\omega_g - \mathbb{1}_m^T\Gamma\mathbf{cos}(\eta)$, which is strictly convex at the point $(\overline{\omega}_g, \overline{\eta})$ under Assumption 5.3.2. ■

	State variables
P_{gi}	Governor output
P_{ti}	Turbine output power
	Parameters
T_{gi}	Governor time constant
T_{ti}	Turbine time constant
K_i	Droop constant
	Controllable input
θ_i	Power generation control

Table 5.2: Description of the variables and parameters appearing in the turbine-governor dynamics.

Remark 5.3.4 (Boundedness of solutions)**.** *In the proofs of Theorem 5.4.6 and Theorem 5.5.9 we require Assumption 5.3.2 and subsequently Lemma 5.3.3 to ensure that there exists a compact forward invariant set around an equilibrium of (5.3). This allows us to apply LaSalle's invariance principle in the stability analysis.*

In this section we have established that the power network model (5.3) is an output strictly incrementally cyclo-passive system. Furthermore we have shown that under Assumption 5.3.2, the incremental storage function U has a local minimum at its steady state.

5.4 Primary frequency control and Hamiltonian matrices

In this section we study the stability of the structure preserving power network presented in Section 5.1 in closed loop with the second order turbine governor model

$$\begin{aligned} T_g \dot{P}_g &= -P_g - K_i^{-1}\omega_g + \overline{\theta} \\ T_t \dot{P}_t &= -P_t + P_g, \end{aligned} \tag{5.20}$$

where the input $\overline{\theta}$ is a *constant* setpoint. The various symbols are described in Table 5.2 The steady state solution of the closed loop system (5.3) and (5.20) necessarily

satisfies

$$\begin{aligned} \mathbf{0} &= \mathcal{B}^T\overline{\omega} \\ \mathbf{0} &= -D_g\overline{\omega}_g - \mathcal{B}_g\Gamma\sin(\overline{\eta}) + \overline{P}_t \\ \mathbf{0} &= -D_l\overline{\omega}_l - \mathcal{B}_l\Gamma\sin(\overline{\eta}) - P_d \\ \mathbf{0} &= -\overline{P}_g - K^{-1}\overline{\omega}_g + \overline{\theta} \\ \mathbf{0} &= -\overline{P}_t + \overline{P}_g. \end{aligned} \tag{5.21}$$

As a result of Assumption 5.2.1, a solution to (5.21) exists. From algebraic manipulations of (5.21) we can derive the following lemma that makes the frequency deviation at steady state $\overline{\omega}$ explicit.

Lemma 5.4.1 (Steady state frequency deviation)**.** *Let Assumption 5.2.1 hold, then necessarily $\overline{\omega} = \mathbb{1}_n\omega_*$, with*

$$\omega_* = \frac{\mathbb{1}_{n_g}^T\overline{\theta} - \mathbb{1}_{n_l}^T P_d}{\mathbb{1}_{n_g}^T D_g\mathbb{1}_{n_g} + \mathbb{1}_{n_l}^T D_l\mathbb{1}_{n_l} + \mathbb{1}_{n_g}^T K^{-1}\mathbb{1}_{n_g}}, \tag{5.22}$$

where $\mathbb{1}_n \in \mathbb{R}^n$ is the vector consisting of all ones.

It is clear from Lemma 5.4.1 that it is desirable to have a small value of K_i in order to have a small frequency deviation at steady state. Before we continue with the stability analysis we repeat a useful result which is presented in a more general form in (Isidori 2000).

Lemma 5.4.2 ((Isidori 2000), Theorem 10.9.1)**.** *There exists a symmetric matrix $X_i > \mathbf{0}$ such that*

$$X_iA_{Ri} + A_{Ri}^TX_i + X_iB_{Ri}B_{Ri}^TX_i + C_{Ri}^TC_{Ri} < \mathbf{0}, \tag{5.23}$$

if and only if all the eigenvalues of A_{Ri} have negative real part and the Hamiltonian matrix

$$H_i = \begin{bmatrix} A_{Ri} & B_{Ri}B_{Ri}^T \\ -C_{Ri}^TC_{Ri} & -A_{Ri}^T \end{bmatrix}, \tag{5.24}$$

has no eigenvalues on the imaginary axis.

The relevance of Lemma 5.4.2 will become evident in the proof of Lemma 5.4.5, where we study asymptotic stability of the steady state. More explicit, we can prove asymptotic stability if the following assumption is satisfied, which relates the parameters of generator i to the Hamiltonian matrix defined in Lemma 5.4.2.

Assumption 5.4.3 (A generator related Hamiltonian matrix)**.** *Let for all $i \in \mathcal{V}_g$ the Hamiltonian matrix*

$$H_i = \begin{bmatrix} A_{Ri} & B_{Ri}B_{Ri}^T \\ -C_{Ri}^TC_{Ri} & -A_{Ri}^T \end{bmatrix}, \tag{5.25}$$

be such that it has not eigenvalues on the imaginary axis, where

$$\begin{aligned} A_{Ri} &= \begin{bmatrix} -\frac{1}{2}T_{gi}^{-1} & -\frac{1}{4}T_{gi}^{-1}K_i^{-1}D_{gi}^{-1} \\ \frac{1}{2}T_{ti}^{-1} & -\frac{1}{2}T_{ti}^{-1} \end{bmatrix} \\ B_{Ri}B_{Ri}^T &= \begin{bmatrix} \frac{1}{4}D_{gi}^{-1}T_{gi}^{-2}T_{ti}^{-2} & 0 \\ 0 & 0 \end{bmatrix} \\ C_{Ri}^TC_{Ri} &= \begin{bmatrix} 0 & 0 \\ 0 & \frac{1}{4}D_{gi}^{-1} \end{bmatrix}, \end{aligned} \tag{5.26}$$

Remark 5.4.4 (Determining the eigenvalues of H_i)**.** *Determining the eigenvalues of $H_i \in \mathbb{R}^{4\times 4}$ in Assumption 5.4.3 is straightforward and can be done locally for every generator. It is possible to give an analytic expression of the eigenvalues of matrix H_i, since the associated characteristic polynomial is of fourth order. Obtaining explicit bounds on the generator parameters such that Assumption 5.4.3 is satisfied is left for future research. Furthermore, an interesting question is how system parameters should be altered if the Hamiltonian matrix does have eigenvalues on the imaginary axis (Grivet-Talocia 2004), (Alam et al. 2011).*

A fundamental ingredient to prove asymptotic stability is the existence of an incremental storage function, which has a local minimum at the steady state solution to (5.21), and is negative semi-definite along the solutions to (5.3). The result of the following lemma contributes to establishing such existence and will be exploited in the proof of Theorem 5.4.6.

Lemma 5.4.5 (Existence of a dissipation inequality)**.** *Let Assumption 5.4.3 hold and define with a slight abuse of notation $\dot{\overline{U}}_{gi} = -D_{gi}(\omega_{gi} - \overline{\omega}_{gi})^2 + (\omega_{gi} - \overline{\omega}_{gi})(P_{ti} - \overline{P}_{ti})$. There exists an incremental storage function*

$$\overline{Z}_i = \tfrac{1}{2}\begin{pmatrix} P_{gi} - \overline{P}_{gi} \\ P_{ti} - \overline{P}_{ti} \end{pmatrix}^T X_i \begin{pmatrix} P_{gi} - \overline{P}_{gi} \\ P_{ti} - \overline{P}_{ti} \end{pmatrix}, \tag{5.27}$$

where $X_i > 0$, such that $\dot{\overline{U}}_{gi} + \dot{\overline{Z}}_i < 0$.

Proof. We first write

$$\dot{\overline{U}}_{gi} = (\omega_{gi} - \overline{\omega}_{gi})^T \overbrace{\begin{bmatrix} -D_{gi} \end{bmatrix}}^{W_{1i}} (\omega_{gi} - \overline{\omega}_{gi}) + (\omega_{gi} - \overline{\omega}_{gi})^T \overbrace{\begin{bmatrix} 0 & 1 \end{bmatrix}}^{W_{2i}} \begin{pmatrix} P_{gi} - \overline{P}_{gi} \\ P_{ti} - \overline{P}_{ti} \end{pmatrix}.$$

Bearing in mind the turbine-governor dynamics (5.20) and exploiting the last two

identities in (5.21), it follows that $\overline{Z}_i$ satisfies along the solutions to (5.20)

$$\begin{aligned}\dot{\overline{Z}}_i &= \begin{pmatrix} P_{gi}-\overline{P}_{gi} \\ P_{ti}-\overline{P}_{ti}\end{pmatrix}^T X_i \overbrace{\begin{bmatrix} -T_{gi}^{-1} & 0 \\ T_{ti}^{-1} & -T_{ti}^{-1}\end{bmatrix}}^{W_{3i}} \begin{pmatrix} P_{gi}-\overline{P}_{gi} \\ P_{ti}-\overline{P}_{ti}\end{pmatrix} \\ &\quad + \begin{pmatrix} P_{gi}-\overline{P}_{gi} \\ P_{ti}-\overline{P}_{ti}\end{pmatrix}^T X_i \overbrace{\begin{bmatrix} -T_{gi}^{-1}K_i^{-1} \\ 0\end{bmatrix}}^{W_{4i}} (\omega_{gi}-\overline{\omega}_{gi})\end{aligned} \tag{5.28}$$

Defining $x_i = ((\omega_{gi}-\overline{\omega}_{gi})^T, (P_{gi}-\overline{P}_{gi})^T, (P_{ti}-\overline{P}_{ti})^T)^T$ and $X_i = X_i^T$, we have

$$\dot{\overline{U}}_{gi} + \dot{\overline{Z}}_i = x_i^T \overbrace{\begin{bmatrix} W_{1i} & \frac{1}{2}(W_{2i}+W_{4i}^T X_i^T) \\ \frac{1}{2}(W_{2i}^T + X_i W_{4i}) & \frac{1}{2}(X_i W_{3i} + W_{3i}^T X_i)\end{bmatrix}}^{W_{Ti}} x_i. \tag{5.29}$$

Since $W_{1i} < 0$ it follows that $W_{Ti} < \mathbf{0}$ if and only if the Schur complement of W_{1i} in W_{Ti} is negative definite. The Schur complement of W_{1i} in W_{Ti} is given by

$$\begin{aligned} S_i &= \tfrac{1}{2}(X_i W_{3i} + W_{3i}^T X_i) - \tfrac{1}{2}(W_{2i}^T + X_i W_{4i}) W_{1i}^{-1} \tfrac{1}{2}(W_{2i} + W_{4i}^T X_i^T) \\ &= X_i(\tfrac{1}{2}W_{3i} - \tfrac{1}{4}W_{4i}W_{1i}^{-1}W_{2i}) + (-\tfrac{1}{4}W_{2i}^T W_{1i}^{-1} W_{4i}^T + \tfrac{1}{2}W_{3i}^T)X_i \\ &\quad -\tfrac{1}{4}X_i W_{4i} W_{1i}^{-1} W_{4i}^T X_i - \tfrac{1}{4} W_{2i}^T W_{1i}^{-1} W_{2i}. \end{aligned} \tag{5.30}$$

Defining

$$\begin{aligned} A_{Ri} &= \tfrac{1}{2}W_{3i} - \tfrac{1}{4}W_{4i}W_{1i}^{-1}W_{2i} \\ B_{Ri} &= \tfrac{1}{2}W_{4i}(-W_{1i}^{-1})^{\frac{1}{2}} \\ C_{Ri} &= \tfrac{1}{2}(-W_{1i}^{-1})^{\frac{1}{2}} W_{2i}, \end{aligned} \tag{5.31}$$

one can notice that the condition $S_i = X_i A_{Ri} + A_{Ri}^T X_i + X_i B_{Ri} B_{Ri}^T X_i + C_{Ri}^T C_{Ri} < \mathbf{0}$ is an algebraic Riccati inequality with unknown X_i. It follows from Lemma 5.4.2 that there exists a positive definite solution $X_i > \mathbf{0}$ to the inequality $S_i < \mathbf{0}$ if and only if $A_{Ri} = \frac{1}{2}W_{3i} - \frac{1}{4}W_{4i}W_{1i}^{-1}W_{2i} = \frac{1}{2}W_{3i} - B_{Ri}C_{Ri}$ is Hurwitz and the Hamiltonian matrix H_i, defined in Assumption 5.4.3, has no eigenvalues on the imaginary axis. The latter condition is trivially satisfied by Assumption 5.4.3 and straightforward calculations show that

$$A_{Ri} = \begin{bmatrix} -\frac{1}{2}T_{gi}^{-1} & -\frac{1}{4}T_{gi}^{-1}K_i^{-1}D_{gi}^{-1} \\ \frac{1}{2}T_{ti}^{-1} & -\frac{1}{2}T_{ti}^{-1}\end{bmatrix}, \tag{5.32}$$

and that its characteristic polynomial is given by $p_{A_{Ri}}(s) = s^2 + \frac{1}{2}(T_{gi}^{-1} + T_{ti}^{-1})s + \frac{1}{8}T_{gi}^{-1}T_{ti}^{-1}(2 + K_i^{-1}D_{gi}^{-1})$. It is straightforward to confirm that $p_{A_{Ri}}(s)$ has only negative roots. We can therefore conclude that under Assumption 5.4.3, there exists indeed a positive definite matrix $X_i > 0$, such that $\dot{\overline{U}}_{gi} + \dot{\overline{Z}}_i < 0$. ■

We are now ready to present the main result of this section, namely that the solution to (5.21) is locally asymptotically stable under the assumptions discussed.

Theorem 5.4.6 (Stability of the equilibrium frequency)**.** *Consider system (5.3) with constant power demand P_d and constant control input $\overline{\theta}$ Let Assumptions 5.2.1, 5.3.2 and 5.4.3 hold. Then, the solutions to the closed loop system (5.3) and (5.20) that start in a neighborhood of $(\overline{\eta}, \overline{\omega} = \mathbb{1}_n\omega^*, \overline{P}_g, \overline{P}_t)$ converge asymptotically to the largest invariant set where $\omega = \mathbb{1}_n\omega^*$ characterized in Lemma 5.4.1, $P_g = \overline{P}_g$ and $P_t = \overline{P}_t$.*

Proof. Bearing in mind Lemma 5.3.1, we recall that the incremental storage function

$$\begin{aligned} U(\omega_g, \overline{\omega}_g, \eta, \overline{\eta}) = &\frac{1}{2}(\omega_g - \overline{\omega}_g)^T M(\omega_g - \overline{\omega}_g) \\ &- \mathbb{1}^T\Gamma\cos(\eta) + \mathbb{1}^T\Gamma\cos(\overline{\eta}) - (\Gamma\sin(\overline{\eta}))^T(\eta - \overline{\eta}). \end{aligned} \tag{5.33}$$

satisfies along the solutions to (5.3)

$$\dot{U} = -\|\omega_g - \overline{\omega}_g\|^2_{D_g} - \|\omega_l - \overline{\omega}_l\|^2_{D_l} + (\omega_g - \overline{\omega}_g)^T(P_t - \overline{P}_t). \tag{5.34}$$

We rewrite $\dot{U}$ as

$$\dot{U} \quad = \quad \textstyle\sum_{i\in\mathcal{V}_g} \dot{\overline{U}}_{gi} - \|\omega_l - \overline{\omega}_l\|^2_{D_l},$$

where $\dot{\overline{U}}_{gi} = -D_i(\omega_{gi} - \overline{\omega}_{gi})^2 + (\omega_{gi} - \overline{\omega}_{gi})(P_{ti} - \overline{P}_{ti})$. Notice that the expression of $\dot{\overline{U}}_{gi}$ is the same as in Lemma 5.4.5. From Lemma 5.4.5 and Assumption 5.4.3 it follows that there exists an incremental storage function

$$\overline{Z}_i \quad = \quad \tfrac{1}{2}\begin{pmatrix} P_{gi} - \overline{P}_{gi} \\ P_{ti} - \overline{P}_{ti} \end{pmatrix}^T X_i \begin{pmatrix} P_{gi} - \overline{P}_{gi} \\ P_{ti} - \overline{P}_{ti} \end{pmatrix},$$

where $X_i > 0$, such that $\dot{\overline{U}}_{gi} + \dot{\overline{Z}}_i < 0$. As a consequence of Assumption 5.2.1, the total incremental storage function $U + \sum_{i\in\mathcal{V}_g}\overline{Z}_i$ has a strict local minimum at $(\overline{\eta}, \overline{\omega}, \overline{P}_g, \overline{P}_t)$. Furthermore, $U + \sum_{i\in\mathcal{V}_g}\overline{Z}_i$ satisfies along the solutions to the closed loop system (5.3) and (5.20) $\dot{U} + \sum_{i\in\mathcal{V}_g}\dot{\overline{Z}}_i \leq 0$. Therefore, there exists a compact level set Υ around the equilibrium $(\overline{\eta}, \overline{\omega} = \mathbb{1}_n\omega^*, \overline{P}_g, \overline{P}_t)$, which is forward invariant. By LaSalle's invariance principle the solution starting in Υ asymptotically converges to the largest invariant set contained in $\Upsilon \cap \{(\overline{\eta}, \overline{\omega}, \overline{P}_g, \overline{P}_t) : \omega = \overline{\omega}, P_g = \overline{P}_g, P_t = \overline{P}_t\}$, where $\overline{\omega} = \mathbb{1}_n\omega^*$ characterized in Lemma 5.4.1. ■

Remark 5.4.7 (Relation to other studies)**.** *A related study on primary frequency control is performed in (Zhao and Low 2014) and requires $K_i^{-1} < D_{gi}$ for the system at hand in order to prove asymptotic stability of the steady state. Assumption 5.4.3 is less conservative, but requires additional knowledge of T_{gi} and T_{ti}.*

A consequence of the analysis in this section is that the power network will generally converge to a steady state frequency deviation ω^* unequal to zero. In the next section we address this issue by designing additional secondary control, which regulates the frequency and minimizes generation costs.

5.5 Optimal turbine-governor control

The generated power P_{ti} at generator i is the output of the turbine-governor system. Various turbine-goveror models appear in the literature. In this section we consider two of the most widely used models that have fundamentally different properties. We therefore partition the set of generators $\mathcal{V}_g = (\mathcal{V}_{g1} \cup \mathcal{V}_{g2})$ into the sets $\mathcal{V}_{g1}$ and $\mathcal{V}_{g2}$, where the turbine-governor dynamics are described by first order and second order dynamics respectively. Being able to incorporate both types in a single framework, unifies the various modelling assumptions appearing in conventional AGC and OLFC and increases the modelling flexibility.

The first order and second order turbine-governor dynamics will be discussed separately and controllers are proposed that achieve frequency regulation. To facilitate the controller design using only local information we write (5.18), taking therein and in the remainder of this work $\overline{\omega} = \mathbf{0}$ and $\overline{P}_t = \overline{P}_t^{opt}$, as

$$\begin{aligned} \dot{U} =& - \|\omega_g - \mathbf{0}\|^2_{D_g} - \|\omega_l - \mathbf{0}\|^2_{D_l} + (\omega_g - \overline{\omega}_g)^T (P_t - \overline{P}_t^{opt}) \\ =& \sum_{i \in \mathcal{V}_g} \dot{U}_{gi}(\omega_{gi}, P_{ti}, \overline{P}_{ti}^{opt}) + \sum_{i \in \mathcal{V}_l} \dot{U}_{li}(\omega_{li}), \end{aligned} \tag{5.35}$$

where we define with a slight abuse of notation

$$\begin{aligned} \dot{U}_{gi}(\omega_{gi}, P_{ti}, \overline{P}_{ti}^{opt}) =& - D_{gi}\omega_{gi}^2 + \omega_{gi}(P_{ti} - \overline{P}_{ti}^{opt}) \\ \dot{U}_{li}(\omega_{li}) =& - D_{li}\omega_{li}^2. \end{aligned} \tag{5.36}$$

For the sake of exposition we only consider decentralized controllers in subsections 5.5.1 and 5.5.2 that guarantee frequency regulation without achieving optimality. These results are then instrumental to Subsection 5.5.3 where a distributed control architecture is proposed with controllers that exchange information on their marginal costs with their neighbours over a communication network to achieve optimality.

5.5.1 First order turbine-governor dynamics

We start with the first order turbine-governor dynamics of a single generator $i \in \mathcal{V}_{g1}$. The dynamics are given by

$$T_{ti}\dot{P}_{mi} = -P_{ti} - K_i^{-1}\omega_{gi} + \theta_i, \tag{5.37}$$

where θ_i is an additional control input to be designed. An overview of the used symbols is provided in Table 5.2. In comparison with the previous section, we do not assume that θ is constant. Instead, consider the following controller at bus i:

$$T_{\theta_i}\dot{\theta}_i = -\theta_i + P_{ti}, \tag{5.38}$$

where the controller time constant T_{θ_i} can be chosen to obtain a desirable rate of change of the control input θ_i. As explained before, an additional communication term will be added to controller (5.38) in subsection 5.5.3 to enforce optimality at steady state. The following lemma provides an intermediate result that is useful later on.

Lemma 5.5.1 (Incremental passivity of (5.37), (5.38))**.** *System (5.37), (5.38) with input $-\omega_{gi}$ and output P_{ti} is an incrementally passive system, with respect to $(\overline{\theta}_i, \overline{P}_{ti}^{opt})$ satisfying*

$$0 = -\overline{P}_{ti}^{opt} - K_i^{-1}0 + \overline{\theta}_i^{opt} \tag{5.39}$$

$$0 = -\overline{\theta}_i^{opt} + \overline{P}_{ti}^{opt}, \tag{5.40}$$

Namely, there exists a positive definite storage function $Z_{1i}(\theta_i, \overline{\theta}_i^{opt}, P_{ti}, \overline{P}_{ti}^{opt})$ which satisfies the following incremental dissipation inequality

$$\dot{Z}_{1i} = -K_i(\theta_i - P_{ti})^2 - \omega_{gi}(P_{ti} - \overline{P}_{ti}^{opt}), \tag{5.41}$$

where $\dot{Z}_{1i}$ represents the derivative of $Z_{1i}(\theta_i, \overline{\theta}_i^{opt}, P_{ti}, \overline{P}_{ti}^{opt})$ along the solutions to (5.37), (5.38).

Proof. Consider the incremental storage function

$$Z_{1i} = \frac{T_{\theta_i}K_i}{2}(\theta_i - \overline{\theta}_i^{opt})^2 + \frac{T_{P_{ti}}K_i}{2}(P_{ti} - \overline{P}_{ti}^{opt})^2. \tag{5.42}$$

We note that Z_{1i} satisfies along the solutions to (5.37), (5.38),

$$\begin{aligned}\dot{Z}_{1i} = &-(\theta_i - \overline{\theta}_i^{opt})K_i\theta_i + (\theta_i - \overline{\theta}_i^{opt})K_iP_{ti}\\ &-(P_{ti} - \overline{P}_{ti}^{opt})K_iP_{ti} + (P_{ti} - \overline{P}_{ti}^{opt})K_i\theta_i\\ &-(P_{ti} - \overline{P}_{ti}^{opt})\omega_{gi}\\ = &-K_i(\theta_i - P_{ti})^2 - (P_{ti} - \overline{P}_{ti}^{opt})\omega_{gi},\end{aligned} \tag{5.43}$$

where we exploit identity (5.39) in the second equation. ■

The interconnection of generator dynamics (5.3) and turbine-governor dynamics (5.37) including controller (5.38) can be understood as a feedback interconnection of two incrementally passive systems. The following corollary is then an immediate result from this observation.

Corollary 5.5.2 (Passive interconnection)**.** *Along the solutions to (5.3), (5.37) and (5.38), $Z_{1i}(\theta_i, \overline{\theta}_i^{opt}, P_{ti}, \overline{P}_{ti}^{opt})$ satisfies for $i \in \mathcal{V}_{g1}$*

$$\dot{U}_{gi} + \dot{Z}_{1i} = -D_{gi}\omega_{gi}^2 - K_i(\theta_i - P_{ti})^2 \leq 0, \tag{5.44}$$

where $\dot{U}_{gi}$ and $\dot{Z}_{1i}$ are given in (5.36) and (5.41) respectively.

We now perform a similar analysis for the second order turbine-governor dynamics.

5.5.2 Second order turbine-governor dynamics

Consider the second order turbine-governor dynamics of a single generator $i \in \mathcal{V}_{g2}$. The dynamics are given by

$$\begin{aligned} T_{gi}\dot{P}_{gi} &= -P_{gi} - K_i^{-1}\omega_{gi} + \theta_i \\ T_{ti}\dot{P}_{mi} &= -P_{ti} + P_{gi}, \end{aligned} \tag{5.45}$$

where θ_i is again an additional dynamic control input to be designed. In contrast to the first order dynamics, the second order dynamics do not possess a useful passivity property. This can be readily concluded from the observation that system (5.45) with input ω_{gi} and output P_{ti} has relative degree 2. We now propose a different controller than (5.38) to accommodate the higher order turbine-governor model, namely

$$T_{\theta_i}\dot{\theta}_i = -\theta_i + P_{gi} - (1 - K_i^{-1})\omega_{gi}, \tag{5.46}$$

where K^{-1} is the droop constant appearing in (5.45). Similar to (5.38) we postpone adding an additional communication term until the next subsection.

Lemma 5.5.3 (Storage function for second order dynamics)**.** *There exists a positive definite storage function $Z_{2i}(\theta_i, \overline{\theta}_i^{opt}, P_{gi}, \overline{P}_{gi}, P_{ti}, \overline{P}_{ti}^{opt})$ which satisfies along the solutions to (5.3), (5.45) and (5.46)*

$$\dot{U}_{gi} + \dot{Z}_{2i} = \begin{bmatrix} \omega_{gi} \\ P_{gi} - P_{ti} \\ P_{gi} - \theta_i \end{bmatrix}^T W_i \begin{bmatrix} \omega_{gi} \\ P_{gi} - P_{ti} \\ P_{gi} - \theta_i \end{bmatrix}, \tag{5.47}$$

with

$$W_i = \begin{bmatrix} -D_{gi} & -\frac{1}{2}K_i^{-1} - \frac{1}{2} & -\frac{1}{2}K_i^{-1} + \frac{1}{2} \\ -\frac{1}{2}K_i^{-1} - \frac{1}{2} & -T_{gi}T_{ti}^{-1} & -\frac{1}{2} \\ -\frac{1}{2}K_i^{-1} + \frac{1}{2} & -\frac{1}{2} & -1 \end{bmatrix}. \tag{5.48}$$

Proof. Consider the incremental storage function

$$\begin{aligned} Z_{2i} &= \frac{T_{\theta_i}}{2}(\theta_i - \overline{\theta}_i^{opt})^2 + \frac{1}{2}T_{gi}(P_{gi} - \overline{P}_{gi}^{opt})^2 + \frac{1}{2}T_{gi}(P_{gi} - P_{ti})^2 \\ &= \frac{T_{\theta_i}}{2}(\theta_i - \overline{\theta}_i^{opt})^2 + T_{gi}(P_{gi} - \overline{P}_{gi}^{opt})^2 \\ &\quad + \frac{T_{gi}}{2}(P_{ti} - \overline{P}_{ti}^{opt})^2 - T_{gi}(P_{gi} - \overline{P}_{gi}^{opt})(P_{ti} - \overline{P}_{ti}^{opt}). \end{aligned} \tag{5.49}$$

It can be readily confirmed that Z_{2i} is positive definite. We have that $Z_{2i}(\theta_i, \overline{\theta}_i^{opt}, P_{gi}, \overline{P}_{gi}, P_{ti}, \overline{P}_{ti}^{opt})$ satisfies along the solutions to (5.45), (5.46),

$$\begin{aligned} \dot{Z}_{2i} &= (\theta_i - \overline{\theta}_i^{opt})(-\theta_i + P_{gi} - (1 - K_i^{-1})\omega_{gi}) \\ &\quad + 2(P_{gi} - \overline{P}_{gi}^{opt})(-P_{gi} - K_i^{-1}\omega_{gi} + \theta_i) \\ &\quad + T_{gi}T_{ti}^{-1}(P_{ti} - \overline{P}_{ti}^{opt})(-P_{ti} + P_{gi}) \\ &\quad - T_{gi}T_{ti}^{-1}(P_{gi} - \overline{P}_{gi}^{opt})(-P_{ti} + P_{gi}) \\ &\quad - (P_{ti} - \overline{P}_{ti}^{opt})(-P_{gi} - K_i^{-1}\omega_{gi} + \theta_i) \\ &= - T_{gi}T_{ti}^{-1}(P_{gi} - P_{ti})^2 - (P_{gi} - \theta_i)^2 \\ &\quad - K_i^{-1}(P_{gi} - P_{ti})\omega_{gi} - K_i^{-1}(P_{gi} - \theta_i)\omega_{gi} \\ &\quad - (P_{gi} - P_{ti})(P_{gi} - \theta_i) \\ &\quad - (\theta_i - \overline{\theta}_i^{opt})\omega_{gi}, \end{aligned} \tag{5.50}$$

where we exploited in the second identity the fact that in steady state

$$\begin{aligned} 0 &= - \overline{P}_{gi}^{opt} - K_i^{-1}0 + \overline{\theta}_i^{opt} \\ 0 &= - \overline{P}_{ti}^{opt} + \overline{P}_{gi}^{opt} \\ 0 &= - \overline{\theta}_i^{opt} + \overline{P}_{gi}^{opt} - (1 - K_i^{-1})0. \end{aligned} \tag{5.51}$$

We recall that $\dot{U}_{gi} = -D_{gi}\omega_{gi}^2 + \omega_{gi}(P_{ti} - \overline{P}_{ti}^{opt})$ and notice that

$$\begin{aligned} & \omega_{gi}(P_{ti} - \overline{P}_{ti}^{opt}) - (\theta_i - \overline{\theta}_i^{opt})\omega_{gi} \\ = \; & \omega_{gi}(P_{ti} - \theta_i) \\ = \; & \omega_{gi}(P_{gi} - \theta_i) - \omega_{gi}(P_{gi} - P_{ti}). \end{aligned} \tag{5.52}$$

The expression for W_i then follows from writing $\dot{U}_{gi} + \dot{Z}_{2i}$ as a quadratic form. ■

We now address under what conditions W_i is negative definite, which is important for the stability analysis in the next subsection.

Assumption 5.5.4 (Conditions on K_i^{-1})**.** *Let the permanent droop constant K_i be such that the following inequalities hold*

$$1 - \frac{T_{ti}}{T_{gi}} - \sqrt{\alpha_i} < K_i^{-1} < 1 - \frac{T_{ti}}{T_{gi}} + \sqrt{\alpha_i}, \tag{5.53}$$

where

$$\alpha_i = T_{ti}^2 T_{gi}^{-2}(4T_{gi}T_{ti}^{-1} - 1)(D_{gi}T_{gi}T_{ti}^{-1} - 1). \tag{5.54}$$

Additonally, let D_{gi}, T_{gi}, T_{ti} be such that

$$\begin{aligned} 4T_{gi}T_{ti}^{-1} &> 1 \\ D_{gi}T_{gi}T_{ti}^{-1} &> 1, \end{aligned} \tag{5.55}$$

are satisfied.

Remark 5.5.5 (Locally verifiable)**.** *The power network generally consists of many generators. It is therefore important to note that the validity of Assumption 5.5.4 can be checked at each generator using only information that is locally available.*

Lemma 5.5.6 (Negative definiteness of W_i)**.** *Let Assumption 5.5.4 hold. Then $W_i < 0$.*

Proof. Inequality (5.55) guarantees that

$$X_i = \begin{bmatrix} -T_{gi}T_{ti}^{-1} & -\frac{1}{2} \\ -\frac{1}{2} & -1 \end{bmatrix} < 0. \tag{5.56}$$

It follows that $W_i < 0$ if and only if the Schur complement of X_i in W_i is negative definite. This Schur complement is given by

$$S_i = -D_{gi} - \begin{bmatrix} -\frac{1}{2}K_i^{-1} - \frac{1}{2} \\ -\frac{1}{2}K_i^{-1} + \frac{1}{2} \end{bmatrix}^T X_i^{-1} \begin{bmatrix} -\frac{1}{2}K_i^{-1} - \frac{1}{2} \\ -\frac{1}{2}K_i^{-1} + \frac{1}{2} \end{bmatrix}, \tag{5.57}$$

and is quadratic in K_i^{-1}. By Cramer's rule we have

$$X_i^{-1} = \frac{1}{T_{gi}T_{ti}^{-1} - \frac{1}{4}} \begin{bmatrix} -1 & \frac{1}{2} \\ \frac{1}{2} & -T_{gi}T_{ti}^{-1} \end{bmatrix}, \tag{5.58}$$

and a straightforward calculation yields

$$S_i = -D_{gi} + \frac{\frac{1}{4}T_{gi}T_{ti}^{-1}K_i^{-2} + (\frac{1}{2} - \frac{1}{2}T_{gi}T_{ti}^{-1})K_i^{-1} + \frac{1}{2} + \frac{1}{4}T_{gi}T_{ti}^{-1}}{T_{gi}T_{ti}^{-1} - \frac{1}{4}}. \tag{5.59}$$

The solution to $S_i = 0$ is given by the quadratic formula resulting in

$$K_i^{-1} = \frac{-b_i}{2a_i} \pm \sqrt{\frac{b_i^2 - 4a_i c_i}{4a_i^2}}, \tag{5.60}$$

with

$$\begin{aligned} a_i &= \frac{1}{4} T_{gi} T_{ti}^{-1} \\ b_i &= \frac{1}{2} - \frac{1}{2} T_{gi} T_{ti}^{-1} \\ c_i &= -D_{gi}(T_{gi} T_{ti}^{-1} - \frac{1}{4}) + \frac{1}{2} + \frac{1}{4} T_{gi} T_{ti}^{-1}. \end{aligned} \tag{5.61}$$

Algebraic manipulations then yield

$$\begin{aligned} \frac{-b_i}{2a_i} &= 1 - \frac{T_{ti}}{T_{gi}} \\ \frac{b_i^2 - 4a_i c_i}{4a_i^2} &= T_{ti}^2 T_{gi}^{-2} - T_{ti} T_{gi}^{-1}(4 + D_{gi}) + 4D_{gi} \\ &= T_{ti}^2 T_{gi}^{-2}(4 T_{gi} T_{ti}^{-1} - 1)(D_{gi} T_{gi} T_{ti}^{-1} - 1) \\ &= \alpha_i. \end{aligned} \tag{5.62}$$

It can now be readily confirmed that $S_i < 0$ when (5.53) holds, where $\sqrt{\alpha_i}$ is real as a result of inequality (5.55). ■

5.5.3 Stability analysis and optimal distributed control

Having discussed the separate control of the various turbine-governors, we now turn our attention to the question of how the different controllers in the network can cooperate to ensure minimization of the generation costs at steady state. To this end we add an additional communication term to controllers (5.38) and (5.46) representing the exchange of information on the marginal costs among the controllers

$$T_{\theta_i} \dot{\theta}_i = -\theta_i + P_{ti} - K_i^{-1} q_i \sum_{j \in \mathcal{N}_i^{com}} (q_i \theta_i + r_i - (q_j \theta_j + r_j)), \quad \forall i \in \mathcal{V}_{g1} \tag{5.63}$$

$$T_{\theta_i} \dot{\theta}_i = -\theta_i + P_{gi} - (1 - K_i^{-1}) \omega_{gi} - q_i \sum_{j \in \mathcal{N}_i^{com}} (q_i \theta_i + r_i - (q_j \theta_j + r_j)), \quad \forall i \in \mathcal{V}_{g2} \tag{5.64}$$

where $\mathcal{N}_i^{com}$ is the set of buses connected via a communication link to bus i. The additional communication term can be interpreted as a consensus algorithm, where

generator i compares its marginal cost with the marginal costs of connected generators, such that the overall network converges to the state where there is consensus in the marginal costs (see Theorem 5.5.9). Due to the modified dynamics of the controller state θ_i, the derivatives of Z_{1i} and Z_{21} along the solutions to (5.63), (5.64) need to be reevaluated. We exploit the result in the proof of Theorem 1, but is discussed separately for the sake of readability.

Remark 5.5.7 (Communication induced modifications)**.** *As a result of the additional communication term in (5.63), (5.64), the expressions for $\dot{Z}_{1i}$ and $\dot{Z}_{2i}$ given in respectively (5.41) and (5.50) need to be modified. Notice that*

$$q_i \sum_{j \in \mathcal{N}_i^{com}} (q_i\theta_i + r_i - (q_j\theta_j + r_j)) = \big(Q\mathcal{L}^{com}(Q\theta + R)\big)_i, \tag{5.65}$$

where $\mathcal{L}^{com}$ is the Laplacian matrix reflecting the topology of the communication network. Therefore, we add the following term to $\dot{Z}_{1i}$ and $\dot{Z}_{2i}$

$$-(\theta_i - \overline{\theta}_i^{opt})\big(Q\mathcal{L}^{com}(Q\theta + R)\big)_i \tag{5.66}$$

Summing over all buses $i \in \mathcal{V}_g$ then yields

$$\begin{aligned} &- \sum_{i \in \mathcal{V}_g} (\theta_i - \overline{\theta}_i^{opt})\big(Q\mathcal{L}^{com}(Q\theta + R)\big)_i \\ &= -(\theta - \overline{\theta}^{opt})^T Q\mathcal{L}^{com}(Q\theta + R) \\ &= -(Q\theta + R - (Q\overline{\theta}^{opt} + R))^T \mathcal{L}^{com}(Q\theta + R - (Q\overline{\theta}^{opt} + R)), \end{aligned} \tag{5.67}$$

where we exploited

$$\mathcal{L}^{com}(Q\overline{\theta}^{opt} + R) = \mathbf{0}, \tag{5.68}$$

which is a result of $\overline{\theta}^{opt} = \overline{P}_t^{opt}$, $Q\overline{\theta}^{opt} + R \in \mathrm{Im}(\mathbb{1}_{n_g})$ and $\mathrm{Ker}(\mathcal{L}^{com}) = \mathrm{Im}(\mathbb{1}_{n_g})$.

The communication network is utilized to ensure that all marginal costs converge to the same value throughout the network (see the proof of Theorem 1), leading to the following assumption:

Assumption 5.5.8 (Connectivity)**.** *The graph reflecting the topology of information exchange among the controllers is undirected and connected, but can differ from the topology of the power network.*

We are now ready to state the main result of this section.

Theorem 5.5.9 (Distributed optimal LFC)**.** *Let Assumptions 1, 2, 3 and 4 hold. Consider the power network (5.3), turbine-governor dynamics (5.37), (5.45) and the distributed controllers (5.63), (5.64). Then, solutions that start sufficiently close to* $(\overline{\eta}, \overline{\omega} = \mathbf{0}, \overline{P}_t^{opt}, \overline{P}_g^{opt}, \overline{\theta}^{opt})$ *converge to the set where we have frequency regulation and where the power generation solves optimization problem (5.9), i.e.* $\overline{\omega} = \mathbf{0}$ *and* $\overline{P}_t = \overline{P}_t^{opt}$.

Proof. As a result of Lemma 5.3.1, Corollary 1, Lemma 5.5.3 and Remark 5.5.7, we have that $U + \sum_{i\in\mathcal{V}_{g1}} Z_{1i} + \sum_{i\in\mathcal{V}_{g2}} Z_{2i}$ satisfies

$$\begin{aligned}
&\dot{U} + \sum_{i\in\mathcal{V}_{g1}} \dot{Z}_{1i} + \sum_{i\in\mathcal{V}_{g2}} \dot{Z}_{2i} \\
&= -\|\omega_l\|_{D_l}^2 + \sum_{i\in\mathcal{V}_{g1}} -D_{gi}\omega_{gi}^2 - K_i(\theta_i - P_{ti})^2 \\
&+ \sum_{i\in\mathcal{V}_{g2}} \begin{bmatrix} \omega_{gi} \\ P_{gi} - P_{ti} \\ P_{gi} - \theta_i \end{bmatrix}^T W_i \begin{bmatrix} \omega_{gi} \\ P_{gi} - P_{ti} \\ P_{gi} - \theta_i \end{bmatrix} \\
&- (Q\theta + R - (Q\overline{\theta}^{opt} + R))^T \mathcal{L}^{com} (Q\theta + R - (Q\overline{\theta}^{opt} + R)) \\
&\leq 0,
\end{aligned} \tag{5.69}$$

along the solutions to the power network (5.3), turbine-governor dynamics (5.37), (5.45) and the distributed controllers (5.63), (5.64). Particularly, it follows from Assumption 5.5.8 that $W_i < 0$. Since $(\overline{\eta}, \overline{\omega} = \mathbf{0}, \overline{P}_t^{opt}, \overline{P}_g^{opt}, \overline{\theta}^{opt})$ is a strict local minimum of $U + \sum_{i\in\mathcal{V}_{g1}} Z_{1i} + \sum_{i\in\mathcal{V}_{g2}} Z_{2i}$ as a consequence of Assumption 5.3.2, there exists a compact level set Υ around $(\overline{\eta}, \overline{\omega} = \mathbf{0}, \overline{P}_t^{opt}, \overline{P}_g^{opt}, \overline{\theta}^{opt})$ which is forward invariant. By LaSalle's invariance principle, any solution starting in Υ asymptotically converges to the largest invariant set contained in $\Upsilon \cap \{(\eta, \omega, P_t, P_g, \theta) : \omega = \mathbf{0}, P_t = \theta, Q\theta + R = Q\overline{\theta}^{opt} + R + c(t)\mathbb{1}\}$, where $c(t) : \mathbb{R}_{\geq 0} \to \mathbb{R}$ is a function, and $Q\theta + R = Q\overline{\theta}^{opt} + R + c(t)\mathbb{1}$ follows from the connectedness of the communication graph. On this invariant set the power network satisfies

$$\begin{aligned}
\mathbf{0} &= \mathcal{B}^T \mathbf{0} \\
\mathbf{0} &= -D_g \mathbf{0} - \mathcal{B}_g \Gamma \sin(\eta) + \overline{P}_t^{opt} + c(t) Q^{-1} \mathbb{1}_{n_g} \\
\mathbf{0} &= -D_l \mathbf{0} - \mathcal{B}_l \Gamma \sin(\eta) - P_d.
\end{aligned} \tag{5.70}$$

Premultiplying the second and third line of (5.70) with $\mathbb{1}_n^T$, we have

$$\mathbb{1}_n^T \begin{bmatrix} -D_g \mathbf{0} - \mathcal{B}_g \Gamma \sin(\eta) + \overline{P}_t^{opt} + c(t) Q^{-1} \mathbb{1}_{n_g} \\ -D_l \mathbf{0} - \mathcal{B}_l \Gamma \sin(\eta) - P_d. \end{bmatrix} = 0. \tag{5.71}$$

Since $\mathbb{1}_n^T \begin{bmatrix} D_g \\ D_l \end{bmatrix} = \mathbf{0}$, $\mathbb{1}_{n_g}^T \overline{P}_t^{opt} - \mathbb{1}_{n_l}^T P_d = 0$ and Q^{-1} is a diagonal matrix with only positive elements, it follows that necessarily $c(t) = 0$. We can therefore conclude that the system indeed converges to the set where $\omega = \mathbf{0}$ and $P_t = \overline{P}_t^{opt}$, characterized in Lemma 5.2.3. ■

Remark 5.5.10 (Region of attraction)**.** *The local nature of our result is a consequence of the considered incremental storage function having a local minimum at the desired steady state. Nevertheless, the provided results are helpful to further characterize various sublevel sets of the incremental storage function (Dvijotham et al. 2015), (Vu and Turitsyn 2016), (De Persis and Monshizadeh 2017), for instance by numerically assessing the sublevel sets that are compact. We leave a thorough analysis of the region of attraction as an interesting future direction.*

Remark 5.5.11 (Primal-dual based approaches)**.** *A popular alternative to the consensus based algorithm (5.63), (5.64) is a primal-dual gradient based approach. To obtain a distributed solution, optimization problem (5.9) is equivalently replaced*[2] *by*

$$\begin{aligned} &\min_{P_t} C(P_t) \\ \text{s.t.} \quad &\mathbf{0} = -\mathcal{B}v + \begin{bmatrix} P_t \\ -P_d \end{bmatrix}. \end{aligned} \tag{5.72}$$

The associated Lagrangian function is given by

$$L(P_t, \lambda) = C(P_t) + \lambda^T \big(-\mathcal{B}v + \begin{bmatrix} P_t \\ -P_d \end{bmatrix} \big), \tag{5.73}$$

where λ is called the Lagrange multiplier. Under convexity of (5.72), strong duality holds and the solution to (5.72) is equivalent (Boyd and Vandenberghe 2004) to the solution to

$$\max_{\lambda} \min_{P_t} L(P_t, \lambda). \tag{5.74}$$

Following (Zhang and Papachristodoulou 2015), (Li et al. 2016), (Stegink et al. 2017), a continuous primal-dual algorithm can be exploited to solve (5.74). However, since the evolution of P_t is described by the turbine dynamics, we cannot design its dynamics. Bearing in mind that controller (5.38) and (5.46) enforce a steady state where $P_t = \theta$, we solve instead

$$\max_{\lambda} \min_{\theta} L(\theta, \lambda), \tag{5.75}$$

[2]See Lemma 2.3.3 for a discussion on the equivalence of (5.9) and (5.72).

where the dynamics of θ can be freely adjusted. Inspired by the results in (Zhang and Papachristodoulou 2015), (Li et al. 2016), (Stegink et al. 2017), we replace the communication term in (5.63), (5.64),

$$-q_i \sum_{j \in \mathcal{N}_i^{com}} (q_i \theta_i + r_i - (q_j \theta_j + r_j)) \tag{5.76}$$

by

$$\frac{\partial L}{\partial \theta_i} = -\nabla C_i(\theta_i) + \lambda_i, \tag{5.77}$$

yielding the modified controllers

$$T_{\theta_i} \dot{\theta}_i = -\theta_i + P_{ti} - K_i^{-1}(\nabla C_i(\theta_i) - \lambda_i), \quad \forall i \in \mathcal{V}_{g1} \tag{5.78}$$

$$T_{\theta_i} \dot{\theta}_i = -\theta_i + P_{gi} - (1 - K_i^{-1})\omega_{gi} - (\nabla C_i(\theta_i) - \lambda_i). \quad \forall i \in \mathcal{V}_{g2} \tag{5.79}$$

The variables v and λ evolve according to

$$\begin{aligned} \dot{v} &= \frac{\partial L}{\partial v} = -\mathcal{B}^T \lambda \\ \dot{\lambda} &= -\frac{\partial L}{\partial \lambda} = \mathcal{B} v - \begin{bmatrix} \theta \\ -P_d \end{bmatrix}. \end{aligned} \tag{5.80}$$

The analysis of Theorem 5.5.9 can now be repeated with the additional storage term

$$Z_3 = \frac{1}{2}(v - \overline{v})^T (v - \overline{v}) + \frac{1}{2}(\lambda - \overline{\lambda})^T (\lambda - \overline{\lambda}). \tag{5.81}$$

We notice that in this case only convexity of $C(\cdot)$ is required and that the load P_d appears in (5.80).

Remark 5.5.12 (Load control)**.** *Incorporating load control in the LFC has been recently studied in e.g. (Zhao et al. 2013), (Chen et al. 2012), (Weckx et al. 2015) and can be incorporated within the presented framework with minor modifications with respect to the previous discussion. To do so, we modify the dynamics at the load buses $i \in \mathcal{V}_l$ to become*

$$\begin{aligned} \dot{\delta}_i &= \omega_{li} \\ 0 &= -D_{li}\omega_{li} - \sum_{j \in \mathcal{N}_i} V_i V_j B_{ij} \sin(\delta_i - \delta_j) - P_{li} - u_{li}, \end{aligned} \tag{5.82}$$

where u_{li} is the additional controllable load. Associated to every controllable load is a strictly concave benefit function of the form

$$C_i^B(u_{li}) = \frac{1}{2} q_i u_{li}^2 + r_i u_{li} + s_i, \tag{5.83}$$

which is a common approach to quantify the benefit of the consumed power. Instead of minimizing the total generation costs as in (5.9) we now aim at maximizing the so-called 'social welfare' (Berger and Schweppe 1989), (Kiani and Annaswamy n.d.),

$$\begin{aligned} &\max_{u_l, P_t} C^B(u_l) - C(P_t) \\ \text{s.t.} \quad &0 = \mathbb{1}_{n_g}^T \overline{P}_t - \mathbb{1}_{n_l}^T (P_d + u_l), \end{aligned} \tag{5.84}$$

where $C^B(u_l) - C(P_t) = \sum_{i \in \mathcal{V}_l} C_i^B(u_{li}) - \sum_{i \in \mathcal{V}_g} C_i(P_{ti})$. Notice that (5.84) is equivalent to (5.9) in the absence of controllable loads. A straightforward but remarkable extension of Lemma 5.3.1 is that $U(\omega_g, \overline{\omega}_g, \eta, \overline{\eta})$ as in (5.17) now satisfies along the solutions to (5.3) and (5.82)

$$\begin{aligned} \dot{U} = &- \|\omega_g - \overline{\omega}_g\|_{D_g}^2 - \|\omega_l - \overline{\omega}_l\|_{D_l}^2 \\ &+ (\omega_g - \overline{\omega}_g)^T (P_t - \overline{P}_t) \\ &- (\omega_l - \overline{\omega}_l)^T (u_l - \overline{u}_l), \end{aligned} \tag{5.85}$$

i.e. the power network is also output strictly cyclo-incrementally passive with respect to the additional input-output pair $(u_l, -\omega_l)$. This property allows to incorporate load control in the same manner as the generation control. A thorough discussion on all possible load dynamics is outside the scope of this work, although the considered turbine-governor dynamics can be straightforwardly adapted. In the case there are no restrictions on the design, a possible load controller is given by

$$\begin{aligned} T_{\theta_i} \dot{\theta}_i &= \omega_{li} - q_i \sum_{j \in \mathcal{N}_i^{com}} (q_i \theta_i + r_i - (q_j \theta_j + r_j)) \qquad \forall i \in \mathcal{V}_l \\ u_{li} &= \theta_{li}. \end{aligned} \tag{5.86}$$

The analysis of Theorem 5.5.9 can now be repeated with the additional storage term

$$Z_{3i} = \frac{1}{2} \sum_{i \in \mathcal{V}_l} (\theta_i - \overline{\theta}_i^{opt})^2. \tag{5.87}$$

5.6 Case study

To illustrate the proposed control scheme we adopt the 6 bus system from (Wood and Wollenberg 1996). Its topology is shown in Figure 5.1. The relevant generator and load parameters are provided in Table 5.3 , whereas the transmission line parameters are provided in Table 5.4. The used numerical values are based on (Wood and Wollenberg 1996) and (Venkat et al. 2006). The turbine-governor dynamics are modelled by the second order model (5.45). Every generator is equipped with the

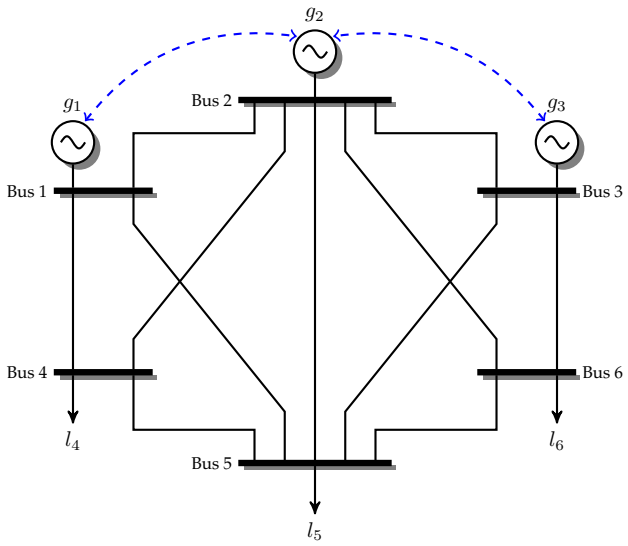

Figure 5.1: Diagram for a 6-bus power network, consisting of 3 generator and 3 load buses. The turbine-governor dynamics of generators are represented by a second order model. The communication links are represented by the dashed lines.

controller presented in (5.64). The communication links between the controllers are also depicted in Figure 5.1. The system is initially at steady state with loads P_{d1}, P_{d2} and P_{d3} being 1.01, 1.20 and 1.18 pu respectively (assuming a base power of 100 MVA). After 10 seconds the loads are respectively increased to 1.15, 1.25 and 1.21 pu. From Figure 5.2 we can see how the controllers regulate the frequency deviation back to zero. The total generation is shared optimally among the different generators such that (5.9) is solved.

5.6.1 Instability

We now show that a wrongly chosen value for the frequency gain $(1 - K_i^{-1})$ in controller (5.64) can lead to instability. To do so, we change the controller at generator 3 into

$$T_{\theta_3}\dot{\theta}_3 = -\theta_3 + P_{s3} - 5(1 - K_3^{-1})\omega_{g3} - q_3 \sum_{j \in \mathcal{N}_3^{com}} (q_3\theta_3 + r_3 - (q_j\theta_j + r_j)), \tag{5.88}$$

for $t > 5$. Leaving all other values identical to the previous simulation, we notice from Figure 5.3 that this change at only one generator can cause instability throughout the whole network.

	Bus 1	Bus 2	Bus 3	Bus 4	Bus 5	Bus 6
M_i	4.6	6.2	5.1	–	–	–
D_{gi}	3.4	3.0	4.2	–	–	–
D_{li}	–	–	–	1.0	1.6	1.2
V_i	1.05	0.98	1.04	1.01	1.03	1.00
T_{gi}	4.0	4.6	5.0	–	–	–
T_{ti}	5.0	6.7	10.0	–	–	–
K_i	0.5	0.5	0.5	–	–	–
$T_{\theta i}$	0.1	0.1	0.1	–	–	–
q_i	2.4	3.8	3.4	–	–	–
r_i	10.5	5.7	8.9	–	–	–
s_i	9.1	14.4	13.2	–	–	–

Table 5.3: Numerical values of the generator and load parameters. The values for K_i satisfy Assumption 3.

B_{ij} (pu)	1	2	3	4	5	6	j
1	–	-4.0	–	-4.7	-3.1	–	
2	-4.0	–	-3.8	-8.0	-3.0	-4.5	
3	–	-3.8	–	–	-3.2	-9.6	
4	-4.7	-8.0	–	–	-2.0	–	
5	-3.1	-3.0	-3.2	-2.0	–	-3.0	
6	–	-4.5	-9.6	–	-3.0	–	
i							

Table 5.4: Susceptance B_{ij} of the transmission line connecting bus i and bus j. Values are per unit on a base of 100 MVA.

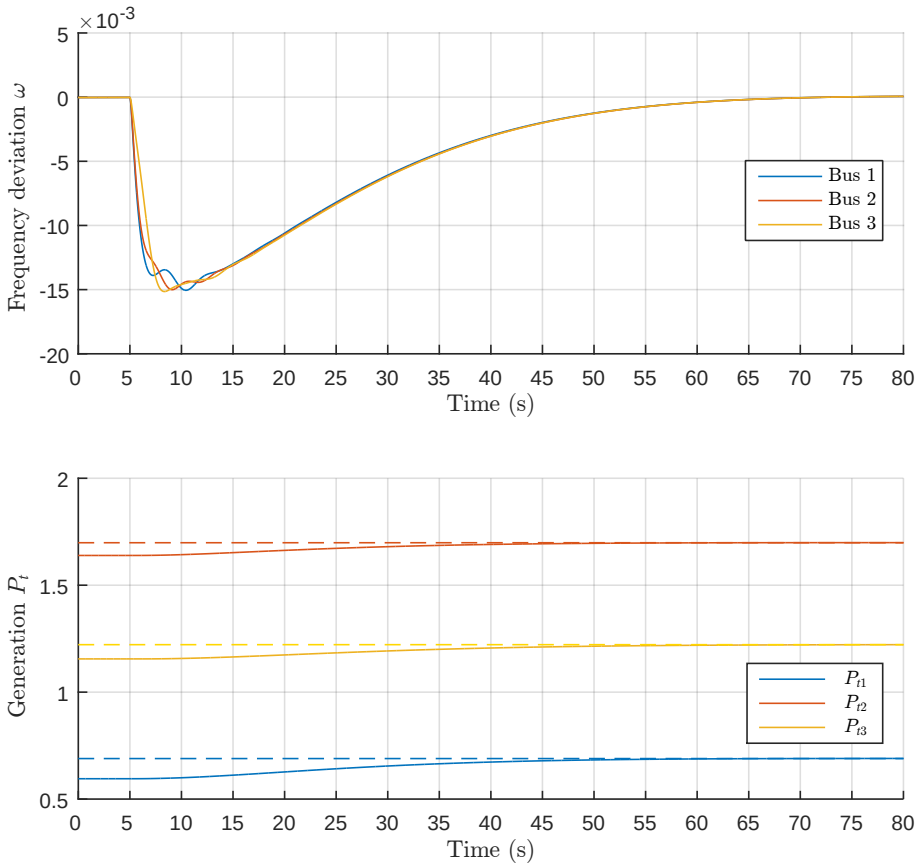

Figure 5.2: Frequency response and generated power at the generator buses using the controllers (5.64). The load is increased at timestep 5, whereafter the frequency deviation is regulated back to zero and generation costs are minimized. The cost minimizing generation $\overline{P}_t^{opt}$ for $t > 5$, characterized in Lemma 5.2.3, is given by the dashed lines.

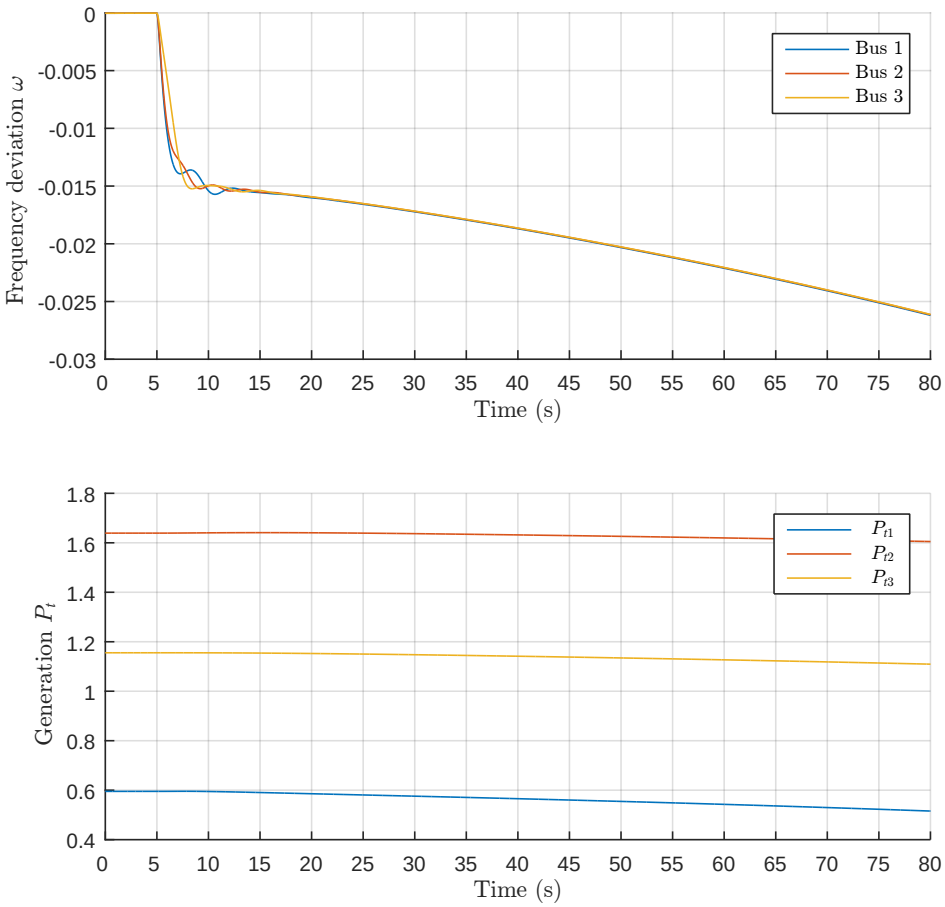

Figure 5.3: Frequency response and generated power at the generator buses using the controllers (5.64). The load is increased at timestep 5 and the controller at generator 3 is replaced by (5.88). Both the frequency deviation and the power generation become unstable.

Published in:

S. Trip, M. Cucuzella, C. De Persis, A.J. van der Schaft and A. Ferrara – *"Passivity based design of sliding modes for optimal Load Frequency Control,"* 2017, under review.

M. Cucuzella, S. Trip, C. De Persis and A. Ferrara – *"Distributed second order sliding modes for Optimal Load Frequency Control,"* Proceedings of the 2017 American Control Conference (ACC), pp. 3451–3456, Seattle, WA, USA, 2017.

Chapter 6

Passivity based design of sliding modes

Abstract

This chapter proposes a distributed sliding mode control strategy for optimal *Load Frequency Control (OLFC) in power networks, where besides frequency regulation also minimization of generation costs is achieved (economic dispatch). We study a nonlinear power network partitioned into control areas, where each area is modelled by an equivalent generator including voltage and second order turbine-governor dynamics. Desired passivity properties of the turbine-governor suggest the design of a sliding manifold, such that the turbine-governor system is passive once the sliding manifold is attained. This chapter offers a new perspective on OLFC by means of sliding mode control, and in comparison with the previous chapter, we relax required assumptions on the system parameters.*

6.1 Control areas with second order turbine-governor dynamics

The considered model in this chapter extends the control area model studied in Chapter 2, with the second order turbine-governor dynamics discussed in Section 5.5. For convenience we will recall the associated dynamics and state the previously established incremental passivity property of the control area model in a slightly different manner. Consequently, we again consider a power network consisting of n interconnected control areas. The network topology is represented by a connected and undirected graph $\mathcal{G} = (\mathcal{V}, \mathcal{E})$, where the nodes $\mathcal{V} = \{1, ..., n\}$, represent the control areas and the edges $\mathcal{E} = \{1, ..., m\}$, represent the transmission lines connecting the areas. The topology can be described by its corresponding incidence matrix $\mathcal{B} \in \mathbb{R}^{n \times m}$. Then, by arbitrarily labeling the ends of edge k with a $+$ and a $-$, one

has that

$$\mathcal{B}_{ik} = \begin{cases} +1 & \text{if } i \text{ is the positive end of } k \\ -1 & \text{if } i \text{ is the negative end of } k \\ 0 & \text{otherwise.} \end{cases}$$

A control area is represented by an equivalent generator and a load, where the governing dynamics of the i-th area are described by the so called 'flux-decay' or 'single-axis model' given as (Machowski et al. 2008):

$$\begin{aligned} \dot{\delta}_i &= \omega_i \\ T_{pi}\dot{\omega}_i &= -\omega_i + K_{pi}\Big(\sum_{j\in\mathcal{N}_i} V_i V_j B_{ij}\sin(\delta_i-\delta_j) - P_{di} + P_{ti}\Big) \\ T_{Vi}\dot{V}_i &= \overline{E}_{fi} - \big(1-(X_{di}-X'_{di})B_{ii}\big)V_i - (X_{di}-X'_{di})\sum_{j\in\mathcal{N}_i} V_j B_{ij}\cos(\delta_i-\delta_j), \end{aligned} \tag{6.1}$$

where $\mathcal{N}_i$ is the set of control areas connected to the i-th area by transmission lines. Moreover, P_{ti} in (6.1) is the power generated by the i-th (equivalent) plant and can be expressed as the output of the following second order dynamical system that describes the behaviour of both the governor and the turbine:

$$\begin{aligned} T_{ti}\dot{P}_{ti} &= -P_{ti} + P_{gi} \\ T_{gi}\dot{P}_{gi} &= -\frac{1}{K_i}\omega_i - P_{gi} + u_i. \end{aligned} \tag{6.2}$$

The symbols used in (6.1) and (6.2) are described in Table 6.1. We aim at the design of a continuous control input u_i to achieve both frequency regulation and economic efficiency (optimal Load Frequency Control).
To study the power network we write system (6.1) compactly for all areas $i \in \mathcal{V}$ as

$$\begin{aligned} \dot{\eta} &= \mathcal{B}^T\omega \\ T_p\dot{\omega} &= -\omega + K_p(P_t - P_d - \mathcal{B}\Gamma(V)\sin(\eta)) \\ T_V\dot{V} &= -(X_d - X'_d)E(\eta)V + \overline{E}_f, \end{aligned} \tag{6.3}$$

and the turbine-governor dynamics in (6.2) as

$$\begin{aligned} T_t\dot{P}_t &= -P_t + P_g \\ T_g\dot{P}_g &= -K^{-1}\omega - P_g + u, \end{aligned} \tag{6.4}$$

where $\eta = \mathcal{B}^T\delta \in \mathbb{R}^m$ is vector describing the differences in voltage angles. Furthermore, $\Gamma = \text{diag}\{\Gamma_1, \ldots, \Gamma_m\}$, where $\Gamma(V)_k = V_i V_j B_{ij}$, with $k \sim \{i, j\}$, i.e., line k

	State variables
δ_i	Voltage angle
ω_i	Frequency deviation
V_i	Voltage
P_{ti}	Turbine output power
P_{gi}	Governor output
	Parameters
T_{pi}	Time constant of the control area
T_{ti}	Time constant of the turbine
T_{gi}	Time constant of the governor
T_{Vi}	Direct axis transient open-circuit constant
K_{pi}	Gain of the control area
K_i	Speed regulation coefficient
X_{di}	Direct synchronous reactance
X'_{di}	Direct synchronous transient reactance
B_{ij}	Transmission line susceptance
	Inputs
u_i	Control input to the governor
$\overline{E}_{fi}$	Constant exciter voltage
P_{di}	Unknown power demand

Table 6.1: Description of the used symbols

connects areas i and j. The components of the matrix $E(\eta) \in \mathbb{R}^{m\times m}$ are defined as

$$\begin{aligned} E_{ii}(\eta) =& \frac{1}{X_{di} - X'_{di}} - B_{ii} && i \in \mathcal{V} \\ E_{ij}(\eta) =& B_{ij}\cos(\eta_k) = E_{ji}(\eta) && k \sim \{i,j\} \in \mathcal{E} \\ E_{ij}(\eta) =& 0 && \text{otherwise.} \end{aligned} \tag{6.5}$$

The remaining symbols follow straightforwardly from (6.1) and (6.2), and are vectors and matrices of suitable dimensions. To permit the controller design in the next sections, the following assumption is made on the *unknown* demand (unmatched disturbance) and the available measurements:

Assumption 6.1.1 (Available information)**.** *The variables ω_i, P_{ti} and P_{gi} are locally available at control area i. The unmatched disturbance P_{di} is unknown, and can be bounded as*

$$|P_{di}| \leq \mathcal{D}_i, \tag{6.6}$$

where $\mathcal{D}_i$ is a positive constant available at control area i.

Before recalling the incremental passivity property for the considered power network model, we first need the following assumption on the existence of a steady state solution.

Assumption 6.1.2 (Steady state solution)**.** *The unknown power demand (unmatched disturbance) P_d is constant and for a given P_d, there exist a $\overline{u}$ and a state $(\overline{\eta}, \overline{\omega}, \overline{V}, \overline{P}_t, \overline{P}_g)$ that satisfies*

$$\begin{aligned} \mathbf{0} &= \mathcal{B}^T \overline{\omega} \\ \mathbf{0} &= -\overline{\omega} + K_p(\overline{P}_t - P_d - \mathcal{B}\Gamma(\overline{V})\sin(\overline{\eta})) \\ \mathbf{0} &= -(X_d - X_d')E(\overline{\eta})\overline{V} + \overline{E}_f, \end{aligned} \tag{6.7}$$

and

$$\begin{aligned} \mathbf{0} &= -\overline{P}_t + \overline{P}_g \\ \mathbf{0} &= -K^{-1}\overline{\omega} - \overline{P}_g + \overline{u}. \end{aligned} \tag{6.8}$$

To state an incremental passivity property of (6.3), we make use of the following storage function (Trip et al. 2016), (De Persis and Monshizadeh 2017):

$$S_1(\eta, \omega, V) = \frac{1}{2}\omega^T T_p \omega + \frac{1}{2} V^T E(\eta) V, \tag{6.9}$$

that can also be interpreted as a Hamiltonian function of the system (Stegink et al. 2017).

Lemma 6.1.3 (Incremental cyclo-passivity of (6.3))**.** *System (6.3) with input P_t and output ω is a strictly output incrementally cyclo-passive system, with respect to the constant $(\overline{\eta}, \overline{\omega}, \overline{V})$ satisfying (6.7).*

Proof. For notational convenience we define $x = (\eta, \omega, V)$. Following the calculation in Chapter 2, evaluation of (note the use of a calligraphic $\mathcal{S}$)

$$\mathcal{S}_1(x) = S_1(x) - S_1(\overline{x}) - \nabla S_1(\overline{x})^T (x - \overline{x}), \tag{6.10}$$

shows that $\mathcal{S}_1(x)$ satisfies (see Chapter 2)

$$\begin{aligned} \dot{\mathcal{S}}_1(x) = &-\omega^T K_p^{-1} \omega - \dot{V}^T T_V (X_d - X_d')^{-1} \dot{V} \\ &+ (\omega - \overline{\omega})^T (P_t - \overline{P}_t), \end{aligned} \tag{6.11}$$

along the solutions to (6.3). ■

For the stability analysis in Section 6.4 the following technical assumption is needed on the steady state that eventually allows us to infer boundedness of solutions.[1]

Assumption 6.1.4 (Steady state voltages and voltage angles)**.** *Let $\overline{V} \in \mathbb{R}^n_{>0}$ and let differences in steady state voltage angles satisfy*

$$\overline{\eta}_k \in (-\frac{\pi}{2}, \frac{\pi}{2}) \quad \forall k \in \mathcal{E}. \tag{6.12}$$

Furthermore, for all $i \in \mathcal{V}$ it holds that

$$\frac{1}{X_{di} - X'_{di}} - B_{ii} - \sum_{k \sim \{i,j\} \in \mathcal{E}} \frac{B_{ij}(\overline{V}_i + \overline{V}_j \sin^2(\overline{\eta}_k))}{\overline{V}_i \cos(\overline{\eta}_k)} > 0 \tag{6.13}$$

The assumption above holds if the generator reactances are small compared to the line reactances and the differences in voltage (angles) are small (De Persis and Monshizadeh 2017). It is important to note that this holds for typical operation points of the power networks. The main consequence of Assumption 6.1.4 is that the incremental storage function $\mathcal{S}_1$ now obtains a strict local minimum at a steady state satisfying (6.7).

Lemma 6.1.5 (Local minimum of $\mathcal{S}_1$)**.** *Let Assumptions 6.1.4 hold. Then, the incremental storage function $\mathcal{S}_1$ has a local minimum at $(\overline{\eta}, \overline{\omega}, \overline{V})$ satisfying (6.7).*

Proof. Under Assumption 6.1.4, the Hessian of (6.9), evaluated at $(\overline{\eta}, \overline{\omega}, \overline{V})$, is positive definite (Chapter 3). Consequently, $S_1(\overline{\eta}, \overline{\omega}, \overline{V})$ is strictly convex. The incremental storage function (6.10) is defined as a Bregman distance (Bregman 1967) associated with (6.9) for the points (η, ω, V) and $(\overline{\eta}, \overline{\omega}, \overline{V})$. Due to the strict convexity of $S_1(\overline{\eta}, \overline{\omega}, \overline{V})$, (6.10) has a local minimum at $(\overline{\eta}, \overline{\omega}, \overline{V})$. ■

Remark 6.1.6 (Sliding mode control for different power network models)**.** *The focus of this work is to achieve OLFC by distributed sliding mode control for the nonlinear power network, explicitly taking into account the turbine-governor dynamics. Equations (6.3) well represent power systems for the purpose of frequency regulation and are often further simplified by assuming constant voltages, leading to the so called 'swing equations'. To the analysis in this chapter the incremental passivity property established above is essential, which has been derived for various other models, including microgrids. It is therefore expected that the presented approach can be straightforwardly applied to a wider range of models than the one we consider here.*

[1] In case boundedness of solutions can be inferred by other means, Assumption 6.1.4 can be omitted.

6.2 Frequency regulation and economic dispatch

In this section we recall, for convenience and to make this chapter consistent, the control objectives of optimal load frequency control, that we have considered before in Chapter 2 and Chapter 5. Before doing so, we first note that the steady state frequency deviation $\overline{\omega}$, is generally different from zero without proper adjustments of $\overline{u}$.

Lemma 6.2.1 (Steady state frequency)**.** *Let Assumption 6.1.2 hold, then necessarily* $\overline{\omega} = \mathbb{1}_n\omega^*$ *with*

$$\omega^* = \frac{\mathbb{1}_n^T(\overline{u} - \overline{P}_d)}{\mathbb{1}_n^T(K_p^{-1} + K^{-1})\mathbb{1}_n}, \tag{6.14}$$

where $\mathbb{1}_n \in \mathbb{R}^n$ *is the vector consisting of all ones.*

This leads us to the first objective, concerning the regulation of the frequency deviation.

Objective 6.2.2 (Frequency regulation)**.**

$$\lim_{t\to\infty} \omega(t) = \mathbf{0}. \tag{6.15}$$

From (6.14) it is clear that it is sufficient that $\mathbb{1}_n^T(\overline{u} - \overline{P}_d) = 0$, to have zero frequency deviation at the steady state. Therefore, there is flexibility to distribute the total required generation optimally among the various control areas. To make the notion of optimality explicit we assign to every control area a strictly convex linear-quadratic cost function $C_i(P_{ti})$ related to the generated power P_{ti}:

$$C_i(P_{ti}) = \frac{1}{2}q_iP_{ti}^2 + r_iP_{ti} + s_i \quad \forall i \in \mathcal{V}. \tag{6.16}$$

Minimizing the total generation cost, subject to the constraint that allows for a zero frequency deviation can then be formulated as the following optimization problem:

$$\begin{aligned} &\min \sum_{i\in\mathcal{V}} C_i(P_{ti}) \\ \text{s.t.} \quad &\mathbb{1}_n^T(\overline{u} - \overline{P}_d) = 0. \end{aligned} \tag{6.17}$$

The lemma below, which is identical to Lemma 5.2.3 makes the solution to (6.17) explicit:

Lemma 6.2.3 (Optimal generation)**.** *The solution* $\overline{P}_t^{opt}$ *to (6.17) satisfies*

$$\overline{P}_t^{opt} = Q^{-1}(\overline{\lambda}^{opt} - R), \tag{6.18}$$

where

$$\overline{\lambda}^{opt} = \frac{\mathbb{1}_n \mathbb{1}_n^T (\overline{P}_d + Q^{-1} R)}{\mathbb{1}_n^T Q^{-1} \mathbb{1}_n}, \tag{6.19}$$

and $Q = diag(q_1, \ldots, q_n)$, $R = (r_1, \ldots, r_n)^T$.

From (6.18) it follows that the marginal costs $Q\overline{P}_t^{opt} + R$ are identical. Note that (6.18) depends explicitly on the *unknown* power demand P_d. We aim at the design of a controller solving (6.17) without measurements of the power demand, leading to the second objective.

Objective 6.2.4 (Economic dispatch)**.**

$$\lim_{t \to \infty} P_t(t) = \overline{P}_t^{opt}, \tag{6.20}$$

with $\overline{P}_t^{opt}$ *as in (6.18), without measurements of* P_d.

In order to achieve Objective 6.2.2 and Objective 6.2.4 we refine Assumption 6.1.2 that ensures the feasibility of the objectives.

Assumption 6.2.5 (Existence of a optimal steady state)**.** *Assumption 6.1.2 holds when* $\overline{\omega} = \mathbf{0}$ *and* $\overline{P}_t = \overline{P}_g = \overline{P}_t^{opt}$*, with* $\overline{P}_t^{opt}$ *as in (6.18).*

Remark 6.2.6 (Varying power demand)**.** *To allow for a steady state solution, the power demand (unmatched disturbance) is required to be constant. This is not needed to reach the desired sliding manifold discussed in the next section, but is required only to establish the asymptotic convergence properties in Objective 6.2.2 and Objective 6.2.4.*

6.3 Distributed sliding mode control

In Section 6.1 we discussed a passivity property of the power network (6.3), with input P_t and output ω. Unfortunately, the turbine-governor system (6.4) does not immediately allow for a passive interconnection, since (6.4) is a linear system with relative degree two, when considering $-\omega$ as the input and P_t as the output. To alleviate this issue we propose a *distributed* Suboptimal Second Order Sliding Mode (D–SSOSM) control algorithm that simultaneously achieves Objective 6.2.2 and Objective 6.2.4, by passifying (6.4) and by exchanging information on the marginal costs. As a first step (see also Remark 6.3.2 below), we augment the turbine-governor

dynamics (6.4) with a distributed control scheme, resulting in:

$$\begin{aligned} T_t\dot{P}_t &= -P_t + P_g \\ T_g\dot{P}_g &= -K^{-1}\omega - P_g + u \\ T_\theta\dot{\theta} &= -\theta + P_t - A\mathcal{L}^{com}(Q\theta + R). \end{aligned} \tag{6.21}$$

Here, $Q\theta + R$ reflects the 'virtual' marginal costs and $\mathcal{L}^{com}$ is the Laplacian matrix corresponding to the topology of an underlying communication network. The diagonal matrix $T_\theta \in \mathbb{R}^{n\times n}$ provides additional design freedom to shape the transient response and the matrix A is suggested later to obtain a suitable passivity property. We note that $\mathcal{L}^{com}(Q\theta + R)$ represents the exchange information on the marginal costs among the control areas. To guarantee an optimal coordination of generation among *all* the control areas the following assumption is made:

Assumption 6.3.1 (Communication topology)**.** *The graph corresponding to the communication topology is undirected and connected.*

Remark 6.3.2 (First order turbine-governor dynamics)**.** *The rational behind this seemingly ad-hoc choice of the augmented dynamics is that for the controlled first order turbine-governor dynamics, where $u = \theta$ and $P_g = -K^{-1}\omega + \theta$, system*

$$\begin{aligned} T_t\dot{P}_t &= -P_t - K^{-1}\omega + \theta \\ T_\theta\dot{\theta} &= -\theta + P_t - K^{-1}Q\mathcal{L}^{com}(Q\theta + R), \end{aligned} \tag{6.22}$$

has been shown to be incrementally passive with input $-\omega$ and output P_t, and is able to solve Objective 6.2.2 and Objective 6.2.4 (Chapter 5 and (Trip and De Persis 2017b)). We aim at the design of u and A in (6.21), such that (6.21) behaves similarly as (6.22). This is made explicit in Lemma 6.4.2.

To facilitate the discussion, we recall some definitions that are essential to sliding mode control. To this end, consider system

$$\dot{x} = \zeta(x, u) \tag{6.23}$$

with $x \in \mathbb{R}^n$, $u \in \mathbb{R}^m$.

Definition 6.3.3 (Sliding function)**.** *The sliding function $\sigma(x) : \mathbb{R}^n \to \mathbb{R}^m$ is a sufficiently smooth output function of system* (6.23)*.*

Definition 6.3.4 (r–sliding manifold)**.** *The r–sliding manifold*[2] *is given by*

$$\{x, u \in \mathbb{R}^n : \sigma(x) = L_\zeta \sigma(x) = \cdots = L_\zeta^{(r-1)} \sigma(x) = \mathbf{0}\}, \tag{6.24}$$

where $L_\zeta^{(r-1)}\sigma(x)$ is the $(r-1)$-th order Lie derivative of $\sigma(x)$ along the vector field $\zeta(x,u)$. With a slight abuse of notation we also write $L_\zeta \sigma(x) = \dot{\sigma}(x)$.

Definition 6.3.5 (r–sliding mode)**.** *A r–order sliding mode is enforced from $t = T_r \geq 0$, when, starting from an initial condition $x(0) = x_0$, the state of* (6.23) *reaches the r–sliding manifold* (6.24)*, and there remains for all $t \geq T_r$.*

Note that the order of a sliding mode controller is identical to the order of the sliding mode that it is aimed at enforcing.

We now propose a sliding function $\sigma(\omega, P_t, P_g, \theta)$ and a matrix A for system (6.21), which will allow us to prove convergence to the desired state. The choices are motivated by the stability analysis in the next section, but are stated here for the sake of exposition. First, the sliding function $\sigma : \mathbb{R}^{4n} \to \mathbb{R}^n$ is given by

$$\sigma(\omega, P_t, P_g, \theta) = M_1\omega + M_2 P_t + M_3 P_g + M_4\theta, \tag{6.25}$$

where $M_1 > \mathbf{0}$, $M_2 \geq \mathbf{0}$, $M_3 > \mathbf{0}$ are diagonal matrices and $M_4 = -(M_2 + M_3)$. Therefore, $\sigma_i, i \in \mathcal{V}$, depends only on the locally available variables that are defined on node i, facilitating the design of a distributed controller (see Remark 6.3.7). Second, the diagonal matrix $A \in \mathbb{R}^{n\times n}$ is defined as

$$A = (M_2 + M_3)^{-1} M_1 Q. \tag{6.26}$$

By regarding the sliding function (6.25) as the output function of system (6.3), (6.21), it appears that the relative degree[3] of the system is equal to 1. This implies that a first order sliding mode controller can be *naturally* applied (Utkin 1992) in order to attain in a finite time, the sliding manifold defined by $\sigma = \mathbf{0}$. Note however that the control input u appears in the first time derivative of the sliding function. Since the sliding mode controller will generate a discontinuous control signal, this leads potentially to a discontinuous control input to the governor. Then, in order to provide a continuous control input u to the governor, we also require $\dot{\sigma} = \mathbf{0}$. Therefore, the desired sliding manifold is given by:

$$\{(\eta, \omega, V, P_t, P_g, \theta) : \sigma = \dot{\sigma} = \mathbf{0}\}. \tag{6.27}$$

We continue by discussing a possible controller attaining the desired sliding manifold (6.27) while providing a continuous control input u.

[2] For the sake of simplicity, the order r of the sliding manifold is omitted in the following.

[3] The relative degree is the minimum order ρ of the time derivative $\sigma_i^{(\rho)}, i \in \mathcal{V}$, of the sliding function associated to the i-th node in which the control $u_i, i \in \mathcal{V}$, explicitly appears.

6.3.1 Suboptimal Second Order Sliding Mode controller

To prevent chattering, it is important to provide a continuous control input u to the governor. Since sliding mode controllers generate a discontinuous control signal, we adopt the procedure suggested in (Bartolini et al. 1998a) and first integrate the discontinuous signal, yielding for system (6.21):

$$\begin{aligned} T_t\dot{P}_t &= -P_t + P_g \\ T_g\dot{P}_g &= -K^{-1}\omega - P_g + u \\ T_\theta\dot{\theta} &= -\theta + P_t - A\mathcal{L}^{com}(Q\theta + R) \\ \dot{u} &= w, \end{aligned} \tag{6.28}$$

where w is the new (discontinuous) input generated by a sliding mode controller discussed below. A consequence is that the system relative degree (with respect to the new control input w) is now 2, and we need to rely on a second order ($r = 2$) sliding mode control strategy to attain the sliding manifold (6.25) in a finite time (Levant 2003). To make the controller design explicit, we discuss a specific second order sliding mode controller, the so-called 'Suboptimal Second Order Sliding Mode' (SSOSM) controller proposed in (Bartolini et al. 1998a). We introduce two auxiliary variables $\xi_1 = \sigma \in \mathbb{R}^n$ and $\xi_2 = \dot{\sigma} \in \mathbb{R}^n$, and define the so-called auxiliary system as:

$$\begin{cases} \dot{\xi}_1 = \xi_2 \\ \dot{\xi}_2 = \phi(\eta, \omega, V, P_t, P_g, \theta) + Gw. \end{cases} \tag{6.29}$$

Bearing in mind hat $\dot{\xi}_2 = \ddot{\sigma} = \phi + Gw$, the expressions for the mapping ϕ and matrix G can be straightforwardly obtained from (6.25) by taking the second derivative of σ with respect to time, yielding for the latter[4] $G = M_3 T_g^{-1} \in \mathbb{R}^{n\times n}$. We assume that the entries of ϕ and G have known bounds

$$|\phi_i| \leq \Phi_i \qquad \forall i \in \mathcal{V} \tag{6.30}$$

$$0 < G_{\min_i} \leq G_{ii} \leq G_{\max_i} \qquad \forall i \in \mathcal{V} \tag{6.31}$$

with Φ_i, $G_{\min_i}$ and $G_{\max_i}$ being positive constants. Second, w is a discontinuous control input described by the SSOSM control algorithm (Bartolini et al. 1998a), and consequently for each area $i \in \mathcal{V}$, the control law w_i is given by

$$w_i = -\alpha_i W_{\max_i} \operatorname{sgn}\left(\xi_{1_i} - \frac{1}{2}\xi_{1,\max_i}\right), \tag{6.32}$$

[4]The expression for ϕ is rather long and is omitted.

with

$$W_{\max_i} > \max\left(\frac{\Phi_i}{\alpha_i^* G_{\min_i}}; \frac{4\Phi_i}{3G_{\min_i} - \alpha_i^* G_{\max_i}}\right), \tag{6.33}$$

$$\alpha_i^* \in (0,1] \cap \left(0, \frac{3G_{\min_i}}{G_{\max_i}}\right), \tag{6.34}$$

α_i switching between α_i^* and 1, according to (Bartolini et al. 1998a, Algorithm 1). Note that indeed the input signal to the governor, $u(t) = \int_0^t w(\tau)d\tau$, is continuous, since the input w is piecewise constant.

The extremal values $\xi_{1,\max_i}$ in (6.32) can be detected by implementing for instance a peak detection as in (Bartolini et al. 1998b).

Remark 6.3.6 (Uncertainty of ϕ and G)**.** *The mapping ϕ and matrix G are uncertain due to the presence of the unmeasurable power demand P_d and voltage angle θ, and possible uncertainties in the system parameters. In practical cases the bounds in* (6.30) *and* (6.31) *can be determined relying on data analysis and physical insights. However, if these bounds cannot be a-priori estimated, the adaptive version of the SSOSM algorithm proposed in (Incremona et al. 2016) can be used to dominate the effect of the uncertainties.*

Remark 6.3.7 (Distributed control)**.** *Given A in (6.26), the dynamics of θ_i in* (6.21) *read for node $i \in \mathcal{V}$ as*

$$T_{\theta i}\dot{\theta}_i = -\theta_i + P_{ti} - \frac{Q_i M_{1_{ii}}}{M_{2_{ii}} + M_{3_{ii}}} \sum_{j \in \mathcal{N}_j^{com}} (Q_i\theta_i + R_i - Q_j\theta_j - R_j), \tag{6.35}$$

where $\mathcal{N}_j^{com}$ is the set of controllers connected to controller i. Furthermore, (6.32) *depends only on σ_i, i.e. on states defined at node i. Consequently, the overall controller is indeed distributed and only information on marginal costs needs to be shared among neighbours.*

Remark 6.3.8 (Alternative SOSM controllers)**.** *In this work we rely on the SOSM control law proposed in (Bartolini et al. 1998a). However, to constrain system* (6.3) *augmented with dynamics* (6.28) *on the sliding manifold (6.27), where $\sigma = \dot{\sigma} = \mathbf{0}$, any other SOSM control law that does not need the measurement of $\dot{\sigma}$ can be used. An interesting continuation of the presented results is to study the performance of various SOSM controllers within the setting of (optimal) LFC.*

Remark 6.3.9 (Relaxed conditions on the system parameters)**.** *In comparison to the previous chapter, we do not require the parameters in (6.3) and (6.4) to satisfy Assumption 5.5.4.*

6.4 Stability analysis and main result

In this section we study the stability of the proposed control scheme, based on an enforced passivity property of (6.21) on the sliding manifold defined by (6.25). First, we establish that the second order sliding mode controller (6.29)–(6.34) constrains the system in finite time to the desired sliding manifold.

Lemma 6.4.1 (Convergence to the sliding manifold)**.** *Let Assumption 6.1.1 hold. The solutions to system (6.3), augmented with* (6.28)*, in closed loop with controller* (6.29)–(6.34) *converge in a finite time T_r to the sliding manifold (6.27) such that*

$$P_g = -M_3^{-1}(M_1\omega + M_2P_t + M_4\theta) \quad \forall t \geq T_r. \tag{6.36}$$

Proof. Following (Bartolini et al. 1998a), the application of (6.29)–(6.34) to each control area guarantees that $\sigma = \dot{\sigma} = \mathbf{0},\ \forall\, t \geq T_r$. The details are omitted, and are an immediate consequence of the used SSOSM control algorithm (Bartolini et al. 1998a). Then, from (6.25) one can easily obtain (6.36), where M_3 is indeed invertible. ■

Exploiting relation (6.36), on the sliding manifold where $\sigma = \dot{\sigma} = \mathbf{0}$, the so-called equivalent system is as follows:

$$\begin{aligned} M_3T_t\dot{P}_t &= -(M_2 + M_3)P_t - M_4\theta - M_1\omega \\ T_\theta\dot{\theta} &= -\theta + P_t - A\mathcal{L}^{com}(Q\theta + R). \end{aligned} \tag{6.37}$$

As a consequence of the feasibility assumption (Assumption 6.1.2), the system above admits the following steady state:

$$\begin{aligned} \mathbf{0} &= -(M_2 + M_3)\overline{P}_t^{opt} - M_4\overline{\theta} - M_1\mathbf{0} \\ \mathbf{0} &= -\overline{\theta} + \overline{P}_t^{opt} - A\mathcal{L}^{com}(Q\overline{\theta} + R). \end{aligned} \tag{6.38}$$

Now, we show that system (6.37), with A as in (6.26), indeed possesses a passivity property with respect to the steady state (6.38). Note that, due to the discontinuous control law (6.32), the solutions to the closed loop system are understood in the sense of Filippov. Following the equivalent control method (Utkin 1992), the solutions to the equivalent system are however continuously differentiable.

Lemma 6.4.2 (Incremental passivity of (6.37)**.** *System (6.37) with input $-\omega$ and output P_t is an incrementally passive system, with respect to the constant $(\overline{P}_t^{opt}, \overline{\theta})$ satisfying (6.38).*

Proof. Consider the following incremental storage function

$$\begin{aligned}\mathcal{S}_2 = &\frac{1}{2}(P_t - \overline{P}_t^{opt})^T M_1^{-1} M_3 T_t (P_t - \overline{P}_t^{opt}) \\ &+ \frac{1}{2}(\theta - \overline{\theta})^T M_1^{-1}(M_2 + M_3) T_\theta (\theta - \overline{\theta}),\end{aligned} \tag{6.39}$$

which is positive definite, since $M_1 > \mathbf{0}, M_2 \geq \mathbf{0}$ and $M_3 > \mathbf{0}$. Then, we have that $\mathcal{S}_2$ satisfies along the solutions to (6.37)

$$\begin{aligned}\dot{\mathcal{S}}_2 = &\frac{1}{2}(P_t - \overline{P}_t^{\text{opt}})^T M_1^{-1} M_3 T_t \dot{P}_t \\ &+ \frac{1}{2}(\theta - \overline{\theta})^T M_1^{-1}(M_2 + M_3) T_\theta \dot{\theta} \\ = &\frac{1}{2}(P_t - \overline{P}_t^{opt})^T (-M_1^{-1}(M_2 + M_3) P_t - \omega - M_1^{-1} M_4 \theta) \\ &+ \frac{1}{2}(\theta - \overline{\theta})^T M_1^{-1}(M_2 + M_3)(P_t - \theta - A\mathcal{L}^{com}(Q\theta + R)).\end{aligned}$$

In view of $M_4 = -(M_2 + M_3)$, $A = (M_2 + M_3)^{-1} M_1 Q$ and equality (6.38), it follows that

$$\begin{aligned}\dot{\mathcal{S}}_2 = &- (P_t - \theta)^T M_1^{-1}(M_2 + M_3)(P_t - \theta) \\ &- (Q\theta + R - Q\overline{\theta} - R)\mathcal{L}^{com}(Q\theta + R - Q\overline{\theta} - R) \\ &- (P_t - \overline{P}_t^{opt})^T(\omega - \mathbf{0}).\end{aligned}$$

■

Remark 6.4.3 (Reducing the relative degree)**.** *An important consequence of the proposed sliding mode controller* (6.29)–(6.34) *is that the relative degree of system (6.37) is one with input $-\omega$ and output P_t. This is in contrast to the 'original' system (6.4) that has relative degree two with the same input–output pair.*

Now, relying on the interconnection of incrementally passive systems, we can prove the main result of this chapter concerning the evolution of the augmented system controlled via the proposed distributed SSOSM control strategy.

Theorem 6.4.4 (Main result: distributed OLFC)**.** *Let Assumptions 6.1.1–6.3.1 hold. Consider system* (6.3) *and* (6.21)*, controlled via* (6.29)–(6.34)*. Then, the solutions of the closed-loop system starting in a neighbourhood of the equilibrium $(\overline{\eta}, \overline{\omega} = \mathbf{0}, \overline{V}, \overline{P}_t^{opt}, \overline{P_g}, \overline{\theta})$ approach the set where $\overline{\omega} = \mathbf{0}$ and $\overline{P}_t = \overline{P}_t^{opt}$, with $\overline{P}_t^{opt}$ given by (6.18).*

Proof. Following Lemma 6.4.1, we have that the SSOSM control enforces system (6.21) to evolve $\forall\, t \geq T_r$ on the sliding manifold (6.27), resulting in the reduced order system (6.37). Consider the overall incremental storage function $\mathcal{S} = \mathcal{S}_1 + \mathcal{S}_2$, with $\mathcal{S}_1$ given by (6.10) and $\mathcal{S}_2$ given by (6.39). In view of Lemma 6.1.5, we have that $\mathcal{S}$ has a local minimum at $(\overline{\eta}, \overline{\omega} = \mathbf{0}, \overline{V}, \overline{P}_t^{opt}, \overline{\theta})$ and satisfies along the solutions to (6.3), (6.37)

$$\begin{aligned}\dot{\mathcal{S}} =& -\omega^T K_p^{-1}\omega - \dot{V}^T T_V (X_d - X_d')^{-1}\dot{V} \\ & - (P_t - \theta)^T M_1^{-1}(M_2 + M_3)(P_t - \theta) \\ & - (Q\theta + R - Q\overline{\theta} - R)\mathcal{L}^{com}(Q\theta + R - Q\overline{\theta} - R) \\ \leq\, & 0.\end{aligned}$$

Consequently, there exists a forward invariant set, Υ around $(\overline{\eta}, \overline{\omega} = \mathbf{0}, \overline{V}, \overline{P}_t^{opt}, \overline{\theta})$ and by LaSalle's invariance principle the solutions that start in Υ approach the largest invariant set contained in

$$\begin{aligned}\Upsilon \cap \{(\eta, \omega, V, P_t, \theta) : \omega = \mathbf{0}, V = \big((X_d - X_d')E(\overline{\eta})\big)^{-1}\overline{E}_f, \\ P_t = \theta, \theta = \overline{\theta} + Q^{-1}\mathbb{1}\alpha(t)\},\end{aligned} \tag{6.40}$$

where $\alpha(t) \in \mathbb{R}$ is a scalar. On this invariant set the controlled power network satisfies

$$\begin{aligned}\dot{\eta} &= \mathcal{B}^T\mathbf{0} \\ \mathbf{0} &= K_p(\overline{\theta} + Q^{-1}\mathbb{1}\alpha(t) - P_d - \mathcal{B}\Gamma(V)\sin(\eta)) \\ \mathbf{0} &= -(X_d - X_d')E(\eta)V + \overline{E}_f \\ M_3 T_t \dot{P}_t &= \mathbf{0} \\ T_\theta \dot{\theta} &= \mathbf{0}.\end{aligned} \tag{6.41}$$

Pre-multiplying both sides of the second line of (6.41) with $\mathbb{1}_n^T K_p^{-1}$ yields $0 = \mathbb{1}_n^T(\overline{\theta} + Q^{-1}\mathbb{1}\alpha(t) - P_d)$. Since $\overline{\theta} = \overline{P}_t^{opt}$, $\mathbb{1}_n^T(\overline{P}_t^{opt} - P_d) = 0$ and Q is a diagonal matrix with only positive elements, it follows that necessarily $\alpha(t) = 0$. We can conclude that the solutions to the system (6.3) and (6.21), controlled via (6.29)–(6.34), indeed approach the set where $\overline{\omega} = \mathbf{0}$ and $\overline{P}_t = \overline{P}_t^{opt}$, with $\overline{P}_t^{opt}$ given by (6.18). ■

Remark 6.4.5 (Robustness to failed communication)**.** *The proposed control scheme is distributed and as such requires a communication network to share information on the marginal costs. However, note that the term $-A\mathcal{L}^{com}(Q\theta + R)$ in (6.21) is not needed to enforce the passivity property established in Lemma 6.4.2, but is required to prove convergence to the economic efficient generation $\overline{P}_t^{opt}$. In fact, setting $A = \mathbf{0}$ still permits to infer frequency regulation following the argumentation of Theorem 6.4.4.*

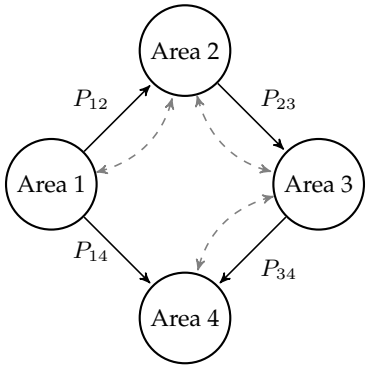

Figure 6.1: Scheme of the considered power network partitioned into 4 control areas, where $P_{ij} = B_{ij}V_iV_j \sin(\delta_i - \delta_j)$. The arrows indicate the positive direction of the power flows through the power network, while the dashed lines represent the communication network.

Remark 6.4.6 (Region of attraction)**.** *LaSalle's invariance principle can be applied to all bounded solutions. As follows from Lemma 6.1.5, we have that the considered incremental storage function has a local minimum at the desired steady state, whereas the time to converge to the sliding manifold can be made arbitrarily small by properly choosing the gains of the SSOSM control. This guarantees that solutions starting in the vicinity of the steady state of interest remain bounded. A preliminary (numerical) assessment indicates that the region of attraction is large, but a thorough analysis is left as future endeavour.*

6.5 Case study

In this section, the proposed control solution is assessed in simulation, by implementing a power network partitioned into four control areas (e.g. the IEEE New England 39-bus system (Nabavi and Chakrabortty 2013)). The topology of the power network is represented in Figure 6.1, together with the communication network (dashed lines). The line parameters are $B_{12} = -5.4$ p.u., $B_{23} = -5.0$ p.u., $B_{34} = -4.5$ p.u. and $B_{14} = -5.2$ p.u., while the network parameters and the power demand ΔP_{di} of each area are provided in Table 6.2, where a base power of 1000MW is assumed. The matrices in (6.25) are chosen as $M_1 = 3I_4$, $M_2 = I_4$, $M_3 = 0.1I_4$ and $M_4 = -(M_2 + M_3)$, $I_4 \in \mathbb{R}^{4\times 4}$ being the identity matrix, while the control amplitude $W_{\max_i}$ and the parameter α_i^*, $i = 1, \ldots, 4$, in (6.32) are 10 and 1, respectively, for all $i \in \mathcal{V}$. For the sake of simplicity, in the cost function (6.16) we select $R_i = s_i = 0$

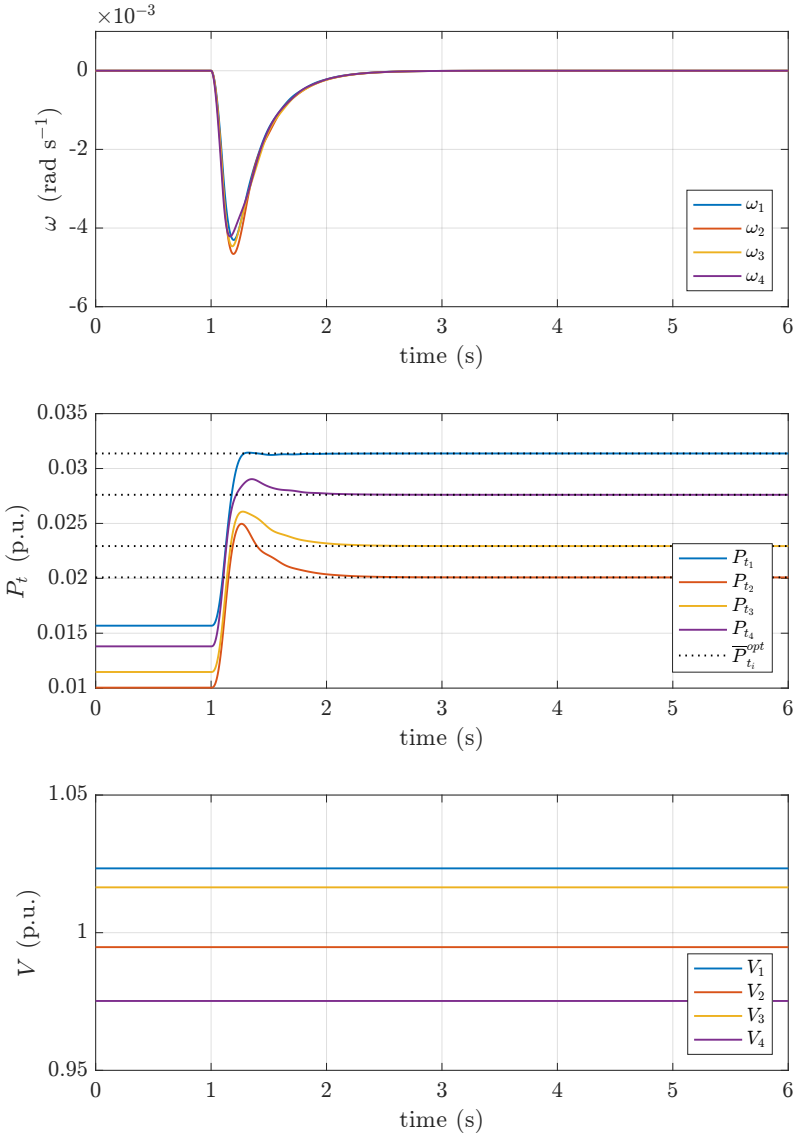

Figure 6.2: Time evolution of the frequency deviation, generated power and voltage dynamics considering a power demand variation at the time instant $t = 1s$.

		Area 1	Area 2	Area 3	Area 4
T_{pi}	(s)	21.0	25.0	23.0	22.0
T_{ti}	(s)	0.30	0.33	0.35	0.28
T_{gi}	(s)	0.080	0.072	0.070	0.081
T_{Vi}	(s)	5.54	7.41	6.11	6.22
K_{pi}	(Hz p.u.$^{-1}$)	120.0	112.5	115.0	118.5
K_i	(Hz p.u.$^{-1}$)	2.5	2.7	2.6	2.8
X_{di}	(p.u.)	1.85	1.84	1.86	1.83
X'_{di}	(p.u.)	0.25	0.24	0.26	0.23
$\overline{E}_{fi}$	(p.u.)	1.0	1.0	1.0	1.0
B_{ii}	(p.u.)	-13.6	-12.9	-12.3	-12.3
$T_{\theta i}$	(s)	0.33	0.33	0.33	0.33
q_i	(\$ p.u.$^{-1}$)	2.42	3.78	3.31	2.75
ΔP_{di}	(p.u.)	0.010	0.015	0.012	0.014

Table 6.2: Network Parameters and power demand

for all $i \in \mathcal{V}$. The system is initially at the steady state. Then, at the time instant $t = 1$s, the power demand in each area is increased according to the values reported in Table 6.2. From Figure 6.2, one can observe that the frequency deviations converge asymptotically to zero after a transient where the frequency drops because of the increasing load. Indeed, one can note that the proposed controllers increase the power generation in order to reach again a zero steady state frequency deviation. Moreover, the total power demand is shared among the areas, minimizing the total generation costs. More precisely, by applying the proposed D-SSOSM, the total generation costs are 10 % less than the generation costs when each area would produce only for its own demand.

Part III

Power networks as cyber-physical systems

Introduction

Increased penetration of renewable energy sources has revived the interest in power network related control issues. The power network is developing towards a situation where it consists of an ever increasing amount of small and volatile generation units. As a consequence it becomes more difficult to maintain the frequency close to its nominal value and traditional control strategies might turn out to be incapable to deal with the changing network. Technological advances in computer-based control offer possibilities to maintain the high reliability of the power network and at the same time to lower operational costs. A critical aspect of many new control strategies is however the use of an underlying communication network. This poses the question of how the communication structure impacts the stability of the physical system and how the required amount of communication can be reduced. In this work we show how these questions can be addressed within a hybrid systems framework.

Various solutions to improve the efficiency of power networks have been recently proposed that generally follow one of the following two approaches. In the first approach, the economic dispatch problem is distributively solved by a primal-dual algorithm converging to the solution of the associated Lagrangian dual problem (Zhang and Papachristodoulou 2015), (Li et al. 2016). In the second approach, a consensus algorithm is employed to converge to a state of identical marginal costs, solving the economic dispatch problem in the unconstrained case (Simpson-Porco et al. 2013), (Trip et al. 2016), (Trip and De Persis 2017b). An important aspect of the aforementioned approaches is the requirement of *continuous* communication between different parts in the network. With an increasing number of generation units the required bandwidth might however exceed the capacity of the underlying communication network and a more efficient communication infrastructure is desirable (Fan et al. 2016).

Contributions

In Part III of this thesis, we focus on reducing the required information exchange among the controllers. Particularly, we study the possibility to exchange information at discrete time instances, while the physical network is still evolving continuously. The approach chosen in this part, to study the stability of the interconnected cyber-physical system, is closely related to the approach used in (De Persis and Postoyan 2017) and in (Postoyan et al. 2015), where (event-)triggered coordination algorithms are proposed for networked control systems, resulting in hybrid systems. We analyze the obtained hybrid system using the formalism of (Goebel et al. 2012). Various works on cyber-physical systems have addressed discrete communication times, where the interplay between digital control and the continuous physical system is explicitly taken into account. Early works have focussed on discrete information exchange for single and double integrator dynamics to obtain consensus (Dimarogonas et al. 2012), (Heemels et al. 2012), (Seyboth et al. 2013). Compared to these results, we propose an alternative approach to design rules that determine the moments when information is exchanged, where the design and analysis are based on a non-quadratic storage function and an invariance principle for hybrid systems. In the proposed methodology, we start with a given storage function for a system that is stable under the assumption of continuous exchange of information. We then propose an additional storage term that takes into account the cyber part of the system. The stability study then prescribes the maximum amount of time between sampling instances such that stability can still be guaranteed and is in the same spirit as (Carnevale et al. 2007), where a maximum allowable transfer interval for networked control systems is proposed and analyzed using Lyapunov arguments. Our approach permits to reuse results from the previous chapters and allows us to straightforwardly relax the assumption of continuous information exchange.

Outline

Chapter 7

The presented work provides a contribution towards relaxing the predominant assumption of continuous communication between various nodes in a power network. To achieve this we adapt our previous results (Bürger et al. 2014), (Trip et al. 2016), where an incremental passivity property of the power network is established and used to design distributed controllers achieving economically efficient frequency regulation in the presence of unknown and possibly time-varying chan-

ges in the load. This work focuses on a master-slave control structure, similar to the one presented in (Dörfler and Grammatico 2016). The proposed solution in this paper achieves frequency regulation and minimizes required generation costs, i.e. it achieves an economic dispatch. We furthermore show that the formalism for hybrid systems (Goebel et al. 2012) is suitable to extend the Lyapunov-based controller design for power networks to explicitly include the digital nature of the control structure. Specifically, we are able to design a maximum time that is allowed between two sampling instances. We therefore provide a further analytical understanding of the communication requirements in power networks that facilitates the reduction of current, 'as high as possible', sampling rates. As the proposed controller design exploits the incremental passivity property of the physical network, the proposed solution can be straightforwardly adapted to other networks possessing such a property as well. As we show in the case study a sampling rate that is too slow can destabilize a system that would be stable under fast sampling, stressing the importance to study the stability of a cyber-physical system in a coherent way.

Chapter 8

This chapter continues the efforts of Chapter 7, to further relax the assumption of continuous communication. Where Chapter 7 focussed on a more centralized control scheme, this chapter investigates the digital nature of the consensus algorithm (Section 8.1). First, the consensus algorithm is studied as an autonomous system, where the nodes in the network broadcast the value of their state at discrete time instances to their neighbours (Section 8.2). Stability is proven by exploiting an invariance principle for hybrid systems. Particularly, we design a suitable storage function that takes into account the digital nature of the communication. The stability analysis then suggest a minimal broadcasting frequency at every node that guarantees stability of the overall network. In Section 8.3, the (hybrid) consensus algorithm is studied in closed loop with a nonlinear system, leading to a new characterization of the minimal broadcasting frequency. A case study on the autonomous consensus protocol and a case study on optimal Load Frequency Control confirm the obtained theoretical results (Section 8.4).

Published in:

S. Trip and C. De Persis – *"Communication requirements in a master-slave control structure for optimal load frequency control,"* Proceedings of the 2017 IFAC World Congress, pp. 10519–10524, Toulouse, FR, 2017.

Chapter 7

Communication requirements in a master-slave control structure

Abstract

To have economically efficient frequency control in power networks, the communication between the generators and controllers is essential. In this chapter we adopt a master-slave control structure where a control center (master) optimally allocates the required power generation among the units (slaves). We investigate the communication and sampling rate requirements such that frequency regulation and optimality are guaranteed. The analysis of the continuous physical system and the discrete-time communication protocol is carried out within the framework of hybrid systems and relies on an invariance principle. Based on Lyapunov arguments a minimum sampling rate is established. A case study indicates that a low sampling rate can indeed lead to instability.

7.1 The Bergen-Hill model

This chapter considers the same Bergen-Hill model of the power network as we have discussed in Chapter 5. For convenience we repeat the overall network model, but refer for the details to Section 5.1. The power network model considered is given by

$$\begin{aligned} \dot{\delta} &= \omega \\ M\dot{\omega}_g &= -D_g\omega_g - \mathcal{B}_g\Gamma\sin(\mathcal{B}^T\delta) + \hat{u}_g \\ \mathbf{0} &= -D_l\omega_l - \mathcal{B}_l\Gamma\sin(\mathcal{B}^T\delta) - P_d, \end{aligned} \tag{7.1}$$

where in comparison with equation (5.3), the input P_t is replaced by $\hat{u}_g$. Particularly, we do not consider a continuous adjustment of the generated power, but study how the set-points for the generated power can be discretely updated. In the next section we propose a possible controller that adjusts $\hat{u}_g$, obtaining frequency regulation and an economic dispatch.

7.2 Cyber-layer and control structure

From Lemma 5.2.2 it follows that we require that $\mathbb{1}_{n_g}^T \overline{u}_g - \mathbb{1}_{n_l}^T P_d = 0$ in order to have a steady state frequency deviation of zero. Similar to Chapter 5, we aim at an *optimal* distribution of generation among the generators such that $\overline{u}_g$ solves the optimization problem

$$\begin{array}{ll} & \min_{\hat{u}_g} C(\hat{u}_g) = \min_{\hat{u}_g} \sum_{i\in\mathcal{V}_g} C_i(\hat{u}_{gi}) \\ \text{s.t.} & \mathbb{1}_{n_g}^T \hat{u}_g - \mathbb{1}_{n_l}^T P_l = 0, \end{array} \tag{7.2}$$

where $C_i(\hat{u}_{gi})$ represents the quadratic cost function of generator i. The solution $\overline{u}_g^{opt}$ to (7.2) can be made explicit, and we recall Lemma 5.2.3:

Lemma 7.2.1 (Optimal generation)**.** *Let*

$$C(\hat{u}_g) = \frac{1}{2}\hat{u}_g^T Q \hat{u}_g + R^T \hat{u}_g + \mathbb{1}_{n_g}^T s, \tag{7.3}$$

with $Q > 0$ and diagonal. The solution $\overline{u}_g^{opt}$ to (7.2) must satisfy

$$\overline{u}_g^{opt} = Q^{-1}(\overline{\lambda}^{opt} - R), \tag{7.4}$$

where $\overline{\lambda}^{opt} = \frac{\mathbb{1}_{n_g}(\mathbb{1}_{n_l}^T P_d + \mathbb{1}_{n_g}^T Q^{-1} R)}{\mathbb{1}_{n_g}^T Q^{-1} \mathbb{1}_{n_g}} \in \mathrm{Im}(\mathbb{1}_{n_g})$, with $Q = \mathrm{diag}(q_1, \ldots, q_{n_g})$, $R = (r_1, \ldots, r_{n_g})^T$ and $s = (s_1, \ldots, s_{n_g})^T$.

Various controllers that continuously adjust $\hat{u}_g$ to achieve frequency regulation and economic efficiency have been proposed in the literature. These works generally require a continuous exchange of information over a communication network, which hampers practical application of the controllers. In this chapter we focus on relaxing this requirement for a master-slave control structure. Extending the presented results to a fully distributed controller is done in the next chapter. Before formalizing the control structure, we provide an informal discussion on the idea. To this end, consider the following controller:

$$\begin{array}{rcl} \dot{\theta}_{gi} & = & -q_i^{-1}\omega_{gi} \\ \hat{u}_{gi} & = & q_i^{-1}(\alpha \sum_{j=1}^{n_g} \hat{\theta}_{gj} - r_i), \end{array} \tag{7.5}$$

where $\hat{\theta}_{gi}$ refers to a sampled version of θ_{gi}, implying the existence of a clock that determines when $\hat{\theta}_{gi}$ and therefore $\hat{u}_{gi}$ are updated. The constants q_i and r_i are defined by the cost function (7.3) and the constant $\alpha \in \mathbb{R}_{>0}$ is an additional tuning parameter. For all nodes the controller writes as

$$\begin{array}{rcl} \dot{\theta}_g & = & -Q^{-1}\omega_g \\ \hat{u}_g & = & Q^{-1}(\alpha \mathbb{1}_{n_g}\mathbb{1}_{n_g}^T \hat{\theta}_g - R). \end{array} \tag{7.6}$$

Notice that at a steady state where $\omega_g = \mathbf{0}$, we have that $\hat{u}_g = \overline{u}_g = Q^{-1}(\alpha \mathbb{1}_{n_g} \mathbb{1}_{n_g}^T \overline{\theta}_g - R)$. Comparing this to relation (7.4) where $\omega = \mathbf{0}$, we have that necessarily

$$\alpha \mathbb{1}_{n_g} \mathbb{1}_{n_g}^T \overline{\theta}_g = \overline{\lambda}^{opt}, \tag{7.7}$$

and therefore that $\hat{u}_g = \overline{u}_g^{opt}$. The challenge lies therefore in the design of a clock that determines the time instances when the values of $\hat{\theta}$ and $\hat{u}_g$ are updated and that guarantees $\lim_{t\to\infty} \omega(t) = \mathbf{0}$. To do so, we assume the existence of a clock at the control center of the following form:

$$\dot{\phi} = f(\phi), \tag{7.8}$$

where $f(\phi) : \mathbb{R} \to \mathbb{R}_{<0}$ is a smooth function to be defined later. The update of $\hat{\theta}_g$ and $\hat{u}_g$ occurs when $\phi = a \in \mathbb{R}_+$, whereafter the clock is reset to $\phi = b > a$. The design of $f(\phi)$ that guarantees $\lim_{t\to\infty} \omega(t) = \mathbf{0}$ is the subject of the following sections.

Remark 7.2.2 (A master-slave control structure)**.** *The control structure of controller (7.5) can be understood as follows. Each generator integrates its own frequency deviation. At a sampling instant, a centralized controller (control center / master) collects the values of $\hat{\theta}_i$ and transmits the sum, $\sum_{j\in\mathcal{V}_g} \hat{\theta}_j$, to all generators (slaves) in the network. A similar control structure has been discussed in (Dörfler and Grammatico 2016) where continuous sampling and communication is assumed.*

Remark 7.2.3 (Imperfect communication)**.** *We assume that the communication and the computation of $\sum_{i\in\mathcal{V}_g} \hat{\theta}_{gi}$ is synchronous and instantaneous. Interesting extensions include robustness to delays (Efimov et al. 2016), asynchronous communication ((De Persis and Postoyan 2017), (Postoyan et al. 2015)) and resiliency to denial of service (De Persis and Tesi 2014).*

7.3 The power network as a hybrid system

Besides continuous differential equations, the overall system (7.1), (7.6), (7.8) consists of discontinuous jumps (resets) of the clock state and associated jump (reset) conditions. The framework discussed in (Goebel et al. 2012) turns out to be suitable for analyzing such systems and this section focuses on formalizing the system at hand as a hybrid system within that framework. We refer for the details of the framework to (Goebel et al. 2012), but we provide some basic preliminaries in Section 1.4 that helps to understand the used formalism.

7.3.1 The power network as a hybrid system

We now formalize system (7.1), (7.6), (7.8) as a hybrid system where we additionally define $\eta = \mathcal{B}^T\delta \in \mathbb{R}^m$ and $\Theta = \mathbb{1}_{n_g}^T\theta_g \in \mathbb{R}$ (see also Remark 7.4.8 below). The flow set is $C = \{(\eta, \omega_g, \Theta, \hat{\Theta}, \phi) \in \mathbb{R}^m \times \mathbb{R}^{n_g} \times \mathbb{R} \times \mathbb{R} \times [a, b]\}$. The flow map is

$$\left.\begin{aligned} \dot{\eta} &= \mathcal{B}^T\omega \\ M\dot{\omega}_g &= -D_g\omega_g - \mathcal{B}_g\Gamma\sin(\eta) + \hat{u}_g \\ \mathbf{0} &= -D_l\omega_l - \mathcal{B}_l\Gamma\sin(\eta) - P_d \\ \dot{\Theta} &= -\mathbb{1}_{n_g}^T Q^{-1}\omega_g \\ \dot{\hat{\Theta}} &= \mathbf{0} \\ \hat{u}_g &= Q^{-1}(\alpha\mathbb{1}_{n_g}\hat{\Theta} - R) \\ \dot{\phi} &= f(\phi) \end{aligned}\right\} F(\eta, \omega_g, \Theta, \hat{\Theta}, \phi). \tag{7.9}$$

The jump set is $D = \{(\eta, \omega_g, \Theta, \hat{\Theta}, \phi) \in \mathbb{R}^m \times \mathbb{R}^{n_g} \times \mathbb{R} \times \mathbb{R} \times \{a\}\}$. The jump map is

$$\left.\begin{aligned} \eta^+ &= \eta \\ \omega_g^+ &= \omega_g \\ \Theta^+ &= \Theta \\ \hat{\Theta}^+ &= \Theta \\ \phi^+ &= b \end{aligned}\right\} G(\eta, \omega_g, \Theta, \hat{\Theta}, \phi). \tag{7.10}$$

The hybrid system with the data above will be represented by the notation $\mathcal{H} = (C, F, D, G)$ or, briefly, by $\mathcal{H}$. The stability analysis in the next section is based on an invariance principle for hybrid systems that requires the system to be nominally well posed. This property is established for system at hand in the following lemma:

Lemma 7.3.1 (Nominally well posed)**.** *The system $\mathcal{H}$ is nominally well posed.*

Proof. Following (Goebel et al. 2012, Theorem 6.8) it is sufficient that the system $\mathcal{H}$ satisfies the following hybrid basic conditions:

1. C and D are closed subsets of $\mathcal{X} := \mathbb{R}^m \times \mathbb{R}^{n_g} \times \mathbb{R} \times \mathbb{R} \times \mathbb{R}$,
2. $F : \mathcal{X} \rightrightarrows \mathcal{X}$ is outer semicontinuous and locally bounded relative to C, $C \subset$ dom F, and $F(x)$ is convex for every $x \in C$,
3. $G : \mathcal{X} \rightrightarrows \mathcal{X}$ is outer semicontinuous and locally bounded relative to D, $D \subset$ dom G.

Condition 1. can be readily verified. Condition 2. is satisfied by $F : \mathcal{X} \to \mathcal{X}$, being a continuous function. Condition 3. is satisfied by $G : \mathcal{X} \to \mathcal{X}$ and having a closed graph. Notice that we replaced $\rightrightarrows$ with $\to$, since F and G are multivariate functions. ■

Furthermore, the solutions to the system $\mathcal{H}$ have a persistent dwell time that will be discussed in more detail in Section 7.5.

7.4 Design of clock dynamics

In this section we design the clock dynamics $\dot{\phi}$, such that the overall system converges to the desired set where $\omega = \mathbf{0}$ and $\Theta = \overline{\Theta}^{opt}$, with $\hat{u}_g = \overline{u}_g^{opt} = Q^{-1}(\alpha \mathbb{1}_{n_g} \overline{\Theta}^{opt} - R)$ the solution to the optimization problem (7.2). The analysis is performed relying on Lyapunov arguments. For this purpose we take a similar approach as in (De Persis and Postoyan 2017) and introduce a storage function taking into account the physical component of the system and a storage function taking into account the cyber component of the system (sampling and clock dynamics). The convergence of the overall cyber-physical system is then established using an invariance principle for hybrid systems.

7.4.1 The physical component

We adapt here a useful result from Section 8.3, where an incremental cyclo-passivity property is established for the Bergen-Hill power network model, representing the physical component of the system (states η and ω).

Remark 7.4.1 (Incremental passivity for hybrid systems)**.** *The notion of passivity for hybrid systems has been previously defined in e.g, (Naldi and Sanfelice 2013). Different other useful passivity notions exist for continuous systems such as, cyclo-passivity (van der Schaft 1999), equilibrium independent passivity (Hines et al. 2011) and incremental passivity (Pavlov and Marconi 2008). Although some of the relations we establish below seem to be related to those passivity properties, we do not formalize this as it requires some additional work that is beyond the scope of thesis.*

Lemma 7.4.2 (Dissipation of the physical component)**.** *Let Assumption 5.2.1 hold when taking $\overline{P}_t = \overline{u}_g$. There exists a storage function $U_1(\omega_g, \overline{\omega}_g, \eta, \eta)$[1] that satisfies along the*

[1]The variable ω_l can be eliminated by exploiting the identity $\omega_l = D_l^{-1}(-\mathcal{B}_l \Gamma \sin(\overline{\eta}) - P_d)$.

flows of the system $\mathcal{H}$

$$\begin{aligned}\dot{U}_1(\omega_g,\overline{\omega}_g,\eta,\overline{\eta}) \leq & -\|\omega_g-\overline{\omega}_g\|^2_{D_g}-\|\omega_l-\overline{\omega}_l\|^2_{D_l} \\ & +(\omega_g-\overline{\omega}_g)^T Q^{-1}\alpha\mathbb{1}_{n_g}(\hat{\Theta}-\overline{\Theta}),\end{aligned} \tag{7.11}$$

and at the jumps

$$U_1^+(\omega_g^+,\overline{\omega}_g,\eta^+,\overline{\eta}) = U_1(\omega_g,\overline{\omega}_g,\eta,\overline{\eta}).$$

Proof. Consider the incremental storage function

$$\begin{aligned}U_1(\omega_g,\overline{\omega}_g,\eta,\overline{\eta}) &= \tfrac{1}{2}(\omega_g-\overline{\omega}_g)^T M(\omega_g-\overline{\omega}_g) \\ &\quad -\mathbb{1}^T\Gamma\cos(\eta)+\mathbb{1}^T\Gamma\cos(\overline{\eta})-\left(\Gamma\sin(\overline{\eta})\right)^T(\eta-\overline{\eta}).\end{aligned} \tag{7.12}$$

We have that U_1 satisfies along the flows of the system $\mathcal{H}$

$$\begin{aligned}\dot{U}_1 &= (\omega_g-\overline{\omega}_g)^T(-D_g\omega_g-\mathcal{B}_g\Gamma\sin(\eta)+Q^{-1}(\alpha\mathbb{1}_{n_g}\hat{\Theta}-R)) \\ &\quad +(\Gamma\sin(\eta)-\Gamma\sin(\overline{\eta}))^T(\mathcal{B}_g^T\omega_g+\mathcal{B}_l^T\omega_l) \\ &= -\|\omega_g-\overline{\omega}_g)\|^2_{D_g} \\ &\quad +(\omega_g-\overline{\omega}_g)^T Q^{-1}\alpha\mathbb{1}_{n_g}(\hat{\Theta}-\overline{\Theta}) \\ &\quad +(\Gamma\sin(\eta)-\Gamma\sin(\overline{\eta}))^T\mathcal{B}_l^T(\omega_l-\overline{\omega}_l) \\ &= -\|\omega_g-\overline{\omega}_g)\|^2_{D_g} \\ &\quad +(\omega_g-\overline{\omega}_g)^T Q^{-1}\alpha\mathbb{1}_{n_g}(\hat{\Theta}-\overline{\Theta}) \\ &\quad +(\mathcal{B}_l\Gamma\sin(\eta)+P_d)^T D_l^{-1}D_l(\omega_l-\overline{\omega}_l) \\ &\quad -(\mathcal{B}_l\Gamma\sin(\overline{\eta})+P_d)^T D_l^{-1}D_l(\omega_l-\overline{\omega}_l) \\ &= -\|\omega_g-\overline{\omega}_g\|^2_{D_g}-\|\omega_l-\overline{\omega}_l\|^2_{D_l} \\ &\quad +(\omega_g-\overline{\omega}_g)^T Q^{-1}\alpha\mathbb{1}_{n_g}(\hat{\Theta}-\overline{\Theta}),\end{aligned} \tag{7.13}$$

where we have exploited in the first line the identity $\dot{\eta}=\mathcal{B}^T\omega=\mathcal{B}_g^T\omega_g+\mathcal{B}_l^T\omega_l$. In the second identity we used the existence of $(\overline{\eta},\overline{\omega}_g,\overline{\Theta})$ satisfying

$$\begin{aligned}\mathbf{0} &= \mathcal{B}^T\overline{\omega} \\ M\mathbf{0} &= -D_g\overline{\omega}_g-\mathcal{B}_g\Gamma\sin(\overline{\eta})+Q^{-1}(\alpha\mathbb{1}_{n_g}\overline{\Theta}-R) \\ \mathbf{0} &= -D_l\overline{\omega}_l-\mathcal{B}_l\Gamma\sin(\overline{\eta})-P_d.\end{aligned} \tag{7.14}$$

Since $\omega_g^+=\omega$ and $\eta^+=\eta$, it follows trivially that $U_1^+(\omega_g^+,\overline{\omega}_g,\eta^+,\overline{\eta})=U_1(\omega_g,\overline{\omega}_g,\eta,\overline{\eta})$. ■

The result of Lemma 7.4.2 holds in particular when $\overline{\omega}=\mathbf{0}$ and $\overline{\Theta}=\overline{\Theta}^{opt}$.

Remark 7.4.3 (Applicability on the coordination of different networks)**.** *We focus on the Bergen-Hill model introduced in Chapter 5. The essential property we exploit is that the system (7.1) is output strictly incrementally passive along the flows. It is therefore expected that the presented results can be applied to networks that share the same property.*

7.4.2 A cyber-physical system

We now consider the interconnection of the cyber component to the physical component, starting with the integrator dynamics (7.6).

Lemma 7.4.4 (Dissipation of the cyber-physical system)**.** *There exists a storage function $U_2(\Theta, \overline{\Theta}^{opt})$ such that $U_1(\omega_g, \overline{\omega}_g = \mathbf{0}, \eta, \overline{\eta}) + U_2(\Theta, \overline{\Theta}^{opt})$ satisfies along the flows of the system $\mathcal{H}$*

$$\begin{aligned} &\dot{U}_1(\omega_g, \overline{\omega}_g = \mathbf{0}, \eta, \overline{\eta}) + \dot{U}_2(\Theta, \overline{\Theta}^{opt}) \\ &\leq -\|\omega_g\|^2_{D_g} - \|\omega_l\|^2_{D_l} + \omega_g^T Q^{-1} \alpha \mathbb{1}_{n_g}(\hat{\Theta} - \Theta), \end{aligned} \tag{7.15}$$

and at the jumps

$$\begin{aligned} &U_1^+(\omega_g^+, \overline{\omega}_g = \mathbf{0}, \eta^+, \overline{\eta}) + U_2^+(\Theta^+, \overline{\Theta}^{opt}) \\ &= U_1(\omega_g, \overline{\omega}_g = \mathbf{0}, \eta, \overline{\eta}) + U_2(\Theta, \overline{\Theta}^{opt}). \end{aligned} \tag{7.16}$$

Proof. Consider the storage function

$$U_2(\Theta, \overline{\Theta}^{opt}) \quad = \quad \tfrac{\alpha}{2}(\Theta - \overline{\Theta}^{opt})^2. \tag{7.17}$$

We have that $U_1(\omega_g, \overline{\omega}_g = \mathbf{0}, \eta, \overline{\eta}) + U_2(\Theta, \overline{\Theta}^{opt})$ satisfies along the flows of the system $\mathcal{H}$

$$\begin{aligned} \dot{U}_1 + \dot{U}_2 = &- \|\omega_g\|^2_{D_g} - \|\omega_l\|^2_{D_l} \\ &+ \omega_g^T Q^{-1} \alpha \mathbb{1}_{n_g}(\hat{\Theta} - \overline{\Theta}^{opt}) \\ &- \omega_g^T Q^{-1} \alpha \mathbb{1}_{n_g}(\Theta - \overline{\Theta}^{opt}) \\ = &- \|\omega_g\|^2_{D_g} - \|\omega_l\|^2_{D_l} \\ &+ \omega_g^T Q^{-1} \alpha \mathbb{1}_{n_g}(\hat{\Theta} - \Theta), \end{aligned} \tag{7.18}$$

where we applied Lemma 7.4.2 with $\overline{\omega} = \mathbf{0}$ and $\overline{\Theta} = \overline{\Theta}^{opt}$. Since $(\eta^+, \omega_g^+, \Theta^+) = (\eta, \omega_g, \Theta)$, it follows that $U_1^+(\omega_g^+, \overline{\omega}_g = \mathbf{0}, \eta^+, \overline{\eta}) + U_2^+(\Theta^+, \overline{\Theta}^{opt}) = U_1(\omega_g, \overline{\omega}_g = \mathbf{0}, \eta, \overline{\eta}) + U_2(\Theta, \overline{\Theta}^{opt})$. ■

We now proceed with considering the clock dynamics that determine the sampling instances. More specifically, we aim at finding a storage function that can compensate for the perturbative term $\omega_g^T Q^{-1} \alpha \mathbb{1}_{n_g}(\hat{\Theta} - \Theta)$ appearing in $\dot{U}_1 + \dot{U}_2$.

Remark 7.4.5 (Continuous communication)**.** *In the case of continuous communication and measurements we have that $\hat{\Theta} = \Theta$, such that $\dot{U}_1 + \dot{U}_2 \leq 0$. This simplifies the analysis since no additional clock dynamics need to be considered and can be regarded as a special case within the current setting.*

Before we design the clock dynamics $\dot{\phi} = f(\phi)$ that ensure the stability of the system we make the following assumption on the steady state difference in voltage angles $\overline{\eta}$, that is required to establish boundedness of solutions as we will see in Theorem 7.4.7.

Assumption 7.4.6 (Steady state differences in voltage angles)**.** *The steady state differences in voltage angles $\overline{\eta}$ satisfy $\overline{\eta} = (\frac{-\pi}{2}, \frac{\pi}{2})^m$.*

We are now ready to state the main result of this chapter.

Theorem 7.4.7 (Frequency control with discrete communication)**.** *Let Assumptions 5.2.1 and 7.4.6 hold. Let $\dot{\phi} = f(\phi) = -\frac{\alpha}{\epsilon}(1+\phi)^2$, with*

$$\epsilon < \frac{D_{gi}}{q_i^{-1}(\sum_{j\in\mathcal{V}_g} q_j^{-1})} \tag{7.19}$$

for all $i \in \mathcal{V}_g$. Then, maximal solutions of the system $\mathcal{H}$ that start in a neighborhood of $(\overline{\eta}, \overline{\omega} = \mathbf{0}, \overline{\Theta}^{opt}, \overline{\Theta}^{opt}, \phi(0))$ converge asymptotically to the largest invariant set where $\omega = \mathbf{0}$ and $\hat{\Theta} = \overline{\Theta}^{opt}$, so that $\hat{u}_g = \overline{u}_g^{opt}$ characterized in Lemma 7.2.1.

Proof. Consider the storage function

$$U_3(\Theta, \hat{\Theta}, \phi) \quad = \quad \tfrac{\alpha\phi}{2}(\hat{\Theta} - \Theta)^2. \tag{7.20}$$

We have that $U = U_1(\omega_g, \overline{\omega}_g = \mathbf{0}, \eta, \overline{\eta}) + U_2(\Theta, \overline{\Theta}^{opt}) + U_3(\Theta, \hat{\Theta}, \phi)$ satisfies along the flows of the system $\mathcal{H}$

$$\begin{aligned}
\dot{U} = \dot{U}_1 + \dot{U}_2 + \dot{U}_3 = \\
&- \|\omega_g\|^2_{D_g} - \|\omega_l\|^2_{D_l} + \omega_g^T Q^{-1}\alpha \mathbb{1}_{n_g}(\hat{\Theta} - \Theta) \\
&+ \alpha\phi(\hat{\Theta} - \Theta)(\mathbb{1}_{n_g}^T Q^{-1}\omega_g) \\
&+ \frac{\alpha f(\phi)}{2}(\hat{\Theta} - \Theta)^T(\hat{\Theta} - \Theta) \\
=& - \|\omega_g\|^2_{D_g} - \|\omega_l\|^2_{D_l} + \alpha(1+\phi)\big(\omega_g^T Q^{-1}\mathbb{1}_{n_g}(\hat{\Theta} - \Theta)\big) \\
&+ \frac{\alpha f(\phi)}{2}(\hat{\Theta} - \Theta)^2 \\
\leq& - \|\omega_g\|^2_{D_g} - \|\omega_l\|^2_{D_l} \\
&+ \frac{\alpha^2(1+\phi)^2}{2\epsilon}(\hat{\Theta} - \Theta)^2 + \frac{\epsilon}{2}(\mathbb{1}_{n_g}^T Q^{-1}\omega_g)^2 \\
&+ \frac{\alpha f(\phi)}{2}(\hat{\Theta} - \Theta)^2 \\
=& - \omega_g^T(D_g - \frac{\epsilon}{2}Q^{-1}\mathbb{1}_{n_g}\mathbb{1}_{n_g}^T Q^{-1})\omega_g - \|\omega_l\|^2_{D_l} \\
&+ \frac{\alpha^2(1+\phi)^2}{2\epsilon}(\hat{\Theta} - \Theta)^2 + \frac{\alpha f(\phi)}{2}(\hat{\Theta} - \Theta)^2,
\end{aligned} \tag{7.21}$$

where we have applied Young's inequality. By the Gershgorin circle theorem we have that $D_g - \frac{\epsilon}{2} Q^{-1} \mathbb{1}_{n_g} \mathbb{1}_{n_g}^T Q^{-1} > \mathbf{0}$ if $\epsilon < \frac{D_{gi}}{q_i^{-1}(\sum_{j \in \mathcal{V}_g} Q_j^{-1})}$ for all $i \in \mathcal{V}_g$. Choosing $f(\phi) = -\frac{\alpha}{\epsilon}(1+\phi)^2$ it follows then that $\dot{U} \leq -\|\omega_g\|_\zeta^2 - \|\omega_l\|_{D_l}^2$ with $\zeta = D_g - \frac{\epsilon}{2} Q^{-1} \mathbb{1}_{n_g} \mathbb{1}_{n_g}^T Q^{-1} > \mathbf{0}$. Notice furthermore that $U(G(\eta, \omega_g, \Theta, \hat{\Theta}, \phi)) = U(\eta, \omega_g, \Theta, \hat{\Theta}, \phi)$, such that

$$\dot{U}(x) \leq u_c(x) \quad \forall x \in C \tag{7.22}$$

$$U(G(x)) - U(x) \leq u_d(x) \quad \forall x \in D, \tag{7.23}$$

where $x = (\eta, \omega_g, \Theta, \hat{\Theta}, \phi)$ and

$$u_c(x) = \begin{cases} -\|\omega_g\|_\zeta^2 - \|\omega_l\|_{D_l}^2 & x \in C \\ -\infty & \text{otherwise} \end{cases} \tag{7.24}$$

$$u_d(x) = \begin{cases} 0 & x \in D \\ -\infty & \text{otherwise.} \end{cases} \tag{7.25}$$

Since $U_1 + U_2$ has a local minimum at $(\overline{\eta}, \overline{\omega} = \mathbf{0}, \overline{\Theta}^{opt})$ as a consequence of Assumption 7.4.6, $0 < a \leq \phi \leq b$ and $\dot{U} \leq 0$, there exists a compact level set around $(\overline{\eta}, \overline{\omega} = \mathbf{0}, \overline{\Theta}^{opt}, \overline{\Theta}^{opt}, \phi(0))$ which is forward invariant. It follows that the maximal solutions to the system $\mathcal{H}$ that start sufficient close to $(\overline{\eta}, \overline{\omega} = \mathbf{0}, \overline{\Theta}^{opt}, \overline{\Theta}^{opt}, \phi(0))$ are bounded. Since solutions to $\mathcal{H}$ are also complete, they are precompact. Because U is continuous, solutions that start in a neighbourhood of $(\overline{\eta}, \overline{\omega} = \mathbf{0}, \overline{\Theta}^{opt}, \overline{\Theta}^{opt}, \phi(0))$ approach the largest weakly invariant subset $\mathcal{S}$ of

$$U^{-1}(r) \cap \mathcal{X} \cap \left[\overline{u_c^{-1}(0)} \cup \left(u_d^{-1}(0) \cap G(u_d^{-1}(0))\right)\right], \tag{7.26}$$

where $r \in U(\mathcal{X})$ and $\mathcal{X} := \mathbb{R}^m \times \mathbb{R}^{n_g} \times \mathbb{R} \times \mathbb{R} \times \mathbb{R}$ (Goebel et al. 2012, Theorem 8.2). Since $u_d^{-1}(0) \cap G(u_d^{-1}(0)) = \emptyset$ and

$$\overline{u_c^{-1}(0)} = -\|\omega_g\|_\zeta^2 - \|\omega_l\|_{D_l}^2, \tag{7.27}$$

we can conclude that the maximal solutions to system $\mathcal{H}$ approach the largest we-

akly invariant set where $\omega = \mathbf{0}$. On this set we have

$$\left.\begin{aligned} \dot{\eta} &= \mathcal{B}^T \mathbf{0} \\ \mathbf{0} &= -D_g \mathbf{0} - \mathcal{B}_g \Gamma \sin(\eta) + \hat{u}_g \\ \mathbf{0} &= -D_l \mathbf{0} - \mathcal{B}_l \Gamma \sin(\eta) - P_d \\ \dot{\Theta} &= -\mathbb{1}_{n_g}^T Q^{-1} \mathbf{0} \\ \dot{\hat{\Theta}} &= \mathbf{0} \\ \hat{u}_g &= Q^{-1}(\alpha \mathbb{1}_{n_g} \hat{\Theta} - R) \\ \dot{\phi} &= f(\phi) \end{aligned}\right\} F(\eta, \mathbf{0}, \Theta, \hat{\Theta}, \phi) \tag{7.28}$$

and

$$\left.\begin{aligned} \eta^+ &= \eta \\ \mathbf{0}^+ &= \mathbf{0} \\ \Theta^+ &= \Theta \\ \hat{\Theta}^+ &= \Theta \\ \phi^+ &= b \end{aligned}\right\} G(\eta, \mathbf{0}, \Theta, \hat{\Theta}, \phi). \tag{7.29}$$

Premultiplying the concatenated second and third line of $F(\eta, \mathbf{0}, \Theta, \hat{\Theta}, \phi)$ with $\mathbb{1}_n^T$ yields $0 = \mathbb{1}_{n_g}^T Q^{-1}(\alpha \mathbb{1}_{n_g} \hat{\Theta} - R) - \mathbb{1}_{n_l}^T P_d$. Bearing in mind that $\hat{\Theta} = \overline{\Theta}^{opt}$ is the only value satisfying this relation, it follows that $\hat{u}_g = Q^{-1}(\alpha \mathbb{1}_{n_g} \hat{\Theta} - R)$ converges to $\overline{u}_g^{opt} = Q^{-1}(\alpha \mathbb{1}_{n_g} \overline{\Theta}^{opt} - R)$ characterized in Lemma 7.2.1. ■

Remark 7.4.8 (Change of variables)**.** *In order to apply the invariance principle in the proof of Theorem 7.4.7 we require boundedness of solutions. This can be established for η and Θ, but becomes more difficult for δ_i and θ_i and is the reason to introduce the variables η and Θ in Section 7.3.*

In the next section we further analyse the obtained clock dynamics and establish a minimum sampling rate.

7.5 Minimum sampling rate

The choice of a and b and the clock dynamics

$$\dot{\phi} = -\frac{\alpha}{\epsilon}(1 + \phi)^2, \tag{7.30}$$

where α is the tuning variable in (7.5), determine the sampling rate. Now we turn our attention to the question how much time T elapses between a clock reset $\phi(t) = b$ until the following reset at $\phi(t + T) = a$.

Theorem 7.5.1 (Inter sampling time)**.** *The inter sampling time T is given by*

$$T = \frac{\epsilon}{\alpha}\big(\frac{1}{a+1} - \frac{1}{b+1}\big) \tag{7.31}$$

Proof. We solve $\dot{\phi} = -\frac{\alpha}{\epsilon}(1+\phi)^2$, satisfying the boundary condition $\phi(0) = b$. It can be readily confirmed that the solution is

$$\phi(t) = \frac{1 - \frac{1}{b+1} - \frac{\alpha}{\epsilon}t}{\frac{\alpha}{\epsilon}t + \frac{1}{b+1}}. \tag{7.32}$$

Solving (7.32) with boundary condition $\phi(T) = a$ then yields $T = \frac{\epsilon}{\alpha}\big(\frac{1}{a+1} - \frac{1}{b+1}\big)$. ■

From the result above we can furthermore conclude that the solutions to the system $\mathcal{H}$ have indeed a persistent dwell time. In order to determine the minimum sampling rate, it is interesting to see what the maximum value of T is. We define the maximum allowed time between to sampling instances T_{max}, as $T_{max} = \lim_{b\to\infty, a\to 0} T$. From Theorem 7.5.1 the following result is immediate:

Corollary 7.5.2 (Minimum sampling rate)**.** *The maximum allowed time between two sampling instances is $T_{max} = \frac{\epsilon}{\alpha}$.*

The implication of this section is that despite the nonlinear clock dynamics $\dot{\phi} = -\frac{\alpha}{\epsilon}(1+\phi)^2$, we can rely on a simple counter to determine the sampling instances.

Remark 7.5.3 (Gain tuning)**.** *In this work we present a theoretical bound on the minimum sampling rate. In a practical setting we can adjust the variables $\alpha \in \mathbb{R}_{>0}$ and ϵ satisfying (7.19) to obtain a desired transient response.*

7.6 Case study

This section we study the effect of the chosen sampling rate on the convergence properties of power network for an academic example of the power network. To do so, we adopt the 6 bus system from (Wood and Wollenberg 1996). The topology of the power network as well as the communication links are shown in Figure 7.1. The relevant generator and load parameters are provided in Table 7.1, whereas the transmission line parameters are provided in Table 7.1. The numerical values are identical to the ones used in (Trip and De Persis 2016a) and are based on the values provided in (Wood and Wollenberg 1996) and (Ourari et al. 2006). The system is initially at steady state with loads P_{d1}, P_{d2} and P_{d3} being 1.54, 1.62 and 1.50 pu respectively (assuming a base power of 100 MVA). After 20 seconds the loads are respectively increased to 1.62, 1.88 and 1.64 pu. We now consider two cases. In the first case we use a sampling rate that is too slow, whereas in the second case we choose a sampling rate that is sufficiently fast.

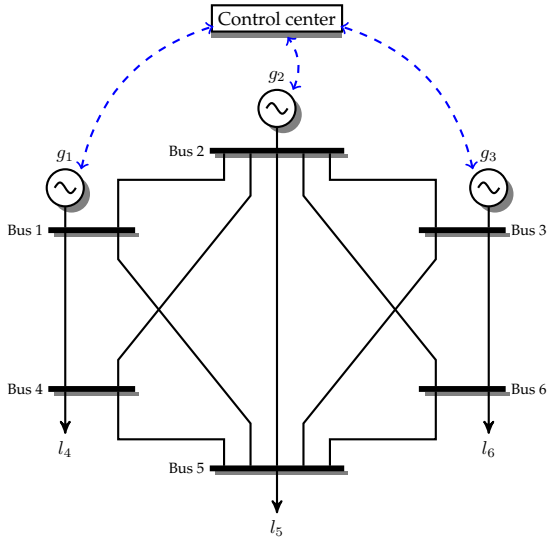

Figure 7.1: Diagram for the 6 bus power network model, consisting of 3 generator and 3 load buses. The communication links are represented by the dashed lines.

		Bus 1	Bus 2	Bus 3	Bus 4	Bus 5	Bus 6
M_i	(pu)	4.62	4.17	5.10	–	–	–
D_i	(pu)	1.41	1.28	1.72	0.42	0.61	0.51
V_i	(pu)	1.05	0.98	1.04	1.01	1.03	1.00
q_i	(10^2 \$/h)	2.42	3.78	3.31	–	–	–
r_i	(10^2 \$/h)	11.1	10.7	13.0	–	–	–
s_i	(10^2 \$/h)	9.1	17.4	13.2	–	–	–
α		1	1	1	–	–	–

Table 7.1: Numerical values of the generator and load parameters.

7.6.1 Too slow sampling

From Corollary 7.5.2 it follows that $T_{max} = 6.60$. In this case study we deliberately sample slower than the estimated minimum rate, namely with an inter sampling time of $T = 20$. From Figure 7.2 we see that frequency deviations and generated power are unstable.

B_{ij} (pu)	1	2	3	4	5	6	j
1	–	-4.0	–	-4.7	-3.1	–	
2	-4.0	–	-3.8	-8.0	-3.0	-4.5	
3	–	-3.8	–	–	-3.2	-9.6	
4	-4.7	-8.0	–	–	-2.0	–	
5	-3.1	-3.0	-3.2	-2.0	–	-3.0	
6	–	-4.5	-9.6	–	-3.0	–	
i							

Table 7.2: Susceptance B_{ij} of the transmission line connecting bus i and bus j. Values are per unit on a base of 100 MVA.

7.6.2 Sufficiently fast sampling

We now increase the sampling rate such that $T = 3$. From Figure 7.3 we see that the frequency deviation converges to zero. Furthermore, the power generation approaches the cost minimizing power generation $\overline{u}_g^{opt}$ characterized in Lemma 7.2.1.

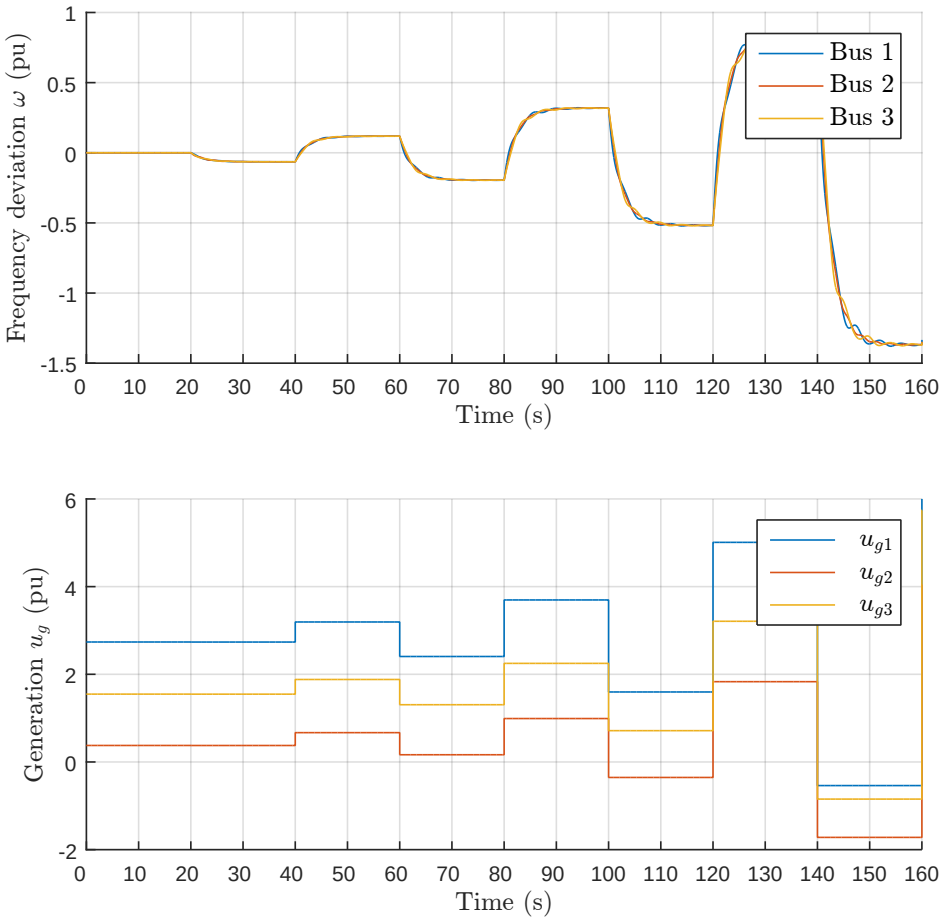

Figure 7.2: Frequency response and control input at the generator buses with inter sampling time $T = 20$. The constant load is increased at timestep 20, whereafter the frequency deviation becomes unstable.

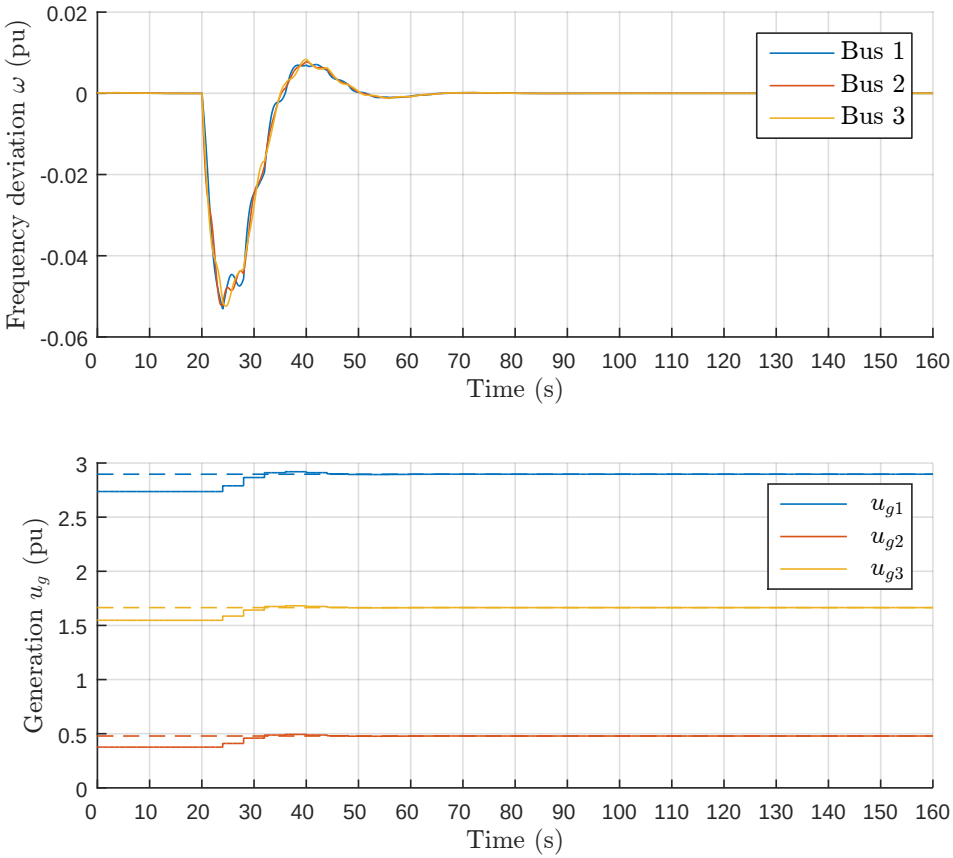

Figure 7.3: Frequency response and control input at the generator buses with inter sampling time $T = 3$. The constant load is increased at timestep 20, whereafter the frequency deviation is regulated back to zero and the generation costs are minimized. The cost minimizing generation $\overline{u}_g^{opt}$ for $t > 10$, characterized in Lemma 7.2.1, is given by the dashed lines.

Published in:
S. Trip, C. De Persis and P. Tesi – *"Coordination of nonlinear cyber-physical systems, from a continuous consensus to a discrete broadcasting protocol (tentative)'*, 2017, in preparation.

Chapter 8

Distributed control with discrete communication

Abstract

This chapter investigates the digital nature of the consensus algorithm, that has been employed throughout this thesis, to achieve an optimal allocation of inputs to a network. We focus on a particular digital implementation of the communication to which we will refer as a 'discrete broadcasting protocol'. That is, a node in a network broadcasts a certain value to its neighbors at discrete time instances. The contribution of this chapter includes the design of a storage function, taking into account the digital nature of the communication, that allows us to determine a lower bound on the broadcasting frequency guaranteeing stability of an underlying system, that is proven to be stable in the presence of continuous communication. First, for illustrative purposes we consider a simple example of a consensus algorithm, whereafter we discuss the consensus algorithm in closed loop with a nonlinear system.

8.1 From continuous consensus to discrete broadcasting

In this chapter we study a 'discrete broadcasting' implementation of the thoroughly studied consensus algorithm

$$\begin{aligned}\dot{\theta} &= -\mathcal{B}\Gamma\mathcal{B}^T\theta \\ &= -\mathcal{L}\theta,\end{aligned} \tag{8.1}$$

where $\mathcal{L}$ is the (weighted) Laplacian matrix associated to a connected and undirected graph $\mathcal{G} = (\mathcal{V}, \mathcal{E})$ consisting of n nodes and where $\theta \in \mathbb{R}^n$ is the state. With broadcasting we, informally, mean that a node i sends (broadcasts) its current value of θ_i to its neighbouring nodes at discrete time instances. Despite the fact that many result on this topic are available, there are still some open questions (Nowzari et al. 2016) and we believe that the provided results in this chapter contribute to

a further understanding of interconnected physical and digital systems. To facilitate a discrete broadcasting implementation, we impose a few assumptions on the communication network.

Assumption 8.1.1 (Communication network)**.** *Throughout this chapter we make the following assumptions:*

- *The communication network is connected and undirected, i.e. if node i can communicate with node j, then also the converse is possible.*
- *Each node knows (an upper bound on) its (weighted) degree.*
- *Each node broadcasts its current state, with a (possibly varying) frequency, to all its neighbouring nodes.*
- *The communication is without delays and errors.*

It is worth mentioning that in comparison with (De Persis and Postoyan 2017), where clocks or events are defined on the edges of the network, we focus on the design of 'rules', determining the broadcasting instances, that are implemented at the nodes, which is more in line with implementation practises. Within a setting of wireless transmission, the set of neighbouring nodes of node i is generally the set of nodes that is within the communication range of node i. The main objective is to determine a scheduling of information transmission on each node, using only information that is locally available at a node, such that convergence to a consensus state is guaranteed. In this chapter we first study the autonomous system (8.1) that provide preparatory results for the remainder, whereafter we will study system (8.1) interconnected with output strictly incrementally passive distribution systems that include e.g. the various power networks that have appeared in this thesis.

Remark 8.1.2 (Relaxing Assumption 8.1.1)**.** *Although Assumption 8.1.1 covers a large class of networks, important extensions include incorporating delays and time-varying communication topologies. These extensions have been studied extensively within continuous consensus protocols, and an interesting endeavor is to study if the developed methods for the continuous protocol, can be incorporated within the setting studied here.*

8.2 Average preserving consensus

In this section we propose a modification of the continuous consensus algorithm (8.1). Specifically, we consider the case where every node broadcasts at certain time

instances, determined by a local clock at each node, its actual value of θ_i to its adjacent nodes, resulting in the system

$$\dot{\theta} = -\mathcal{L}\hat{\theta}, \tag{8.2}$$

where, $\hat{\theta}_i$, is the latest broadcasted value of θ_i. First, note that (8.2) preserves the average of initial values, since

$$\mathbb{1}_n^T \dot{\theta} = -\mathbb{1}_n^T \mathcal{L}\hat{\theta} = 0. \tag{8.3}$$

Therefore, we aim at characterizing a scheduling of information transmission under which system (8.2) convergence to consensus, i.e.

$$\lim_{t\to\infty} \theta(t) = \overline{\theta}, \tag{8.4}$$

where

$$\overline{\theta} = \mathbb{1}_n \frac{\sum_i^n \theta_i(0)}{n} \in \mathrm{Im}(\mathbb{1}_n). \tag{8.5}$$

8.2.1 Hybrid system

To formalize the idea outlined above we introduce at every node $i \in \mathcal{V}$ a local 'clock variable' ϕ_i whose dynamics are given by

$$\dot{\phi}_i = -2\mathrm{deg}(i)(\frac{1}{4} + \phi_i + \phi_i^2) - \epsilon_i, \tag{8.6}$$

with $\epsilon_i \in \mathbb{R}_{>0}$ a constant. With $\mathrm{deg}(i)$ we denote the (weighted) degree of node $i \in \mathcal{V}$, i.e.

$$\mathrm{deg}(i) = \sum_{k\in\mathcal{E}_i} \Gamma_k, \tag{8.7}$$

with $\mathcal{E}_i$ being the set of edges incident to node i and Γ_k the weight of edge k. Broadcasting of θ_i occurs when $\phi_i = a_i$, whereafter the clock is reset to $\phi_i^+ = b_i$, where $0 < a_i < b_i$, for all $i \in \mathcal{V}$. Furthermore, as we will show in Subsection 8.2.4, there exists a minimum time between two broadcasting instances of node $i \in \mathcal{V}$.

Remark 8.2.1 (Broadcasting with time-varying frequencies)**.** *For a given b_i and a_i, equation (8.6) determines the broadcasting frequency. The analysis in this chapter permits to include a time-varying broadcasting frequency by considering instead of (8.6), the differential inclusion*

$$\dot{\phi}_i \in \big[-M_i, -2\mathrm{deg}(i)(\frac{1}{4} + \phi_i + \phi_i^2) - \epsilon_i\big], \tag{8.8}$$

where $\epsilon_i \in \mathbb{R}_{>0}$, and $M_i \in \mathbb{R}_{>0}$ are constants. The corresponding analysis is pursued in a future publication. However, periodic broadcasting has its advantages due to its simplicity and can be implemented straightforwardly and permits e.g. a 'round robin' scheduling of transmission.

Remark 8.2.2 (Clock dynamics)**.** *The choice of (8.6) is a result of the stability analysis performed later in this section. We provide the clock dynamics here for the sake of exposition, but its rational will become clear in the proof of Lemma 8.2.5. It is important to note that every node possesses its own clock, allowing for asynchronous communication and that (8.6) does not depend on any global information of the network. Furthermore, (8.6) allows us to determine the minimum broadcasting frequency and we do so in Subsection 8.2.4.*

To analyze the convergence properties we formulate the system within the hybrid system framework given in (Goebel et al. 2012), for which a few basic concepts are recalled in Subsection 1.4.3. For the present study, the corresponding flow set is $C := \{(\theta, \hat{\theta}, \phi) \in \mathbb{R}^n \times \mathbb{R}^n \times [a, b]\}$, with $[a, b] = [a_1, b_1] \times \ldots \times [a_n, b_n]$. The flow map $F(\theta, \hat{\theta}, \phi)$ is

$$\left.\begin{aligned} \dot{\theta} &= -\mathcal{L}\hat{\theta} \\ \dot{\hat{\theta}} &= 0 \\ \dot{\phi} &= \alpha(\phi) \end{aligned}\right\} := F(\theta, \hat{\theta}, \phi), \tag{8.9}$$

where $\alpha_i(\phi_i) = -2\deg(i)(\frac{1}{4} + \phi_i + \phi_i^2) - \epsilon_i$,, given by (8.6) above. The jump set is $D := \{(\theta, \hat{\theta}, \phi) \in \mathbb{R}^n \times \mathbb{R}^n \times [a, b] : \exists i \in \{1, \ldots, n\} \text{ s.t. } \phi_i = a_i\}$. The jump map $G(\theta, \hat{\theta}, \phi)$ is defined by

$$G(\theta, \hat{\theta}, \phi) := \{G_i(\theta, \hat{\theta}, \phi) : i \in \{1, \ldots, n\} \text{ and } \phi_i = a_i\}, \tag{8.10}$$

with

$$\left.\begin{aligned} \theta^+ &= \theta \\ \hat{\theta}_i^+ &= \theta_i \\ \hat{\theta}_j^+ &= \hat{\theta}_j \quad j \neq i \\ \phi_i^+ &= b_i \\ \phi_j^+ &= \phi_j \quad j \neq i \end{aligned}\right\} := G_i(\theta, \hat{\theta}, \phi). \tag{8.11}$$

The definition of the jump map (8.10) ensures that at each jump, only one clock variable is reset. In case multiple clocks have reached their lower bound, multiple, but a finite number, successive jumps occur without flows in between. We provide further details on this in the proof of Theorem 8.2.8. The hybrid system with the data

above will be represented by the notation $\mathcal{H}_1 = (C, F, D, G)$ or, briefly, by $\mathcal{H}_1$. The stability analysis in the next subsection 8.2.3 is based on an invariance principle for hybrid systems that requires the system to be nominally well posed. This property is established for system at hand in the following lemma:

Lemma 8.2.3 (Nominally well posed)**.** *The system $\mathcal{H}_1$ is nominally well posed.*

Proof. Following (Goebel et al. 2012, Theorem 6.8) it is sufficient that the system $\mathcal{H}_1$ satisfies the following hybrid basic conditions:

1. C and D are closed subsets of $\mathcal{X} := \mathbb{R}^n \times \mathbb{R}^n \times \mathbb{R}^n$,
2. $F : \mathcal{X} \rightrightarrows \mathcal{X}$ is outer semicontinuous and locally bounded relative to C, $C \subset$ dom F, and $F(z)$ is convex for every $z \in C$,
3. $G : \mathcal{X} \rightrightarrows \mathcal{X}$ is outer semicontinuous and locally bounded relative to D, $D \subset$ dom G.

Condition 1) can be readily verified. Condition 2) is satisfied by $F : \mathcal{X} \to \mathcal{X}$ being a continuous mapping. Condition 3) is satisfied since G is locally bounded and is given by the union of graphs of the continuous mappings $G_i, i \in \{1, \ldots, n\}$, which is closed. ■

8.2.2 Precompactness of solutions

In this subsection we show that the maximal solutions to $\mathcal{H}_1$ are precompact, i.e. they are complete and the closure of their range is compact. Before proving the precompactness of the solutions we establish an important lemma that is essential to the remainder of this section. Consider the storage function[1]

$$V_1(\theta, \hat{\theta}, \phi) = \frac{1}{2}(\theta - \overline{\theta})^T(\theta - \overline{\theta}) + (\theta - \hat{\theta})^T[\phi](\theta - \hat{\theta}), \tag{8.12}$$

with $\overline{\theta}$ given by (8.5).

Remark 8.2.4 (An alternative expression of V_1)**.** *Noting that $\frac{1}{2}(\theta - \overline{\theta})^T(\theta - \overline{\theta})$ can be written as $\|\Pi\theta\|^2$, with $\Pi = I - \frac{1}{n}\mathbb{1}_n\mathbb{1}_n^T$, we can write 8.12 as*

$$V_1 = \begin{bmatrix} \theta \\ \hat{\theta} \end{bmatrix}^T \begin{bmatrix} \frac{1}{2}\Pi + [\phi] & -[\phi] \\ -[\phi] & [\phi] \end{bmatrix} \begin{bmatrix} \theta \\ \hat{\theta} \end{bmatrix}. \tag{8.13}$$

[1] We denote diag$(\phi_1, \ldots, \phi_n)$ by $[\phi]$.

Lemma 8.2.5 (Evolution of V_1)**.** *The storage function V_1 given in (8.12) satisfies*

$$\begin{aligned} \dot{V}_1(\theta,\hat{\theta},\phi) &= \begin{bmatrix}\theta\\ \hat{\theta}\end{bmatrix}^T Z_1 \begin{bmatrix}\theta\\ \hat{\theta}\end{bmatrix} \leq 0 \quad (\theta,\hat{\theta},\phi)\in C \\ V_1(\theta^+,\hat{\theta}^+,\phi^+) &\leq V_1(\theta,\hat{\theta},\phi) \quad (\theta,\hat{\theta},\phi)\in D, \end{aligned} \tag{8.14}$$

along the solutions to $\mathcal{H}_1$, where Z_1 is given by

$$Z_1 = \begin{bmatrix} [\alpha] & -[\alpha]-\frac{1}{2}(I+2[\phi])\mathcal{L} \\ -[\alpha]-\frac{1}{2}((I+2[\phi])\mathcal{L})^T & [\alpha]+[\phi]\mathcal{L}+\mathcal{L}[\phi] \end{bmatrix}. \tag{8.15}$$

Proof. First, we consider the evolution of $V_1(\theta,\hat{\theta},\phi)$ during the flows. We have that

$$\begin{aligned} \dot{V}_1(\theta,\hat{\theta},\phi) &= -\theta^T\mathcal{L}\hat{\theta} + \dot{\phi}^T[\theta-\hat{\theta}](\theta-\hat{\theta}) + 2\phi^T[\theta-\hat{\theta}](-\mathcal{L}\hat{\theta}) \\ &= -\theta^T\mathcal{L}\hat{\theta} + \alpha^T[\theta-\hat{\theta}](\theta-\hat{\theta}) + 2\phi^T[\theta-\hat{\theta}](-\mathcal{L}\hat{\theta}) \\ &= \begin{bmatrix}\theta\\ \hat{\theta}\end{bmatrix}^T Z_1 \begin{bmatrix}\theta\\ \hat{\theta}\end{bmatrix}, \end{aligned} \tag{8.16}$$

where the matrix Z_1 is given by (8.15). Note that $[\alpha]$ is negative definite, and in order to have that $Z_1 \leq \mathbf{0}$ it is sufficient that the Schur complement S_1 of block $[\alpha]$ of matrix Z_1 satisfies $S_1 \leq \mathbf{0}$. This Schur complement is given by[2]

$$\begin{aligned} S_1 &= [\alpha]+[\phi]\mathcal{L}+\mathcal{L}[\phi] \\ &\quad -\big(-[\alpha]-\frac{1}{2}((I+2[\phi])\mathcal{L})^T\big)[\alpha]^{-1}\big(-[\alpha]-\frac{1}{2}(I+2[\phi])\mathcal{L}\big) \\ &= [\alpha]+[\phi]\mathcal{L}+\mathcal{L}[\phi] \\ &\quad -[\alpha][\alpha]^{-1}[\alpha] \\ &\quad -\frac{1}{4}(\mathcal{L}+2[\phi]\mathcal{L})^T[\alpha]^{-1}(\mathcal{L}+2[\phi]\mathcal{L}) \\ &\quad -[\alpha][\alpha]^{-1}(\frac{1}{2}(I+2[\phi])\mathcal{L}) \\ &\quad -(\frac{1}{2}((I+2[\phi])\mathcal{L})^T)[\alpha]^{-1}[\alpha] \\ &= -\mathcal{L}-\frac{1}{4}(\mathcal{L}+2[\phi]\mathcal{L})^T[\alpha]^{-1}(\mathcal{L}+2[\phi]\mathcal{L}) \\ &= -\mathcal{L}-\mathcal{L}([\alpha]^{-1}(\frac{1}{4}I+[\phi]+[\phi][\phi]))\mathcal{L} \\ &= -\mathcal{B}\Gamma^{\frac{1}{2}}(I+\Gamma^{\frac{1}{2}}\mathcal{B}^T([\alpha]^{-1}(\frac{1}{4}I+[\phi]+[\phi][\phi]))\mathcal{B}\Gamma^{\frac{1}{2}})\Gamma^{\frac{1}{2}}\mathcal{B}^T. \end{aligned} \tag{8.17}$$

[2]We write $\Gamma = \Gamma^{\frac{1}{2}}\Gamma^{\frac{1}{2}}$, where $\Gamma = \mathrm{diag}(\Gamma_1,\ldots,\Gamma_k)$; the diagonal matrix consisting of the weights of the edges.

A sufficient condition for $S_1 \leq \mathbf{0}$ is

$$I + \Gamma^{\frac{1}{2}}\mathcal{B}^T([\alpha]^{-1}(\frac{1}{4}I + [\phi] + [\phi][\phi]))\mathcal{B}\Gamma^{\frac{1}{2}} > \mathbf{0}. \tag{8.18}$$

This requires that all eigenvalues of $\Gamma^{\frac{1}{2}}\mathcal{B}^T([\alpha]^{-1}(\frac{1}{4}I + [\phi] + [\phi][\phi]))\mathcal{B}\Gamma^{\frac{1}{2}}$ are greater than -1. Studying this problem is equivalent to finding the smallest eigenvalue of the weighted edge-Laplacian $\Gamma^{\frac{1}{2}}\mathcal{B}^T X\mathcal{B}\Gamma^{\frac{1}{2}}$, with $X = [\alpha]^{-1}(\frac{1}{4}I + [\phi] + [\phi][\phi])$ This is equivalent to find $\lambda_{\min}(X\mathcal{B}\Gamma\mathcal{B}^T) = \lambda_{\min}(X\mathcal{L})$. By Gershgorin circle theorem we have that every eigenvalue of $X\mathcal{L}$ lies within at least one of the Gershgorin discs with center $(XL)_{ii}$ and radius, $R_i = \sum_{j\in\mathcal{N}_i}(X\mathcal{L})_{ij}$, where in this case we have that $(X\mathcal{L})_{ii} = \deg(i)X_{ii} = R_i$. To ensure that $\lambda_{\min}(X\mathcal{L}) > -1$ we need to enfore $2\deg(i)X_{ii} > -1$ for all i. Bearing in mind the definition of X it follows that if $\alpha_i < -2\deg(i)(\frac{1}{4} + \phi_i + \phi_i^2)$, then $S_1 \leq \mathbf{0}$ and consequently $Z_1 \leq \mathbf{0}$. Since we picked in (8.6) $\alpha_i = -2\deg(i)(\frac{1}{4}+\phi_i+\phi_i^2)-\epsilon_i$, with $\epsilon_i \in \mathbb{R}_{>0}$, we have indeed $\dot{V}_1(\theta, \hat{\theta}, \phi) \leq 0$.

Second, $V_1(\theta^+, \hat{\theta}^+, \phi^+) \leq V_1(\theta, \hat{\theta}, \phi)$, since $\theta_i = \hat{\theta}_i$ whenever the value of ϕ_i is increased during a jump. ■

Exploiting the previous lemma we can now establish the following result.

Lemma 8.2.6 (Precompactness of solutions)**.** *Every maximal solution to system $\mathcal{H}_1$ is precompact.*

Proof. For any $(\theta, \hat{\theta}, \phi) \in C \cup D = C$, we have that $(\theta, \hat{\theta}, \phi) \in D$ or that $(\theta, \hat{\theta}, \phi)$ is in the interior of C. Furthermore, $G(D) \subset C \cup D$. Since the domain of a maximal solution to $\mathcal{H}_1$ is unbounded it follows from (Goebel et al. 2012, Proposition 6.10) that there exists from every initial condition a nontrivial solution and every maximal solution is complete. Furthermore, we note that by construction $\phi \in \times[a, b]$ is bounded and positive. Exploiting Lemma 8.2.5, where we have proven that

$$\begin{aligned} \dot{V}_1(\theta, \hat{\theta}, \phi) &\leq 0 \quad (\theta, \hat{\theta}, \phi) \in C \\ V_1(\theta^+, \hat{\theta}^+, \phi^+) &\leq V_1(\theta, \hat{\theta}, \phi) \quad (\theta, \hat{\theta}, \phi) \in D \end{aligned} \tag{8.19}$$

it follows from (8.12) that both $\theta - \overline{\theta}$ and $\theta - \hat{\theta}$ are bounded over time. Since $\overline{\theta}$ is a constant, θ is bounded, and consequently $\hat{\theta}$ is bounded as well. We can conclude that the solutions to system $\mathcal{H}_1$ remain bounded and that the closure of their range is compact. We can therefore conclude that every maximal solution is precompact. ■

8.2.3 Stability analysis

According to the previous subsections the system $\mathcal{H}_1$ is nominally well posed and its maximal solutions are precompact. To infer that the solutions approach the desired (consensus) state, we rely on an invariance principle for hybrid systems (Lemma 1.4.17). Before we do so, we establish the following lemma that we will use to characterize the set that the solutions to $\mathcal{H}_1$ approach.

Lemma 8.2.7 (Nullspace of Z_1)**.** *The nullspace of Z_1 given in (8.15) satisfies*

$$\mathrm{Ker}(Z_1) = \mathrm{Im}(\mathbb{1}_{2n}). \tag{8.20}$$

Proof. (i) $\mathrm{Im}(\mathbb{1}_n) \subseteq \mathrm{Ker}(Z_1)$.

Take $v = \beta\mathbb{1}_n \in \mathrm{Im}(\mathbb{1}_n)$, with some scalar $\beta \in \mathbb{R}$. The claim follows from

$$\begin{aligned} Z_1 v =& \beta \begin{bmatrix} [\alpha]\mathbb{1}_n - [\alpha]\mathbb{1}_n - \frac{1}{2}(I + 2[\phi])\mathcal{L}\mathbb{1}_n \\ -[\alpha]\mathbb{1}_n - \frac{1}{2}((I + 2[\phi])\mathcal{L})^T\mathbb{1}_n + [\alpha]\mathbb{1}_n + [\phi]\mathcal{L}\mathbb{1}_n + \mathcal{L}[\phi]\mathbb{1}_n \end{bmatrix} \\ =& \beta \begin{bmatrix} \mathbf{0} \\ -\frac{1}{2}\mathcal{L}\mathbb{1}_n - \mathcal{L}[\phi]\mathbb{1}_n + \mathcal{L}[\phi]\mathbb{1}_n \end{bmatrix} = \mathbf{0}. \end{aligned} \tag{8.21}$$

(ii) $\mathrm{Im}(\mathbb{1}_n) \supseteq \mathrm{Ker}(Z_1)$.
Note first the following factorization of the matrix Z_1, where indeed $\det(A) \neq 0$:

$$Z_1 = \begin{bmatrix} A & B \\ B^T & C \end{bmatrix} = \begin{bmatrix} I & \mathbf{0} \\ CA^{-1} & I \end{bmatrix} \begin{bmatrix} A & \mathbf{0} \\ \mathbf{0} & S \end{bmatrix} \begin{bmatrix} I & A^{-1}B \\ \mathbf{0} & I \end{bmatrix}$$

Let $v \in \mathrm{Ker}(Z_1)$. Then $Z_1 v = \mathbf{0}$. The latter is equivalent to

$$\begin{bmatrix} A & \mathbf{0} \\ \mathbf{0} & S \end{bmatrix} \begin{bmatrix} I & A^{-1}B \\ \mathbf{0} & I \end{bmatrix} z = \mathbf{0},$$

or

$$\begin{aligned} Az_1 + Bz_2 &= \mathbf{0} \\ Sz_2 &= \mathbf{0}. \end{aligned}$$

Recall from (8.17), that $S = -\mathcal{B}Y\mathcal{B}^T$, with

$$Y = I + \Gamma^{\frac{1}{2}}\mathcal{B}^T([\alpha]^{-1}(\frac{1}{4}I + [\phi] + [\phi][\phi]))\mathcal{B}\Gamma^{\frac{1}{2}}, \tag{8.22}$$

If $Y > \mathbf{0}$, then $\mathrm{Ker}(S) = \mathrm{Im}(\mathbb{1}_n)$.[3] The latter and $Sz_2 = \mathbf{0}$ imply $z_2 = \mathbb{1}_n\beta$ for some β. Replacing it in $Az_1 + Bz_2 = \mathbf{0}$ and bearing in mind the expressions for A, B, we have

$$\begin{aligned} \mathbf{0} &= [\alpha]z_1 - ([\alpha] + \tfrac{1}{2}(I + 2[\phi])\mathcal{L})z_2 \\ &= [\alpha]z_1 - ([\alpha] + \tfrac{1}{2}(I + 2[\phi])\mathcal{L})\mathbb{1}\beta \\ &= [\alpha]z_1 - [\alpha]\mathbb{1}_n\beta, \end{aligned}$$

from which it follows that $z_1 = \mathbb{1}_n\beta$, that is

$$z = \begin{bmatrix} z_1 \\ z_2 \end{bmatrix} = \mathbb{1}_{2n}\beta,$$

and therefore $z \in \mathrm{Im}(\mathbb{1}_{2n})$. This proves claim (ii) and the thesis is complete.

■

Using the lemma above, we are now ready to state the main result of this section.

Theorem 8.2.8 (Approaching consensus)**.** *The maximal solutions of system $\mathcal{H}_1$ approach the set where $\theta = \hat{\theta} = \overline{\theta}$, with*

$$\overline{\theta} = \mathbb{1}_n \frac{\sum_i \theta_i(0)}{n} \in \mathrm{Im}(\mathbb{1}_n). \tag{8.23}$$

Proof. We first note that the average value of $x(0)$ is preserved since during flows

$$\mathbb{1}_n^T\dot{\theta} = -\mathbb{1}_n^T\mathcal{L}\hat{\theta} = 0, \tag{8.24}$$

and at a the jumps $\theta^+ = \theta$. According to Lemma 8.2.5,

$$\dot{V}_1(\theta, \hat{\theta}, \phi) \leq u_c(\theta, \hat{\theta}, \phi) \quad \forall (\theta, \hat{\theta}, \phi) \in C \tag{8.25}$$

$$V_1(\theta^+, \hat{\theta}^+, \phi^+) - V_1(\theta, \hat{\theta}, \phi) \leq u_d(\theta, \hat{\theta}, \phi) \quad \forall (\theta, \hat{\theta}, \phi) \in D, \tag{8.26}$$

where

$$u_c(\theta, \hat{\theta}, \phi) = \begin{cases} \begin{bmatrix} \theta \\ \hat{\theta} \end{bmatrix}^T Z_1 \begin{bmatrix} \theta \\ \hat{\theta} \end{bmatrix} & (\theta, \hat{\theta}, \phi) \in C \\ -\infty & \text{otherwise} \end{cases} \tag{8.27}$$

$$u_d(\theta, \hat{\theta}, \phi) = \begin{cases} 0 & (\theta, \hat{\theta}, \phi) \in D \\ -\infty & \text{otherwise.} \end{cases} \tag{8.28}$$

[3] Trivially $\mathrm{Im}(\mathbb{1}_n) \subseteq \mathrm{Ker}(S)$. Let now $v \in \mathrm{Ker}(S)$. Then $BYB^Tv = \mathbf{0}$, which implies $v^TBYB^Tv = 0$. Since $Y > \mathbf{0}$, then necessarily $B^Tv = \mathbf{0}$ and hence $v \in \mathrm{Im}(\mathbb{1}_n)$, which proves $\mathrm{Ker}(S) \subseteq \mathrm{Im}(\mathbb{1}_n)$. Hence $\mathrm{Ker}(S) = \mathrm{Im}(\mathbb{1}_n)$.

Here, we have introduced u_c and u_d to define the evolution of V_1 outside the flow and jump set, respectively, as is required to invoke the invariance principle (Goebel et al. 2012, Theorem 8.2). Now, in view of Lemmas 8.2.3, 8.2.5, 8.2.6, and (Goebel et al. 2012, Theorem 8.2), any maximal solutions to system $\mathcal{H}_1$ approach the largest weakly invariant subset of

$$\Upsilon = V_1^{-1}(r) \cap \mathcal{X} \cap \big[\overline{u_c^{-1}(0)} \cup \big(u_d^{-1}(0) \cap G(u_d^{-1}(0))\big)\big],$$

where $r \in V_1(\mathcal{X})$ and $\mathcal{X} := \mathbb{R}^n \times \mathbb{R}^n \times [a, b]$. Note that $u_d^{-1}(0) = D$, but that not necessarily $D \cap G(D) = \emptyset$, as potentially multiple clocks reach at the same (hybrid) time their lower bound. We continue by showing that any maximal solution to $\mathcal{H}_1$ in a weakly forward invariant subset of Υ is in the subset $V_1^{-1}(r) \cap \mathcal{X} \cap \overline{u_c^{-1}(0)}$. Assume, *ad absurdum*, that there exists a maximal solution q in Υ with initialization $q(t_0, k_0) \notin \overline{u_c^{-1}(0)}$, for which $V_1^{-1}(r) \cap \mathcal{X} \cap \big[u_d^{-1}(0) \cap G(u_d^{-1}(0))\big]$ is a weakly forward invariant subset. In this case, $q(t_0, k_0) \in D \cap G(D)$. The solution q experiences a finite number of m jumps until all clocks which are equal to their lower bound are reset. After the jumps $q(t_0, k_0 + m) \in C \backslash D$. This implies that $q(t_0, k_0 + m) \in \overline{u_c^{-1}(0)}$, since it would be otherwise no longer in the set Υ. This contradicts the original claim, and we can conclude that any maximal solution in approaches the largest weakly invariant subset of $\overline{u_c^{-1}(0)}$. Then, in view of (8.27), any maximal solution to $\mathcal{H}_1$ approaches the set

$$\{\theta, \hat{\theta}, \phi : \begin{bmatrix} \theta \\ \hat{\theta} \end{bmatrix}^T Z_1 \begin{bmatrix} \theta \\ \hat{\theta} \end{bmatrix} = 0\}. \tag{8.29}$$

Since, according to Lemma 8.2.7, $\mathrm{Ker}(Z_1) = \mathrm{Im}(\mathbb{1}_{2n})$ and since

$$\begin{bmatrix} \overline{\theta} \\ \overline{\theta} \end{bmatrix} \in \mathrm{Im}(\mathbb{1}_{2n}), \tag{8.30}$$

we conclude that $\begin{bmatrix} \theta \\ \hat{\theta} \end{bmatrix}$ approaches the set where

$$\{\theta, \hat{\theta}, \phi : \begin{bmatrix} \overline{\theta} \\ \overline{\theta} \end{bmatrix} + c\mathbb{1}_{2n}\}, \tag{8.31}$$

where $c \in \mathbb{R}$ is some scalar. Since we also have that

$$\mathbb{1}_n^T \theta(t), \tag{8.32}$$

is a conserved quantity, we necessarily have that $c = 0$. ■

8.2.4 Minimum broadcasting frequency

The choice of a_i, b_i and the clock dynamics

$$\dot{\phi}_i = -2\deg(i)(\frac{1}{4} + \phi_i + \phi_i^2) - \epsilon_i, \tag{8.33}$$

determine the broadcasting frequency of node $i \in \mathcal{V}$. To determine the required broadcasting frequency, we study the clock dynamics given by

$$\dot{\phi}_i = -2\deg(i)(\frac{1}{4} + \phi_i + \phi_i^2), \tag{8.34}$$

that provides the upper bound on the maximum inter sampling time for a given a_i and b_i. Now we turn our attention to the question how much time T_i elapses between a clock reset $\phi_i(t) = b_i$ until the following reset at $\phi_i(t + T_i) = a$.

Theorem 8.2.9 (Inter broadcasting time)**.** *The inter broadcasting time T_i, induced by dynamics (8.34), is given by*

$$T_i = \frac{b_i - a_i}{\deg(i)(2a_ib_i + a_i + b_i + \frac{1}{2})}. \tag{8.35}$$

Proof. We solve $\dot{\phi}_i = -2\deg(i)(\frac{1}{4} + \phi_i + \phi_i^2)$, satisfying the boundary condition $\phi_i(0) = b_i$. It can be readily confirmed that the solution is

$$\phi_i(t) = \frac{b_i(1 - \deg(i)t) - \frac{1}{2}\deg(i)t}{\deg(i)(2b + 1)t + 1}. \tag{8.36}$$

Solving (8.74) with boundary condition $\phi_i(T_i) = a_i$ then yields

$$T_i = \frac{b_i - a_i}{\deg(i)(2a_ib_i + a_i + b_i + \frac{1}{2})}. \tag{8.37}$$

■

We define the upper bound on the allowed time between to broadcasting instances T_i^{max}, as $T_i^{max} = \lim_{b_i\to\infty, a_i\to 0} T_i(a_i, b_i)$. From Theorem 8.2.9 the following result is immediate:

Corollary 8.2.10 (Minimum broadcasting frequency)**.** *The maximum allowed time between two sampling instances satisfies $T_i^{max} < \frac{1}{\deg(i)}$, such that the broadcasting frequency of node $i \in \mathcal{V}$ needs to be faster than the (weighted) degree of node i.*

The implication of this section is that despite the nonlinear clock dynamics $\dot{\phi}_i = -2\deg(i)(\frac{1}{4} + \phi_i + \phi_i^2) - \epsilon_i$, we can rely on a simple counter to determine the broadcasting instances.

8.3 Coordination of distributed dynamical systems

In this section we investigate the broadcasting implementation of the consensus algorithm for (optimal) coordination of distributed dynamical systems. Consider a network of dynamical systems defined on a connected, undirected graph $\mathcal{G} = (\mathcal{V}, \mathcal{E})$. Each node represents a nonlinear system

$$\begin{aligned} \dot{x}_i &= f_i(x_i, u_i, \theta_i, d_i) \\ y_i &= h_i(x_i), \end{aligned} \tag{8.38}$$

where $x_i \in \mathbb{R}_i^r$ is the state, $u_i \in \mathbb{R}$ is the input from other nodes in the system and $y_i \in \mathbb{R}$ is the output. The *unknown* constant disturbance at node i is $d_i \in \mathbb{R}$, whereas θ_i is a controllable external input to node i. Compactly, the dynamics at the nodes are represented by

$$\begin{aligned} \dot{x} &= f(x, u, \theta, d) \\ y &= h(x). \end{aligned} \tag{8.39}$$

The nodes in the network are interconnected by edges, where edge k is described by

$$\begin{aligned} \dot{\xi}_k &= F_k(\xi_k, v_k) \\ \lambda_k &= H_k(\xi_k, v_k), \end{aligned} \tag{8.40}$$

leading to a compact notation for all edges as

$$\begin{aligned} \dot{\xi} &= F(\xi, v) \\ \lambda &= H(\xi, v). \end{aligned} \tag{8.41}$$

The interconnection structure is described by the incidence matrix $\mathcal{B}$, and

$$\begin{aligned} u &= \mathcal{B}\lambda \\ v &= -\mathcal{B}^T y, \end{aligned} \tag{8.42}$$

such that the overall system is given by

$$\begin{aligned} \dot{x} &= f(x, \mathcal{B}H(\xi, \mathcal{B}^T h(x)), \theta, d) \\ \dot{\xi} &= F(\xi, \mathcal{B}^T h(x)). \end{aligned} \tag{8.43}$$

In the same spirit as the previous chapters, we aim at output regulation, by an optimal allocation of the inputs $\theta_i, i \in \mathcal{V}$ to the network. To do so, we make the following assumption, ensuring the existence of a steady state of (8.43):

Assumption 8.3.1 (Existence of steady state with input sharing)**.** *For a given d, there exists a constant $(\overline{x}, \overline{\xi})$ and a constant $\overline{\theta} \in \mathrm{Im}(\mathbb{1}_n)$ satisfying,*

$$\begin{aligned} \mathbf{0} = \ & f(\overline{x}, \mathcal{B}H(\overline{\xi}, \mathcal{B}^T h(\overline{x})), \overline{\theta}, d) \\ \mathbf{0} = \ & F(\overline{\xi}, \mathcal{B}^T h(\overline{x})). \end{aligned} \tag{8.44}$$

Note that we have taken $\overline{\theta} \in \mathrm{Im}(\mathbb{1}_n)$ in the assumption above. This is instead of explicitly posing an optimization problem that prescribes the optimal input $\overline{\theta}$, that generally depends on the particular network dynamics. We consider the following control objective:

Objective 8.3.2 (Output regulation and input sharing)**.** *The output of system (8.43) satisfies*

$$\lim_{t\to\infty} y(t) = \overline{y} = h(\overline{x}), \tag{8.45}$$

while the input to the system satisfies

$$\lim_{t\to\infty} \theta(t) \in \mathrm{Im}(\mathbb{1}_n). \tag{8.46}$$

Furthermore, we assume that the physical network enjoys some useful passivity property that we have established e.g. for several power network models in the previous chapters.

Assumption 8.3.3 (Output strictly incremental passivity)**.** *There exists a radially unbounded incremental storage function $V_2(x, \overline{x}, \xi, \overline{\xi})$ that satisfies*

$$\dot{V}_2 = -(h(x) - h(\overline{x}))^T Y (h(x) - h(\overline{x})) + (h(x) - h(\overline{x}))^T K(\theta - \overline{\theta}), \tag{8.47}$$

along the solutions to (8.43), with constant $\overline{\theta} \in \mathrm{Im}(\mathbb{1}_n)$, $Y \in \mathbb{R}^{n\times n}_{>0}$ positive definite and diagonal matrix and $K \in \mathbb{R}^{n\times n}$ is a diagonal matrix. I.e, system (8.43) is output strictly incrementally passive with respect to the steady state (8.44).

Consider now the controller

$$\dot{\theta} = -\mathcal{L}\theta - K^T(h(x) - h(\overline{x})). \tag{8.48}$$

The following lemma shows that controller (8.48) achieves Objective 8.3.2.

Lemma 8.3.4 (Achieving Objective 8.3.2 by a continuous consensus protocol)**.** *Let Assumption 8.3.1 and Assumption 8.3.3 hold. Controller (8.48) achieves Objective 8.3.2 for system (8.43).*

Proof. The incremental storage function

$$\underbrace{\frac{1}{2}(\theta-\overline{\theta})^T(\theta-\overline{\theta})}_{\Theta(\theta,\overline{\theta})}+V_2(x,\overline{x},\xi,\overline{\xi}), \tag{8.49}$$

is radially unbounded and satisfies

$$\dot{\Theta}+\dot{V}_2=-(h(x)-h(\overline{x}))^TY(h(x)-h(\overline{x}))-\theta^T\mathcal{L}\theta, \tag{8.50}$$

along the solutions to (8.43), (8.48). By LaSalle's invariance principle, the solutions to the closed loop system (8.43), (8.48) approach the largest invariant set where $h(x)=h(\overline{x})$ and $\theta\in\mathrm{Im}(\mathbb{1})$. ■

Similar as in Sections 8.1 and 8.2, we consider the following broadcasting implementation of (8.48)

$$\dot{\theta}=-\mathcal{L}\hat{\theta}-K^T(h(x)-h(\overline{x})), \tag{8.51}$$

and define a clock variable ϕ having the following dynamics

$$\dot{\phi}=\alpha+\beta, \tag{8.52}$$

where

$$\alpha_i=-2\mathrm{deg}(i)(\frac{1}{4}+\phi_i+\phi_i^2)-\epsilon_i\quad\forall i\in\mathcal{V}, \tag{8.53}$$

and

$$\beta_i=-\frac{4(K_i\phi_i)^2}{Y_i}-\epsilon_{2i}\quad\forall i\in\mathcal{V}. \tag{8.54}$$

Here, ϵ_i and ϵ_{2i} are again two arbitrarily small scalars. Accordingly, we study, similarly to the previous section, the following hybrid system with flow set $C:=\{(x,\xi,\theta,\hat{\theta},\phi)\in\mathbb{R}^n\times\mathbb{R}^m\times\mathbb{R}^n\times\mathbb{R}^n\times[a,b]\}$. The flow map $F(x,\xi,\theta,\hat{\theta},\phi)$ is

$$\left.\begin{array}{rcl}\dot{x}&=&f(x,\mathcal{B}H(\xi,\mathcal{B}^Th(x)),\theta,d)\\ \dot{\xi}&=&F(\xi,\mathcal{B}^Th(x))\\ \dot{\theta}&=&-\mathcal{L}\hat{\theta}-K^T(h(x)-h(\overline{x}))\\ \dot{\hat{\theta}}&=&\mathbf{0}\\ \dot{\phi}&=&\alpha+\beta\end{array}\right\}:=F(x,\xi,\theta,\hat{\theta},\phi) \tag{8.55}$$

where α_i and β_i are given by (8.34) and (8.54), respectively. The jump set is $D := \{(x, \xi, \theta, \hat{\theta}, \phi) \in \mathbb{R}^n \times \mathbb{R}^m \times \mathbb{R}^n \times \mathbb{R}^n \times [a, b] : \exists i \in \{1, \ldots, n\} \text{ s.t. } \phi_i = a_i\}$. The jump map $G(x, \xi, \theta, \hat{\theta}, \phi)$ is defined by

$$G(x, \xi, \theta, \hat{\theta}, \phi) := \{G_i(x, \xi, \theta, \hat{\theta}, \phi) : i \in \{1, \ldots, n\} \text{ and } \phi_i = a_i\}, \tag{8.56}$$

with

$$\left.\begin{array}{lll} x^+ = & x & \\ \xi^+ = & \xi & \\ \theta^+ = & \theta & \\ \hat{\theta}_i^+ = & \theta_i & \\ \hat{\theta}_j^+ = & \hat{\theta}_j & j \neq i \\ \phi_i^+ = & b_i & \\ \phi_j^+ = & \phi_j & j \neq i \end{array}\right\} := G_i(x, \xi, \theta, \hat{\theta}, \phi). \tag{8.57}$$

The hybrid system with the data above will be represented by the notation $\mathcal{H} = (C, F, D, G)$ or, briefly, by $\mathcal{H}$. Before analyzing the asymptotical behaviour of $\mathcal{H}$, we establish the following useful lemma:

Lemma 8.3.5 (Evolution of $V = V_1 + V_2$)**.** *The storage function $V = V_1 + V_2$, with V_1 as (8.12) satisfies*

$$\begin{aligned} \dot{V} = \begin{bmatrix} \theta \\ \hat{\theta} \end{bmatrix}^T Z_1 \begin{bmatrix} \theta \\ \hat{\theta} \end{bmatrix} + \begin{bmatrix} \theta - \hat{\theta} \\ h(x) - h(\overline{x}) \end{bmatrix}^T Z_2 \begin{bmatrix} \theta - \hat{\theta} \\ h(x) - h(\overline{x}) \end{bmatrix} \leq 0 \quad (x, \xi, \theta, \hat{\theta}, \phi) \in C \\ V(x^+, \xi^+, \theta^+, \hat{\theta}^+, \phi^+) \leq V(x, \xi, \theta, \hat{\theta}, \phi) \quad (x, \xi, \theta, \hat{\theta}, \phi) \in D, \end{aligned} \tag{8.58}$$

along the solutions to $\mathcal{H}$, where Z_1 and Z_2 are given by

$$Z_1 = \begin{bmatrix} [\alpha] & -[\alpha] - \frac{1}{2}(I + 2[\phi])\mathcal{L} \\ -[\alpha] - \frac{1}{2}((I + 2[\phi])\mathcal{L})^T & [\alpha] + [\phi]\mathcal{L} + \mathcal{L}[\phi] \end{bmatrix}, \tag{8.59}$$

$$Z_2 = \begin{bmatrix} [\beta] & [\phi]K + K^T[\phi] \\ [\phi]K + K^T[\phi] & -Y \end{bmatrix}. \tag{8.60}$$

Proof. First, evaluating 8.12 along the flows of system $\mathcal{H}$ yields

$$\begin{aligned}\dot{V}_1 =& -\theta^T\mathcal{L}\hat{\theta} - (\theta-\overline{\theta})^T K(h(x)-h(\overline{x}))\\ &+\dot{\phi}^T[\theta-\hat{\theta}](\theta-\hat{\theta}) + 2\phi^T[\theta-\hat{\theta}](-\mathcal{L}\hat{\theta}-K(h(x)-h(\overline{x})))\\ =& -\theta^T\mathcal{L}\hat{\theta} + (\alpha+\beta)^T[\theta-\hat{\theta}](\theta-\hat{\theta}) + 2\phi^T[\theta-\hat{\theta}](-\mathcal{L}\hat{\theta}-K(h(x)-h(\overline{x})))\\ =& \begin{bmatrix}\theta\\ \hat{\theta}\end{bmatrix}^T Z_1 \begin{bmatrix}\theta\\ \hat{\theta}\end{bmatrix} - (\theta-\overline{\theta})^T K(h(x)-h(\overline{x}))\\ &-2\phi^T[\theta-\hat{\theta}](-K(h(x)-h(\overline{x}))) + \beta^T[\theta-\hat{\theta}](\theta-\hat{\theta}),\end{aligned} \tag{8.61}$$

where the matrix Z_1 is identical to (8.15). Bearing in mind that

$$\dot{V}_2 = -(h(x)-h(\overline{x}))^T Y(h(x)-h(\overline{x})) + (h(x)-h(\overline{x}))^T K(\theta-\overline{\theta}), \tag{8.62}$$

the incremental storage function V satisfies along the flows to system $\mathcal{H}$

$$\dot{V} = \begin{bmatrix}\theta\\ \hat{\theta}\end{bmatrix}^T Z_1 \begin{bmatrix}\theta\\ \hat{\theta}\end{bmatrix} + \begin{bmatrix}\theta-\hat{\theta}\\ h(x)-h(\overline{x})\end{bmatrix}^T Z_2 \begin{bmatrix}\theta-\hat{\theta}\\ h(x)-h(\overline{x})\end{bmatrix}. \tag{8.63}$$

Furthermore, $Z_2 < \mathbf{0}$ if for all $i \in \mathcal{V}$

$$\beta_i < -\frac{4(K_i\phi_i)^2}{Y_i}. \tag{8.64}$$

Second, $V(x^+,\xi^+,\theta^+,\hat{\theta}^+,\phi^+) \leq V(x,\xi,\theta,\hat{\theta},\phi)$, since $\theta_i = \hat{\theta}_i$ whenever the value of ϕ_i is increased during a jump.

■

The following two lemmas can be established in the same way as Lemma 8.2.3 and Lemma 8.2.6 in the previous section and we omit the details.

Lemma 8.3.6 (Nominally well posed)**.** *The system $\mathcal{H}$ is nominally well posed.*

Lemma 8.3.7 (Precompactness of solutions)**.** *Every maximal solution to system $\mathcal{H}$ is precompact.*

We are now ready to prove the main result of this section.

Theorem 8.3.8 (Achieving output regulation and input sharing)**.** *The maximal solutions of system $\mathcal{H}$ approach the set where $h(x) = y = \overline{y}$ and $\theta = \hat{\theta} = \overline{\theta} \in \mathrm{Im}(\mathbb{1}_n)$.*

Proof. According to Lemma 8.3.5

$$\dot{V}(x,\xi,\theta,\hat{\theta},\phi) \leq u_c(x,\xi,\theta,\hat{\theta},\phi) \quad \forall (x,\xi,\theta,\hat{\theta},\phi) \in C \tag{8.65}$$

$$V(x^+,\xi^+,\theta^+,\hat{\theta}^+,\phi^+) - V(x,\xi,\theta,\hat{\theta},\phi) \leq u_d(x,\xi,\theta,\hat{\theta},\phi) \quad \forall (x,\xi,\theta,\hat{\theta},\phi) \in D, \tag{8.66}$$

where

$$u_c(x,\xi,\theta,\hat{\theta},\phi) = \begin{cases} \begin{bmatrix}\theta\\ \hat{\theta}\end{bmatrix}^T Z_1 \begin{bmatrix}\theta\\ \hat{\theta}\end{bmatrix} + \begin{bmatrix}\theta-\hat{\theta}\\ h(x)-h(\overline{x})\end{bmatrix}^T Z_2 \begin{bmatrix}\theta-\hat{\theta}\\ h(x)-h(\overline{x})\end{bmatrix} & (x,\xi,\theta,\hat{\theta},\phi)\in C \\ -\infty & \text{otherwise} \end{cases} \tag{8.67}$$

$$u_d(x,\xi,\theta,\hat{\theta},\phi) = \begin{cases} 0 & (x,\xi,\theta,\hat{\theta},\phi)\in D \\ -\infty & \text{otherwise.} \end{cases} \tag{8.68}$$

In view of Lemmas 8.3.5, 8.3.6, 8.3.7, and (Goebel et al. 2012, Theorem 8.2), the maximal solutions to system $\mathcal{H}$ approach the largest weakly invariant subset of

$$\Upsilon = V^{-1}(r)\cap\mathcal{X}\cap\big[\overline{u_c^{-1}(0)}\cup\big(u_d^{-1}(0)\cap G(u_d^{-1}(0))\big)\big], \tag{8.69}$$

where $r\in V(\mathcal{X})$ and $\mathcal{X}:=\mathbb{R}^n\times\mathbb{R}^n\times\mathbb{R}^n\times\mathbb{R}^n\times[a,b]$. Similarly as in the proof of Theorem 8.2.8, we can argue that any maximal solution approaches the set $\overline{u_c^{-1}(0)}$. In view of (8.67), this subset is given by

$$\{x,\xi,\theta,\hat{\theta},\phi : \begin{bmatrix}\theta\\ \hat{\theta}\end{bmatrix}^T Z_1 \begin{bmatrix}\theta\\ \hat{\theta}\end{bmatrix} + \begin{bmatrix}\theta-\hat{\theta}\\ h(x)-h(\overline{x})\end{bmatrix}^T Z_2 \begin{bmatrix}\theta-\hat{\theta}\\ h(x)-h(\overline{x})\end{bmatrix} = 0\}. \tag{8.70}$$

Since $Z_1\leq\mathbf{0}$ with $\mathrm{Ker}(Z_1)=\mathrm{Im}(\mathbb{1}_n)$ and since $Z_2<\mathbf{0}$, we conclude that the maximal solutions to system $\mathcal{H}$ approach the set where $h(x)=h(\overline{x})=\overline{y}$ and $\theta=\hat{\theta}=\overline{\theta}\in\mathrm{Im}(\mathbb{1}_n)$. ■

8.3.1 Inter broadcasting time

This section follows Section 8.2.4, where we consider here the clock dynamics

$$\dot{\phi}_i = -2\mathrm{deg}(i)(\frac{1}{4}+\phi_i+\phi_i^2) - \frac{4K_i^2\phi_i^2}{Y_i} - \epsilon_i - \epsilon_{2i}. \tag{8.71}$$

Again, a_i, b_i and (8.34) determine the broadcasting frequency of node i. To determine the required broadcasting frequency, we study the clock dynamics given by

$$\dot{\phi}_i = -2\mathrm{deg}(i)(\frac{1}{4}+\phi_i+\phi_i^2) - \frac{4K_i^2\phi_i^2}{Y_i}, \tag{8.72}$$

that provides the upper bound on maximum inter sampling time for a given a_i and b_i. Now we turn our attention to the question how much time T_i elapses between a clock reset $\phi_i(t)=b_i$ until the following reset at $\phi_i(t+T_i)=a_i$.

Theorem 8.3.9 (Inter broadcasting time)**.** *The inter broadcasting time T_i, induced by dynamics (8.34), is given by*

$$T_i = \frac{2}{\sqrt{c_{1i}c_{2i}}}\left(\arctan\left(\frac{2b_i(c_{1i}+c_{2i})+c_{1i}}{\sqrt{c_{1i}c_{2i}}}\right) - \arctan\left(\frac{2a_i(c_{1i}+c_{2i})+c_{1i}}{\sqrt{c_{1i}c_{2i}}}\right)\right) \tag{8.73}$$

Proof. We solve $\dot{\phi}_i = -2\text{deg}(i)(\frac{1}{4}+\phi_i+\phi_i^2) - \frac{4K_i^2\phi_i^2}{Y_i}$, satisfying the boundary condition $\phi_i(0) = b_i$. It can be readily confirmed that the solution is

$$\phi_i(t) = -\frac{0.5\sqrt{c_{1i}c_{2i}}\tan\left(\frac{1}{2}\sqrt{c_{1i}c_{2i}}\,t - \arctan\left(\frac{2b_i(c_{1i}+c_{2i})+c_{1i}}{\sqrt{c_{1i}c_{2i}}}\right)\right) - 0.5c_{1i}}{c_{1i}+c_{2i}}, \tag{8.74}$$

with

$$\begin{aligned} c_{1i} &= 2\text{deg}(i) \\ c_{2i} &= \frac{4K_i^2}{Y_i} \end{aligned} \tag{8.75}$$

Solving (8.74) with boundary condition $\phi_i(T_i) = a_i$ then yields

$$T_i = \frac{2}{\sqrt{c_{1i}c_{2i}}}\left(\arctan\left(\frac{2b_i(c_{1i}+c_{2i})+c_{1i}}{\sqrt{c_{1i}c_{2i}}}\right) - \arctan\left(\frac{2a_i(c_{1i}+c_{2i})+c_{1i}}{\sqrt{c_{1i}c_{2i}}}\right)\right). \tag{8.76}$$

■

We define the upper bound on the allowed time between to broadcasting instances T_i^{max}, as $T_i^{max} = \lim_{b_i\to\infty, a_i\to 0} T_i(a_i, b_i)$. From Theorem 8.2.9 the following result is immediate:

Corollary 8.3.10 (Inter broadcasting time)**.** *The maximum allowed time between two sampling instances satisfies*

$$T_i^{max} < \frac{2}{\sqrt{c_{1i}c_{2i}}}\left(\frac{\pi}{2} - \arctan\left(\frac{\sqrt{c_{1i}}}{\sqrt{c_{2i}}}\right)\right) \tag{8.77}$$

A further analysis shows also that T_i^{max} given above reduces to the expression in Corollary 8.2.10, if one takes $c_{2i} \to 0$, as one would expect.

8.4 Case study

We perform two case studies to illustrate the results obtained in this chapter. First we study the consensus algorithm in Section 8.2, whereafter we apply the results of Section 8.3 to the power network.

8.4.1 Average preserving consensus

In this case study we perform a simulation of the hybrid system (8.9)–(8.11). Consider a cycle graph of 4 nodes, where the flow dynamics are given by $\dot{\theta} = -\mathcal{L}\hat{\theta}$, with $\mathcal{L}$ the (unweighed) Laplacian matrix. The broadcasting instances are determined by the clock dynamics

$$\dot{\phi}_i = -2\text{deg}(i)(\frac{1}{4} + \phi_i + \phi_i^2), \tag{8.78}$$

where for all nodes $i \in \{1, 2, 3, 4\}$ the lower and upper bound are $a_i = 0$ and $b_i = 50$, respectively. Note that in comparison with (8.6), we have omitted ϵ_i, as this is implicitly incorporated by taking $b_i < \infty$. Initially, the state variables satisfy

$$\theta(0) = \begin{bmatrix} 10 \\ 20 \\ 30 \\ 40 \end{bmatrix} \quad \hat{\theta}(0) = \begin{bmatrix} 5 \\ 1 \\ -10 \\ 4 \end{bmatrix} \quad \phi(0) = \begin{bmatrix} 1 \\ 10 \\ 20 \\ 40 \end{bmatrix}. \tag{8.79}$$

The evolution of the system is given in Figure 8.1, from where we notice that all states θ_i, $i \in \{1, 2, 3, 4\}$ approach the average of the elements of $\theta(0)$.

8.4.2 Optimal Load Frequency Control

This subsection we perform a numerical study on the same power network as in Chapter 2, where we assume for the sake of exposition that the voltages are constant. We incorporate the results from this chapter to obtain discrete time communication among the controllers and we formulate the resulting hybrid system as follows: Consider the flow set $C := \{(\eta, \omega, \theta, \hat{\theta}, \phi) \in \mathbb{R}^m \times, \mathbb{R}^n \times \mathbb{R}^n \times \mathbb{R}^n \times [1^{-10}, 2]^n\}$. Here, we have chosen $a_i = 1^{-10}, b_i = 2$ for all $i \in \{1, \dots 4\}$. The flow map $F(\eta, \omega, \theta, \hat{\theta}, \phi)$ is

$$\left.\begin{aligned} \dot{\eta} &= \mathcal{B}^T\omega \\ M\dot{\omega} &= Q^{-1}\theta - \mathcal{B}\Gamma\sin(\eta) - D\omega - P_d \\ \dot{\theta} &= -\mathcal{L}\hat{\theta} - Q^{-1}\omega \\ \dot{\hat{\theta}} &= \mathbf{0} \\ \dot{\phi} &= -2\text{Deg}\cdot(\tfrac{1}{4}\mathbb{1}_4 + \phi + [\phi]\phi) - 4D^{-1}Q^{-2}[\phi]\phi \end{aligned}\right\} := F(\eta, \omega, \theta, \hat{\theta}, \phi), \tag{8.80}$$

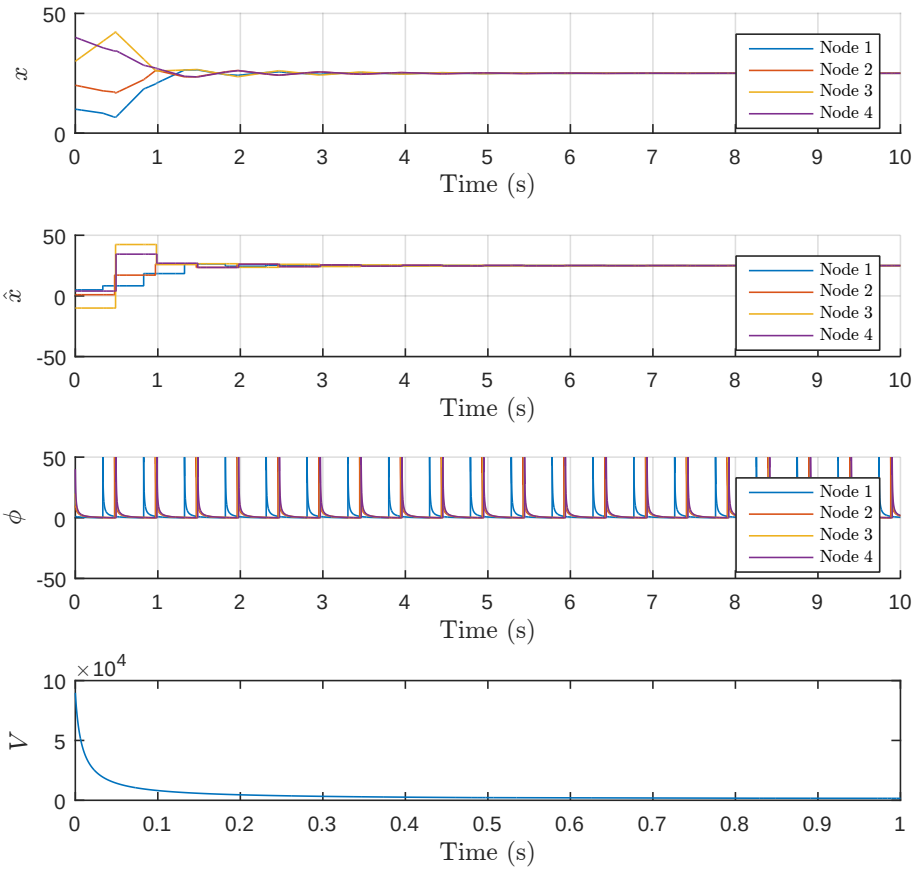

Figure 8.1: Simulation of a 4 node cycle graph. All states θ_i converge to the average of initial conditions, i.e. to 25. Also the value of V_1 given by (8.12) is plotted and is decreasing.

where $\mathrm{Deg} = \mathrm{diag}(\deg(1), \ldots, \deg(4))$, $\mathcal{B}$ is the incidence matrix reflecting the topology of the power network and $\Gamma = \mathrm{diag}(\Gamma_1, \ldots, \Gamma_k)$ describes the line characteristics, with $\Gamma_k = B_{ij} V_i V_j$ for line k connecting areas i and j. The jump set is $D := \{(\eta, \omega, \theta, \hat{\theta}, \phi) \in \mathbb{R}^m \times \mathbb{R}^n \times \mathbb{R}^n \times \mathbb{R}^n \times [1^{-10}, 2]^n : \exists i \in \{1, \ldots, n\} \text{ s.t. } \phi_i = 1^{-10}\}$. The jump map $G(\eta, \omega, \theta, \hat{\theta}, \phi)$ is defined by

$$G(\eta, \omega, \theta, \hat{\theta}, \phi) := \{G_i(\eta, \omega, \theta, \hat{\theta}, \phi) : i \in \{1, \ldots, n\} \text{ and } \phi_i = 1^{-10}\}, \tag{8.81}$$

with

$$\left.\begin{array}{lll} \eta^+ = & \eta & \\ \omega^+ = & \omega & \\ \theta^+ = & \theta & \\ \hat{\theta}_i^+ = & \theta_i & \\ \hat{\theta}_j^+ = & \hat{\theta}_j & j \neq i \\ \phi_i^+ = & 2 & \\ \phi_j^+ = & \phi_j & j \neq i \end{array}\right\} := G_i(\eta, \omega, \theta, \hat{\theta}, \phi). \tag{8.82}$$

The stability analysis is omitted here, but follows essentially the proof of Theorem 8.3.8, under the assumption that steady state differences in voltage angles satisfy $\overline{\eta}_k \in (-\frac{\pi}{2}, \frac{\pi}{2})$, for all $k \in \mathcal{E}$, and taking

$$V_2 = \frac{1}{2}\omega^T M\omega - \mathbb{1}_m^T \Gamma \cos(\eta) + \mathbb{1}_m^T \Gamma \cos(\overline{\eta}) - (\Gamma \sin(\overline{\eta})^T (\eta - \overline{\eta})). \tag{8.83}$$

We illustrate the performance of the controllers on a connected four area network introduced in Section 2.6. The network topology is shown in Figure 8.2. For simpli-

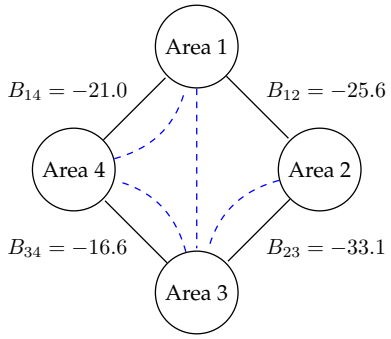

Figure 8.2: A four area equivalent network of the power grid, where B_{ij} denotes the susceptance of the transmission line connecting two areas. The dashed lines represent the communication links.

city, we assume here that the voltages are constant. An overview of the numerical values of the relevant parameters is provided in Table 8.1 below. The communication among the controllers is depicted in Figure 8.2 as well and differs from the topology of the power grid. The system is initially at steady state with a constant load $P_d(t) = (2.00, 1.00, 1.50, 1.00)^T$, $t \in [0, 30)$ and according to their cost functions generators take a different share in the power generation such that the total costs are

	Area 1	Area 2	Area 3	Area 4
M_i	5.22	3.98	4.49	4.22
D_i	1.60	1.22	1.38	1.42
V_i	1	1	1	1
Q_i	1	1	1	1

Table 8.1: An overview of the numerical values used in the simulations.

minimized. $P_d(t) = (2.20, 1.05, 1.55, 1.10)^T$, $t \geq 30$. The frequency response to the control input is given in Figure 8.3. From Figure 8.3 we can see how the frequency drops due to the increased load. Furthermore we note that the controller regulates the power generation such that a new steady state condition is obtained where the frequency deviation is again zero and costs are minimized. Since we have chosen $Q_i = 1$ for all $i \in \{1, \dots 4\}$, we have indeed an identical generation at all nodes at steady state.

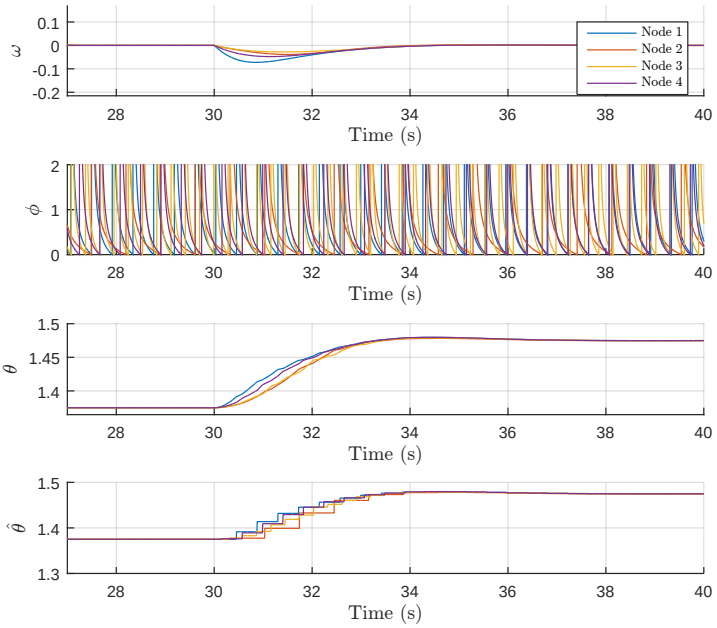

Figure 8.3: Time evolution of the frequency deviation ω, clock ϕ, control input θ, and information exchange $\hat{\theta}$.

Chapter 9

Conclusions and research suggestions

9.1 Conclusions

This thesis provides a framework to design distributed controllers that maintain the frequency of power networks at nominal operating conditions, while retaining economic efficiency. A key insight is that many power network models are incrementally passive systems with respect to their desired steady state solutions. To show this property we study incremental storage functions that interestingly can be interpreted as a Bregman divergence of energy functions, establishing a connection with classical work in the field of power systems. We propose incrementally passive and distributed controllers and study the closed loop behavior of the overall system. We particularly focus on nonlinear models describing high voltage networks and AC microgrids. The passivity property is essential to include the second order turbine-governor dynamics in the stability analysis and we consider two approaches to the controller design. In the first approach, we develop an overall dissipation inequality for the combined power network and turbine-governor system. In the second approach, we apply a distributed sliding mode controller to recover a suitable passivity property of the turbine-governor system once the system reaches the sliding manifold. An important aspect of the proposed distributed controllers is the exchange of information on a communication network. We show that the used incremental storage functions can be adapted to incorporate the discrete time exchange of information. The resulting cyber-physical system is modelled within the framework of hybrid systems and we determine the maximum amount of time that is allowed between two communication instances. Also here, the passivity property of the power network plays a major role in the allowed inter-communication time. An important conclusion of this work is that it is important to incorporate the generation side and the communication network explicitly in the design phase of controllers and that neglecting these aspects can result in an unjustified belief that stability of the network is guaranteed by suggested solutions.

9.2 Research suggestions

This thesis contributed to the (analytical) understanding of the optimal coordination of power networks. Despite the progress made, there are numerous possibilities to extend the presented results, and we discuss below a few that are closely related to this work.

Region of attraction

The incremental storage functions appearing in this thesis, have been mostly used to prove local stability results. An important continuation of these efforts is to study the related level sets of the storage functions in further detail to characterize the regions of attraction of the steady state solutions.

Relaxing assumptions

There are three assumptions appearing throughout this work, that are mainly required to develop suitable incremental storage functions and to prove stability. Relaxing these assumptions would provide new and interesting perspectives on the presented results. First, we mainly assume that the cost function at a node is linear-quadratic, e.g. $C_i(\theta_i) = q_i\theta_i^2$, where θ_i is the power generation. A naturally extension is to consider general strictly convex functions C_i. This leads e.g. to the study of the following system:

$$\begin{aligned} \dot{\eta} &= \mathcal{B}^T\omega \\ M\dot{\omega} &= -D\omega - \mathcal{B}\Gamma\sin(\eta) + \theta - P_d \\ \dot{\theta} &= -\nabla^2 C(\theta)\mathcal{L}\nabla C(\theta) - \omega. \end{aligned} \tag{9.1}$$

Second, it is assumed that the state state voltage angle differences across a line satisfy $\overline{\delta}_i - \overline{\delta}_j = \overline{\eta}_k \in (\frac{-\pi}{2}, \frac{\pi}{2})$, which is required to show that the considered storage functions have a local minimum at the steady state. It is worthwhile to study the stability of the system when this assumption, and other similar 'Hessian conditions', are violated. Third, the transmission lines are assumed to be lossless. Energy functions have been established for power networks where all lines have an identical ratio of susceptance and conductance (Padiyar 2013), and the results in this work are applicable to that case. However, incorporating general lossy networks appears to be very challenging and is a long-standing open problem in analytical power network stability studies.

Generation, transmission and load dynamics

The proposed methodology to study the stability of the power network and to design (distributed) controllers relies on system-theoretical properties, such as incremental passivity. This enabled us to study a power network with nonlinear dynamics, where various components are represented in more detail than is generally done in analytical studies. Incorporating dynamics of the generation and demand side that are on par with the models considered in numerical studies is however still required. This includes e.g. the incorporation of saturation, limiting the generator output power.

New control objectives

The focus of this work is the regulation of the frequency in the power network, while minimizing the generation costs. Future research should additionally include the control of the voltages, which we only have briefly discussed. Also, exact regulation is often not needed in a power network and it is desirable to formulate and analyze objectives where small deviations from the desirable values are allowed. The emphasize of this thesis is on asymptotic stability properties. An important extension is to study the transient behaviour of the system.

Cyber-physical systems

In this work we have made an important step to incorporate the cyber layer of the control structure explicitly, by assuming that the communication occurs at discrete time instances. Other aspects have been neglected, such as delays, quantization effects and (measurement) noise. An interesting endeavour is include those phenomena and to study their effect on the stability of the overall system.

Bibliography

Aguirre, L. A., Rodrigues, D. D., Lima, S. T. and Martinez, C. B.: 2008, Dynamical prediction and pattern mapping in short-term load forecasting, *International Journal of Electrical Power & Energy Systems* **30**, 73 – 82.

Alam, R., Bora, S., Karow, M., Mehrmann, V. and Moro, J.: 2011, Perturbation theory for Hamiltonian matrices and the distance to bounded-realness, *SIAM Journal on Matrix Analysis and Applications* **32**(2), 484–514.

Alessandri, A., Gaggero, M. and Tonelli, F.: 2011, Min-max and predictive control for the management of distribution in supply chains, *IEEE Transactions on Control Systems Technology* **19**(5), 1075–1089.

Alvarado, F., Meng, J., DeMarco, C. and Mota, W.: 2001, Stability analysis of interconnected power systems coupled with market dynamics, *IEEE Transactions on Power Systems* **16**(4), 695–701.

Andreasson, M., Dimarogonas, D. V., Johansson, K. H. and Sandberg, H.: 2013, Distributed vs. centralized power systems frequency control, *Proc. of the 12th European Control Conference (ECC)*, Zürich, Switzerland, pp. 3524–3529.

Andreasson, M., Dimarogonas, D. V., Sandberg, H. and Johansson, K. H.: 2016, Distributed controllers for multi-terminal hvdc transmission systems, *IEEE Transactions on Control of Network Systems* **PP**(99), 1–1.

Apostolopoulou, D., Domínguez-García, A. D. and Sauer, P. W.: 2016, An assessment of the impact of uncertainty on automatic generation control systems, *IEEE Transactions on Power Systems* **31**(4), 2657–2665.

Apostolopoulou, D., Sauer, P. W. and Domínguez-García, A. D.: 2015, Distributed optimal load frequency control and balancing authority area coordination,

Proc. of the 2015 North American Power Symposium (NAPS), Charlotte, NC, USA, pp. 1–5.

Arcak, M.: 2007, Passivity as a design tool for group coordination, *IEEE Transactions on Automatic Control* **52**(8), 1380–1390.

Bai, H., Arcak, M. and Wen, J.: 2011, *Cooperative control design: a systematic, passivity-based approach*, Vol. 89, Springer.

Bartolini, G., Ferrara, A. and Usai, E.: 1998a, Chattering avoidance by second-order sliding mode control, *IEEE Transactions on Automatic Control* **43**(2), 241–246.

Bartolini, G., Ferrara, A. and Usai, E.: 1998b, On boundary layer dimension reduction in sliding mode control of SISO uncertain nonlinear systems, *Proc. of the IEEE International Conference on Control Applications*, Vol. 1, Trieste, Italy, pp. 242 –247.

Bergen, A. and Hill, D.: 1981, A structure preserving model for power system stability analysis, *IEEE Transactions on Power Apparatus and Systems* **PAS-100**(1), 25–35.

Bergen, A. R. and Vittal, V.: 2000, *Power systems analysis*, 2 edn, Prentice Hall.

Berger, A. W. and Schweppe, F. C.: 1989, Real time pricing to assist in load frequency control, *IEEE Transactions on Power Systems* **4**(3), 920–926.

Bertsekas, D. P.: 1998, *Network Optimization: continuous and discrete methods*, Vol. 8, Athena Scientific, Belmont, Massachusetts.

Binetti, G., Davoudi, A., Lewis, F. L., Naso, D. and Turchiano, B.: 2014, Distributed consensus-based economic dispatch with transmission losses, *IEEE Transactions on Power Systems* **29**(4), 1711–1720.

Blanchini, F., Franco, E., Giordano, G., Mardanlou, V. and Montessoro, P. L.: 2016, Compartmental flow control: Decentralization, robustness and optimality, *Automatica* **64**, 18–28.

Boyd, S. and Vandenberghe, L.: 2004, *Convex optimization*, Cambridge university press.

Bregman, L.: 1967, The relaxation method of finding the common point of convex sets and its application to the solution of problems in convex programming, *USSR Computational Mathematics and Mathematical Physics* **7**(3), 200 – 217.

Bürger, M. and De Persis, C.: 2013, Internal models for nonlinear output agreement and optimal flow control, *Proc. of 9th IFAC Symposium on Nonlinear Control Systems (NOLCOS)*, Toulouse, France, pp. 289 – 294.

Bürger, M. and De Persis, C.: 2015, Dynamic coupling design for nonlinear output agreement and time-varying flow control, *Automatica* **51**, 210–222.

Bürger, M., De Persis, C. and Trip, S.: 2014, An internal model approach to (optimal) frequency regulation in power grids, *Proc. of the 21th International Symposium on Mathematical Theory of Networks and Systems (MTNS)*, Groningen, the Netherlands, pp. 577–583.

Cai, D., Mallada, E. and Wierman, A.: 2015, Distributed optimization decomposition for joint economic dispatch and frequency regulation, *Proc. of the 54th IEEE Conf. on Decision and Control (CDC)*, Osaka, Japan, pp. 15–22.

Caliskan, S. and Tabuada, P.: 2014, Compositional transient stability analysis of multimachine power networks, *IEEE Transactions on Control of Network Systems*, **1**(1), 4–14.

Carnevale, D., Teel, A. R. and Nešić, D.: 2007, A Lyapunov proof of an improved maximum allowable transfer interval for networked control systems, *IEEE Transactions on Automatic Control* **52**(5), 892.

Chakrabortty, A., Chow, J. H. and Salazar, A.: 2011, A measurement-based framework for dynamic equivalencing of large power systems using wide-area phasor measurements, *IEEE Transactions on Smart Grid* **2**(1), 68–81.

Chen, L., Li, N., Jiang, L. and Low, S. H.: 2012, Optimal demand response: Problem formulation and deterministic case, *Control and Optimization Methods for Electric Smart Grids* pp. 63–85.

Cherukuri, A. and Cortés, J.: 2016, Initialization-free distributed coordination for economic dispatch under varying loads and generator commitment, *Automatica* **74**, 183–193.

Chiang, H.-D., Chu, C.-C. and Cauley, G.: 1995, Direct stability analysis of electric power systems using energy functions: theory, applications, and perspective, *Proceedings of the IEEE* **83**(11), 1497–1529.

Chu, C.-C. and Chiang, H.-D.: 1999, Constructing analytical energy functions for lossless network-reduction power system models: Framework and new developments, *Circuits, Systems and Signal Processing* **18**(1), 1–16.

Como, G.: 2017, On resilient control of dynamical flow networks, *Annual Reviews in Control* .

Coogan, S. and Arcak, M.: 2015, A compartmental model for traffic networks and its dynamical behavior, *IEEE Transactions on Automatic Control* **60**(10), 2698–2703.

Cox, N., Marconi, L. and Teel, A.: 2012, Hybrid internal models for robust spline tracking, *Proc. of the 51st IEEE Conference on Decision and Control (CDC)*, Maui, HI, USA, pp. 4877 – 4882.

Cucuzella, M., Trip, S., De Persis, C. and Ferrara, A.: 2017, Distributed second order sliding modes for optimal load frequency control, *Proc. of the 2017 American Control Conference (ACC)*, Seattle, WA, USA, pp. 3451–3456.

Cucuzella, M., Trip, S., De Persis, C., Ferrara, A. and van der Schaft, A.: 2017, A robust consensus algorithm for current sharing and voltage regulation in dc microgrids, *(under review)* .

Cucuzzella, M., Lazzari, R., Trip, S., Rosti, S., Sandroni, C. and Ferrara, A.: 2017, Sliding mode voltage control of boost-based dc microgrids, *(under review)* .

De Persis, C.: 2013, Balancing time-varying demand-supply in distribution networks: an internal model approach, *Proc. of the 12th European Control Conference (ECC)*, Zurich, Switzerland, pp. 748 – 753.

De Persis, C. and Jayawardhana, B.: 2014, On the internal model principle in the coordination of nonlinear systems, *IEEE Transactions on Control of Network Systems* **1**(3), 272–282.

De Persis, C. and Monshizadeh, N.: 2017, Bregman storage functions for microgrid control, *IEEE Transactions on Automatic Control* **PP**(99), 1–1.

De Persis, C. and Postoyan, R.: 2017, A lyapunov redesign of coordination algorithms for cyber-physical systems, *IEEE Transactions on Automatic Control* **62**(2), 808–823.

De Persis, C. and Tesi, P.: 2014, On resilient control of nonlinear systems under denial-of-service, *Proc. of the IEEE 53rd Conference on Decision and Control (CDC)*, Los Angeles, CA, USA, pp. 5254–5259.

De Persis, C., Weitenberg, E. and Dorfler, F.: 2016, A power consensus algorithm for dc microgrids, *arXiv preprint arXiv:1611.04192* .

Dimarogonas, D. V., Frazzoli, E. and Johansson, K. H.: 2012, Distributed event-triggered control for multi-agent systems, *IEEE Transactions on Automatic Control* **57**(5), 1291–1297.

Dörfler, F. and Bullo, F.: 2013, Novel insights into lossless ac and dc power flow, *Proc. of the 2013 Power and Energy Society General Meeting (PES)*, Vancouver, Canada, pp. 1–5.

Dörfler, F., Chertkov, M. and Bullo, F.: 2013, Synchronization in complex oscillator networks and smart grids, *Proceedings of the National Academy of Sciences* **110**(6), 2005–2010.

Dörfler, F. and Grammatico, S.: 2016, Amidst centralized and distributed frequency control in power systems, *Proc. of the 2016 American Control Conference (ACC)*, Boston, MA, USA, pp. 5909–5914.

Dörfler, F., Simpson-Porco, J. W. and Bullo, F.: 2016, Breaking the hierarchy: Distributed control and economic optimality in microgrids, *IEEE Transactions on Control of Network Systems* **3**(3), 241–253.

Dvijotham, K., Low, S. and Chertkov, M.: 2015, Convexity of energy-like functions: theoretical results and applications to power system operations, *arXiv preprint arXiv:1501.04052* .

Edwards, C. and Spurgen, S. K.: 1998, *Sliding Mode Control: Theory and Applications*, Taylor and Francis, London, UK.

Efimov, D., Schiffer, J. and Ortega, R.: 2016, Robustness of delayed multistable systems with application to droop-controlled inverter-based microgrids, *International Journal of Control* **89**(5), 909–918.

Falnes, J.: 2007, A review of wave-energy extraction, *Marine Structures* **20**(4), 185 – 201.

Fan, Y., Hu, G. and Egerstedt, M.: 2016, Distributed reactive power sharing control for microgrids with event-triggered communication, *IEEE Transactions on Control Systems Technology* **PP**(99), 1–11.

Goebel, R., Sanfelice, R. G. and Teel, A. R.: 2012, *Hybrid Dynamical Systems: modeling, stability, and robustness*, Princeton University Press.

Grivet-Talocia, S.: 2004, Passivity enforcement via perturbation of Hamiltonian matrices, *IEEE Transactions on Circuits and Systems I: Regular Papers* **51**(9), 1755–1769.

Guerrero, J. M., Vasquez, J. C., Matas, J., De Vicuña, L. G. and Castilla, M.: 2011, Hierarchical control of droop-controlled ac and dc microgridsa general approach toward standardization, *IEEE Transactions on Industrial Electronics* **58**(1), 158–172.

Gupta, S. K., Kar, K., Mishra, S. and Wen, J. T.: 2015, Distributed consensus algorithms for collaborative temperature control in smart buildings, *Proc. of the 2015 American Control Conference (ACC)*, Chicago, IL, USA, pp. 5758–5763.

Ha, Q. P.: 1998, A fuzzy sliding mode controller for power system load-frequency control, *Knowledge-Based Intelligent Electronic Systems*, Vol. 1, pp. 149–154 vol.1.

Haddad, W. M. and Chellaboina, V.: 2008, *Nonlinear dynamical systems and control: a Lyapunov-based approach*, Princeton University Press.

Heemels, W. P. M. H., Johansson, K. H. and Tabuada, P.: 2012, An introduction to event-triggered and self-triggered control, *Proc. of the 51st IEEE Conference on Decision and Control (CDC)*, Maui, HI, USA, pp. 3270–3285.

Hines, G. H., Arcak, M. and Packard, A. K.: 2011, Equilibrium-independent passivity: A new definition and numerical certification, *Automatica* **47**(9), 1949 – 1956.

Ibraheem, Kumar, P. and Kothari, D. P.: 2005, Recent philosophies of automatic generation control strategies in power systems, *IEEE Transactions on Power Systems* **20**(1), 346–357.

Iftar, A.: 1999, A linear programming based decentralized routing controller for congested highways, *Automatica* **35**(2), 279 – 292.

Incremona, G. P., Cucuzzella, M. and Ferrara, A.: 2016, Adaptive suboptimal second-order sliding mode control for microgrids, *International Journal of Control* pp. 1–19.

Isidori, A.: 2000, *Nonlinear Control Systems II*, Springer-Verlag.

Isidori, A., Marconi, L. and Casadei, G.: 2014, Robust output synchronization of a network of heterogeneous nonlinear agents via nonlinear regulation theory, *IEEE Transactions on Automatic Control* **59**(10), 2680–2691.

Jokic, A., Lazar, M. and van den Bosch, P.: 2009, Real-time control of power systems using nodal prices, *International Journal of Electrical Power & Energy Systems* **31**(9), 522 – 530.

Kar, S. and Hug, G.: 2012, Distributed robust economic dispatch in power systems: A consensus + innovations approach, *Proc. of the 2012 IEEE Power and Energy Society General Meeting*, pp. 1–8.

Kasis, A., Devane, E., Spanias, C. and Lestas, I.: 2016, Primary frequency regulation with load-side participation part I: stability and optimality, *IEEE Transactions on Power Systems* **PP**(99), 1–1.

Kasis, A., Monshizadeh, N., Devane, E. and Lestas, I.: 2017, Stability and optimality of distributed secondary frequency control schemes in power networks, *arXiv preprint arXiv:1703.00532* .

Kiani, A. and Annaswamy, A.: n.d., *Proc. of the 50th IEEE Conference on Decision and Control and European Control Conference*, Orlanda, FL, USA, pp. 2202–2207.

Kundur, P., Balu, N. J. and Lauby, M. G.: 1994, *Power system stability and control*, Vol. 7, McGraw-hill New York.

Kundur, P., Paserba, J., Ajjarapu, V., Andersson, G., Bose, A., Canizares, C., Hatziargyriou, N., Hill, D., Stankovic, A., Taylor, C., Cutsem, T. V. and Vittal, V.: 2004, Definition and classification of power system stability IEEE/CIGRE joint task force on stability terms and definitions, *IEEE Transactions on Power Systems* **19**(3), 1387–1401.

Lee, S.-J., Park, D. J., Kim, J. H. and Ahn, H.-S.: 2017, Distributed coordination of asymmetric compartmental systems under time-varying inputs and its applications, *IEEE Transactions on Control Systems Technology* .

Levant, A.: 2003, Higher-order sliding modes, differentiation and output-feedback control, *International Journal of Control* **76**(9-10), 924–941.

Li, N., Chen, L., Zhao, C. and Low, S.: 2014, Connecting automatic generation control and economic dispatch from an optimization view, *Proc. of the the 2014 American Control Conference (ACC)*, Portland, OR, USA, pp. 735–740.

Li, N., Zhao, C. and Chen, L.: 2016, Connecting automatic generation control and economic dispatch from an optimization view, *IEEE Transactions on Control of Network Systems* **3**(3), 254–264.

Liu, Q. and Ilić, M. D.: 2012, Enhanced automatic generation control (e-agc) for future electric energy systems, *Proc. of the 2012 IEEE Power and Energy Society General Meeting*, pp. 1–8.

Machowski, J., Bialek, J. and Bumby, D. J.: 2008, *Power System Dynamics: Stability and Control*, 2 edn, Wiley.

Mi, Y., Fu, Y., Li, D., Wang, C., Loh, P. C. and Wang, P.: 2016, The sliding mode load frequency control for hybrid power system based on disturbance observer, *International Jorunal of Electrical Power and Energy Systems* **74**, 446 – 452.

Mi, Y., Fu, Y., Wang, C. and Wang, P.: 2013, Decentralized sliding mode load frequency control for multi-area power systems, *IEEE Transactions on Power Systems* **28**(4), 4301–4309.

Miao, Z. and Fan, L.: 2016, Achieving economic operation and secondary frequency regulation simultaneously through local feedback control, *IEEE Trans. Power Syst.* **PP**(99), 1–9.

Milan, P., Wächter, M. and Peinke, J.: 2013, Turbulent character of wind energy, *Physical review letters* **110**(13), 138701.

Monshizadeh, N. and De Persis, C.: 2015, Output agreement in networks with unmatched disturbances and algebraic constraints, *arXiv preprint arXiv:1504.03609* .

Monshizadeh, N., De Persis, C., van der Schaft, A. J. and Scherpen, J.: 2016, A novel reduced model for electrical networks with constant power loads, *arXiv preprint arXiv:1512.08250* pp. 3644–3649. Abridged version in the Proc. of the 2016 American Control Conference (ACC).

Moss, F. and Segall, A.: 1982, An optimal control approach to dynamic routing in networks, *IEEE Transactions on Automatic Control* **27**(2), 329–339.

Mudumbai, R., Dasgupta, S. and Cho, B. B.: 2012, Distributed control for optimal economic dispatch of a network of heterogeneous power generators, *IEEE Transactions on Power Systems* **27**(4), 1750–1760.

Nabavi, S. and Chakrabortty, A.: 2013, Topology identification for dynamic equivalent models of large power system networks, *Proc. of the 2013 American Control Conference (ACC)*, Washington, DC, USA, pp. 1138–1143.

Naldi, R. and Sanfelice, R. G.: 2013, Passivity-based control for hybrid systems with applications to mechanical systems exhibiting impacts, *Automatica* **49**(5), 1104 – 1116.

North American Electric Reliability Corporation (NERC): 2016, *Phase Angle Monitoring: Industry Experience Following the 2011 Pacific Southwest Outage Recommendation 27*.

Nowzari, C., Cortes, J. and Pappas, G. J.: 2016, Event-triggered communication and control for multi-agent average consensus, *arXiv preprint arXiv:1609.06984* .

Ourari, M., Dessaint, L.-A. and Do, V.-Q.: 2006, Dynamic equivalent modeling of large power systems using structure preservation technique, *IEEE Transactions on Power Systems* **21**(3), 1284–1295.

Padiyar, K.: 2013, *Structure Preserving Energy Functions in Power Systems: Theory and Applications*, Taylor & Francis.

Pan, C. T. and Liaw, C. M.: 1989, An adaptive controller for power system load-frequency control, *IEEE Transactions on Power Systems* **4**(1), 122–128.

Pandey, S. K., Mohanty, S. R. and Kishor, N.: 2013, A literature survey on load–frequency control for conventional and distribution generation power systems, *Renewable and Sustainable Energy Reviews* **25**, 318 – 334.

Pavlov, A. and Marconi, L.: 2008, Incremental passivity and output regulation, *Systems and Control Letters* **57**, 400 – 409.

Plemmons, R.: 1977, M-matrix characterizations. i–nonsingular m-matrices, *Linear Algebra and its Applications* **18**(2), 175 – 188.

Postoyan, R., Tabuada, P., Nešić, D. and Anta, A.: 2015, A framework for the event-triggered stabilization of nonlinear systems, *IEEE Transactions on Automatic Control* **60**(4), 982–996.

Rahbari-Asr, N., Ojha, U., Zhang, Z. and Chow, M. Y.: 2014, Incremental welfare consensus algorithm for cooperative distributed generation/demand response in smart grid, *IEEE Transactions on Smart Grid* **5**(6), 2836–2845.

Rinaldi, G., Menon, P. P., Edwards, C. and Ferrara, A.: 2017, Distributed observers for state estimation in power grids, *Proc. of the 2017 American Control Conference (ACC)*, Seattle, WA, USA, pp. 5824–5829.

Rockafellar, R. T.: 1984, *Network flows and monotropic optimization*, Wiley-Interscience.

Schiffer, J.: 2015, Stability and power sharing in microgrids, *PhD Thesis, TU Berlin* .

Schiffer, J. and Dörfler, F.: 2016, On stability of a distributed averaging PI frequency and active power controlled differential-algebraic power system model, *Proc. of the 15th European Control Conference (ECC)*, Aalborg, DK, pp. 1487–1492.

Schiffer, J., Ortega, R., Astolfi, A., Raisch, J. and Sezi, T.: 2013, Synchronization of droop-controlled microgrids with distributed rotational and electronic generation, *Proc. of the IEEE 52nd Conference on Decision and Control (CDC)* pp. 2334–2339.

Schiffer, J., Ortega, R., Astolfi, A., Raisch, J. and Sezi, T.: 2014, Conditions for stability of droop-controlled inverter-based microgrids, *Automatica* **50**(10), 2457–2469.

Schiffer, J., Zonetti, D., Ortega, R., Stankovic, A., Sezi, T. and Raisch, J.: 2015, Modeling of microgrids-from fundamental physics to phasors and voltage sources, *arXiv preprint arXiv:1505.00136* .

Scholten, T., S.Trip and De Persis, C.: 2017, Pressure regulation in large scale hydraulic networks with positivity constraints, *(in preparation)* .

Scholten, T., Trip, S. and De Persis, C.: 2017, Pressure regulation in large scale hydraulic networks with input constraints, *Proc. of the 2017 IFAC World Congress*, Toulouse, France, pp. 5534–5539.

Scholten, T. W., De Persis, C. and Tesi, P.: 2015, Modeling and control of heat networks with storage: the single-producer multiple-consumer case, *Proc. of the 14th European Control Conference (ECC)*, Linz, AT, pp. 2247–2252.

Scholten, T. W., De Persis, C. and Tesi, P.: 2016, Optimal steady state regulation of distribution networks with input and flow constraints, *Proc. of the 2016 American Control Conference (ACC)*, Boston, MA, USA, pp. 6953–6958.

Sepulchre, R., Janković, M. and Kokotović, P.: 1997, *Constructive Nonlinear Control*, Communications and control engineering, W.H. Freeman.

Serrani, A., Isidori, A. and Marconi, L.: 2001, Semi-global nonlinear output regulation with adaptive internal model, *IEEE Transactions on Automatic Control* **46**(8), 1178–1194.

Seyboth, G. S., Dimarogonas, D. V. and Johansson, K. H.: 2013, Event-based broadcasting for multi-agent average consensus, *Automatica* **49**(1), 245 – 252.

Shafiee, Q., Guerrero, J. M. and Vasquez, J. C.: 2014, Distributed secondary control for islanded microgrids; a novel approach, *IEEE Transactions on Power Electronics* **29**(2), 1018–1031.

Shaik, F., Zonetti, D., Ortega, R., Scherpen, J. and van der Schaft, A.: 2013, A port-Hamiltonian approach to power network modeling and analysis, *European Journal of Control* **19**(6), 477 – 485.

Simpson-Porco, J. W., Dörfler, F. and Bullo, F.: 2013, Synchronization and power sharing for droop-controlled inverters in islanded microgrids, *Automatica* **49**(9), 2603–2611.

Stegink, T., De Persis, C. and van der Schaft, A.: 2016, Optimal power dispatch in networks of high-dimensional models of synchronous machines, *arXiv preprint arXiv:1603.06688* .

Stegink, T., De Persis, C. and van der Schaft, A.: 2017, A unifying energy-based approach to stability of power grids with market dynamics, *IEEE Transactions on Automatic Control* **62**(6), 2612–2622.

Trip, S., Bürger, M. and De Persis, C.: 2014, An internal model approach to frequency regulation in inverter-based microgrids with time-varying voltages, *Proc. of the IEEE 53rd Conference on Decision and Control (CDC)*, Los Angeles, CA, USA, pp. 223–228.

Trip, S., Bürger, M. and De Persis, C.: 2016, An internal model approach to (optimal) frequency regulation in power grids with time-varying voltages, *Automatica* **64**, 240 – 253.

Trip, S., Cucuzella, M., De Persis, C., van der Schaft, A. and Ferrara, A.: 2017, Passivity based design of sliding modes for optimal load frequency control, *(under review)* .

Trip, S., Cucuzella, M., Ferrara, A. and De Persis, C.: 2017, An energy function based design of second order sliding modes for automatic generation control, *Proc. of the 2017 IFAC World Congress*, Toulouse, France, pp. 12118–12123.

Trip, S. and De Persis, C.: 2016a, Optimal frequency regulation in nonlinear structure preserving power networks including turbine dynamics: an incremental passivity approach, *Proc. of the 2016 American Control Conference (ACC)*, Boston, MA, USA, pp. 3451–3456.

Trip, S. and De Persis, C.: 2016b, Optimal generation in structure-preserving power networks with second order turbine-governor dynamicsl, *Proc. of the 15th European Control Conference (ECC)*, Aalborg, DK, pp. 916–921.

Trip, S. and De Persis, C.: 2017a, Communication requirements in a master-slave control structure for optimal load frequency control, *Proc. of the 2017 IFAC World Congress*, Toulouse, France, pp. 10519–10524.

Trip, S. and De Persis, C.: 2017b, Optimal load frequency control with non-passive dynamics, *IEEE Transactions on Control of Network Systems* **PP**, 1–1.

Trip, S., De Persis, C. and Tesi, P.: 2017, Coordination of nonlinear cyber-physical systems, from a continuous consensus to a discrete broadcasting protocol, *(in preparation)* .

Trip, S., Scholten, T. and De Persis, C.: 2017a, Optimal regulation of flow networks with input and flow constraints, *Proc. of the 2017 IFAC World Congress*, Toulouse, France, pp. 9854–9859.

Trip, S., Scholten, T. and De Persis, C.: 2017b, Optimal regulation of flow networks with transient constraints, *(under review)* .

Utkin, V. I.: 1992, *Sliding Modes in Control and Optimization*, Springer-Verlag.

Van der Hoven, I.: 1957, Power spectrum of horizontal wind speed in the frequency range from 0.0007 to 900 cycles per hour, *Journal of Meteorology* **14**(2), 160–164.

van der Schaft, A. J.: 1999, *L2-Gain and Passivity in Nonlinear Control*, 2 edn, Springer-Verlag New York, Inc., Secaucus, NJ, USA.

van der Schaft, A. and Maschke, B.: 2013, Port-Hamiltonian systems on graphs, *SIAM Journal on Control and Optimization* **51**(2), 906–937.

Variani, M. H. and Tomsovic, K.: 2013, Distributed automatic generation control using flatness-based approach for high penetration of wind generation, *IEEE Transactions on Power Systems* **28**(3), 3002–3009.

Venkat, A. N., Hiskens, I. A., Rawlings, J. B. and Wright, S. J.: 2006, Distributed mpc strategies with application to power system automatic generation control, *Technical report number 2006-05, (abridged version in IEEE Transactions on Control Systems Technology)* .

Vu, T. L. and Turitsyn, K.: 2016, Lyapunov functions family approach to transient stability assessment, *IEEE Transactions on Power Systems* **31**(2), 1269–1277.

Weckx, S., D'Hulst, R. and Driesen, J.: 2015, Primary and secondary frequency support by a multi-agent demand control system, *IEEE Transactions on Power Systems* **30**(3), 1394–1404.

Wieland, P., Sepulchre, R. and Allgöwer, F.: 2011, An internal model principle is necessary and sufficient for linear output synchronization, *Automatica* **47**, 1068 – 1074.

Willems, J.: 2007, Dissipative dynamical systems, *European Journal on Control* **13**, 134 – 151.

Wood, A. and Wollenberg, B.: 1996, *Power Generation, Operation, and Control*, 2 edn, Wiley.

Xi, K., Dubbeldam, J. L., Lin, H. X. and van Schuppen, J. H.: 2017, Power-imbalance allocation control of power systems-secondary frequency control, *arXiv preprint arXiv:1703.02855* .

Xu, Y., Li, F., Jin, Z. and Variani, M. H.: 2016, Dynamic gain-tuning control (dgtc) approach for agc with effects of wind power, *IEEE Transactions on Power Systems* **31**(5), 3339–3348.

Yang, S., Tan, S. and Xu, J. X.: 2013, Consensus based approach for economic dispatch problem in a smart grid, *IEEE Transactions on Power Systems* **28**(4), 4416–4426.

Yang, T., Wu, D., Sun, Y. and Lian, J.: 2016, Minimum-time consensus-based approach for power system applications, *IEEE Transactions on Industrial Electronics* **63**(2), 1318–1328.

Yi, P., Hong, Y. and Liu, F.: 2015, Distributed gradient algorithm for constrained optimization with application to load sharing in power systems, *Systems & Control Letters* **83**, 45 – 52.

Yi, P., Hong, Y. and Liu, F.: 2016, Initialization-free distributed algorithms for optimal resource allocation with feasibility constraints and application to economic dispatch of power systems, *Automatica* **74**, 259 – 269.

You, S. and Chen, L.: 2014, Reverse and forward engineering of frequency control in power networks, *Proc. of the 53rd IEEE Conference on Decision and Control (CDC)*, Los Angeles, CA, USA, pp. 191–198.

Yousef, H. A., AL-Kharusi, K., Albadi, M. H. and Hosseinzadeh, N.: 2014, Load frequency control of a multi-area power system: An adaptive fuzzy logic approach, *IEEE Transactions on Power Systems* **29**(4), 1822–1830.

Zhang, C. K., Jiang, L., Wu, Q. H., He, Y. and Wu, M.: 2013, Delay-dependent robust load frequency control for time delay power systems, *IEEE Transactions on Power Systems* **28**(3), 2192–2201.

Zhang, X. and Papachristodoulou, A.: 2015, A real-time control framework for smart power networks: Design methodology and stability, *Automatica* **58**, 43 – 50.

Zhao, C. and Low, S.: 2014, Optimal decentralized primary frequency control in power networks, *Proc. of the IEEE 53rd Annual Conference on Decision and Control (CDC)*, Los Angeles, CA, USA.

Zhao, C., Mallada, E. and Dörfler, F.: 2015, Distributed frequency control for stability and economic dispatch in power networks, *Proc. of the 2015 American Control Conference (ACC)*, Chicago, IL, USA, pp. 2359–2364.

Zhao, C., Topcu, U., Li, N. and Low, S.: 2014, Design and stability of load-side primary frequency control in power systems, *IEEE Transactions on Automatic Control* **59**(5), 1177–1189.

Zhao, C., Topcu, U. and Low, S. H.: 2013, Optimal load control via frequency measurement and neighborhood area communication, *IEEE Transactions on Power Systems* **28**(4), 3576–3587.

Zhao, J. and Dörfler, F.: 2015, Distributed control and optimization in DC microgrids, *Automatica* **61**, 18 – 26.

Summary

Social and technological developments resulted in an increase of electricity demand, generated by an ever increasing amount of renewable energy sources. Despite its potential benefits, a continuation of these developments poses significant challenges to the planning and operation of the existing power networks. An important operational aspect in power networks is the regulation of its frequency, which is the focus of this work.

In the presence of more and smaller generation units, careful coordination among the individual parts in the power network is needed, ensuring proper overall functioning. We design and analyse distributed controllers, that ensure that actions taken by local controllers are consistent with global optimality objectives, such as the minimization of generation costs. The total energy of the power network plays a major role in this process, enabling the derivation of useful system theoretic properties without detailed knowledge of all components. Particularly, this work shows that energy functions are suitable to derive passivity properties of various nonlinear power system models, that form an excellent staring point for the controller design. Proposed controllers are shown to regulate the frequency and to obtain an economic dispatch.

The presented results explicitly incorporate two aspects that received less attention despite their practical importance. First, since generated control signals continuously adjust set points at the generation side, it is important to take into account the behavior of the generation side in a satisfactory level of detail. To this end, this work incorporates the turbine-governor dynamics in a more realistic manner than generally done in stability studies on optimal frequency regulation.

Second, an important aspect of proposed distributed solutions is the exchange of information among controllers over an underlying communication infrastructure. The combination of the continuous physical system and the digital communication,

leads to an overall (hybrid) cyber-physical system. As a result of the stability analysis, we derive explicit bounds on the required communication intervals.

We show that it is, although challenging, of importance to incorporate the generation side and the communication network explicitly in the design phase of controllers and that neglecting these aspects can result in an unjustified belief that stability of the network is guaranteed by suggested solutions.

Samenvatting

Sociale en technologische ontwikkelingen hebben geleid tot een toename van de vraag naar elektriciteit, gegenereerd door een steeds grotere hoeveelheid hernieuwbare energiebronnen. Ondanks de potentiële voordelen hiervan, vormen deze ontwikkelingen belangrijke uitdagingen voor de planning en de werking van de bestaande elektriciteitsnetwerken. Een belangrijk operationeel aspect in elektriciteitsnetwerken, waarop dit werk zich focust, is de regulering van de frequentie.

In aanwezigheid van meer en kleinere generatie eenheden is een zorgvuldige coördinatie tussen de afzonderlijke onderdelen in het elektriciteitsnet nodig om ervoor te zorgen dat het gehele netwerk juist functioneert. Wij ontwerpen en analyseren gedistribueerde regelaars, die ervoor zorgen dat de acties van lokale regelaars in overeenstemming zijn met de globale optimaliteitsdoelstellingen, zoals de minimalisering van de generatiekosten. De totale energie van het netwerk speelt een belangrijke rol in dit proces, waardoor het mogelijk is om nuttige systeemtheoretische eigenschappen te formuleren zonder gedetailleerde kennis van alle componenten. In het bijzonder blijkt uit dit werk dat energiefuncties geschikt zijn om passiviteitseigenschappen van verschillende niet-lineaire modellen van het systeem te omschrijven. Deze vormen een uitstekend startpunt voor het ontwerp van de regelaar. Verschillende oplossingen worden getoond om de frequentie te regelen en om een economische optimaliteit te verkrijgen.

De gepresenteerde resultaten bevatten expliciet twee aspecten die vaak minder aandacht krijgen, ondanks dat hun praktische relevantie. Ten eerste, aangezien de gegenereerde besturingssignalen de gewenste regelwaarde continu aanpassen aan de generatiezijde, is het belangrijk rekening te houden met het gedrag van de generatiezijde op een bevredigend detailniveau. Daartoe bevat dit werk de dynamiek van de turbine-regulateur op een realistischer manier dan gangbaar is in stabiliteitsstudies van optimale frequentieregeling.

Ten tweede, een belangrijk aspect van de voorgestelde gedistribueerde oplossingen is de uitwisseling van informatie tussen regelaars over een onderliggende communicatienetwerk. De combinatie van het continue fysieke systeem en de digitale communicatie leidt tot een algemeen (hybride) cyber-fysisch systeem. Als gevolg van de stabiliteitsanalyse bepalen we expliciete grenzen op de vereiste communicatie intervallen.

We tonen aan dat het belangrijk is om de generatiezijde en het communicatienetwerk expliciet in de ontwerpfase van regelaars te integreren en dat het achterwege laten kan leiden tot een ongerechtvaardigd geloof dat de stabiliteit van het netwerk is gewaarborgd.